NUMERICAL STUDY OF SMOKE AND FIRE CONFINEMENT USING AIR CURTAINS IN SHOPPING MALLS
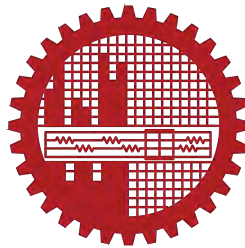

by

Md. Arif Mahmud Shuklo Shoshe

A Thesis Submitted to
Department of Mechanical Engineering
Bangladesh University of Engineering and Technology
Dhaka 1000, Bangladesh.

In Partial Fulfillment of the Requirements for the Degree of
Master of Science in Mechanical Engineering

November 2019

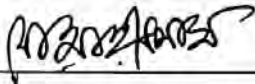# Recommendation of the Board of Examiners

The thesis titled, "NUMERICAL STUDY OF SMOKE AND FIRE CONFINEMENT USING AIR CURTAINS IN SHOPPING MALLS", submitted by Md. Arif Mahmud Shuklo Shoshe, Roll No: 0416102001, Session: April 2016, has been accepted as satisfactory in partial fulfillment of the requirements for the degree of *Master of Science in Mechanical Engineering* on 24 November, 2019.

Board of Examiners

Dr. Md. Ashiqur Rahman
Associate Professor
Dept. of Mechanical Engineering, BUET, Dhaka-1000.

Chairman
(Supervisor)

Dr. Md. Ashraful Islam
Professor & Head
Dept. of Mechanical Engineering, BUET, Dhaka-1000.

Member
(Ex-Officio)

Dr. Md. Zahurul Haq
Professor
Dept. of Mechanical Engineering, BUET, Dhaka-1000.

Member
(Internal)

Dr. Md. Easir Arafat Khan
Assistant Professor
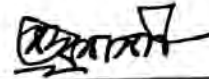Dept. of Chemical Engineering, BUET, Dhaka-1000.

Member
(External)

Certificate of Research

This is to certify that the work presented in this thesis is carried out under the supervision of Dr. Md. Ashiqur Rahman, Associate Professor of Department of Mechanical Engineering, Bangladesh University of Engineering and Technology, Dhaka-1000.
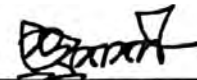
_____

Dr. Md. Ashiqur Rahman

_____

Md. Arif Mahmud Shuklo Shoshe

I would like to dedicate this thesis to my family.

Declaration

I, Md. Arif Mahmud Shuklo Shoshe, hereby declare that, this thesis contains no material that has been submitted previously, in whole or in part, for the award of any other academic degree or diploma. Also, declare that, except where specific reference is made to the work of others, the contents of this dissertation are my own work and are in accordance with academic rules and ethical conduct.

Md. Arif Mahmud Shuklo Shoshe
November 2019

Acknowledgements

Abstract

Fire incidents in densely populated urban areas can rapidly results in a catastrophic multi-death scenario, in absence of adequate fire-fighting equipment. As smoke generated during fire hazards is predominantly responsible for loss of life, confining smoke and heat at the source of fire is essential to facilitate safe evacuation. Shopping mall and marketplace fires represent a high percentage (18%) of the total number of fire incidents that occur in the country. The use of air curtains is quite common in the many shopping malls, especially in the typical, old-fashioned ones in both staircases/exits and in storefronts, for the purpose of acting as aerodynamic sealing. The present study aims to examine the effects of air curtains in confining the propagation of fire and smoke from a source of fire in the event of a typical shopping mall fire in the context of Bangladesh.

Smoke and flame propagation through shopping malls with air curtains are analyzed numerically from evacuation perspective, with strategic variations of operating conditions, and compared with the no air curtain case. Three different designs of shopping malls with distinct geometric and architectural features, two fuel types, and three distinct fuel arrangements are examined to imitate the diversities present in actual shopping malls. The parametric variation of air curtain operating parameters includes the variation of air curtain jet velocity in the range of 3 m/s to 10 m/s, jet angles from 0º to 60º, with a flow rate of 1250 m^3/h to 5000 m^3/h, and jet width of 7.62 cm to 30.48 cm. Single and twin jet configuration of air curtains, with 0 to 4 jet distance between two jets, and placement of air curtain in different combinations, at critically appraised positions during evacuation, are also examined. The numerical studies are conducted in PyroSim, a graphical user interface (GUI) for Fire Dynamics Simulator (FDS), a widely accepted fire simulation tool.

The proposition of injecting additional oxidizers into flame is more involved than common understanding and the phenomenon is addressed comprehensively. An off-the-shelf aircurtain installed at fire source shop door can confine the fire generated heat and smoke inside source shop substantially for all fuel type and arrangements considered, enabling crucial increment in safe evacuation time. About 37.1% of the fire generated

heat could be confined within the source and the flashover event could be delayed for 18s with air curtain at fire source. Use of air curtains with a reduction in the actual, extremely dense, arrangements of fuels, typically present in shops of Bangladesh, to a standard amount and arrangement is found to be beneficial to mitigate devastation during a fire incident. The flashover event can be further delayed with air curtains in combination with standard fuel arrangements but cannot be completely avoided in case of stores with high fuel density.

The effectiveness of air curtains in confining the heat and smoke transfer from the source as observed from the findings of the present study are quite encouraging. Air curtains operated at optimum parameters and placed at multiple critical positions are found to be even more beneficial to the evacuation process. A maximum of 59.4% heat confinement at source and about 120s increment in safe evacuation time through staircase could be achieved for the best case scenario. The findings of the present study provide a comprehensive insight into the role and effectiveness of air curtains in confining the heat and smoke and hence assisting safe evacuation in case of fire incidents in typical shopping malls in Bangladesh.

Table of Contents

List of Figures

List of Tables

Nomenclature

Roman Symbols

c_p constant-pressure specific heat

$\mathbf{f}_b$ external force vector (excluding gravity)

g acceleration of gravity

H total pressure divided by the density (Bernoulli integral)

h_s sensible enthalpy

I radiation intensity per unit of solid angle

I_b radiation blackbody intensity per unit of solid angle

k thermal conductivity

$\dot{m}_\alpha'''$ production rate per unit volume of species α by chemical reactions

Pr Prandtl number

p pressure

$\bar{p}_0$ atmospheric pressure profile

$\bar{p}_m$ background pressure of mth pressure zone

$\tilde{p}$ pressure perturbation

$\dot{q}'''$ heat release rate per unit volume

$\dot{\mathbf{q}}''$ heat flux vector

$\dot{q}_{\mathrm{r}}''$ radiative heat flux

$\dot{Q}$ total heat release rate

$\dot{Q}^*$ fire source Froude number

R universal gas constant

Re   Reynolds number

s   unit vector in direction of radiation intensity

Sc   Schmidt number

T temperature

t time

$\mathbf{u} = (u, v, w)$ velocity vector

W_α molecular weight of gas species α

$\overline{W}$ molecular weight of the gas mixture

$\mathbf{x} = (x, y, z)$ position vector

X_α volume fraction of species α

Y_α mass fraction of species α

$\hat{Y}_\alpha$ mass fraction of species α in mixed zone of a computation cell

Y_F mass fraction of fuel

Z_α species mixture α

Greek Symbols

Δ LES filter width

Δh heat of combustion

δ film thickness

κ absorption coefficient

μ dynamic viscosity

ν_α stoichiometric coefficient, species α

ρ density

τ_{ij} viscous stress tensor

ϕ porosity

χ_{r} radiative loss fraction

σ Stefan-Boltzmann constant

Subscripts

0   initial value

b bulk phase property

c convective

d drag

F   fuel

ijk gas phase cell indices

p pressure

r radiative

s sensible

t turbulent

α gas species index

∞ ambient condition

Acronyms / Abbreviations

$BFSCDA$ Bangladesh Fire Service and Civil Defense Authority

$BNBC$ Bangladesh National Building Code

CAD Computer-Aided Design

CFD Computational Fluid Dynamics

CFT Critical Flame Temperature

$Co-Op$ Co-Operative Market

$CS1$ Fire Source shop 1 with Clothing fuel

$CS2$ Fire Source shop 2 with Clothing fuel

$CS1AC$ Fire Source shop 1 with Clothing fuel & Air Curtain discharged

$CS2AC$ Fire Source shop 2 with Clothing fuel & Air Curtain discharged

$CS1D$ Fire Source shop 1 with Clothing in Display distribution

$CS1ACD$ Fire Source 1 with Clothing in Display distribution & Air Curtain discharged

$CS1G$ Fire Source shop 1 with Clothing in Grid distribution

$CS1ACG$ Fire Source 1 with Clothing in Grid distribution & Air Curtain discharged

DCC Dhaka City Corporation

$DNCC$ Dhaka North City Corporation

DNS Direct Numerical Simulation

DS_TJ Double-Stream Twin Jet

EDC Eddy Dissipation Concept

FDS Fire Dynamics Simulator

FFT Fast Fourier Transforms

$FS1$ Fire Source shop 1 with Furniture fuel

$FS2$ Fire Source shop 2 with Furniture fuel

$FS1AC$ Fire Source shop 1 with Furniture fuel with Air Curtain discharged

$FS2AC$ Fire Source shop 2 with Furniture fuel with Air Curtain discharged

GUI Graphical User Interface

HRR Heat Release Rate

LES Large Eddy Simulation

LOI Limiting Oxygen Index

MP MultiPlan Shopping Complex

$NFPA$ National Fire Protection Association

$NIST$ National Institute of Standards and Technology

$ODAC$ Opposite Double-jet Air Curtain

$RANS$ Reynolds-Averaged Navier–Stokes

RTE Radiation Transport Equation

$S1$ Fire Source Shop 1

$S2$ Fire Source Shop 2

SGS Sub-Grid Scale

TET Total Evacuation Time

VOC Volatile Organic Compound

Chapter 1

Introduction

1.1 Background of this Study

Fire hazard in Bangladesh is an alarmingly frequent and devastating phenomenon. In recent months Dhaka witness some deadly and heart melting scenarios involving massive fire incidents. During the Eid-ul Adha vacation around 2000 tin shacks in Dhaka's Mirpur district were destroyed leaving almost 10,000 people homeless, The Guardian reports, The Guardian (2019). On March 2019, 22-storey FR Tower in Dhaka's Banani area ripped by a deadly fire, killing 25 peoples, The Daily Star (2019*b*). Another fire at Mirpur 12 on March 2019, completely destroyed hundreds of shanties in a slum where nearly 25,000 people used to live in some 7,000-8,000 shanties, Prothom Alo reports, Prothom Alo (2019). A blazing inferno at Dhaka city's Chawkbazar area in February left people speechless as it took at least 70 lives within hours, The New York Times reports, Gettleman (2019). Bashundhara City, a popular choice of city dwellers, witness two devastating fire incidents in 2009 and 2016, The Daily Star (2009), Rabbi (2016). Dhaka North City Corporation (DNCC) market in Gulshan-1 also faced two consecutive fire incidents, one at 2017, where 400 shops were destroyed and an estimated loss of Tk. 500∼600 crores, Hasan et al. (2017). And another one at 2019, where 211 tin tin-shed business establishments were completely razed in fire, The Daily Star reports, The Daily Star (2019*a*). The list could go on and on as according to a recent article published in Dhaka Tribune, on average there was as many as 53 fire incidents per day in 2018, United News of Bangladesh (2019). And for previous year, according to Fire Chief of Bangladesh Fire Service and Civil Defense Authority (BFSCDA), there were as many as 18,048 fire incidents from July 2016 to June 2017, causing an estimated loss of Taka 430 crores, Bangladesh Shongbad Shongstha (2017). Figure 1.1 shows the number of fire incidents in Bangladesh according to Bangladesh
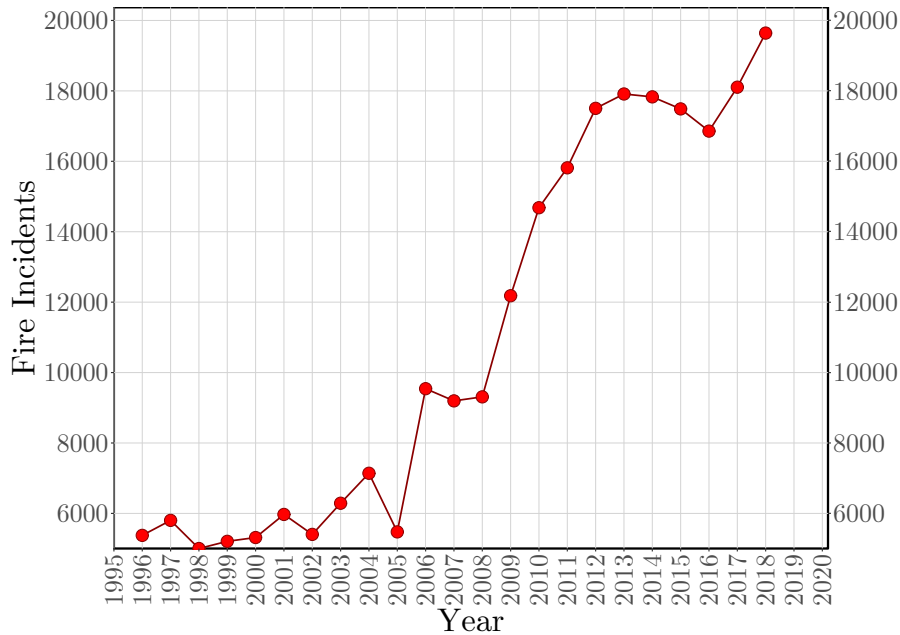
Fig. 1.1 Number of fire incidents in Bangladesh according to Bangladesh Fire Service and Civil Defense Authority (BFSCDA), from 1996 to 2018, *BFSCDA Annual Fire Report* (2019).

Fire Service and Civil Defense Authority (BFSCDA) from 1996 to 2018, and figure 1.2 shows estimated amount of money lost in those fire incidents, according to official report of Bangladesh Fire Service and Civil Defense, *BFSCDA Annual Fire Report* (2019). The number of fire incidents are tripled in last 22 years as seen from the figure 1.1. In last 10 years the estimated loss in fire hazard is over 425 crores on average per year. The statistics presented do support the claim made earlier about the frequency and devastation of fire incidents in Bangladesh. The reasons behind these reoccurring fire incidents should be identified and nullified for betterment of dwellers of Dhaka city as well as Bangladesh.

Careful observation of the follow up reports from International and National dailies after those fire incidents indicated that, the actual reasons were nothing but substandard equipment usage, negligence on fire safety protocol and unawareness of people. The follow up by The New Work Times, Gettleman (2019) on fire incident in Chawkbazar, revealed substandard equipment usage on the vehicle responsible, surrounding street side restaurants, a plastic storage and an illegal chemical storage. A bench of Justice in High Court, later that month ruled the Chawkbazar incident as negligence on fire safety protocol not accident, UNB (2019). On the Banani FR Tower fire incident, The Guardian wrote, 'The builders don't care', Ahmed and Safi (2019), indicating the
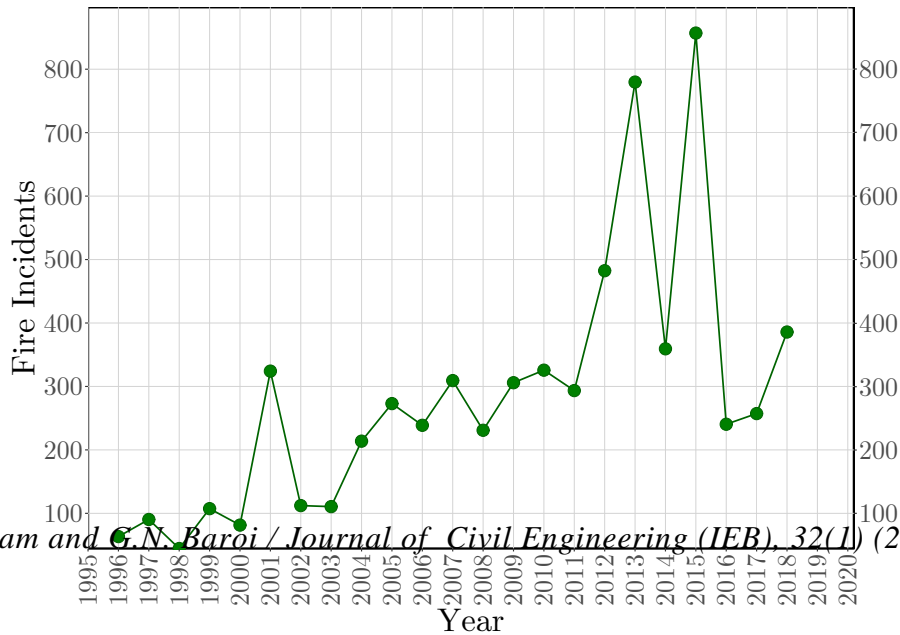
percent of the total incidents. It is followed by fire incidents at residential buildings and 'electricity and gas' installations with 15 and 14 percent, respectively.

Fig. 1.2 Estimated amount of money lost in fire incidents in Bangladesh according to Bangladesh Fire Service and Civil Defense Authority (BFSCDA) from 1996 to 2018, *BFSCDA Annual Fire Report* (2019).
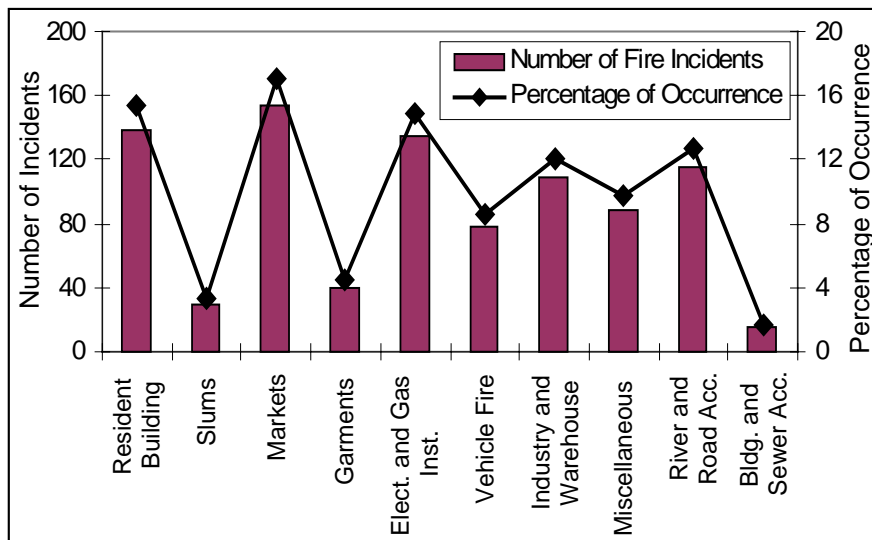
Fig. 1.3 Number and percentage of fire incidents along with the places of occurrence, Alam and Baroi (2004).

Fig. 1. Places of occurrence of fire incidents

5.2   Spatial pattern

building codes were not enforced and thus the consequences. And shockingly after the second fire of DNCC market, experts said, no safety protocol was implemented in DNCC supermarket after the first incident. In separate studies, ten years apart,

On the basis of frequency of fire hazards, the city is categorized in five groups of hazard zones (Sayeeduzzaman, 1992). The distribution of fire hazards and zonal mapping are shown in Fig. 2. From the analysis, Tejgon industrial area, Fulbaria and Postogola wards are found to be most hazardous having more than thirty incidences per year. These areas are classified as highly hazardous area (Hazard Zone Type -1). Wards with fire incidence frequency in between twenty to thirty are considered as moderately hazardous area (Hazard Zone Type -2). Jatrabari, Sadrghat, Shakaribazar, Oize ghat, Simson road, New
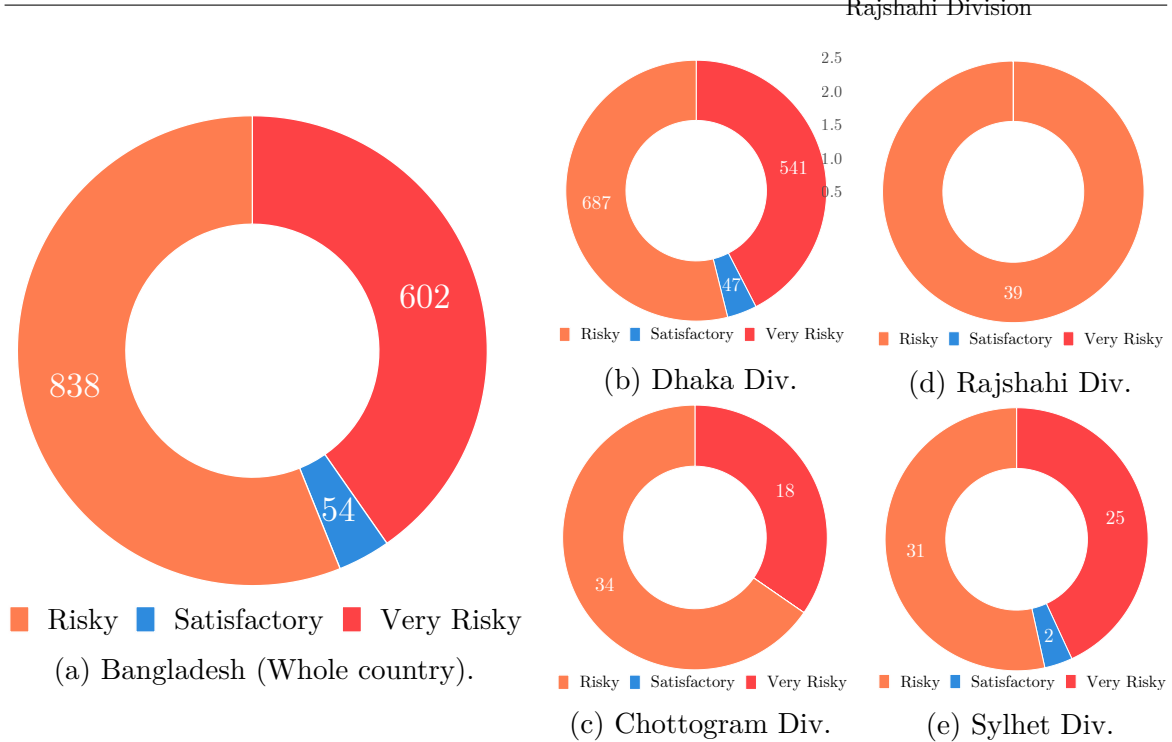
Fig. 1.4 Shopping mall safety scenarios in Bangladesh, according to Bangladesh Fire Service and Civil Defence (BFSCD) Statistics of 2018.

electrical short circuit is still the primary cause of fire incidents, closely followed by cooking/ stove burner fire, Islam and Adri (2008), Islam and Hossain (2018). It was a shocking revelation that, in spite of all the indications, the implementations of building code, adequate fire equipment and safety drills for the occupants, and raise of awareness in people of every social class are still to see day light.

1.1.1 Scenario of shopping mall fire in Bangladesh

Study showed, as seen in figure 1.3, among all the fire incidents in Bangladesh, maximum number of incidents were shopping mall fire, and was 17% of the total incidents Alam and Baroi (2004). And, there are already 3000 shopping malls in Dhaka city and the numbers are increasing continuously, Rahman (2010). Figure 1.4 shows hopping mall safety scenarios in Bangladesh, according to Bangladesh Fire Service and Civil Defence (BFSCD) two inspection statistics conducted in 2018. Only 3.6% shopping malls in the country meet the safety standards required, and 56.1% and 40.3% lies in 'risky' and 'very risky' situation, i.e., prone to devastation in case of any fire incidents due to poor or no fire-fighting systems. These statistics sadly indicate that, at the present conditions, the question on fire incidents is not 'if', rather 'when'. Thus, the scope of

this study was focused on shopping mall fire incidents, in context of Bangladesh, in a hope to lessen the loss of lives and resources during insufferable future fire events. A survey on shopping malls of Dhaka city was conducted to observe the present scenario of shopping malls of Bangladesh, specially in Dhaka city.

1.2 Survey of Shopping Malls in Dhaka City

1.2.1 Shopping Mall-1 (Gulshan-1 DCC market, Dhaka)

Several shopping malls from different regions of Dhaka city were surveyed to examine the actual fuel distribution on the shopping malls and the architectural position of the staircase with respect to shops and corridors. As DCC market of Gulshan-1 was

(a)　　　　　　　　　　　　　　　(b)

(c)　　　　　　　　　　　　　　　(d)

Fig. 1.5 Photographed clothing stores in first florr of Gulshan-1 DCC market during the survey.

Fig. 1.6 Photographed miscellaneous shops of Gulshan-1 DCC market during the survey. Figures show, (a) Plastic store, (b) Shoe store of first floor, and (c) Grocery store, (d) Carpet store, (e) Furniture store of ground floor from Gulshan-1 DCC market respectively.

affected twice in recent years by fire hazard, it was an obvious first choice. Residing on the center of Gulshan-1 circle, the DCC market is a two-story shopping mall hosing mainly furniture shops in ground floor, and plenty of clothing shops, toy shops, and grocery shops on first floor. Shops of DCC market are arranged along long corridors, and similar shops are clustered together. The fuel distributions found in DCC market in shops were extremely high due to compact stacking. Figure 1.5 shows photographs, taken with permission during the survey, of shop outside in inside for two clothing stores in DCC market. The compact stacking inside the shop were visible in both shops. Furthermore, high amount of cloths also stored in shop front corridors, which will create obstruction during evacuation and serve as extra fuel loads to aid propagate fire along the corridor in case of any fire incident. Figure 1.6 shows photographs of a plastic store, a shoe store, a grocery store, a carpet store and a furniture store respectively from top left to bottom. As seen from these figures and as seen on other shops during survey, other type of stores also had high density of fuels stacked inside and outside the sources too. In short, nearly all shops of DCC market had extremely high density of fuel loads.

1.2.2   Shopping Mall-2 (Co-Operative market of Mirpur-1, Dhaka)

Co-Operative market a prominent shopping mall of Mirpur-1 were also surveyed and photographed. The shopping mall had clusters of shop blocks and narrow corridors around them, a different geometric configuration than DCC market. And, the survey revealed that, this shopping mall also had compact stacking of high-density fuel loads. The figure 1.7 shows the photographs of clothing stores in Co-Operative market. A unique design of Co-Operative market was a wooden platform on shop floor. And, on top of this platform as seen from the figure 1.7, compact stacking of high-density fuel loads were stored. The survey also revealed cloths and other products stored again in shop front corridors and almost blocking free movement on corridors, for this shopping mall too.

1.2.3   Shopping Mall-3 (MultiPlan Shopping Complex of New Elephant Road, Dhaka)

MultiPlan shopping complex of New Elephant Road was surveyed next to observe the fuel load distribution on that shopping complex. Although popular for computer related electronic products, up until recent redecoration, the ground floor of the market hosted clothing stores. Figure s five clothing stores and one shoe store of that

Fig. 1.7 Photographed clothing stores in Mirpur-1 Co-Operative Market during the survey.

shopping mall. Among the other surveyed shopping malls, the fuel distribution of MultiPlan shopping complex was much lower and without any shop front fuel storage, an ideal condition, among all other shopping malls. Another significant characteristic of MultiPlan shopping complex was the presence of an open space around the middle surrounding the escalator.

1.2.4 Shopping Mall-4 (Muktijoddha market of Mirpur-1, Dhaka)

Muktijoddha market, another prominent shopping malls of Mirpur-1 were also surveyed and photographed. Like Co-operative market of Mirpur-1, this shopping mall also had clusters of shop blocks and narrow corridors around them, a unique geometric configuration. And again, this shopping mall had compact stacking of high-density fuel loads. Figure 1.9 shows corridors of Muktijoddha market from Mirpur-1. Different
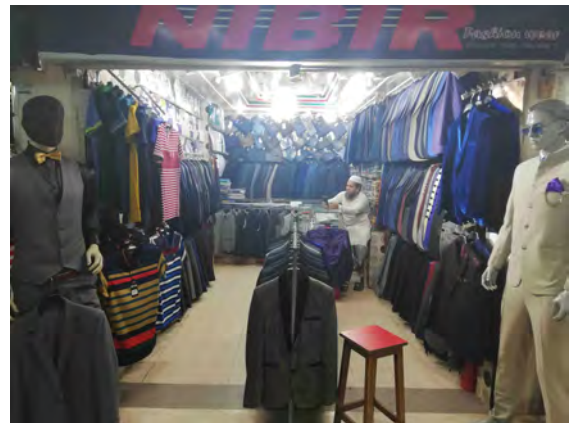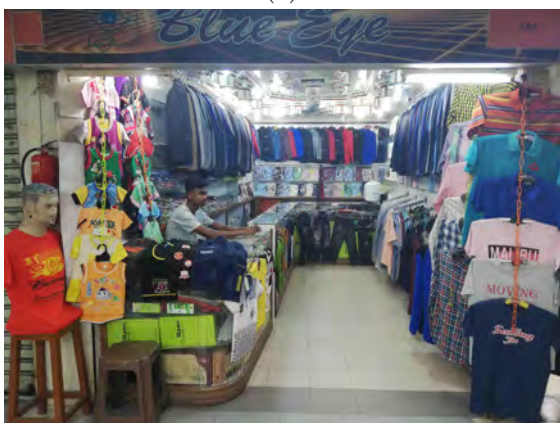
Fig. 1.8 Photographed clothing stores in MultiPlan shopping complex of New Elephant Road during the survey.

(a)

(b)
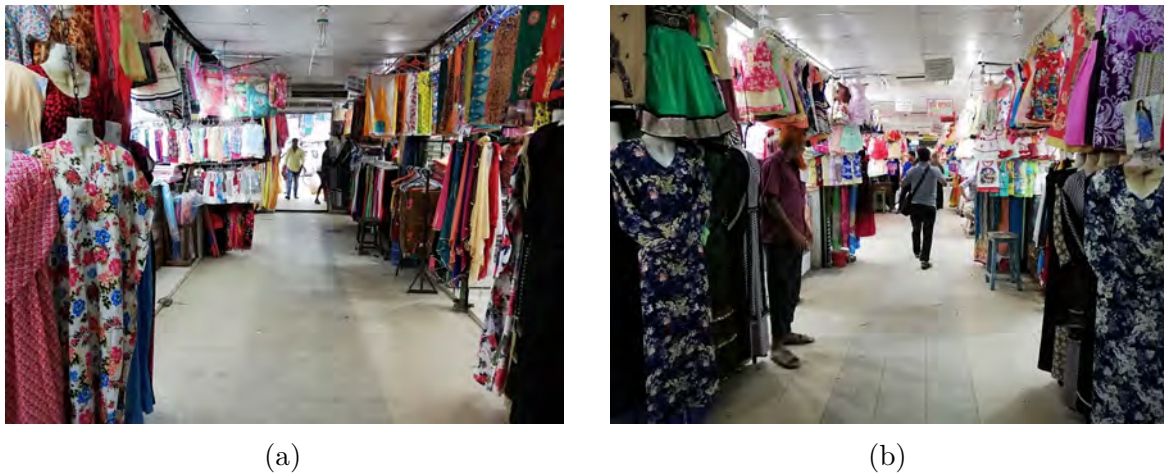
Fig. 1.9 Photographed clothing stores in Mirpur-1 Muktijoddha market during the survey.

types of clothing again stored in shop front corridor, by the shop owners, as seen in the figure, hampering the free movement in corridors.

1.2.5   Shopping Mall-5 (Nurjahan Supermarket of Mirpur Road, Dhaka)

The shopping malls on Mirpur road near Dhaka college were one of the most crowded and buzzing place for shopping as young generation of Dhaka city prefers the affordable and fashionable products choices offered there. Nurjahan Supermarket of Mirpur Road is such a place and figure 1.10 shows some shop insides of the shopping mall. As seen from the figure 1.10, this shopping mall had the most extreme situation on the compact stacking of fuels on the smallest of shops around the narrowest of corridors, among the other surveyed shopping malls.

1.2.6   Other surveyed Shopping malls in Dhaka

Apart from the reported shopping malls, several other shopping malls were also surveyed for their architectural and geometric differences. And figure 1.11 shows such two of these malls, in (a) UAE Maitry complex, Kemal Ataturk Avenue and (b) Genetic Plaza of Dhanmondi-27. The wide space in front of the UAE Maitry complex on Kemal Ataturk Avenue, a preferable one during any hazards, sadly was absent in many other shopping malls. Genetic Plaza of Dhanmondi-27 along other shopping complexes of

(a)
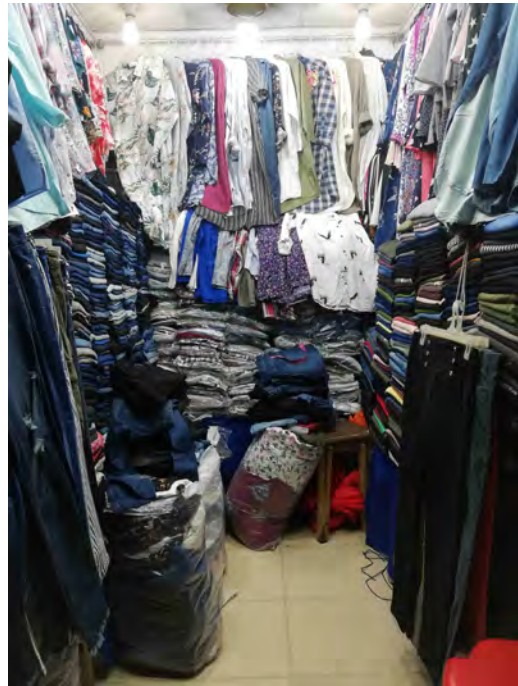
(b)

(c)

(d)

Fig. 1.10 Photographed clothing stores in Nurjahan Supermarket of Mirpur Road during the survey.

<p align="center">(a)   (b)</p>
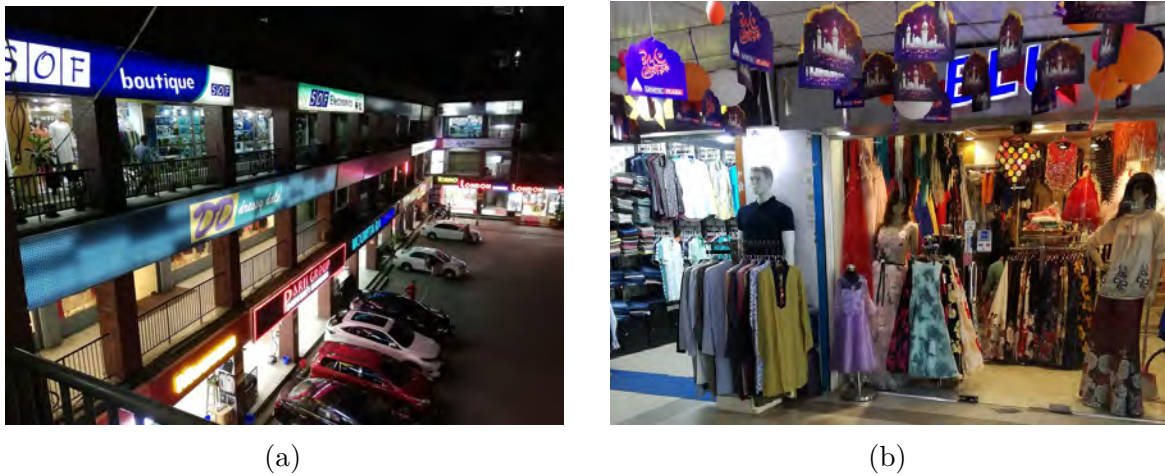
Fig. 1.11 Photographed stores in (a) UAE Maitry complex, Kemal Ataturk Avenue and (b) Genetic Plaza of Dhanmondi-27 during the survey.

<p align="center">(a)   (b)   (c)</p>

Fig. 1.12 Photographed staircase of (a) UAE Maitry complex, (b) Muktijoddha market, and (c) Nurjahan Supermarket during the survey.

Dhanmondi area also hosts clothing stores with compact stacking of cloths inside and outside the shops.

From the survey it could be concluded that, shopping malls of Bangladesh, especially in Dhaka city, contains high density of fuel loads in compact stacking, which will lead to a catastrophic incident in case of any fire hazard. The survey also revealed the limited, outdated or absent fire-fighting equipment in those malls. Staircase, an important location during evacuation from a multi storied building often found to be inadequate considering the population during peak hours. Figure 1.12 shows photographs of staircase of UAE Maitry complex, Muktijoddha market, and Nurjahan Supermarket during the survey. Although shopping malls tends to have wide staircases in mall front, the staircases inside the long corridors of the market were narrow and might not be

<p align="center">12</p>

adequate for the occupants of the mall during a fire hazard. Bangladesh National Building Code (BNBC) required that for unsprinklered area, the maximum travel distance to an exit door should be 23 m and maximum travel path to staircase should be 60 m in case of a commercial building, BNBC (2015). Although the staircase conditions might be met, emergency exit signs and exit doors were not present at any of the surveyed shopping malls. The next section deals with the inadequate and somewhat absent fire-fighting systems in the shopping malls of Bangladesh.

1.3 Heat and Smoke confinement provisions in shopping malls and the use of air curtains

At the beginning of a fire, smoke and toxic gases generate in large amounts, and propagate rapidly through the fire affected area. Due to smoke buoyancy, accumulation of smoke and toxic gases normally started at ceiling and gradually lowered down, and on the way reduce the visibility of evacuees. This in turn cause slower evacuation and more exposure to the toxic gases for the evacuees. Consequently, one of the major causes of deaths in fire related hazards is this toxic smoke inhalation and subsequent asphyxiation, Besserre and Delort (1997). Study revealed in building fire nearly 85% people killed in because of toxic gases, Alarie (2002), Fan et al. (2013). Among other gases, carbon monoxide, a colorless, tasteless, and odorless gas, upon inhalation binds with hemoglobin much faster than oxygen and creates chemical asphyxiation and hypoxia, which will ultimately result in death of the affected person.

Fire resistant doors, fire resistant walls and smoke control systems are traditionally used to confine the heat and smoke propagation in case of a fire incident. Figure 1.13 shows examples of some commercially available fire doors. The application of such fire doors or any other solid obstruction without proper escape route markings can have negative impact on identifying exit paths thus, could hamper the evacuation at early stages of fire. Moreover, application of solid obstructions to control smoke movement may not be practical in many real-life situations like in a shopping mall corridor or a road tunnel. As confinement of the smoke and flame propagation after the initial fire incident should be the primary concern to provide a safe evacuation process, the introduction of aerodynamic sealing might be more appropriate for heat and smoke confinement in channels with high personal load. Air curtains hence can be a viable alternative to fire doors and other solid obstructions as it will not impair visibility and maneuverability in the installed space. Furthermore, in case of shopping malls, fire doors are actually impractical, as the shop doors are usually remained open to allow

<div align="center">(a)   (b)</div>

Fig. 1.13 Commercially available fire doors. Figure (a) Fire Doors at Target Store by Mike Mozart from flickr, (b) From GMP Technical Solutions.

easy access of customers to shop insides. And, thus, in case of fire incidents in any shop, these open doors could provide an easy route for fire and smoke to propagate to other areas and lead to catastrophic disasters. Suggestions regarding the use of fire doors or any other solid obstruction at shop front, as a preventive measure to minimize the devastation in case of a fire hazard, will not be practical for business for reason stated earlier.

On the other hand, a large number of traditional shopping malls in Bangladesh do not have central air conditioning system hence, aiming for better business, shop owners use split Air-Conditioner inside the shops, for thermal comfort of customers. During operation, the air conditions will face high load if the shop door remained open and will consume high energy. And, a closed door to shops may seem unwelcoming to customers. Using an air curtain on an open door, as seen in figure 1.14a might be a solution to this paradox. Researchers used air curtains for sealing heat and mass transfer, odour and contaminant dispersion, dust and smoke confinement successfully. Guyonnaud et al. (2000) reported the mean flow rate of air curtain as the essential consideration to ensure aerodynamic sealing against heat and mass transfer in tunnels after conducting scale down model. Foster et al. (2006) improved the effectiveness of an off-the-self air curtain from 31% to 77% by changing the jet velocity and jet angle in case of cold room infiltration. Pavageau et al. (2001) experimentally investigate a double flux air curtain prototype for confining odour and volatile organic compound (VOC) in large enclosures and reported improved performance over traditional ones. Shih et al. (2011)

1.3 Heat and Smoke confinement provisions in shopping malls and the use of air curtains

Shut-out Functions

Increased Cold Storage Efficiency and Shut-Out Effect Test

This test ascertained the effectiveness of Mitsubishi Electric Air Curtains in reducing temperature increases in a cold storage facility. Without an air curtain, the inside temperature increased from -5 to +4 °C in as little as two minutes. With an air curtain installed this time was extended to about 10 minutes, or approximately five times as long. If the door was left open for five minutes, the temperature increased up to 10°C if no air curtain was used, as opposed to 2°C when one was used. It was established that 50% less energy was required to reduce the inside temperature to -5°C when an air curtain was used.

Insect* Shut-Out Test

This night time test ascertained the effectiveness of Mitsubishi Electric Air Curtains in shutting out insects. A 40W mercury lamp was placed inside an air curtain and ejected from a 48m wide vent at a velocity of 8m/sec. The insect shut-out rate was 70-80%.
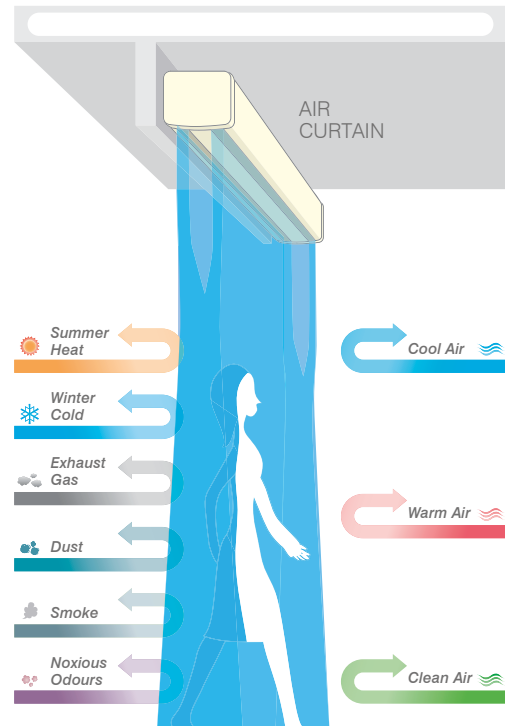
*Insects such as flies which have high flying power may fly into the room along the surface of the floor where wind velocity is comparatively low.

AIR CURTAIN

Summer Heat — Cool Air
Winter Cold
Exhaust Gas — Warm Air
Dust
Smoke
Noxious Odours — Clean Air

(a) (b)

Fig. 1.14 (a) Air curtain installed in shop front, photo from Thermoscreens air curtains, (b) Air curtain's Shut-out Functions, photo from Mitsubishi Electric air curtains.

Twin Nozzle

The twin nozzle design allows the Air Curtain to generate larger air velocity distribution with less air intake.

Resistance to the influence of external airflow has been strengthened, greatly improving insulation against heat and cold.

Propeller Fan   Protector Guard

Motor

Twin Nozzle

investigated the performance of air curtain to control pollutant spread inside a clean room with changing the velocity and injection angle. The results indicated that at 5 m/s velocity and 15°C injection angle the sealing efficiency was 0.87. Shen et al. (2017) used an air curtain to create non-uniform thermal environment in neighboring rooms with an effectiveness of 69.3% which in turn saved energy consumption. These studies affirmed the capability of air curtain as an aerodynamic sealing predicted earlier. A schematic representation of air curtain's shut out functions, from Mitsubishi Electric air curtains, is presented in figure 1.14b. Using commercially available air curtains, could thus be financially beneficial, and is supported by recent studies. Air curtains were reported to reduce the total energy consumption of a retail store by 4.84%, as reported by Bahman et al. (2012) and air curtain at building entrance could reduce 2.3% of annual energy consumption as reported by Wang (2013). This is because with air curtain discharged, the air condition unit, unlike the open door condition, get comparatively cooler air at inlet, thus reducing its energy consumption. Also, the initial investment on a typical air curtain might return within two air-conditioning seasons, as reported by Lawton and Howell (1995). Thus, air curtains could be a viable
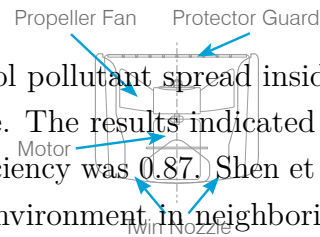
Air Curtain Shut-out Effect – Economic Benefits

	Cooling Mode – Load factors (kW)			Load Factor	Heating Mode – Load factors (kW)			Load factor
Open plan premises, doors kept open and no air curtain	Energy loss due to other causes 8.5	20.5	Energy loss from door area	41.5 kW	Energy loss due to other causes 8.7	37.8	Energy loss from door area	47.5 kW
Open plan premises with air curtain automatic door	8.5	4.1	Energy saved 16.4	12.6 kW	8.7	11.3	Energy saved 26.5	20 kW
Open plan premises with curtain and automatic door	8.5	1	Energy saved 19.5	9.5 kW	8.7	2.8	Energy saved 35	8.5 kW

Assumptions for economic benefits calculations:
Environmental factors – Floor space is 66.4m². Shop height 2.75m, depth 7.3m and width 9.1m. Two door openings of 0.5m (w) and 2.4m (h). Shop is housed in a two-story building surrounded by other buildings on 3 sides (back, left and right). Both the air conditioner and the air curtain have the specifications and characteristics of 50Hz. Cooling mode: indoor temperature 28°C and humidity 70%, outdoor temperature 32°C and humidity 60%. Heating mode: indoor temperature 18°C and outdoor temperature 0°C.

15

option to be used as a heat and smoke confinement purpose in these shopping malls. And, it will also provide easy access to shop insides for customers through the open door thus maintaining good business.

1.3.1 Use of Air Curtains: Existing Scenario

Although using air curtain in shop entrances as a fire and smoke confinement equipment in case of a fire incident is unprecedented in the context of Bangladesh, the technology itself is not an alien one, as many shopping malls already have air curtains at the mall entrance or on the storefront to reduce the cooling load. Figure 1.15, shows photographs of already installed air curtains in mall entrance in figure 1.15a, at staircase entrance in figure 1.15b, and 1.15b of different shopping malls visited during the survey. Interestingly, shops at many shopping malls already had air curtains installed at the shop doors as seen in figure 1.15d, to reduce its air conditioning load. Figure 1.16 and 1.17 photographs of already installed air curtains in mall entrance at Nurjahan market in Mirpur Road, Co-Operative market of Mirpur-1, and MultiPlan Shopping Complex of New Elephant Road, respectively. The concept of forming an aerodynamic sealing, during fire incidents, with air curtains is not an unprecedented one, as researchers used air curtain to confine heat and mass transfer in case of fire in long tunnels and multi storied buildings. However, air curtains have never been studied before for its applicability and effectiveness in shopping mall fires. The following section shed lights to the numerical procedure executed in this study.

1.4 Use of Air Curtains in Confining Fire and Smoke

Implementation of air curtain as aerodynamic sealing to confine fire propagation and smoke dispersion by researchers were successful in many practical scenarios like tunnel fire, building fire and compartment fire etc. Gupta et al. (2007) experimentally investigated single-jet and twin-jet air curtain systems with and without air recirculation ducts in a short section of a tunnel to compare the efficiency as a bilateral aeraulic confinement. The injection velocities were varied in between 1 to 10 m/s and jet width ratios were 10 and 20 for the tests. The result suggested using a recirculated double jet provided at least 30% improvement over non-recirculating single jet. And, at lower nozzle velocity single jet design performed better than a twin jet design. After analyzing all configurations, they reported a recirculated single jet with recirculation nozzle intake inside the confinement area as the best arrangement. They also reported

(a)

(b)

(c)

(d)

Fig. 1.15 Photographs of already installed air curtains in mall entrance in (a), at staircase entrance in (b), (c), and at shop entrance in (d), of different shopping malls visited during the survey.

(a)   (b)

Fig. 1.16 Photographs of already installed air curtains in mall entrance at Nurjahan market in Mirpur Road (left) and Co-Operative market of Mirpur-1 (right), during the survey.

Fig. 1.17 Photographs of already installed air curtains in mall entrance at MultiPlan Shopping Complex of New Elephant Road, during the survey.

that, the operating conditions had dominant influence on behavior and efficiency of an air curtain. Hu et al. (2008) performed experiments on table top model and simulation on Fire Dynamics Simulator (FDS) to study the confinement possibility of smoke and CO in channel fire near fire source with air curtain discharged at different velocities. They reported with increase of air curtain's discharge velocity the gas temperature and CO concentration in curtain protected zone reduced exponentially. The results also suggested that, for discharge velocity up to 3 m/s, introduction of air curtain increased CO concentration around fire source zone than no-curtain condition. And, if the discharge velocity was 4 m/s or more, the CO concentration decreased in fire zone than no-curtain condition. Krajewski and Węgrzyński (2015) developed a mathematical model to predict air curtain velocity under the influence of different flow conditions. They also presented a matrix of application for 10 m/s to 30 m/s outlet velocity and 0° to 30° jet angle for standalone devices to be applicable in context of tunnel fire like scenarios.

Apart from traditional air curtain, varying the orientation and number of jets, prototypes were also investigated to observe the improvements in air curtain effectiveness. Using double-stream twin jet (DS-TJ), air curtains to confine heat and mass transfer in case of a tunnel fire with recirculating hot stream and non-recirculating cold stream. In both experimental and numerical investigation yielded DS-TJ as an encouraging option to confine heat and mass transfer in case of tunnel fire, Elicer-Cortés et al. (2009), Lecaros et al. (2010), and Felis et al. (2010). A modified Opposite Double-jet Air Curtain (ODAC) was investigated both experimentally by a 1:12 scale model and in FDS as a smoke confinement unit in case of high-rise building fire in staircase. ODAC proved not only to be effective in protecting staircase, an important region during evacuation, but also drive away the fire generated smoke from the channel. The optimum air curtain velocity depending on the heat release rate (HRR) was also suggested as they report, an increase in jet velocity does not necessarily guarantees increase in effectiveness, Luo, Li, Gao, Tian, Zhang, Mei, Feng and Ma (2013), Luo, Li, Gao, Zhang and Tian (2013), and Luo et al. (2017). As parametric variations changes air curtain's effectiveness, detailed investigation was performed on revealing the dominating parameter of air curtain's effectiveness. Researchers suggested, momentum ratio and deflection modulus were the controlling parameter of air curtain effectiveness, Yu et al. (2016), Frank and Linden (2014). The air curtain effectiveness E, is defined as the fraction of the exchange flow prevented by the air curtain compared to an unobstructed open door. The momentum ratio R is the ratio of the vertically downward air curtain momentum to the horizontal smoke layer momentum, and the deflection modulus D_m is the ratio

between the momentum flux of the air curtain and the to the displacement ventilation forces. Using Fire Dynamics Simulator (FDS 6.0.1), Yu et al. (2016) suggested with momentum ratio $R = 8 - 10$, sealing effectiveness, $E \approx 60\%$ was attainable. Yu et al. (2018) conducted a parametric study to observe the effect of air curtain's velocity, injection angle, slot width and total heat transfer rates (HRRs) on air curtain's sealing effect against fire induced smoke propagation with small scale experiment studied. They reported up to 70% sealing effectiveness with injection angle variation. Upon detailed observation they suggested injection angle of 30º inclined to the fire source and a momentum ratio of, $R \approx 10$ for optimum sealing against smoke propagation. Viegas and Cruz (2019) carried out full size experiments with air curtain at the top of a permanent opening to assess smoke-tightness. During the tests, velocity of the air curtain nozzle was ranging from 8.3 m/s to 19.9 m/s, and the nozzle thickness was ranging from 0.017 m to 0.045 m. The smoke temperature was between 182ºC to 351ºC and the angle between the air curtain axis and vertical plane was in between 18º to 26º. The smoke-tightness limit was reported as $B = \Delta P_a / \Delta P_s = 0.30 u_a / u_{a\_min} + 1.25$ (with $1.30 \leq u_a / u_{a\_min} \leq 1.67$).

As the present study concerns with fire in shops, a confined, generally non ventilated compartment of a shopping mall, the theories explaining fire behavior specific to this type of scenarios should be reviewed in order to understand the underlying physics. The following section give tributes to this thought.

1.5   Enclosure Fire Dynamics

Enclosure Fire Dynamics deals with fire behavior within a compartment or room, studying the physical and chemical mechanisms controlling the fire growth and decay. After ignition a fire either self-extinguishes or might become life threateningly devastating. Established burning is a state after initial combustion process, when fuel, oxidizer and radiant feedback are sufficient enough to continue combustion unless external forces acts on it. After established burning, the fire growth will follow one of the paths shown in figure 1.18, termed as fire growth curve. Fuel orientation and distribution are vital during early stages of enclosure fire. At this stage of fire, the controlling factor is the amount of fuel available to sustain combustion and defined as fuel-controlled fire. After combustion, the products of combustion have higher temperature than ambient as less density due to increased temperature. The buoyant flow of combustion byproducts is termed as fire plume. In enclosure fire this natural upward flow of fire plume is intersected by ceiling, which deviate the buoyant flow beneath the ceiling and
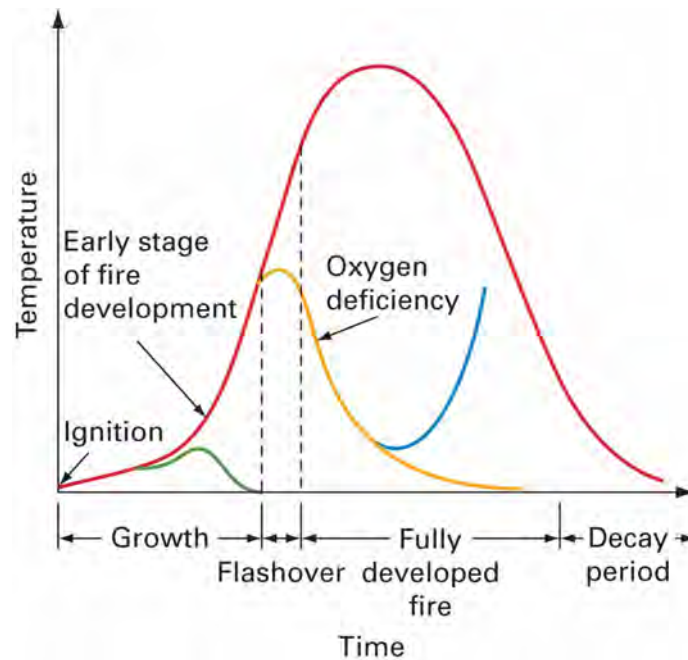
Fig. 1.18 Idealized fire growth curve showing different types of fire behavior, for enclosure fire, Bengtsson (2001), Gorbett, et al. (2016).

the process is termed as *stratification*. As the fire plume followed the least resistant path after being redirected by the ceiling, over time a relatively uniform layer of gases accumulated below the ceiling, this layer is defined as an upper layer or a smoke layer. As the buoyant fire plume raised, cooler air is drawn to fire and the process is referred as *entrainment*. The upper layer is gradually increased as fire continues to burn and the increase in volume makes the upper layer to grow and descend downward from the ceiling. Another movement in upper layer is observed because of the pressure difference between the hot upper layer inside the compartment and cool outside air. At normal atmospheric conditions, due the pressure increase inside the upper layer, smoke is expected to flow out of the source, in absence of wind. Figure 1.19 shows the neutral plane in between the hot upper layer and ambient, where no pressure driven flow occurs. In figure 1.20 the pressure driven flow out of a source for enclosure fire is shown, Gorbett et al. (2016).

In the next phase fire could follow one of the three paths, self-extinguished due to lack of fuel, slow full-room involvement, fast full-room involvement with flashover. The green curve of figure 1.18 portraits the fire growth curve for self-extinguishing fire. The red curve in figure 1.18, shows the fire growth for fire with a fast transition to full-room involvement due to flashover. According to National Fire Protection
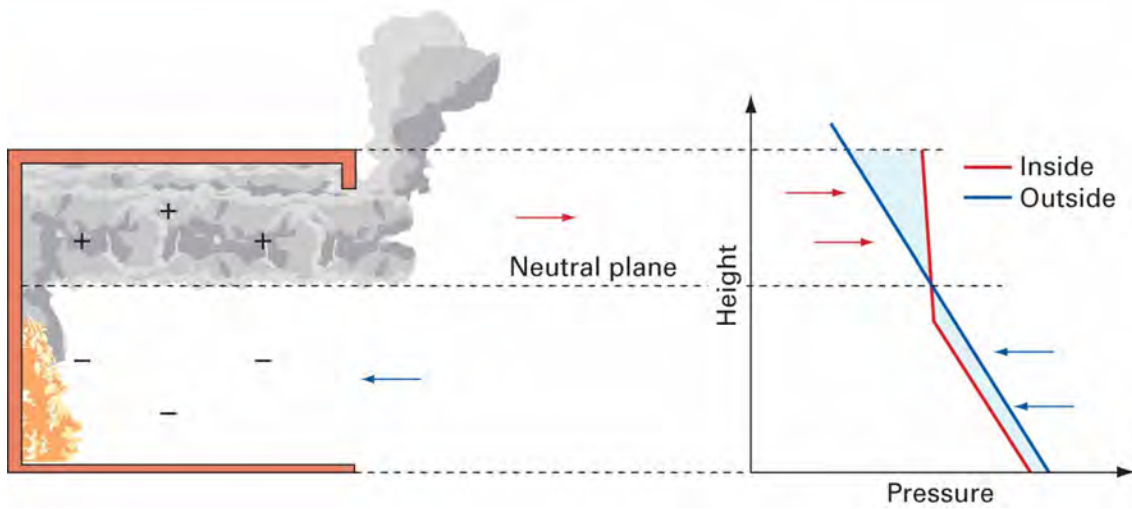
Fig. 1.19 Schematic of neutral plane in enclosure fire, Gorbett et al. (2016).

Fig. 1.20 Pressure driven flow out of source in case of enclosure fire, Gorbett et al. (2016).

Pressure-driven flow from compartment.
Source: Photo by authors.

Association (NFPA), Massachusetts, USA, the preferred definition of flashover is, *'A transitional phase in the development of a compartment fire in which surfaces exposed to thermal radiation reach ignition temperature more or less simultaneously and fire spreads rapidly throughout the space, resulting in full-room involvement or total involvement of the compartment or enclosed area'*, Gorbett et al. (2016). Figure 1.21 of NFPA 921: 'Guide for Fire and Explosion Investigations' shows the flashover conditions in
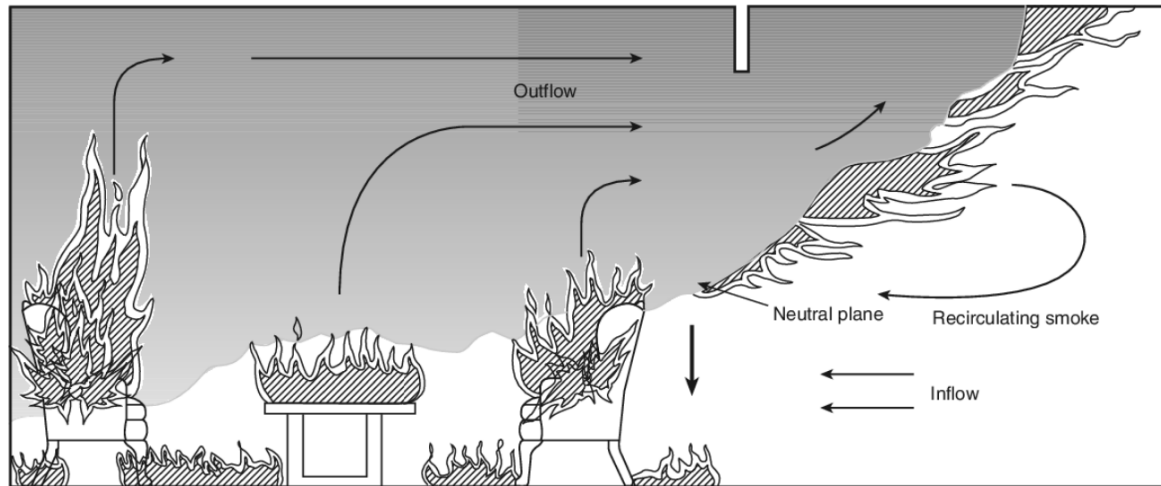
Fig. 1.21 Flashover condition in enclosure fire, National Fire Protection Association (2013).

case of a enclosure fire, National Fire Protection Association (2013). In the event of flashover every combustibles in the enclosed compartment is ignited and fire can not be contained within the compartment. At this point dominant heat transfer method is radiant heat from the ever deepening upper layer and this helped fire spread without direct flame contact. After this stage enclosure fire becomes ventilation-controlled fire, where combustion is affected by the lack of oxygen inside the compartment. The yellow curve of figure 1.18 represents fire growth curve of under ventilated enclosure fire which extinguished due to inadequate oxygen supply. The ventilation-controlled fire can also follow another path as shown with blue color in figure 1.18, progression with backdraft. In case of under ventilated fire lack of oxygen prevents burning but if temperature is high enough, pyrolysis products are being added to upper layer constantly and as upper layer descends, the compartment nearly filled up in volume with the pyrolysis products. Then if a vent is suddenly opened, a gravity current is created, an ignitable mixture is formed at the interface, and if this mixture ignited, a flame front propagates through the compartment. Which in turn increase the pressure inside the compartment rapidly and the fuel rich mixture then forced outside the source through the vent. After being forced out the fuel rich mixture then ignites rapidly with available oxygen outside the compartment and creates a colossal fireball upon exile. This path is termed as fire growth with backdraft for under-ventilated condition in ventilated-controlled enclosure fire.

1.6 Fire Dynamics Simulator (FDS)

This study investigates the fire hazard scenario in shopping malls in context of Bangladesh, with or without air curtains at shop doors, numerically in Fire Dynamics Simulator (FDS), a Large Eddy Simulation (LES) code developed by the National Institute of Standards and Technology (NIST), Maryland, United States, a widely used fire simulation tool. Following section narrates the acceptability of using FDS code to simulate fire by the scientific community. Ryder et al. (2004) and Ryder et al. (2006) investigated Fire Dynamics Simulator (FDS), for several small and large scale models of common fire scenarios. The results were well agreed with the experimental data with appreciable accuracy. They suggested FDS as more effective in simulating fire and smoke dispersion, than traditional Computational Fluid Dynamics (CFD) codes, and also reported that, FDS required less computational power than traditional CFD codes to handle transient solution for longer runs. Shen et al. (2008) validated FDS in a hotel arson fire in Taiwan using Fire dynamics simulator (version 4.0.5) and utilizing the parallel processing facility of FDS. They reported the FDS results agreed well with evidence from scene and illustration from evacuees in regard of the development of fire and smoke movement. Wahlqvist and Van Hees (2013) validated pre-release version of FDS 6 in much sophisticated well-confined mechanically ventilated fire scenarios with the likes of nuclear industry. The challenge of this type of fire was that, variation of pressure to high extent could lead to modification of the confinement levels and subsequently compromise the safety standards. FDS 6 was able to predict the pressure induced phenomena with satisfactory accuracy when compared against the full-scale experiments within the PRISME project. Due to this wide spread acceptability of FDS software, researchers are now highly depended on FDS to investigate the fire propagation and smoke dispersion in large open spaces like shopping mall, subway atrium and underground tunnels. FDS was also widely used to simulate fire hazards in shopping malls or atrium like structures by researchers in recent years. Khan et al. (2017) with Fire Dynamic Simulator with an evacuation software and predicted the total evacuation time for seven fire scenarios with 100 evacuees in a single storied 64 m^2 floor area shopping mall consisting seven shops. They reported a 390% increase in the total evacuation time (TET) for a 50% increase in soot yield, thus concluded that the evacuation is highly affected by the fuel's thermal and reaction properties. Gawad et al. (2015) simulated four scenarios of fire for a two storied shopping mall of 50,753 m2 floor area in each floor having 144 stores with FDS. They reported that the smoke propagated to the second floor at approximately 180s and covered the total floor within

900s after ignition. Gao et al. (2012) with large eddy simulator (LES) studied the dispersion of fire induced smoke in a subway atrium for six fire scenarios. They reported, within 200s of ignition the atrium was filled with smoke and mechanical ventilation was found useful to disperse the smoke effectively. To reduce the horizontal dispersion of smoke roof windows were suggested. Ji et al. (2015) proposed an empirical correlation for predicting the maximum upstream temperature in inclined urban road tunnel fires with FDS. They reported the dimensionless upstream maximum temperature had a nonlinear and non-monotonous relationship with tunnel slope. In the next section literature regarding air curtains as a fire confining mechanism were reviewed briefly to analyze the present situation of this approach.

1.7 Objectives of this Study

Fire incidents in Bangladesh are frequent and devastating, and number of fire incidents in Bangladesh tripled in last 22 years. Study suggests that a majority of these fire incidents occurred in shopping malls. Although significant portion of shopping malls in Bangladesh are in risk of potential fire incidents, most of the shops have extremely dense fuel arrangements, making the situation even worse. Primary cause of death in building fires is inhalation of toxic smoke and subsequent asphyxiation. Suggestions regarding the use of fire doors, fire screens or any other solid obstruction at shop front, as a preventive measure to confine smoke and fire propagation, in case of a fire hazard, will not be practical for business and early stages of evacuation process. The introduction of aerodynamic sealing might be more appropriate for heat and smoke confinement and thus, air curtains could be a viable alternative to fire doors and other solid obstructions as it will not impair visibility and maneuverability in the installed space. And, air curtain's capability to confine heat and mass transfer is already tested for tunnel fire and building fire scenarios. Moreover, air curtains could also reduce the energy consumption as shop owners tend to use split AC inside the shops, for thermal comfort of customers. In spite of the fact that, the use of air curtain as an aerodynamic sealing against heat and dust is quite common for typical shopping malls of Bangladesh, air curtain's confinement capability in case of shopping mall fire in context of Bangladesh is an uncharted territory.

The present study thus, aims to analyze the effectiveness of air curtains to confine fire and smoke propagation in case of a shopping mall fire, especially in the context of Bangladesh. A section of shopping mall with an adjacent staircase is considered for a typical fire scenario with and without air curtain and is numerically analyzed for

air curtain effectiveness to prevent the fire and smoke propagation. Specific aims and possible outcomes of this study are listed below:

1. To develop a detailed model of some popular shopping complex of Dhaka, and perform simulation of heat and smoke transport in case of fire using Fire Dynamics Simulator (FDS), and validate the simulation results with the experimental findings from available literature.

2. To analyze the effects of heat release rate of different ordinary combustibles and arrangements of fuel loads on fire propagation and smoke generation.

3. To numerically investigate the effectiveness of air curtains as a fire and smoke confinement mechanism in case of shopping mall fires.

4. To examine different air curtain parameters, such as velocity of jet, angle of jet, number and arrangements of jets, flow rate, orientation of jets and strategic positions of air curtain, on smoke and heat management.

The findings of this study will help to identify the desired air curtain characteristics required to ensure adequate prevention against fire-smoke propagation for different stores having a range of combustible materials. Analyzing the findings, comment on the possible use of air curtains as heat and smoke barriers in large shopping malls can be made in a quantitative manner. The knowledge gained from this study might be useful in improving the fire-safety performance of different shopping malls in Bangladesh and can be used in implementing a low-cost, easy-to-implement alternative where fire door is not suitable as a fire and smoke preventative barrier.

Chapter 2

Simulation Methodology

2.1 Governing Equations

2.1.1 Fire Dynamics Simulator (FDS)

The numerical studies were conducted in PyroSim (version 2018.3.1210) from Thunderhead Engineering. PyroSim is a graphical user interface (GUI) for Fire Dynamics Simulator FDS, (version 6.7.0 released on June 20, 2018). The user interface in PyroSim provides immediate input feedback, offers complex geometry creation features, enables import options from other CAD software, and ensures correct format of FDS code. FDS is a Large Eddy Simulation (LES) code developed by the National Institute of Standards and Technology (NIST), Maryland, United States, which is a widely used fire simulation tool. FDS solves Navier-Stokes equations with low Mach number approximation. This approximation filters out acoustic waves and allows large variations in temperature and density, suitable for low speed, thermal convective processes. Turbulence modeling was performed with large-eddy simulation (LES), first proposed by Smagorinsky (1963), and it is second order accurate in space and time.

2.1.2 Large Eddy Simulation (LES)

In LES large eddies of turbulent flow are computed in full detail, and only sub-grid scale (SGS) motions are modelled. This approach reduces computational cost in LES, significantly from direct numerical simulation (DNS). And, as LES captures large eddies in directly it is more precise than the Reynolds-averaged Navier–Stokes (RANS) approach. This is because the large eddies, with which most of the turbulent mixing and momentum transfer occurs, are also modelled in RANS approach. And secondly,

LES models the SGS motions with a separate approach, where in RANS model both large eddies and small eddies are modelled with a single model. Finite volume method has become a favored numerical approach for LES as the equations are integrated over control volume an implicit filter is inherently applied. One shortcoming of LES method is, if refining of mesh is performed continuously the LES computation is eventually transformed into a DNS computation. Thus, genuine mesh independence is impossible to achieve Zhiyin (2015).

For the LES filter width, in FDS is taken as cube root of the cell volume, defined as $\Delta = V_c^{1/3}$, where, $V_c = \delta x \delta y \delta z$. Then a filtered field ϕ, for any continuous field, could be defined as

$$\bar{\phi}(x, y, z, t) \equiv \frac{1}{V_c} \int_{x-\delta x/2}^{x+\delta x/2} \int_{y-\delta y/2}^{y+\delta y/2} \int_{z-\delta z/2}^{z+\delta z/2} \phi(x', y', z', t) dx' dy' dz' \qquad (2.1)$$

2.1.2.1 The LES momentum equation

The LES momentum equation is derived from DNS momentum equation with careful filtering. The DNS momentum equation for ith component of velocity in conservative form is as follows:

$$\frac{\partial \rho u_i}{\partial t} + \frac{\partial}{\partial x_j}(\rho u_i u_j) = -\frac{\partial p}{\partial x_i} - \frac{\partial \tau_{ij}}{\partial x_j} + \rho g_i + f_{d,i} + \dot{m}_b''' u_{b,i} \qquad (2.2)$$

The drag force due to unresolved Lagrangian particles is represented by $f_{d,i}$, and the effects of evaporation or pyrolysis is considered by the bulk source term, $\dot{m}_b''' u_{b,i}$. Applying the filtered field ϕ of equation 2.1 to the DNS momentum equation of 2.2, the following equation is generated

$$\frac{\partial \overline{\rho u_i}}{\partial t} + \frac{\partial}{\partial x_j}(\overline{\rho u_i u_j}) = -\frac{\partial \bar{p}}{\partial x_i} - \frac{\partial \bar{\tau}_{ij}}{\partial x_j} + \bar{\rho} g_i + \bar{f}_{d,i} + \overline{\dot{m}_b'''} \tilde{u}_{b,i} \qquad (2.3)$$

Here, ρ is density, $\bar{p}$ is filtered pressure, $\bar{u}_i$ is filtered velocity, and τ_{ij} is the deviatoric part of viscous stress. The cell mean value, $\overline{\rho u_i u_j}$ could not be evaluated advance of equation 2.3, thus needed separation of terms. After applying the mass-weighted or Favre filter, $\bar{\rho} \tilde{\phi} \equiv \overline{\rho \phi}$ to equation 2.3

$$\frac{\partial \bar{\rho} \tilde{u}_i}{\partial t} + \frac{\partial}{\partial x_j}(\bar{\rho} \widetilde{u_i u_j}) = -\frac{\partial \bar{p}}{\partial x_i} - \frac{\partial \bar{\tau}_{ij}}{\partial x_j} + \bar{\rho} g_i + \bar{f}_{d,i} + \overline{\dot{m}_b'''} \tilde{u}_{b,i} \qquad (2.4)$$

If the solution of $\bar{p}$ is available, first term could be separated now, but the filtered $\widetilde{u_i u_j}$ still could not be calculated. Thus, a subgrid-scale (SGS) stress is introduced as

$$\tau_{ij}^{\text{sgs}} \equiv \bar{p}(\widetilde{u_i u_j} - \tilde{u}_i \tilde{u}_j) \tag{2.5}$$

Substituting the subgrid-scale (SGS) stress of equation 2.5 to equation 2.4, the LES momentum equation is formed.

$$\frac{\partial \bar{\rho} \tilde{u}_i}{\partial t} + \frac{\partial}{\partial x_j}(\bar{\rho} \tilde{u}_i \tilde{u}_j) = -\frac{\partial \bar{p}}{\partial x_i} - \frac{\partial \bar{\tau}_{ij}}{\partial x_j} - \frac{\partial \tau_{ij}^{\text{sgs}}}{\partial x_j} + \bar{\rho} g_i + \bar{f}_{d,i} + \overline{\dot{m}_b'''} \tilde{u}_{b,i} \tag{2.6}$$

All term of this equation are computable when total derivative stress is modeled with decomposed SGS stress and Newton's law of viscosity as follows:

$$\tau_{ij}^{\text{dev}} \equiv \bar{\tau}_{ij} + \tau_{ij}^{\text{sgs}} - \frac{1}{3}\tau_{kk}^{\text{sgs}}\delta_{ij} = -2(\mu + \mu_t)\left(\tilde{S}_{ij} - \frac{1}{3}(\nabla \cdot \tilde{\mathbf{u}})\delta_{ij}\right) \tag{2.7}$$

Here, δ_{ij} is the Kronecker delta, μ_t is the turbulent viscosity and is the filtered scale strain rate tensor. Defining a sub-grid kinetic energy and a modified filtered pressure as

$$k_{\text{sgs}} \equiv \frac{1}{2}\tau_{kk}^{\text{sgs}} \tag{2.8}$$

$$\bar{p} \equiv \bar{p} + \frac{2}{3}k_{\text{sgs}} \tag{2.9}$$

Substituting the τ_{ij}^{dev} and $\bar{p}$ of equation 2.7 and equation 2.9 in LES momentum equation of 2.6, we have

$$\frac{\partial \bar{\rho} \tilde{u}_i}{\partial t} + \frac{\partial}{\partial x_j}(\bar{\rho} \tilde{u}_i \tilde{u}_j) = -\frac{\partial \bar{p}}{\partial x_i} - \frac{\partial \tau_{ij}^{\text{dev}}}{\partial x_j} + \bar{\rho} g_i + \bar{f}_{d,i} + \overline{\dot{m}_b'''} \tilde{u}_{b,i} \tag{2.10}$$

2.1.2.2 Subgrid Kinetic Energy

By dot product of the LES momentum equation with the resolved velocity vector, the transport equation for the resolved kinetic energy per unit mass $K \equiv \frac{1}{2}\tilde{u}_i \tilde{u}_j$, is derived as follows, (in which the subgrid kinetic energy term is within the RHS)

$$\bar{\rho}\frac{DK}{Dt} + \frac{\partial}{\partial x_j}([\bar{p}\delta_{ij} + \tau_{ij}^{\text{dev}}]\tilde{u}_i) = \bar{p}\frac{\partial \tilde{u}_i}{\partial x_i} + \tau_{ij}^{\text{dev}}\frac{\partial \tilde{u}_i}{\partial x_j} + (\bar{\rho} g_i + \bar{f}_{b,i})\tilde{u}_i \tag{2.11}$$

2.1.2.3 Deardorff's Model for Turbulent Viscosity

FDS 6.7.0 uses a variation of Deardorff's model for computing the SGS turbulent viscosity, μ_t defined as:

$$\mu_t = \rho C_v \Delta \sqrt{k_{\mathrm{sgs}}} \tag{2.12}$$

$$k_{\mathrm{sgs}} = \frac{1}{2}\left((\bar{u} - \hat{\bar{u}})^2 + (\bar{v} - \hat{\bar{v}})^2 + (\bar{w} - \hat{\bar{w}})^2\right) \tag{2.13}$$

Where $\bar{u}$ is the average value of u at the grid cell center and $\hat{\bar{u}}$ is a weighted average of u over the adjacent cells. The constant $C_v = 0.1$ is used from existing literature, Deardorff (1980).

$$\bar{u_{ijk}} = \frac{u_{ijk} + u_{i-1,jk}}{2} \tag{2.14}$$

$$\hat{u_{ijk}} = \frac{\bar{u_{ijk}}}{2} + \frac{\bar{u_{i-1,jk}} + \bar{u_{i+1,jk}}}{4} \tag{2.15}$$

2.1.2.4 Turbulent Diffusivity

The thermal conductivity k_t, and mass diffusivity $(\rho D)_t$, are related to the turbulent viscosity by constant turbulent Prandtl number $\mathrm{Pr_t}$ (for thermal diffusivity), and constant turbulent Schmidt number $\mathrm{Sc_t}$ (for mass diffusivity), as follows:

$$k_t = \frac{\mu_t c_p}{\mathrm{Pr_t}} \tag{2.16}$$

$$(\rho D)_t = \frac{\mu_t}{\mathrm{Sc_t}} \tag{2.17}$$

2.1.2.5 Coupling Velocity and Pressure Term

To solve the finite difference form of momentum equation for the velocity components, discretized form of the Poisson equation is solved using Fast Fourier Transforms (FFT). The consistence of the divergence of the fluid from this hydrodynamic solver is satisfied against the divergence constraint from the conservative form of sensible enthalpy equation (discussed later in this section) in predictor-corrector steps.

2.1.3 Convection–Diffusion Equations for Mass, Species and Enthalpy

As, with the low Mach number assumption the compressibility effects are eliminated, an alternative approach to equation of state, the solve of finite difference form of mass and species conservation equations with large time steps, and the use of flow divergence

as a surrogate for the enthalpy transport equation were possible. The energy equation is implicitly defined with combustion and radiation source terms embedded within the flow divergence.

2.1.3.1 The Equation of State

The pressure term could be decomposed into a 'background' component $\overline{p}(z, t)$, and flow-induced perturbation $\tilde{p}(x, y, z, t)$, for low speed application like fire, Rehm and Baum (1978). The pressure field within the mth zone, thus becomes:

$$p(\mathbf{x}, t) = \overline{p}_m(z, t) + \tilde{p}(\mathbf{x}, t) \tag{2.18}$$

For low Mach number flows, the temperature and density could be assumed to be inversely proportional and an approximation of the equation of state could be done with this decomposed pressure term as

$$\overline{p}_m = \rho T R \sum_\alpha \frac{Z_\alpha}{W_\alpha} = \frac{\rho T R}{\overline{W}} \tag{2.19}$$

Here, Z_α is the mass fraction of lumped species α. Replacing the pressure term p by $\overline{p}_m$, in the state and energy equations, filter out the acoustic waves which travels much faster than flow speeds expected in fire applications, and reduced one dependent variable in the system of equations. $\overline{p}_0(z)$ denotes the ambient pressure field and is derived from

$$\frac{\mathrm{d}\overline{p}_0(z)}{\mathrm{d}z} = -\rho_0(z)g \tag{2.20}$$

Using the above stated form of equation of state, the mean cell gas temperature, T is derived as:

$$T_{ijk} = \frac{\overline{p}_m}{\rho_{ijk} R \sum_{\alpha=0}^{N_s} (Z_{\alpha,ijk}/W_\alpha)} \tag{2.21}$$

2.1.3.2 Transport Equations of Mass and Species

A predictor-corrector scheme is used for solving the species transport equations with advection terms in flux divergence (conservative) form. The predictor step, shown below, uses information from the previous time step to predict the mass density in any cell ijk at any time step.

$$\frac{(\rho Z_\alpha)^*_{ijk} - (\rho Z_\alpha)^n_{ijk}}{\delta t} + \nabla \cdot (\overline{\rho Z_\alpha}^{\mathrm{FL}} \mathbf{u})^n_{ijk} = \nabla \cdot (\rho D_\alpha \nabla Z_\alpha)^n_{ijk} + (\dot{m}'''_\alpha + \dot{m}'''_{b,\alpha})^n_{ijk} \quad (2.22)$$

The quantity $\overline{\rho Z_\alpha}^{\mathrm{FL}}$ is an interpolation scheme *flux limiter*, applied to cell faces to avoid intolerable levels of dispersion error. The corrector step is defined as:

$$\frac{(\rho Z_\alpha)^{n+1}_{ijk} - \frac{1}{2}\left[(\rho Z_\alpha)^n_{ijk} + (\rho Z_\alpha)^*_{ijk}\right]}{\frac{1}{2}\delta t} + \nabla \cdot (\overline{\rho Z_\alpha}^{\mathrm{FL}} \mathbf{u})^*_{ijk} = \nabla \cdot (\rho D_\alpha \nabla Z_\alpha)^*_{ijk} + (\dot{m}'''_\alpha + \dot{m}'''_{b,\alpha})^n_{ijk}$$

$$(2.23)$$

2.1.3.3   The Velocity Divergence

Due to low Mach number approximation, the enthalpy, h, internal energy, e, and the thermodynamic (background) pressure can be written as:

$$h = e + \overline{p}/\rho \qquad (2.24)$$

Then the energy conservation equation may be written as follows, with *sensible enthalpy, h_s.*

$$\frac{\partial}{\partial t}(\rho h_s) + \nabla \cdot (\rho h_s \mathbf{u}) = \frac{\mathrm{D}\overline{p}}{\mathrm{D}t} + \dot{q}''' + \dot{q}'''_b - \nabla \cdot \dot{\mathbf{q}}'' \qquad (2.25)$$

The terms $\dot{q}'''$, $\dot{q}'''_b$, and $\dot{\mathbf{q}}''$ are the heat release rate per unit volume from a chemical reaction, the energy transferred to subgrid-scale droplets and particles, and the conductive, diffusive, and radiative heat fluxes, respectively. The energy equation of equation 2.25 is not solved explicitly, rather a velocity divergence is factored out which is satisfied by the hydrodynamic solver thus, ensuring energy is conserved. The velocity divergence is as follows:

$$\nabla \cdot \mathbf{u} = \frac{1}{\rho h_s}\left[\frac{\mathrm{D}}{\mathrm{D}t}(\overline{p} - \rho h_s) + \dot{q}''' + \dot{q}'''_b - \nabla \cdot \dot{\mathbf{q}}''\right] \qquad (2.26)$$

2.1.4   Combustion Model

The combustion model in FDS determines $\dot{m}'''_\alpha$, the mean chemical mass production rate per unit volume of species α and the heat release rate per unit volume, $\dot{q}'''$, an important contributor to flow divergence. The calculation of $\dot{m}'''_\alpha$ requires special treatment as flame thickness is on the order of millimeter, while typically computational grids are

in order of tens of centimeters. A *turbulent batch reactor model,* capable of handling a range of chemical kinetics and mixing conditions, is used to determine $\dot{m}'''_\alpha$. For majority of FDS application, non-premixed and fast chemistry limit is valid, and the reactor model reduced to the Eddy Dissipation Concept (EDC), the 'mixed is burnt' approximation. The generalized combustion model, capable of handling both fast and slow chemistry and a range of mixing conditions, treat each cell as a partially-stirred batch reactor assigned with a specific mixing time. After the mixing, reactants could follow fast chemistry mechanism to Arrhenius rate law depending on the available conditions.

2.1.4.1   The Lumped Species Approach

To simplify the reactions, primitive species are lumped into reacting groups in FDS

$$\text{Fuel} + \text{Air} \longrightarrow \text{Products} \tag{2.27}$$

The Fuel, Air and Products are defined as *lumped species.* The groups of primitive species, when exists in flow in certain proportions, only then are lumped together. For example, Air is assumed to be a lumped species which contains 21% O_2, 79% N_2 and small amount of water vapour and carbon monoxide. The number of transport equations needed to solve is reduced by the assumption that the lumped species groups transport and react together.

2.1.4.2   The Turbulent Combustion Model

The *turbulent batch reactor* model assumed each cell has some amount of mixing in between the existing species at initial concentration and the rate of this mixing is governed by turbulence. The mixing time τ_{mix} depends on the dominant physical process within the cell, diffusion, subgrid-scale (SGS) advection or buoyant acceleration. The mathematical representation is

$$\tau_{\text{mix}} = \max(\tau_{\text{chem}}, \min(\tau_{\text{d}}, \tau_{\text{u}}, \tau_{\text{g}}, \tau_{\text{flame}})) \tag{2.28}$$

After mixing the species, based on specific kinetic parameters, the reaction could either follow the Infinitely Fast Chemistry model or the Finite-rate Chemistry, the Arrhenius Reaction model. For a single reaction, based on limiting reactants, the change in the fuel is

$$\Delta \hat{Y}_\text{F} = -\min\left(\hat{Y}_\text{F}, \hat{Y}_\alpha \frac{\nu_\text{F} W_\text{F}}{\nu_\alpha W_\alpha} \right) \tag{2.29}$$

The Eddy Dissipation Concept of Magnussen and Hjertager (1977), predominantly applicable for large-secle fire scenarios, utilizes the "mixing is burnt" assumption and models the mean chemical source term for fuel F as:

$$\dot{m}_\text{F}''' = -\rho \frac{\min(Y_\text{F}, Y_\text{F}/s)}{\tau_\text{mix}} \tag{2.30}$$

The Arrhenius Reaction model, for mixed reactor zone, finds the rate of change in composition for species α as

$$\frac{\mathrm{d}\hat{Y}_\alpha}{\mathrm{d}t} = \frac{1}{\rho} \sum_i r'_{\alpha,i} \tag{2.31}$$

Here for species α the mass rate of reaction per unit volume, and the rate of reaction for fuel is

$$r'_{\alpha,i} = \left(\frac{\nu_{\alpha,i} W_\alpha}{\nu_{\text{F},i} W_\text{F}} \right) r'_{\text{F},i} \tag{2.32}$$

$$r'_{\text{F},i} = -A'_i \rho^{\sum a_{\alpha,i}} T^{n_i} \mathrm{e}^{-E_i/RT} \prod Y_\alpha^{a_{\alpha,i}} \tag{2.33}$$

In the time step δt, the mass fraction of the species α, in the mixed reactor zone is obtained from the concentration change in fuel for all the N_r reactions. And, then the heat release rate per unit volume could be found from heat of formation and mass production rate of the species.

$$\hat{Y}_\alpha(\delta t) = \widetilde{Y}_\alpha^0 + \sum_{i=1}^{N_r} \left(\frac{\nu_{\alpha,i} W_\alpha}{\nu_{\text{F},i} W_{\text{F},i}} \right) \Delta \hat{Y}_{\text{F},i} \tag{2.34}$$

$$\dot{q}''' = \rho \sum_\alpha \left(\widetilde{Y}_\alpha(\delta t) - \widetilde{Y}_\alpha^0 \right) \Delta h_{\text{f},\alpha}^0 \tag{2.35}$$

2.1.4.3 Extinction Model

The default mixing-control reaction model, although sufficient for modelling well-ventilated fires, but is not suited for under-ventilated or suppressed fire scenarios. Thus, extinction process in FDS uses empirical constrains on species concentration and local cell temperature. There are two extinctions options and both are based on critical flame temperature (CFT). CFT is based on the *limiting oxygen index* (LOI),

the volume fraction of oxygen at the point of flame extinction. The mass fraction of oxygen within a control volume, the adiabatic flame temperature and oxygen at the LOI are

$$Y_{O_2} = \frac{\overline{c_p}(T_f - T)}{\Delta H / r_{O_2}} \tag{2.36}$$

$$T_{OI} = T_\infty + Y_{OI}\left(\frac{\Delta H / r_{O_2}}{\overline{c_p}}\right) \tag{2.37}$$

$$Y_{OI} = \frac{X_{OI} W_{O_2}}{X_{OI} W_{O_2} + (1 - X_{OI}) W_{N_2}} \tag{2.38}$$

The simple extinction model in FDS, referred as Model 1, is based on oxygen only and checks if $Y_{OI} < Y_{O_2,\text{lim}}$, and then local extinction is assumed in which $\dot{m}_\alpha''' = 0$ and $\dot{q}''' = 0$ for that grid for that time step is forced.

$$Y_{O_2,\text{lim}}(T) = Y_{OI}\left(\frac{T_{OI} - T}{T_{OI} - T_\infty}\right) \tag{2.39}$$

The second extinction model considered both fuel and oxygen and referred as Model 2, checks in the ability of the potential heat release rate of from a grid to raise the cell temperature above the critical flame temperature T_{CFT}, if not it suppressed the combustion.

2.1.4.4 Thermal Radiation

The energy equation has the following thermal ration component as:

$$\dot{q}_r''' \equiv -\nabla \cdot \dot{\mathbf{q}}_r''(\mathbf{x}) = \kappa(\mathbf{x})[U(\mathbf{x}) - 4\pi I_b(\mathbf{x})] \quad ; \quad U(\mathbf{x}) = \int_{4\pi} I(\mathbf{x}, \mathbf{s}')d\mathbf{s}' \tag{2.40}$$

Here $\kappa(\mathbf{x})$ and $I_b(\mathbf{x})$ are the absorption coefficient and the source term respectively. From the radiation transport equation (RTE), $I(\mathbf{x}, \mathbf{s})$ is the solution for non-scattering grey gas, represented as:

$$\mathbf{s} \cdot \nabla I(\mathbf{x},\mathbf{s}) = \kappa(\mathbf{x})[I_b(\mathbf{x}) - I(\mathbf{x},\mathbf{s})] \tag{2.41}$$

The values of κ, the mean absorption coefficient, values are obtained from RadCal model, a narrow-band model for finding the spectral dependence, Grosshandler (1993). As grid cells for a large scale fire simulation are typically in orders of tens of centimeters,

flame sheets cannot be resolved, and the computed cell temperature can be significantly lower than actual case. Thus, instead of computing, the source term, I_b, is approximated in grid cells containing fuel and oxygen reactions. While on other grids the temperature field is homogeneous and can be computed directly:

$$\kappa I_b = \begin{cases} \kappa \sigma T^4 / \pi & \text{Outside the flame zone,} \quad \dot{q}''' = 0 \\ C \kappa \sigma T^4 / \pi & \text{Inside the flame zone,} \quad \dot{q}''' > 0 \end{cases} \tag{2.42}$$

As, typically a sooty fire radiates approximately one-third of the total combustion energy, χ_r, thermal radiation contribution to total energy emitted, estimated empirically, was used to with the constant C, to satisfy the radiation emission constrains. Lastly, Mie theory provides necessary coefficients for water droplets, which can absorb and scatter the thermal radiation. The details of the governing equations discussed here can be found from 'NIST Special Publication 1018-1, Fire Dynamics Simulator Technical Reference Guide Volume 1: Mathematical Model (Sixth Edition),' by McGrattan et al. (2018).

2.2   The Physical Model

The physical dimensions of DCC supermarket was available as a CAD file, depending on the location of staircase and shops around the staircase three small segments of DCC markets were designed as 3D models. Figure 2.1 shows 3D models of the aforementioned three segments of DCC market. Among the models figure 2.1a was selected for investigation in FDS. After DCC market, three markets from Mirpur-1, Dhaka, two from Dhanmondi and one from New Elephant road were considered and photographed during the survey for the fuel loads and architectural design. As none of the surveyed shopping malls, except DCC market, had CAD design available, measurements were taken manually during the survey for modelling the architectural design in a 3D model environment. Figure 2.2 shows 3D models of sections of Co-Operative Market, Muktijoddha market, and Mukto Bangla market, the three surveyed shopping malls of Mirpur-1. Co-Operative Market in figure 2.2a was selected among these shopping malls and black border in the figure shows the chosen computational geometry for FDS. 3D models of MultiPlan shopping complex of New Elephant Road, Rapa Plaza, and Genetic Plaza of Dhanmondi-27 are shown in figure 2.3. From these bunddle of shopping malls MultiPlan shopping complex figure 2.3a was selected and again the black border shows the chosen computational geometry. The reason behind choosing specific malls was to obtain variation in computation geometry, also covering the range of shopping malls accessed by different social class of Dhaka metropolitan city. While choosing the total floor area of the shopping malls for investigation in FDS, requirement of the computational resources was a pivoting factor. Although only a segment from each shopping malls were selected, careful consideration was taken to retain the specific architectural design of the mall. Also, each selected segment had a

| (a) | (b) | (c) |
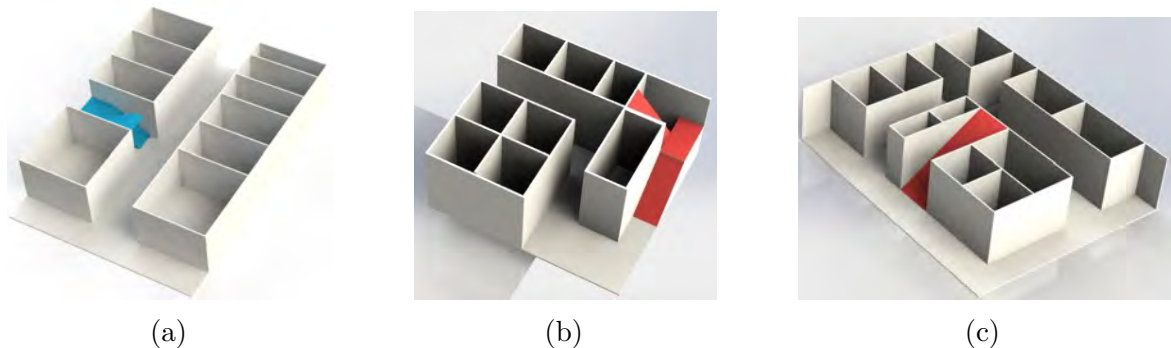
Fig. 2.1 3D models of Gulshan-1 DCC market sections from the available CAD drawing of the floor plan. Figure 2.1a was selected for investigation.

| (a) | (b) | (c) |
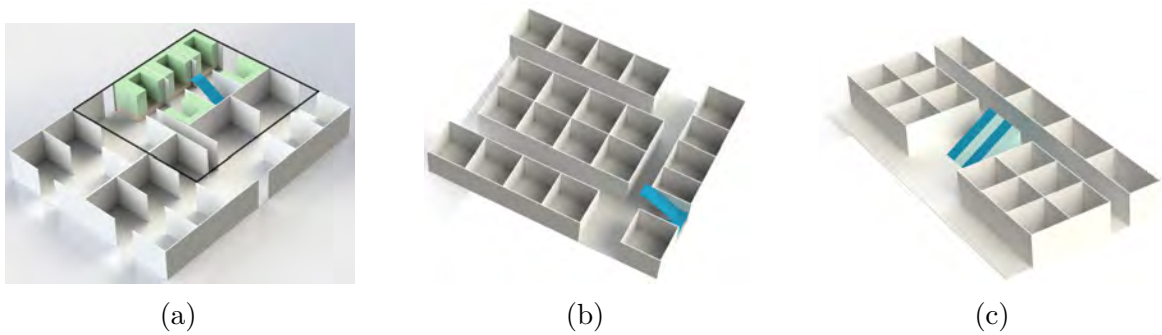
Fig. 2.2 3D models of (a) Co-Operative Market, (b) Muktijoddha market, and (c) Mukto Bangla market of Mirpur-1. Models were designed from data collected during survey. Co-Operative Market in figure 2.2a was selected among these shopping malls and black border shows the chosen computational geometry.

| (a) | (b) | (c) |
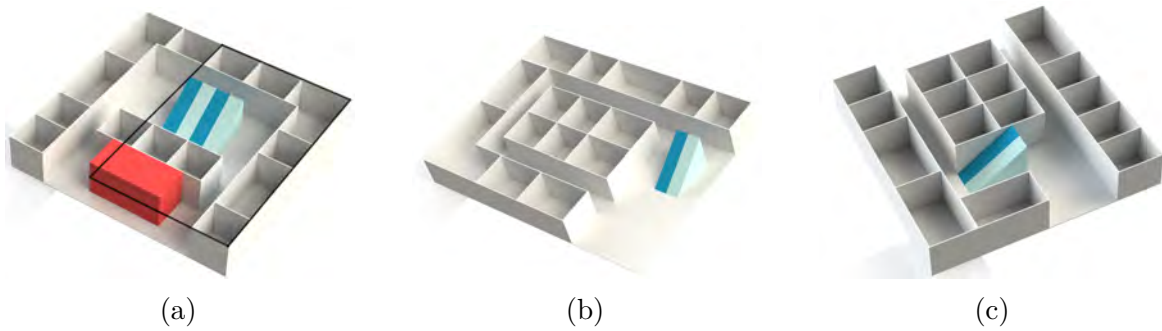
Fig. 2.3 3D models of (a) MultiPlan shopping complex of New Elephant Road, (b) Rapa Plaza, and (c) Genetic Plaza of Dhanmondi-27. Models were designed from data collected during survey. MultiPlan shopping complex figure **??** was selected from these shopping malls and black border shows the chosen computational geometry.

staircase and at least two rows of shops around the staircase. The selected segment of DCC market had 257.71 m^2 floor area, and eleven shops in two rows along a long corridor, the unique architectural design of DCC market, and a staircase in one row. For the Co-Operative market model, a 246.31 m^2 floor area was chosen. The unique feature of Co-Operative market was cluster of shops in blocks and narrow corridors around the blocks. The selected segment had eleven shops around three narrow corridors and a staircase. The selected segment of MultiPlan shopping complex had 315.36 m^2 floor area, nine shops around a large open space where the escalator was present, an atrium like structure, different from other selected segments. The selected segments then designed in PyroSim with actual fuel distribution seen during the survey to investigate the fire and smoke propagation along the computation geometry with and without air curtain discharged. Before proceeding with the current study, previous experimental

room.

The mounting was as follows. First the wall panels were mounted. On top of these wall panels the roof panel was mounted. Specific corner profiles and/or sealants were used depending on the practice used by the supplier of the product. The ends of the panels close to the door wall were sealed with ceramic or mineral wool to avoid ignition of exposed core material.

Fig. 2.4 An ISO-9705 compatible room with all dimensions, and positions of devices and burner (Diagschematiceally, wilgarsstor roomVoorlted te (2060)u) according to ISO 9705.

works on related field done by researchers were validated first, and presented in next section.

2.3 Validation and Mesh Independence

2.3.1 Clothing Fuel HRR

Zalok and Hadjisophocleous (2007) tested a typical clothing store fuel package in an ISO-9705 compatible room. The dimensions of the room and positions of the burner and gas analyzer devices can be seen in figure 2.4. An 1 m × 1 m fuel package, with wood, cloth, plastic hangers and bags, typical combustibles that should be present to display the cloths to the customers was burned inside the room with propane T-burner. Figure 2.5 shows the test setup before and during the fire. They reported that fuel package with 86% cloths, and 12% wood and 2% plastic, had a peak heat release rate of 1538 kW and followed a medium t^2 fire. The present study took the peak heat release rate (HRR) and the ramp up time according to the cloth test, named C, from the study of Zalok and Hadjisophocleous (2007), for designing the clothing fuel in

Figure 8. Photographs show the test progress, Test B.

Fig. 2.5.Photographs showing the test progress of Zalok and Hadjisophocleous (2007)
for clothing test. Figure 9. Photographs show the test progress, Test C.

temperatures were measured at the middle of the room, at the ceiling, at the west wall sur
sampling point inside the duct, see Fig 13. For Test S, the maximum temperatures r
29, 708, 344, and 65 C respectively. For Test W, the maximum temperatures measu
70, 383, and 75 C respectively and for Test C, the maximum temperatures measured w
73, and 193°C respectively

PyroSim. The HRR value had the wooden frame and plastic hanger intrinsically, thus
eliminate the requirement of designing wooden frames for the cloths as seen in reality,
in PyroSim and hence reduced complexity of the simulation process.

2.3.2 Mesh Independence

be seen that clothing stores that have wood as the main combustible (Test W) had al
The mesh independence study was performed by reproducing the ISO-9705 compatible
as temperatures at various points inside the room as in small clothing stores (Test S),
room with various points from the study of Zalok and Hadjisophocleous (2007) are
urned in a similar fashion. However, it can be seen when comparing clothing stores t
mesh in commercial CFD software. In general, the computational domain is
s the major combustible (Test C) with the first two tests (Test S and Test W) that Te
divided into small parts, called mesh. In general, finer mesh (Three better 1.5 may
erably higher temperature at the middle of the room and at the sampling point inside the
but require more resources in terms of computation in CFD. And in LES simulation,
small mesh size will compute smaller eddies instead of modelling, thus, in LES also be
three tests (Test S, W, and C), the maximum heat flux meter recorded value was 3.74,
closer to DNS. and hence the temperature at the A the truly resolvable right beside
(kW/m^2) respectively, and the temperature at the thermocouple right beside the heat fl
air impossible to achieve in LES. Zhiyin (2015), a trade-off had to be made. According
, 48, and 142°C respectively, see Fig 14.
to SFPE (Society of Fire Protection Engineers, Bethesda, Maryland) handbook chapter
on modelling enclosure fire in Computational Fluid Dynamics (CFD), Cox and Kumar
(2002), the source Froude number Q^*, is defined as,

www.see.ed.a

$$Q^* = \frac{\dot{Q}}{\rho_\infty c_\infty T_\infty D^{*2}\sqrt{gD^*}} \tag{2.43}$$

40

Table 2.1 Summary of the mesh sensitivity analysis

Mesh	D^*/dx	Cell Size (cm)	Elements	Time[1]
Coarser	2.5	40	288	0.0044
Coarse	4	28.4	768	0.044
Moderate	10	11.36	18432	1
Fine	16	7.1	64800	4
Finer	25	4.5	218700	34.67

[1] Dimensionless computation time McDermott et al. (2010)

Taking the value of source Froude number of equation 2.43 as 1, for critical flow, where the surface wave speed and flow velocity are same, the characteristic fire diameter D^* is defined as,

$$D^* = \left(\frac{\dot{Q}}{\rho_\infty c_\infty T_\infty \sqrt{g}}\right)^{\frac{2}{5}} \tag{2.44}$$

Here, $\dot{Q}$ is the total heat release rate of the fire, ρ_∞, c_∞, T_∞ are the ambient density, specific heat, and temperature. As suggested in the FDS user guide (sixth edition) by NIST, McGrattan et al. (2013), a non-dimensional expression D^*/dx could be used to find the mesh resolved case. Study suggested, $D^*/dx = 10$ would be sufficient for a mesh resolved case McDermott et al. (2010). The present study thus, considered five values of $D^*/dx = 2.5$, 4, 10, 16 and 25, to design the works of Zalok and Hadjisophocleous (2007) in PyroSim, for mesh independence analysis. The mesh name, cell size, number of elements and computation time of each case was provided in Table 2.1. To observe the improvement in results by cost of resources, a dimensionless computation time was introduced, by dividing the computation time required for each case by the computation time required for the recommended case of $D^*/dx = 10$, (named moderate in this study). Increasing the D^*/dx value beyond 16 drastically increase the resource requirement.

The heat release rate in function of simulation time for different mesh size are presented in figure 2.6. The simulation data were scattered around the experimental curve for first three mesh size, named coarser, coarse and moderate. For next two mesh size fine and finer the data were more precise and closely followed the experimental curve. Figure 2.7 shows the temperature profile at middle of the room for different mesh size and experimental data. Here the simulation data was offset from experimental data. This might be due to the unavailability of exact dimensions and geometric position of the fuel package. Here, the FDS user guide suggested moderate mesh closely

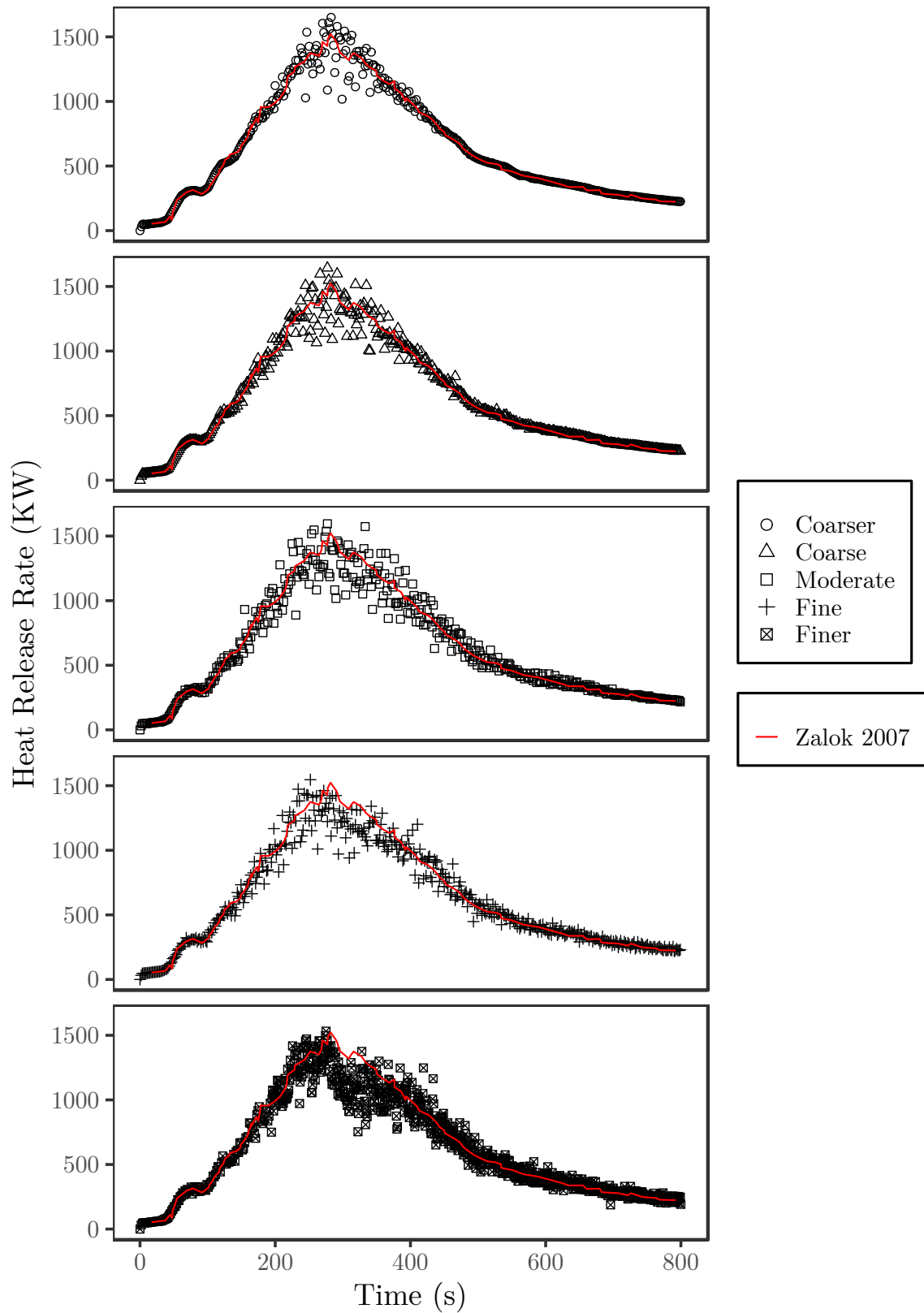Fig. 2.6 Validation of Heat Release Rate (HRR) in PyroSim with Zalok and Hadjisophocleous (2007) and mesh sensitivity analysis.
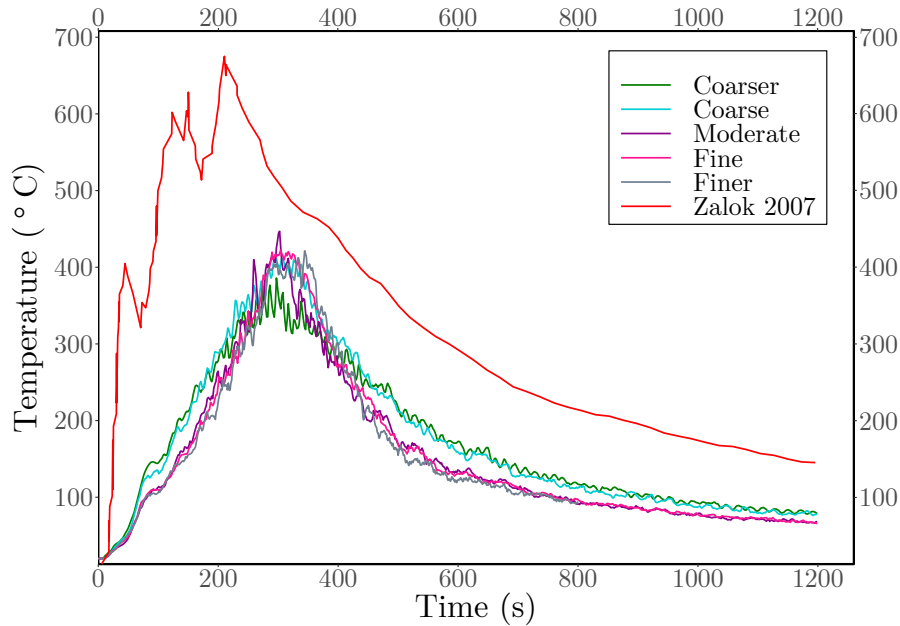
Fig. 2.7 Validation of temperature profile in PyroSim with Zalok and Hadjisophocleous (2007) with mesh sensitivity analysis.

follow the fine and finer mesh curve, while coarser and coarse mesh follow another line together, indicate that the moderate mesh indeed produce good results. Figure 2.8 shows the carbon monoxide concentration at the exhaust duct for the experimental setup and at door for simulation case for different mesh size. Again, the moderate mesh produces nearly equivalent fit of fine and finer mesh, while the coarser and coarse mesh had scattered data. Analyzing the results of mesh sensitivity analysis, conclusion could be drawn as, moderate mesh, suggested sufficient by FDS user guide McGrattan et al. (2013), indeed produce good fit with the experimental data. Lowering the D^*/dx value below 4 might not yield appropriate results. And, increasing the D^*/dx to 16, as in fine mesh case, produced better approximation of experimental data. Further increase in D^*/dx value to 25, finer mesh case for this study did not produce much improvement over fine mesh at nine times the computation cost of fine mesh. Thus, the present study was conducted in $D^*/dx = 15$ slightly lower than fine mesh value due to air curtain jet width constrain, for the fire source shop throughout the total range of simulations performed.
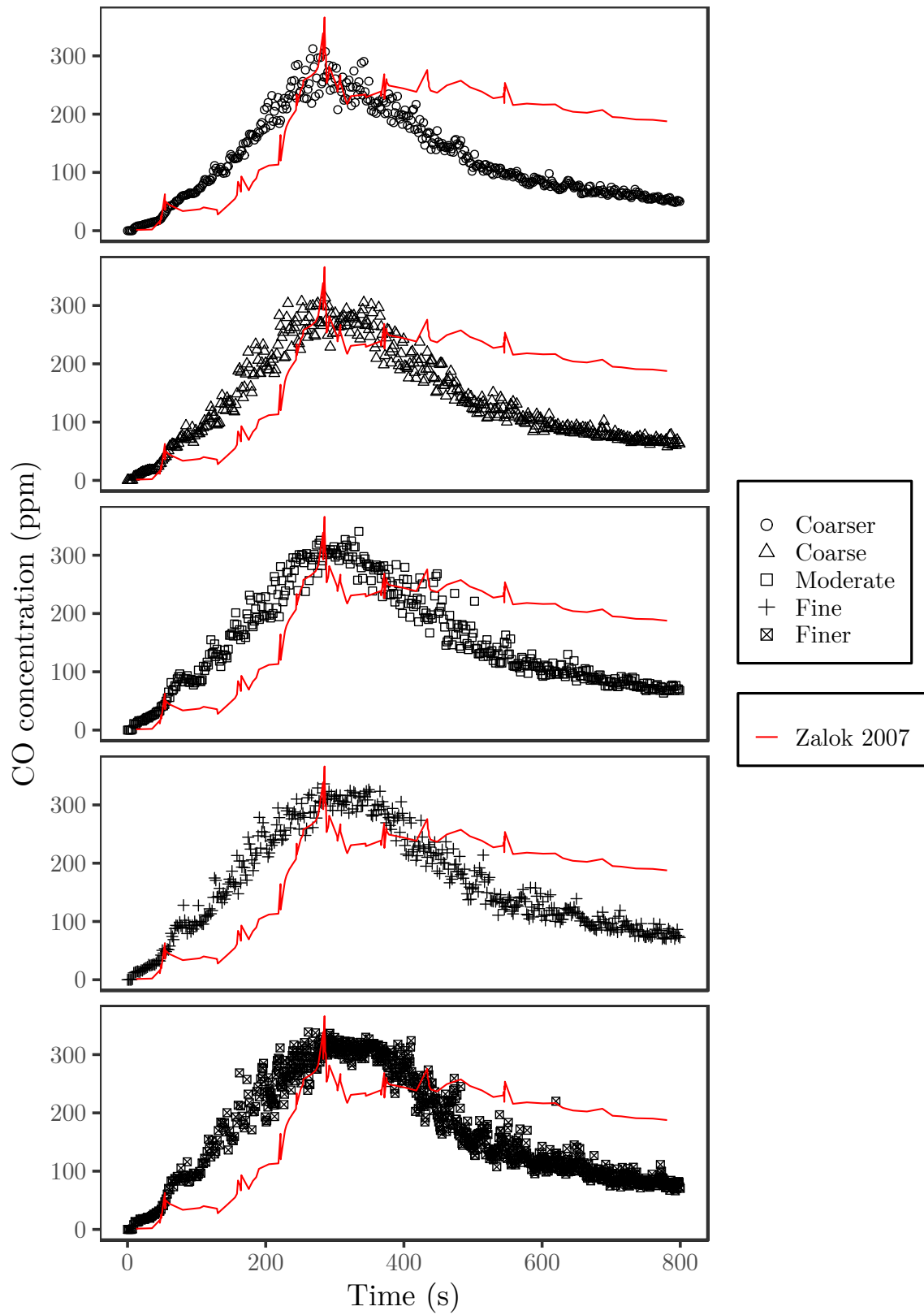
Fig. 2.8 Validation of carbon monoxide concentration in PyroSim with Zalok and Hadjisophocleous (2007) with mesh sensitivity analysis.

2.3.3 Simulation of Air curtains in FDS

The introduction of the air curtains in the FDS model was validated with experimental work of Hu et al. (2008). They conducted experiments on a bench scale model of 3.6 m length and 0.6 m width and 0.66 m height, with an opening of 0.2 m width and 0.42 m height at one end and the fire section was closed on the other end. A circular pool diesel fire was investigated with an air curtain discharged at different velocities mounted at top of the test section 2.4 m from the fire section end. The model was reproduced in PyroSim as shown in figure 2.9 with the actual configuration shown in inset. The reported smoke temperature 0.12 m below the ceiling before and after 0.6 m of the air curtain position, named 'A' and 'D' respectively in the study.

Figure 2.10 represents the comparison of thermocouple temperatures at 'A' before, and at 'D' after the air curtain, discharged at 3 m/s, for FDS simulation and experimental works of Hu et al. (2008). The trends of simulation results agree well with the experimental work, but the numerical values were somewhat offset, and the simulated thermocouple at position 'D' did not show any change in reading throughout the entire simulation. This may be caused by some assumptions that had to made, to conduct the simulation, due to lack of geometric information in the experimental report, for
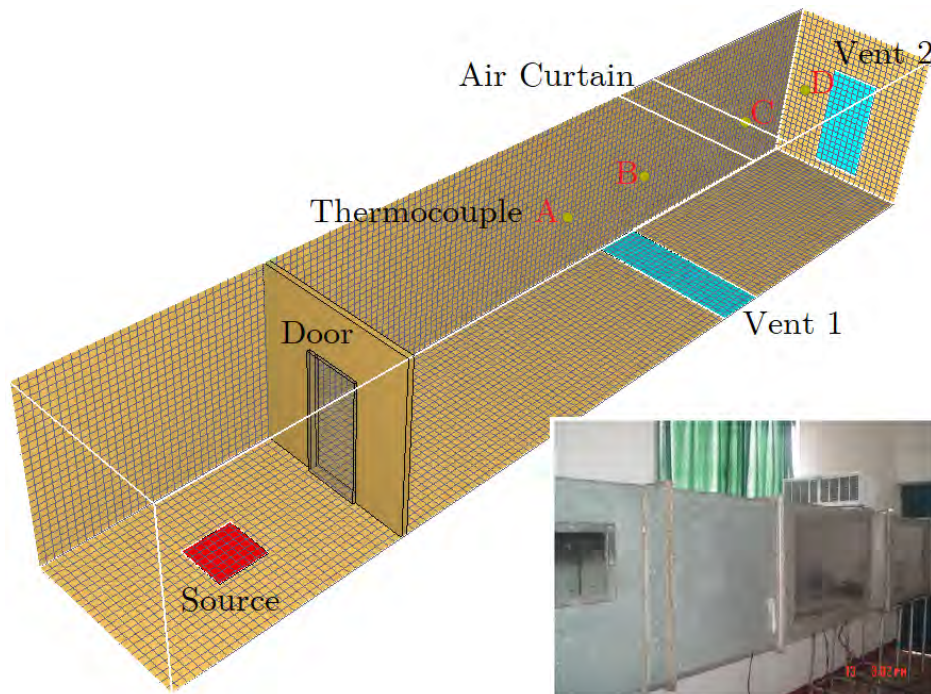

Fig. 2.9 PyroSim model of Hu et al. (2008) designed for validation purpose. Actual setup is shown in inset.
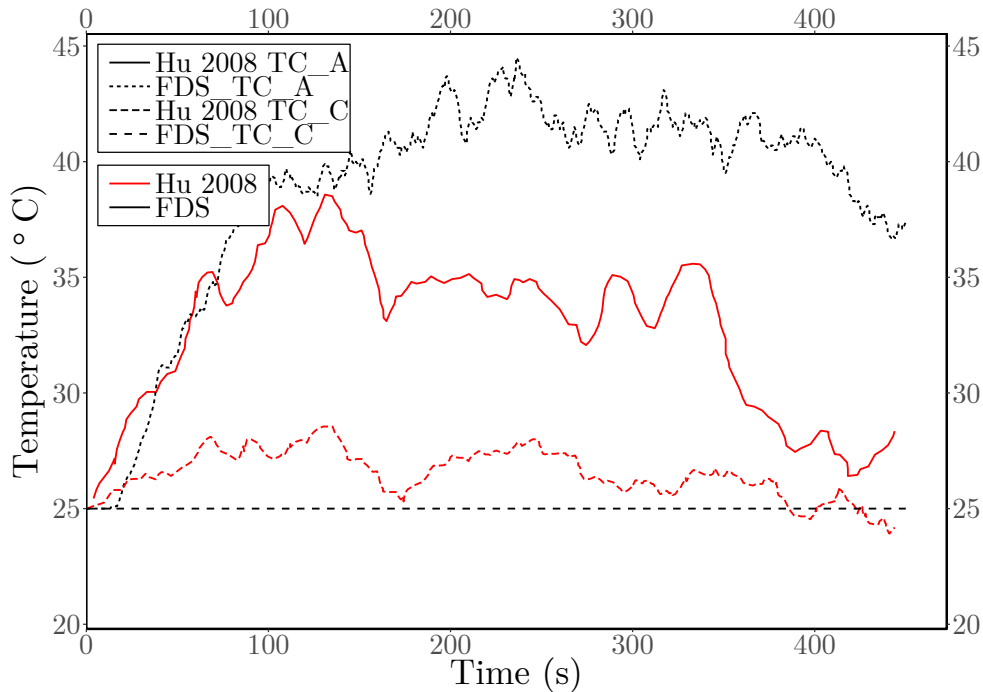
Fig. 2.10 Validation of Hu et al. (2008) for air curtain velocity of 3 m/s.

example, the actual jet width of the air curtain. Another likely cause of the simulated thermocouple no to be responsive to smoke could be the non-circulating air in FDS, while as in experimental setup it should not be the case. Thus, the inlet air curtain air after some experimental time, may vary slightly due to the mixture with hot smoke on other side and exhausted to atmosphere. As seen in figure 2.10 the experimental reading of thermocouple at position 'D' was also vary slightly and the variation was within 2°C.

2.4 Numerical Model

Figure 2.11 represents the designed PyroSim models of DCC market of Gulshan-1, Co-Operative market of Mirpur-1, and MultiPlan shopping complex of New Elephant Road from left to right respectively, with actual fuel distribution seen during the survey. The computation area for DCC market was 257.71 m^2, for Co-Operative market was 246.31 m^2, and for MultiPlan shopping complex 315.36 m^2. The computational geometries include a staircase, and two sources, one near the staircase and one at as furthest possible within the geometry, from staircase. The source shop and shops adjacent to source were designed with fuel loads, which will assist the fire spreading

(a) Shopping Mall-1   (b) Shopping Mall-2   (c) Shopping Mall-3

Fig. 2.11 Designed PyroSim models with clothing as fuel of (a) Shopping Mall-1 (DCC market of Gulshan-1), (b) Shopping Mall-2 (Co-Operative ma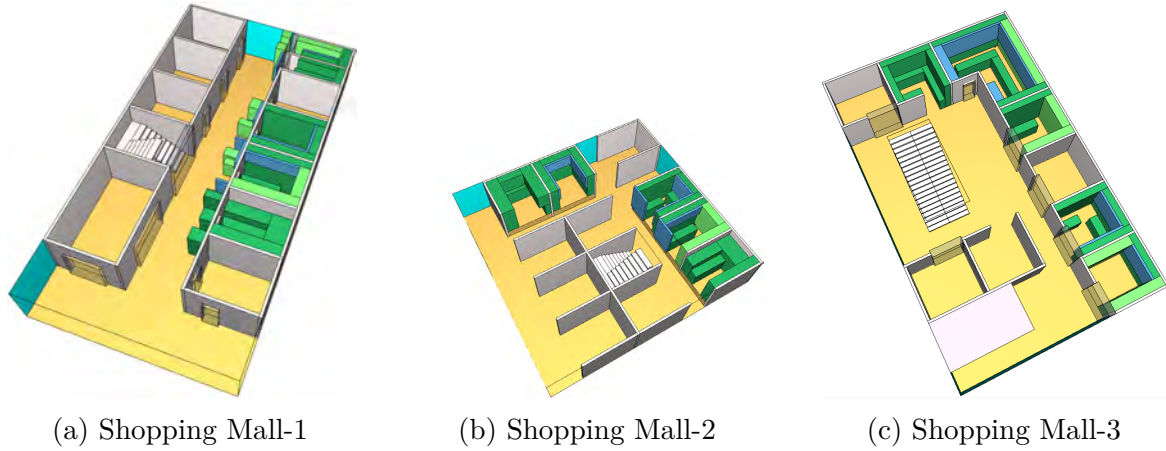rket of Mirpur-1), and (c) Shopping Mall-3 (MultiPlan shopping complex of New Elephant Road). The models were designed with actual fuel distribution seen during the survey.

when happened, while other shops were left empty to reduce the computation load. The source for each simulation was designed with $7.62 \times 7.62 \times 7.62$ cm^3 mesh size, having D^*/dx value of 15, almost identical to the 'Fine' mesh described earlier. A design constrain on the jet width of the air curtain and minimum mesh size with the computational power available prevent lowering the mesh size further. Outside the source a mesh size of $15.24 \times 15.24 \times 15.24$ cm^3 was used having D^*/dx value of 7.5. The outside source mesh size was constrained by mesh alignment condition of FDS. Thermocouple and carbon monoxide measuring devices were placed inside the source, and adjacent shops, also along the hallway, for observing the temperature profile and CO concentration as the fire propagates. Visual representation of flame and smoke propagation during the simulation process could be obtained from FDS-Smokeview, a program to visualize the FDS output, while the network of thermocouple device placed in computational geometry quantifies the fire propagation. Although the smoke dispersion, like fire propagation, could be quantified by several gas devices available in FDS, CO devices were preferred due to the lethal effect of CO gas on evacuees, as the concentrated focus of this study is on evacuation purpose.

The details of DCC market source shop 1 with clothing as fuel is shown in figure 2.12. The fuel distribution, mesh size variation and positions of thermocouple (A, B, C and D), CO devices (A1, B1, C1, and D1), and igniter are visible in this figure. The temperature and CO devices were placed at 2.9 m, 1.524 m and 0.762 m from the floor at each position. The igniter was placed at the furthest corner from the investigated shop door to mimic an event of short circuit. The air curtain was installed at the
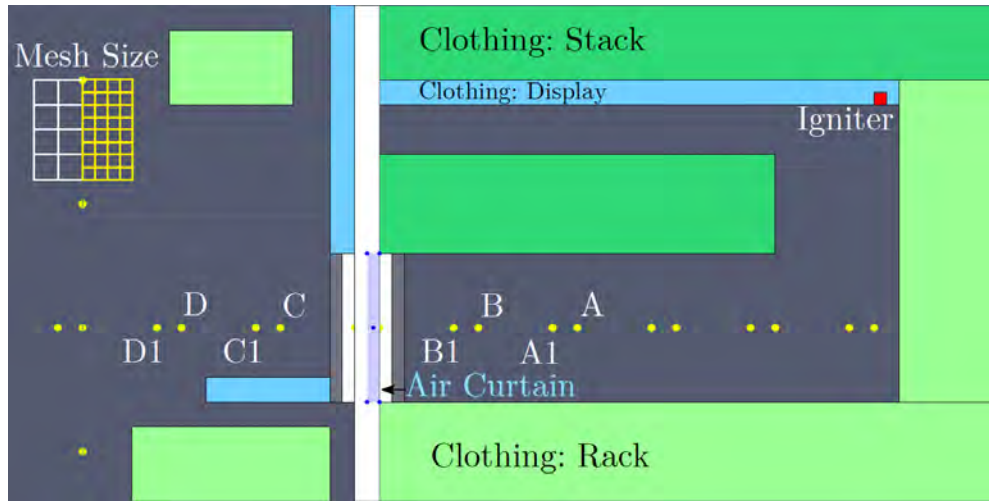
Fig. 2.12 DCC market source shop 1 as designed in PyroSim.

Table 2.2 Mesh division for all geometric models

Geometry	Source	Mesh size (m²)	Cell Size (m³)		D^*/dx		Mesh Elements
			Source	Exterior	Source	Exterior	
DCC	S1 S2	257.71	0.0762^3	0.1524^3	15	7.5	328,320 285,760
Co-Operative	S1 S2	246.31	0.0762^3	0.1524^3	15	7.5	362,040 419,300
MultiPlan	S1 S2	315.36	0.0762^3	0.1524^3	15	7.5	523,560 409,320

door, as a vent of 7.62 cm (jet width) × 91.4 cm (jet length) at a height of 2.134 m. The details of the clothing fuel and furniture fuel design are described in subsequent section.

The mesh elements for DCC market source 1 (S1) configuration were 328,320, and for source 2 (S2) were 285,760. For Co-Operative market source 1 configuration and source 2 configuration the mesh elements were 362,040 and 419,300 respectively. In MultiPlan shopping complex geometry, the mesh elements were 523,560 and 409,320 for source 1 and source 2 respectively. The details of the mesh divisions are shown in table 2.2. The simulations were executed in a Intel Core i-7 9700K, 8 core, 8 thread, 4.90 Ghz processor with 16 GB 3200 MHz DDR4 ram. The computational geometry was divided into 6 to 8 divisions to utilize the parallel processing option in FDS.

2.4.1 Arrangements of Clothing Fuel in Shops

The typical fuel distribution of shopping malls in context of Bangladesh consists of three types of cloth displaying styles as perceived from the survey conducted. Figure 2.13a and figure 2.13b shows cloths stored in shops vertically in a compact manner by folding and storing on top of another.

(a)

(b)

(c)

Fig. 2.13 (a) & (b) Photographed fuel arrangements in shopping malls defined as 'Stack', (c) Fuel arrangements designed as 'Stack' in Pyrosim, the obstructions of dark green color always represent 'Stack' type fuel arrangements in PyroSim model.

(a)

(b)

(c)
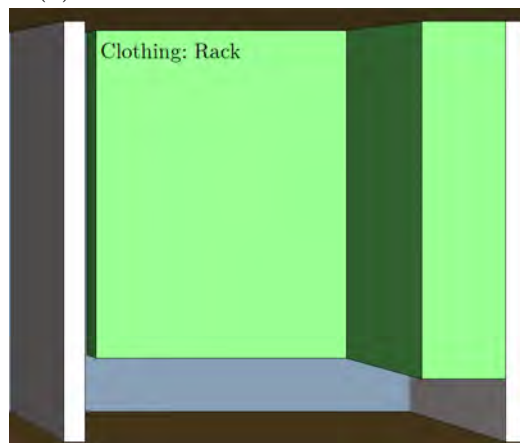
Fig. 2.14 (a) & (b) Photographed fuel arrangements in shopping malls defined as 'Rack', (c) Fuel arrangements designed as 'Rack' in Pyrosim, the obstructions of lime green color always represent 'Rack' type fuel arrangements in PyroSim model.

This pattern of storing is quite normal for common range of products where customers are looking for variations in similar products and shop owners thus had to display them in bulk quantity. In present study this type of clothing storing and display arrangements referred as 'Stack' of clothing. The bulk density of 'Stack' was calculated manually to 387.56 kg/m^3, multiplying an average number of cloths in a typical stack with density of cotton clothing from Bei et al. (2012). Figure 2.13c shows the FDS representation of the stack type clothing, the dark green color was assigned to the stack type cloth storing arrangements and obstructions of dark green color represent stack

(a)

(b)

(c)

Fig. 2.15 (a) & (b) Photographed fuel arrangements in shopping malls defined as 'Display', (c) Fuel arrangements designed as 'Display' in Pyrosim, the obstructions of light blue color always represent 'Display' type fuel arrangements in PyroSim model.
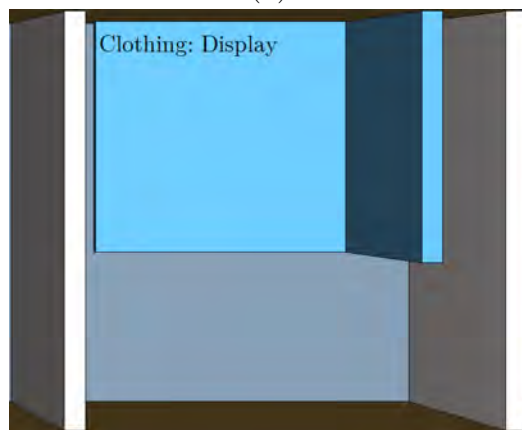
<center>(a)</center>

<center>(b)</center>

Fig. 2.16 (a) Photographed furniture fuel arrangement in DCC market. (b) Five types of furniture designed in Pyrosim and arranged according to real arrangement. Different types of furniture were assigned different color and labeled here. The color always represents the same furniture type throughout the study.

type cloths throughout the study. Another common storing type was putting cloths in hanger and display in a rack as shown in figure 2.14a and figure 2.14b. In FDS this type of stored cloths were designed as obstructions of lime green colors having bulk density of 77.52 kg/m³, and named 'Rack' as seen from figure 2.14c. Lastly there were some expensive and unique designed cloths which were the prime attraction of a shop, displayed in single layer to give maximum exposure as shown in figure 2.15a and 2.15b. These were designed as light blue obstructions of 19.38 kg/m³ bulk density and named 'Display' type of cloth arrangements as seen in figure 2.15c. The self-ignition temperature of cotton cloths was taken as 253ºC slightly lower than the upper limit of cotton linter from Gross and Robertson (1958).

2.4.2   Distribution of Furniture Fuel

For furniture fuel, five different furniture were designed and arranged in computational geometry as seen during the survey, a typical furniture shop of DCC market is shown in figure 2.16a. The furniture of DCC market were typically made of Canadian Red Oak board, thus the density of Red Oak was taken as 660 kg/m³, and heat release rate of Red Oak was taken as 150.0 kW/m² from Tran and White (1992). As in FDS, the furnitures had to designed as rectangular obstructions, additional calculations were done with carpenters to know the amount of wood needed for a specific furniture. Then, the weight of the wood needed was divided by the volume of the furniture and used

<center>52</center>

as input bulk density for that specific furniture. Un-assembled bed, dining table, sofa set, wardrobe and almirah were designed in PyroSim and arranged as actual storing pattern seen during the survey, as shown in figure 2.16b. Additional data were taken from SFPE Handbook Hurley et al. (2015).

2.4.3   Variation of Clothing Fuel Distribution

Three different clothing fuel arrangements were employed in FDS to compare the effect of the extremely compact stacking of fuels typically seen in shopping malls of Bangladesh to ideal case. The actual distribution had high fuel load to area ratio where an ideal grid distribution had moderate fuel distribution with enough space for customers to roam about. The fuel load was further reduced by designing the grid distribution fuel arrangements with 'Display' clothing loads only. Figure 2.17 shows clothing fuel arrangement in DCC market for source shop 1 in 'Actual' distribution, 'Grid' type distribution and 'Display' distribution from left to right respectively. The fuel load to area ratio for 'Actual' distribution was 353.4 kg/m^2, the 'Grid' distribution had 19% fuel load of 'Actual' distribution and designed at 65.7 kg/m^2, and 'Display' distribution had only 4% fuel load of 'Actual' distribution as designed at 16.4 kg/m^2.
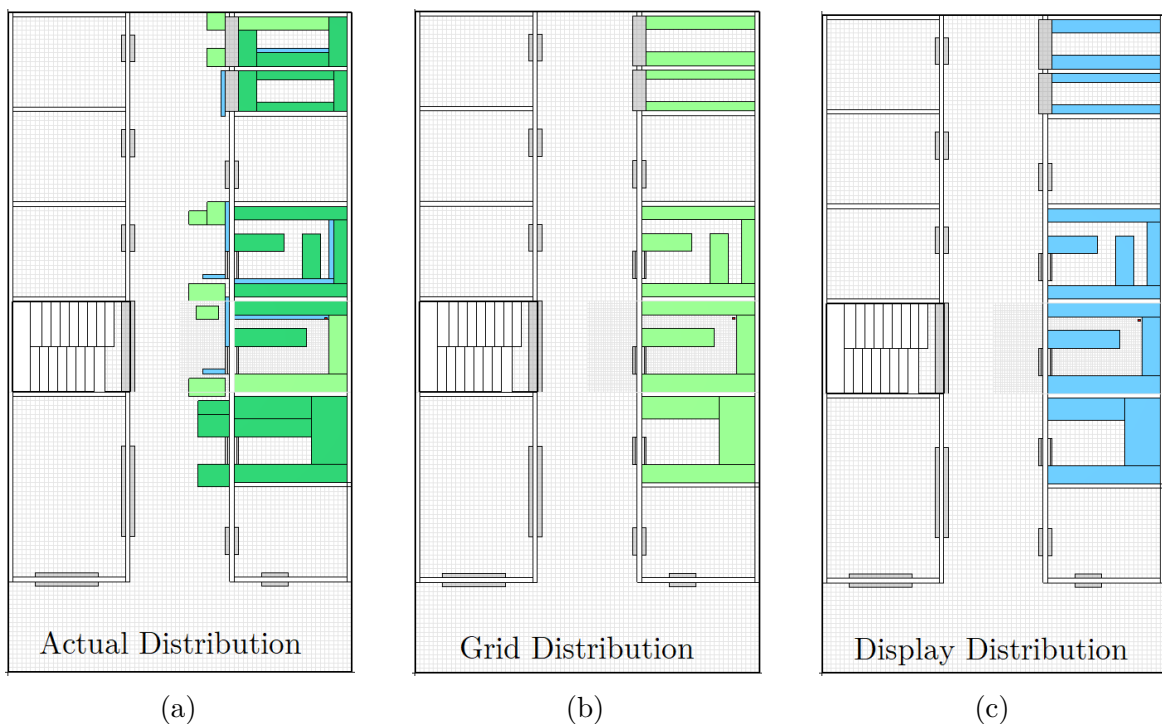

Fig. 2.17 Clothing fuel arrangement in DCC market for (a) 'Actual' distribution (b) 'Grid' type distribution (c) 'Display' distribution.

2.4.4 Air curtain parameters

An air curtain of 7.62 cm (jet width) × 91.4 cm (jet length) was placed at the investigated shop door at 2.13 m height from the floor. The air curtain's injection velocity was varied from 3 m/s to 10 m/s with 1 m/s step size. The injection angle was varied from 0º to 60º with 15º step size. The ratio of the distance between two jets with the jet width, defined as the pitch ratio, for a twin jet air curtain (a commercially available feature), was varied from 0 to 4. The flow rate of the air curtain was varied from 1250 m³/h to 5000 m³/h. The schematic representation of the investigated air curtain parameters are shown in Figure 2.18. Also, two critical position for evacuation were protected varying air curtain installment site in three combinations.

In the present study, three different shopping mall geometry, two sources of fire (two different store locations) for each shopping mall design, and two types of fuel (clothing and furniture) were considered. For each of the above cases, the fire and smoke spread scenario with (air curtains in two different locations) and without air curtains were analyzed. A total of 68 different configurations were studied to determine the optimum location and operating parameters of the air curtain to aid the evacuation process in case of a fire incident compared to the no-air-curtain condition.
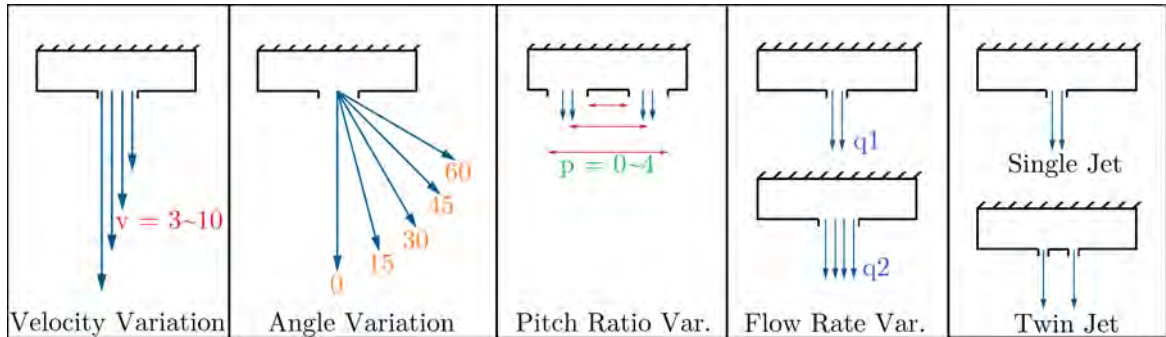

Fig. 2.18 Schematics of air curtain's parametric variations.

Chapter 3

Results and Discussion

This study investigates the effectiveness of air curtain in confining fire induced smoke and flame propagation for a typical shopping mall fire in context of Bangladesh. Design of three popular shopping malls from different parts of Dhaka city were investigated in case of typical fire related hazard with or without air curtain placed at specific positions and parametric variations. The shopping malls were chosen as such so that they had architectural differences. DCC market of Gulshan-1, Co-operative market of Mirpur-1, and MultiPlan shopping complex of Elephant road seemed excellent candidate matching those above mentioned criteria, during a survey conducted by the author in various shopping malls of Dhaka city. DCC market has shops on both sides of some long corridors, Co-operative market has shops in stacks of blocks and narrow corridor around them, and MultiPlan shopping complex has two large open space in middle and the shops are residing around the open spaces. Small units from the respective shopping malls which includes the specific architectural characteristics of the mall with an adjacent staircase, were chosen as the computational geometries. The dimensions of the computational geometries were matched with the actual malls by using CAD drawings, on site measurement and extraction from photographs taken at site with permission. The arrangement of the fuel load in those shops were photographed on site with permission during the survey, and imitated in Fire Dynamics Simulator (FDS) code.

Two types of fuel loads, clothing and furniture, were investigated in this study for their impact during a typical fire incident. The results of the shopping mall survey suggested, a typical clothing store had three types of product orientation for showcasing to customers, exclusive products in full length side by side display, products in racks for customers to browse with, and stocked products in compact stacks with just enough exposure for identification. In numerical simulations they were represented accordingly

with density variations, measured from actual products in those arrangements. To distinguish different clothing arrangements in simulations, arrangements were named and different colors were assigned. Rows of exclusive products named *'Display'* and sky-blue color was used, browsing racks were named *'Racks'* and lime green color was used, lastly, stacked stoked products named *'Stacks'* and forest green color was used to represent in PyroSim (FDS GUI). The furniture fuel distribution was imitated considering a block of furniture in uniform average density, which was obtained by comparing the volume of wood needed and the volume of that particular furniture. Assistance were taken during the measurement of wood for a given furniture from carpenters, and five types of furniture, which were present in almost all the shops surveyed were included during in PyroSim.

Simulations were carried out for two fire source shops in each shopping mall, one adjacent to the staircase and one farthest from the staircase in each case. This enabled to distinguish the architectural effect of the mall on propagation of fire and smoke to the staircase, an important location for evacuees during any fire hazard, if any. Inside the fire source shop the igniter was placed on furthest corner from the door, to allow the fire to build up inside, and in addition, this is a possible location of spark during a short-circuit. The effect of the placement of the air curtain was examined by locating air curtain at the storefront, at the staircase and at both the storefront and staircase. The fire source shopfront air-curtain was placed at the door, the staircase air curtains were also placed at door height. Each case was performed with and without discharging the air curtain to compare the effect of air curtain keeping all other parameters constant. The temperature rise, carbon monoxide concentration, smoke layer velocity, convected and radiated heat were measured at specific positions in FDS to numerically analyze the propagation of smoke and flame in case of a fire hazard and the effectiveness of air curtain to confine the propagation at source.

3.1 Case Studies of Different Fire and Smoke Propagation Scenarios

3.1.1 Shopping Mall-1: DCC Market from Gulshan-1, Dhaka

A section of 258 m^2 area of DCC Market from Gulshan-1 was designed in PyroSim to scale. The dimensions were taken from actual CAD floor plan of DCC Market. The shop interiors were photographed during the survey and designed in PyroSim accordingly. The ground floor of the Gulshan-1 DCC market hosts mainly furniture
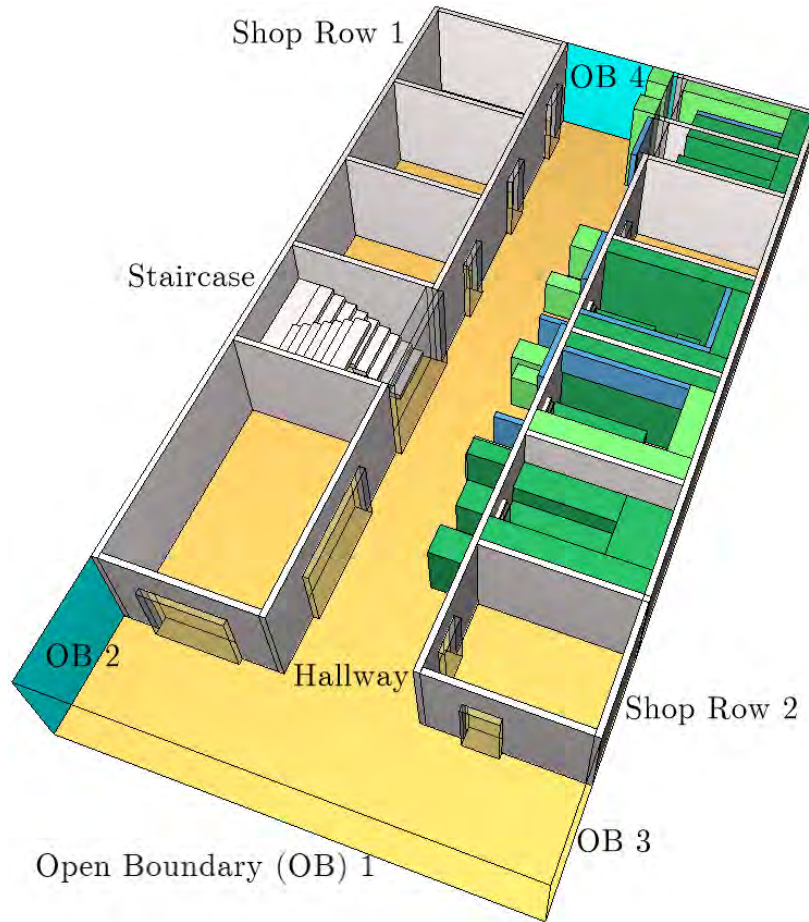
Fig. 3.1 The 3D computational model of DCC Market in PyroSim. The shops are designed with clothing as fuel.

shops, whereas the first floor has clothing, accessories, toys and departmental stores in clusters. As this shopping mall hosts variety of fuel types at any time in case of a fire hazard, it was only logical to study the computational geometry, for multiple fuel scenarios, and this present study concerns with furniture and clothing fire scenarios for the Gulshan-1 DCC market model.

3.1.1.1   Fire and smoke propagation for clothing store fire

The computational geometry was first analyzed for clothing as the fuel load. Figure 3.1 shows the FDS computational model of Gulshan-1 DCC Market in PyroSim. The computational geometry has 11 shops along both side of a long corridor and a staircase, a typical section of the actual DCC market. The floor and ceiling were designed as inert surfaces, ends of the corridors and staircase top were designed as open boundary. Two shops, one in front of the stair case and one at far side of the corridor, were selected as

(a)   (b)

Fig. 3.2 Photographed clothing stores in DCC market during the survey.

the fire source shop in respective simulations. Source shops and shops adjacent to the source shops were designed with fuel loads, while rest of the shops left empty without any fuel load to reduce the complexity during computation. The fuel loads of these shops were taken from the photographs during the survey, two photographs of clothing stores surveyed are shown in figure 3.2

3.1.1.2   Clothing fire in Source Shop 1

Figure 3.3 shows the top view of the FDS model of DCC market for clothing fuel condition. The fire source shop 1 of DCC Market (DCC_S1), was highlighted in blue. The source shop 1 had a floor area of 11.91 m^2 and 4104 kg fuel loads in clothing, yielding a massive fuel load to area ratio of 353.4 kg/m^2. Fire load calculated using 13.2 MJ/kg for 'Textile' products reported by *Chapter 6 - Solid-fuel firing* (1982), was 54175 MJ/m^2, whereas only 661 MJ/m^2 was reported as the 95th percentile of fire load in clothing stores, by Zalok and Hadjisophocleous (2007) during their survey conducted in 2003, in the Canadian cities of Ottawa and Gatineau. This was a clear indication of compact stacking of high-density fuel loads discussed earlier. As, the source shop was immediately in front of the staircase, the path distance was only 4.28 m. Although this small path distance will aid initial evacuation from this source shop, but in case of prolong burning, the fire will soon propagate to the staircase, blocking the subsequent evacuation process completely. The table 3.1 shows the parameters of source shop 1.

The details of the positions of temperature and carbon monoxide measuring devices were shown in yellow circles. In shop and staircase, the devices were placed after 0.61 m
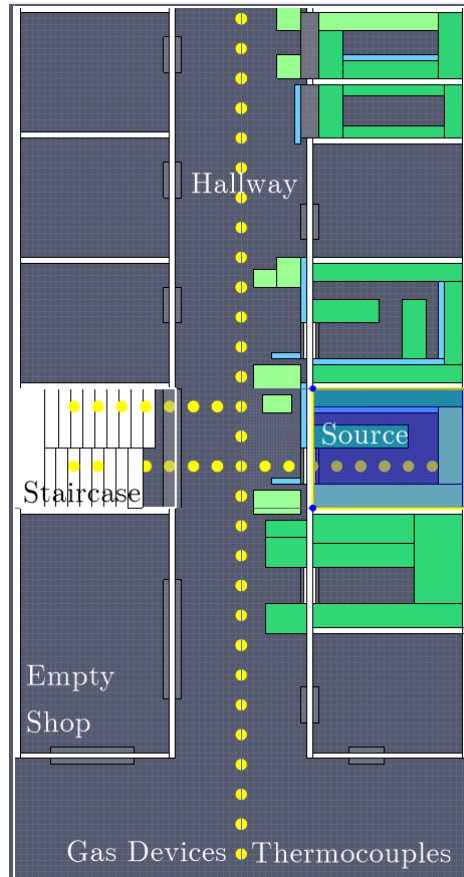
Fig. 3.3 Top view of the computational model of DCC Market in PyroSim for clothing fuel condition, with fire source shop 1 (DCC_S1) highlighted in blue. The position of thermocouple and CO measuring devices are shown in yellow circles.

each, and in corridor after 0.76 m each. For distinguishing purpose, the thermocouple and CO devices were placed 0.15 m apart of one another in same position. Figure 3.4 shows the top view of the fire source shop 1 of DCC Market, DCC_CS1. For DCC_CS1 case, simulation was conducted for 1200s (20 minutes) of simulation time, to observe the growth and propagation of fire inside the computational area. The designed position of igniter to initiate fire, position of air curtain at door, and exact locations of thermocouples (A, B, C, D) and CO devices (A1, B1, C1, D1) both inside the shop and on the corridor are highlighted and labeled respectively. The position of the thermocouple A is 1.37 m horizontally left and 1.83 m vertically downwards of the igniter as seen in the figure 3.4. The CO device A1 is 0.15 m left of thermocouple A, and all thermocouples (A, B, C, D) and CO devices (A1, B1, C1, D1) had 0.61 m distance in between each similar device.

Table 3.1 Parameters of DCC Market source shop 1.

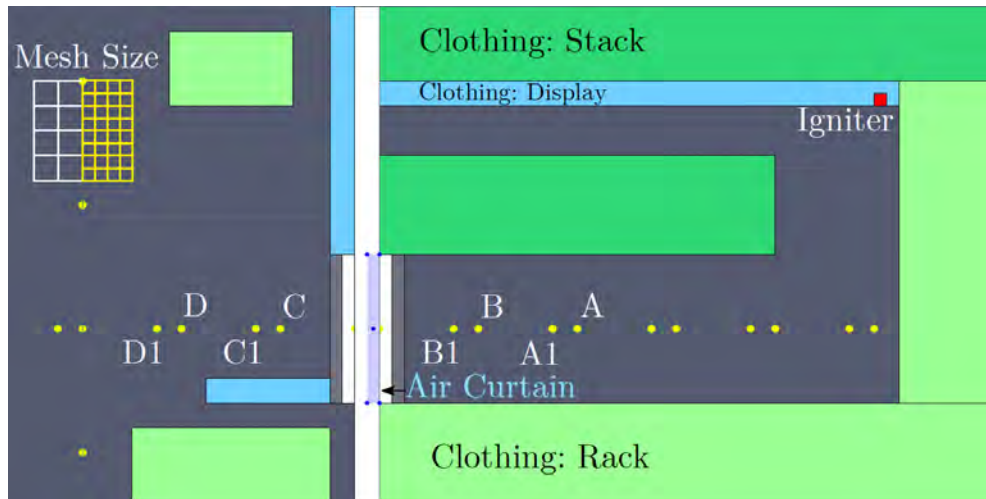| Name	Data
Simulation name	DCC_CS1
Fuel type	Clothing
Heat Release Rate per unit area	1528 kW/m^2
Shop area	11.61 m^2
Path distance to staircase	4.28 m
Fuel load	4104.15 kg
Fuel load to shop area ratio	353.41 kg/m^2
Fire load	54174.84 MJ/m^2
Simulation time	1200s
Total Heat Released	4457.53 Tera Joule
Total Heat Released per unit area	383.8 TJ/m^2 (up to 600s)

Fig. 3.4 Top view of the fire source shop 1 of DCC Market (DCC_S1), in PyroSim for clothing fuel condition. The respective positions of Igniter, Air curtain, Thermocouple (A, B, C, D) and CO devices (A1, B1, C1, D1) are highlighted.

Figure 3.5 and 3.6 present the flame and smoke propagation due to a clothing store fire at source shop 1 of Gulshan-1 DCC Market without air curtain discharged. This simulation was referred as DCC_CS1 through out this study. In figure 3.5 the top row represents the flame propagation only and bottom row represents both the flame and smoke propagation for 50s, 100s, 150s, 200s, 250s and 300s of simulation time respectively from left to right. In figure 3.12 the flame and smoke propagation was represented in a similar manner for 400s, 500s, 600s, 800s, 1000s and 1200s of simulation time. The ignition was stared by an igniter of 4.42×10^{-4} m^3 volume
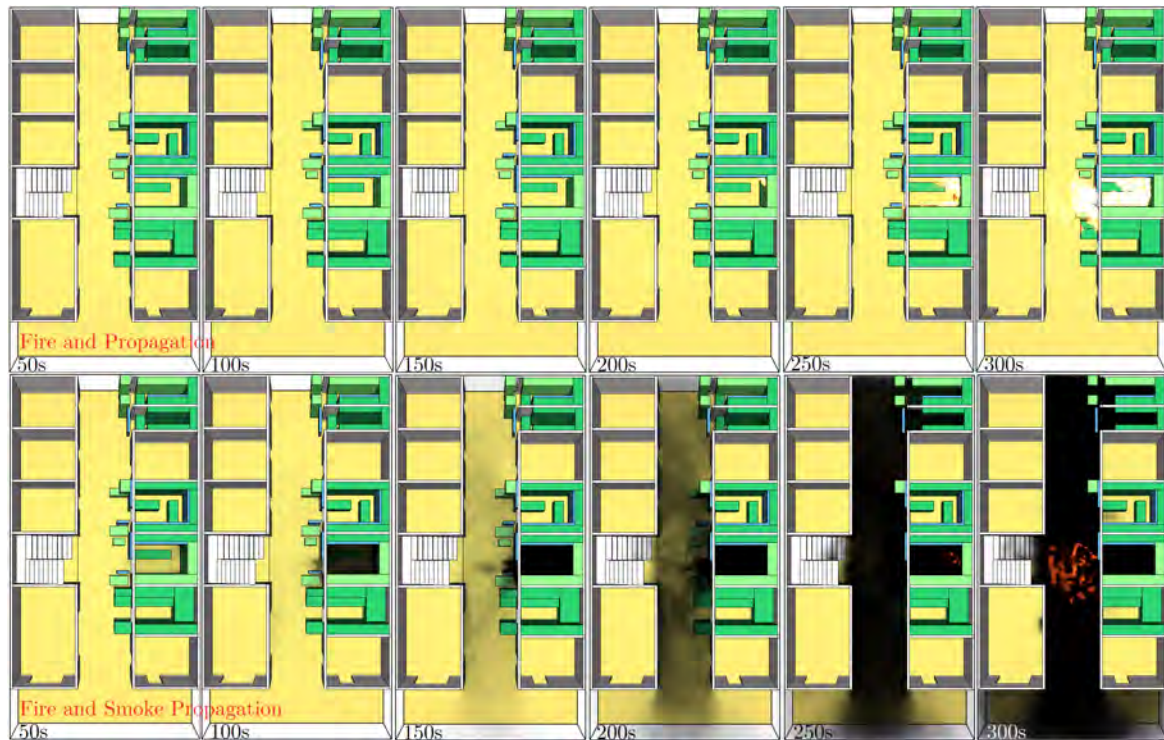
Fig. 3.5 Flame propagation through DCC market source shop 1, DCC_CS1, in case of clothing as fuel load. The top row shows the flame only, and bottom row shows both flame and smoke for 50s, 100s, 150s, 200s, 250s and 300s of simulation time respectively from left to right.

radiating at 1000°C. The total energy radiated by the igniter was tiny, only around 71 kJ for the 1200s simulation time, compared to the total energy of the fire, but was enough to ignite the stack of cloths nearby. Although the igniter was active from 1s of simulation time, visible smoke was spotted after 10s as the fuel need time to reach the flammable limit. Flame was seen from the point of ignition only after 45s, confirming the sustainability of the combustion process initiated by the igniter. Smoke started to build up rapidly inside the shop immediately after ignition, and escaped through the door opening at around 80s. Visibility inside the source shop was lost at 1.524 m, about the average human eye height, due to this smoke build up at around 120s. Flame front was also spreading and igniting new fuel stacks along the way, and finally at around 247s flame front came out of the source shop. At nearly 300s the whole corridor covered in smoke and visibility was hampered at places at eye height. Fire spread to the staircase at 330s, this means that evacuation will not be possible at this stage through this staircase. Fire came out of the source shop and spread on both sides of the corridor at 390s, this was due to the shortage of oxidizer inside the source

Table 3.2 Flame and smoke propagation timeline for DCC market for clothing fuel condition in source shop 1.

Time (s)	Event
45	Visible flame after ignition.
80	Smoke came out of the source shop.
120	Smoke filled up to 1.524 m from the ceiling, inside the source shop.
247	Flame front came out of the shop.
300	Smoke filled up the ceiling of the whole corridor.
330	Fire spread to staircase inside.
390	Fire came out of the source and spread along the corridor.
410	Visibility lost at 1.524 m in total computational area.
430	Fire violently burning in source shop front.
460	Fire fully engulfed the corridor.
560	Fire spread to all adjacent shop insides.
700	Fuel loads disappearing after completely burnt away.
850	Fire completely covered the corridor from floor to ceiling.
1200	Fire sustains as enough fuel load still remains.

shop and availability of unburnt fuel on the smoke propagated to the corridor. The movement of fire along the corridor was further enhanced by the presence of shop front fuel loads, stored by the shopkeepers, residing on the corridor. At around 410s due to this new availability of shop front fuel loads on the corridor, strength of the flame increased and the accumulated smoke covered the whole corridor up to 1.524 m, the average human eye height. Fire started to burn violently in front of the source shop at around 430s. Flames from this extremely intense fire engulfed the corridor completely at around 460s. Flame fronts then spread inside all the adjacent shops around 560s. After this stage from the observation of the fire situation in side the computation geometry, it was clear that, no human could possibly sustain the ongoing hazard without any protective gear. The simulation was continued further and fuel loads started to disappear from the computation geometry indicating complete burn away. There were plenty of fuel loads still to fuel the fire due to the compact stacking of fuels inside those shops. At around 850s the fire was burning from ceiling to floor and sustained in that condition up to 1200s. Some occasional hiccups in the burning region were observed which mainly due to the shortage of oxidizer at that particular location. Table 3.2 presents the complete time line of the clothing store fire in source shop 1 of Gulshan-1 DCC Market.

The temperature distributions at positions A, B (inside the fire source) and C, D (outside the fire source) as shown in figure 3.4, for clothing fire scenario at fire source
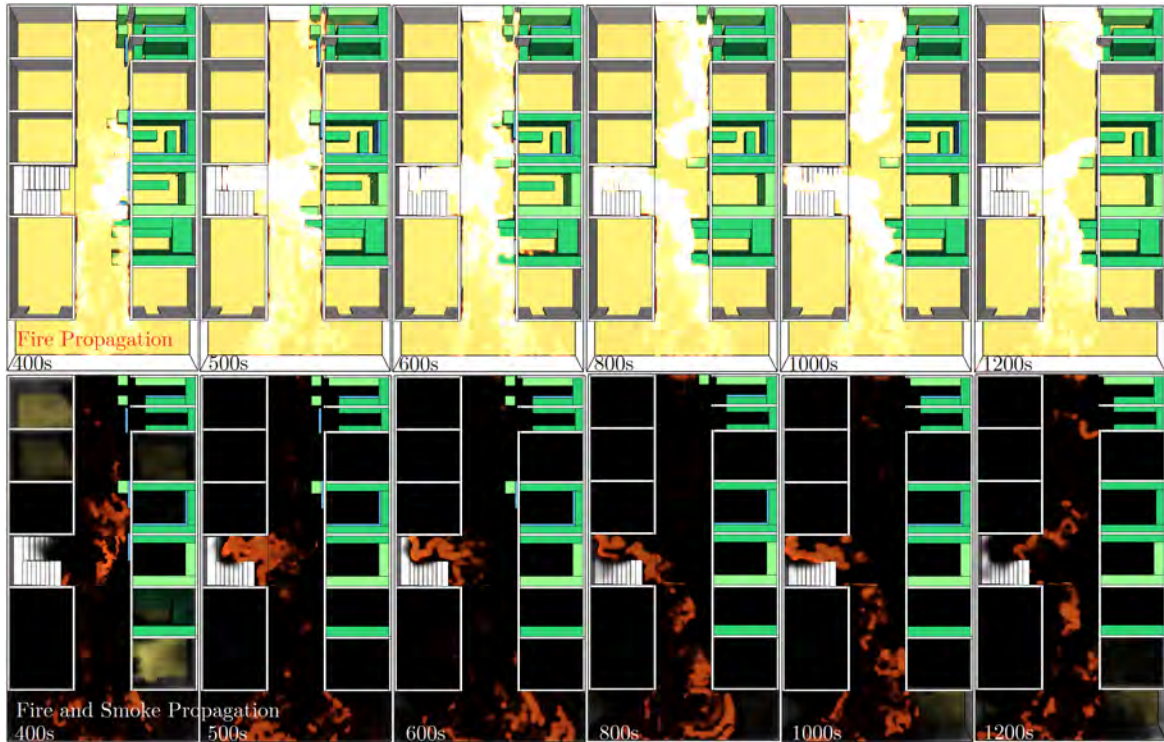
Fig. 3.6 Flame propagation through DCC market source shop 1, DCC_CS1, in case of clothing as fuel load. The top row shows the flame only, and bottom row shows both flame and smoke for 400s, 500s, 600s, 800s, 1000s and 1200s of simulation time respectively from left to right.

shop 1 (DCC_CS1) are shown in Figure 3.7. The temperature measurements were taken at 1.524 m height from the floor with air curtain operating at non-discharged mode. This goes without saying that, ambient temperature increased due to the fire burning at the source shop. The exposure to heat, generated by this fire, can lead to life threat for an evacuee in three ways, namely, hyperthermia, body surface burns and respiratory tract burns. As tenability limits of skin burns normally lower than respiratory burns, considerations of life threat due to fire mainly depends on skin burn threshold and exposure that can cause hyperthermia. Now the body of an evacuee will acquire a 'dose' of heat, both convective and radiative, over time during the evacuation process. If the fraction equivalent dose (FED) of heat accumulated not exceed 0.3, safe evacuation can be assumed even for the more sensitive populations. According to the National Fire Protection Association (NFPA), Massachusetts, USA, standard NFPA 130 (2017) the maximum exposure time, without incapacitation, considering the total FED, is 3.8 minutes at 80°C, National Fire Protection Association (2017). In figure 3.7 the dashed green line represents 80°C, the upper limit of human temperature
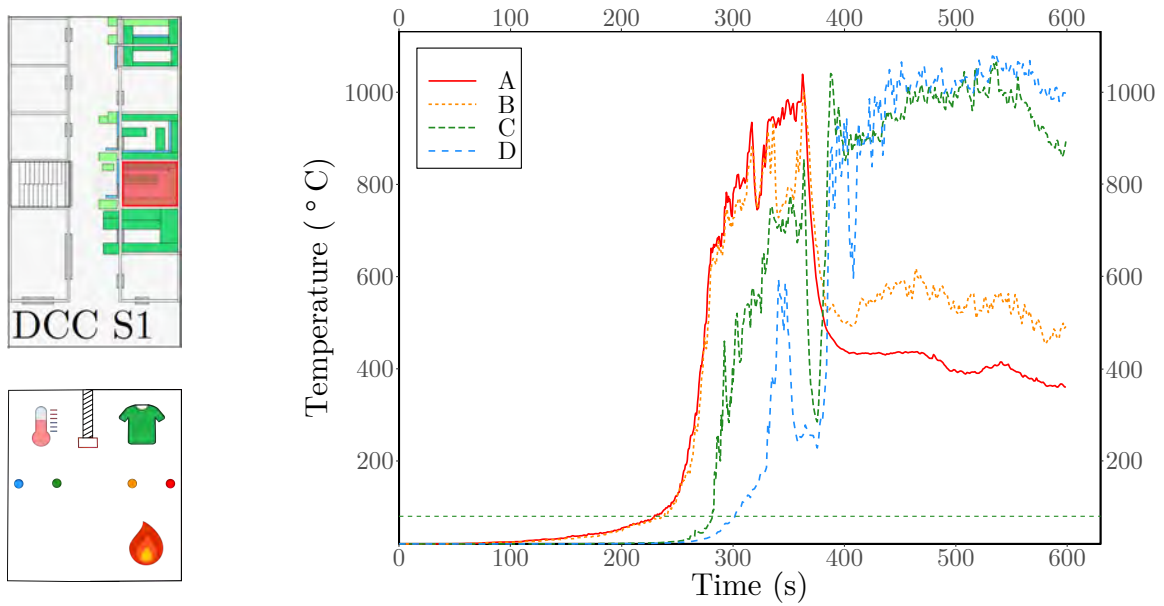
Fig. 3.7 Temperature distributions at positions A, B (inside the fire source) and C, D (outside the fire source) for air curtain at non-discharged condition for clothing fire scenario at fire source shop 1 (DCC_CS1).

tenability for 228s, an arguable time for evacuation from the computational domain considered. Thus at time, when temperature in a specific region went beyond this line, it was considered lethal for the evacuees for that region.

The temperature patterns of thermocouples A and B, the shop inside thermocouples, closely followed each other. The temperature distribution of thermocouples C and D, the shop outside thermocouples, also had matching patterns but had variations from the inside thermocouple temperature patterns. The temperature distributions of shop inside thermocouples crossed the human temperature tenability of 80°C at around 230s. The temperature tenability limit reached at around 280s on position C, and at around 307s at position D. The sharp increase in shop inside temperatures from 190°C at 258s to 500°C at 275s indicated the flashover phase. At around 390s the sharp drop in shop inside temperatures and spike in outside thermocouples indicated the movement of flame front to the corridor from the shop inside. Before dropping sharply the temperature of inside thermocouples crossed 1000°C. And after the sharp increase in temperature for the outside thermocouples, the temperature gradually increased further and stayed around the 1000°C mark for the rest of the simulation. As the temperature above 235°C is labeled critical within less than one minutes of exposure for fire fighters with protections, by Australasian Fire and Emergency Service
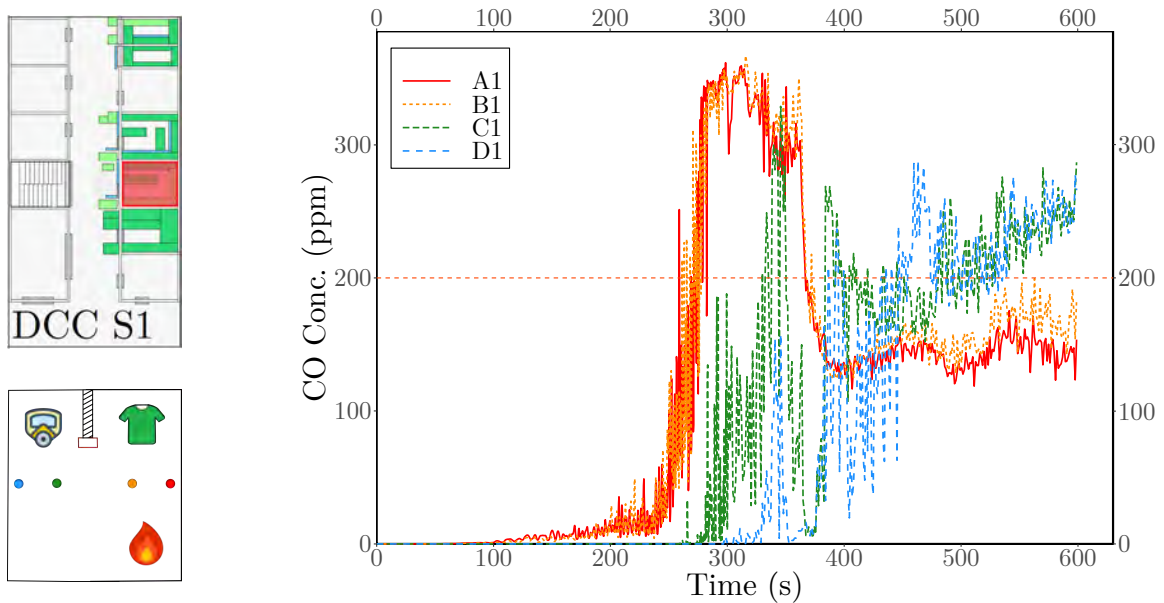
Fig. 3.8 CO concentration at positions A1, B1 (inside the fire source) and C1, D1 (outside the fire source) for air curtain at non-discharged condition for clothing fire scenario at fire source shop 1 (DCC_CS1).

Authorities Council (AFAC), Poh and Engineer (2010), evacuation will not be possible after 400s through the fire engulfed corridor around the source. Although the figure 3.7 plotted only up to 600s of simulation time, for the rest of the simulation pattern of temperature for all four thermocouples are remains same. Details of this curve is attached in appendix A.

The carbon mono-oxide concentration at positions A1, B1 (inside the fire source) and C1, D1 (outside the fire source) as shown in figure 3.4, for clothing fire scenario at fire source shop 1 (DCC_CS1) are shown in Figure 3.8. The CO devices were placed at 1.524 m height from the floor with air curtain operating at non-discharged mode. Inhalation of toxic gases are reported as the main cause of death during a fire hazard, Hietaniemi et al. (1999), Hu et al. (2008). Among other gases the main culprit is the colorless, tasteless, and odorless carbon monoxide, which justifiably termed as the silent killer. The affinity of carbon monoxide to binds with hemoglobin is 200 times larger than oxygen, and thus causing effective oxygen deprivation in cells, medically termed as chemical asphyxiation and hypoxia, in affected evacuee. This will hinder all cell functionality and lead to organ failure which will ultimately result in death of the affected person. And as the inhaled concentration increases, less time is required for the exposure to become lethal. For example at 200 ppm CO concentration, exposure
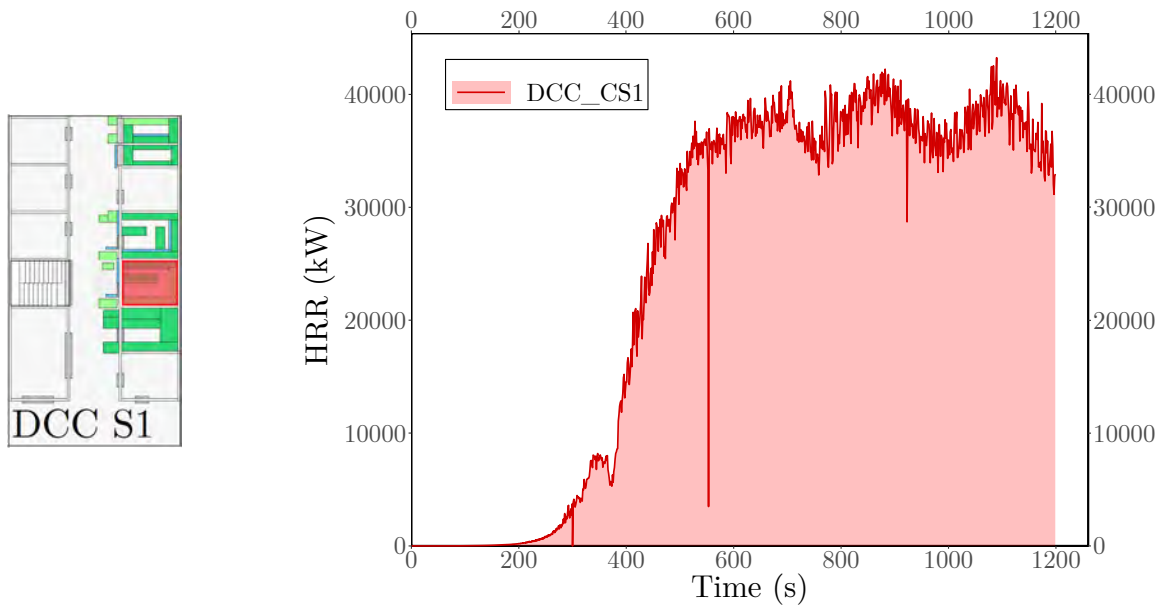
Fig. 3.9 Heat Release Rate (HRR) for clothing fire scenario at fire source shop 1 (DCC_CS1) without air curtain discharged.

for two to three hours will cause loss of judgment for the evacuees, but at 12,800 ppm CO concentration, death will be in less than 3 minutes of exposure, Goldstein (2008). Again taking consideration of the fact that the evacuee will accumulated a dose of CO over time, thus utilizing concept of fractional effective dose, FED, according to NFPA 130 (2017), at 1,700 ppm of CO concentration, the maximum exposure time for evacuees is 4 minutes, National Fire Protection Association (2017).

In the figure 3.8 the CO devices inside the shop showed similar trend for the entire simulation, indicating same conditions prevailed inside the shop at a given time. The CO devices outside the shop also showed same trend in between them, but it was different from the inside devices. For the CO devices at position A1 and B1, the CO concentration spiked at around 250s and breached the 200 ppm bar at 275s. The concentration of CO devices at position C1 and D1 spiked at around 290s, when the smoke started to fill up the corridor. The trend of inside and outside CO devices crossed at around 390s, the time when fire came out of the shop to the corridor due to lack of oxidizer. After 390s, the trend of CO devices remains same with a slow and steady rise for inside devices up to 250 ppm and a slow and steady dip for outside devices down to 294 ppm, to the end of simulation. The detailed CO devices curve is attached at appendix A. Luckily for clothing fire the CO concentration maxed at 375 ppm at around 297s for the CO devices at position A1, which was well below the

lethal limit for short exposure. Thus the temperature distribution is the determining parameter of possible evacuation in case of a fire hazard similar to source 1 conditions. Figure 3.9 shows the heat release rate (HRR), for clothing fire scenario at fire source shop 1 (DCC_CS1) without air curtain discharged. The curve steady increased at first but after 200s the curve increased rapidly and showed a local peak at around 350s and a local drop at 370s. This was around the time when the fire move out of the room due to oxidizer shortage. Then the curve showed an extremely rapid increment as the fire was burning violently on the corridor at this time. After this period the curve steadied up from 600s to 1200s with occasional ups and downs due to oxidizer availability. This steady heat release rate from 560s to end of the simulation, agrees well with the temperature and carbon mono-oxide curve described earlier. During this period the maximum heat release rate was 40 MW, and the curve during the periodic motion never went below 30 MW. The area under the curve of figure 3.9 was calculated by multiple-application Simpson's 1/3 rule by equation 3.1 with $n = 1752$. The result was a staggering 51714 Tera Joule after 1200s of simulation time. When considered for 600s, the total heat released per unit area was 383.8 TJ/m^2. This information will shed light in to the devastation of fire hazards originated from highly compact stacks of fuel like DCC_CS1 in later sections.

$$I \cong (b - a) \frac{f(x_0) + 4 \sum\limits_{i=1,3,5}^{n-1} f(x_i) + 2 \sum\limits_{j=2,4,6}^{n-2} f(x_j) + f(x_n)}{3n} \tag{3.1}$$

3.1.1.3   Clothing fire in Source Shop 2

For the second fire source for DCC Market, the second last shop on the corridor of the computation geometry was chosen. This shop had 6.39 m^2 floor area, smaller than the first shop and comparatively more stacked fuels, weighting nearly 3218.43 kg, thus having a mammoth 504 kg/m^2 fuel load to area ratio. The consequent fire load is 42483.34 MJ/m^2. The path to staircase, an important parameter during evacuation, for this source shop 2 was 12.34 m, highest possible path distance in this geometry. This will enable us to observe the effect of fire propagation from a distant shop to staircase on evacuation. And, from the observation of fire to persists from 600s to 1200s monotonously for DCC_CS1, the subsequent simulations of clothing fire were set for 600s only, to reduce the resource utilization. Table 3.3 shows the parameters of the source shop 2 of DCC Market.
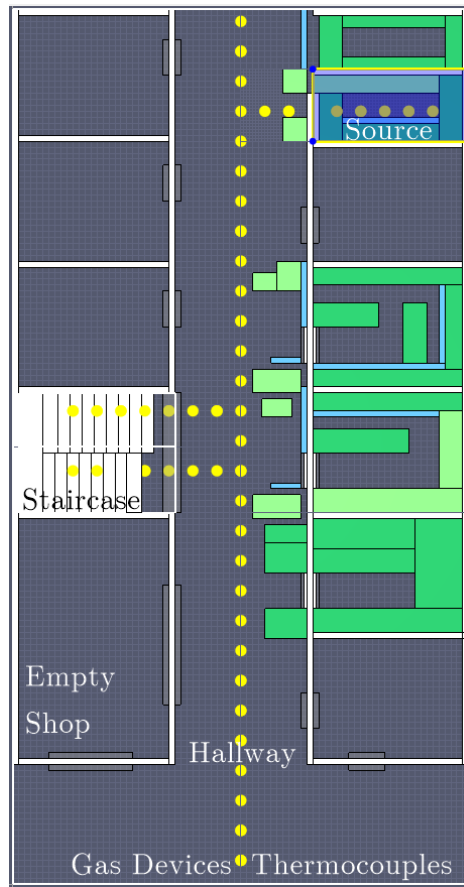
Fig. 3.10 Top view of the computational model of DCC Market in PyroSim for clothing fuel condition, with fire source shop 2 (DCC_S2) highlighted in blue. The position of thermocouple and CO measuring devices are shown in yellow circles.

Table 3.3 Parameters of DCC Market source shop 2.

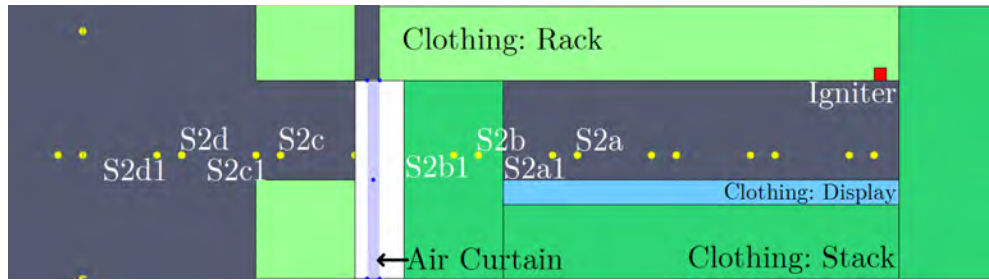| Name	Data
Simulation name	DCC_CS2
Fuel type	Clothing
Heat release rate per unit area	1528 kW/m^2
Shop area	6.39 m^2
Path distance to staircase	12.34 m
Fuel load	3218.43 kg
Fuel load to shop area ratio	503.9 kg/m^2
Fire load	42483.34 MJ/m^2
Simulation time	600s
Total Heat Released	2116.67 Tera Joule
Total Heat Released per unit area	331.4 TJ/m^2

Fig. 3.11 Top view of the fire source shop 2 of DCC Market (DCC_S2), in PyroSim for clothing fuel condition. The respective positions of Igniter, Air curtain, Thermocouple (S2a, S2b, S2c, S2d) and CO devices (S2a1, S2b1, S2c1, S2d1) are highlighted.

Figure 3.10 shows the top view of the FDS model of DCC market for clothing fuel condition with the fire source shop 2 (DCC_S2), highlighted in blue. Here again, the details positions of temperature and carbon monoxide measuring devices were shown in yellow circles. The figure 3.11 showed the designed position of igniter to initiate fire, position of air curtain at door, and exact locations of thermocouples (S2a, S2b, S2c, S2d) and CO devices (S2a1, S2b1, S2c1, S2d1) both inside the shop and on the corridor. The position of the thermocouple S2a is 1.83 m horizontally left and 0.4572 m vertically downwards of the igniter as seen in the figure 3.11. Figure 3.12 shows the fire propagation for the 2nd simulation, referred as DCC_CS2, for clothing fire scenario in source shop 2. The top row shows the flame propagation only, and bottom row shows both flame and smoke for 100s, 200s, 300s, 400s, 500s and 600s of simulation time respectively from left to right. The flame was visible after 60s of simulation time, and smoke came out of the source shop at around 75s. Smoke build up inside the source shop 2 and unlike source 1, it completely filled up the shop inside within 180s. The smoke outside the source accumulated in the corridor ceiling and filled the entire corridor in about 300s. And unlike source shop 1 the smoke layer did not drop to eye height and obstruct vision, rather stayed at nearly 0.9 m below the ceiling up to 550s of simulation time. The flame front came out of the source shop at nearly 333s. The delay in the fire stages of source 2 from source 1 was mainly due to the unavailability of oxidizers inside the shop due to extreme fuel to area ratio. This could be perceived beneficial momentarily, but in the long run the fire will be devastating due to the availability of fuels. At around 410 s the fire spread to inside of the shop immediately adjacent to the source. And at about 430s the flame front reached up to the staircase, this indicating the termination of evacuation through this staircase without any harm. Due to lack of oxidizers the fire came out of the source shop 2 at 440s. Fire was spreading rapidly along the corridor burning the fuel stacks in front of
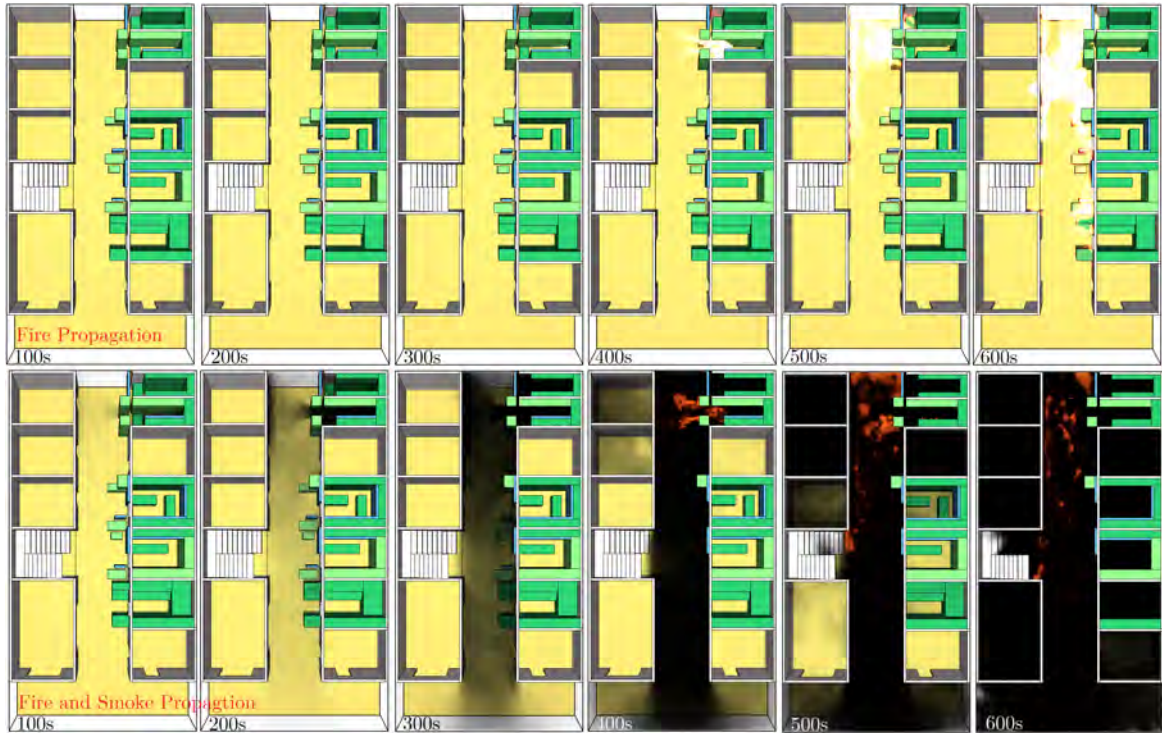
Fig. 3.12 Flame propagation through DCC market source shop 2, DCC_CS2, in case of clothing as fuel load. The top row shows the flame only, and bottom row shows both flame and smoke for 100s, 200s, 300s, 400s, 500s and 600s of simulation time respectively from left to right.

the shops. At 550s the fire gained instant intensity and the smoke from this intense fire quickly filled up the corridor and reduce the visibility after this point. Flame form this intense fire start to burn all shop front fuels inside the computational area. Although the growth nature of this intense fire was similar for both sources, the intensity was much higher for source 1. The fire events for DCC source shop 2 is presented in table 3.4. From the observation of both of the source shop and the fire propagation events, it can be concluded that, both of the fire were ventilation-controlled fire and as no premature decay was observed, it can also be concluded that, the pressure driven flow of the fire from source inside to corridor was indeed an evidence of flashover. According to National Fire Protection Association (NFPA), Massachusetts, USA, the preferred definition of flashover is, '*A transitional phase in the development of a compartment fire in which surfaces exposed to thermal radiation reach ignition temperature more or less simultaneously and fire spreads rapidly throughout the space, resulting in full-room involvement or total involvement of the compartment or enclosed area*', Gorbett et al. (2016).

Table 3.4 Flame and smoke propagation timeline for DCC market for clothing fuel condition in source shop 2.

Time (s)	Event
60	Visible flame after ignition.
75	Smoke came out of the source shop.
180	Smoke filled up the source shop.
300	Smoke filled up the ceiling of the whole corridor.
333	Flame front came out of the shop.
410	Fire spread to adjacent shop.
430	Flame front reached up to the staircase.
440	Fire came out of the source and spread along the corridor.
550	Fire intensely burning in front of source shop 2.
560	Fire spread to all shop front fuel stacks.
600	Fire sustains as enough fuel load still remains.
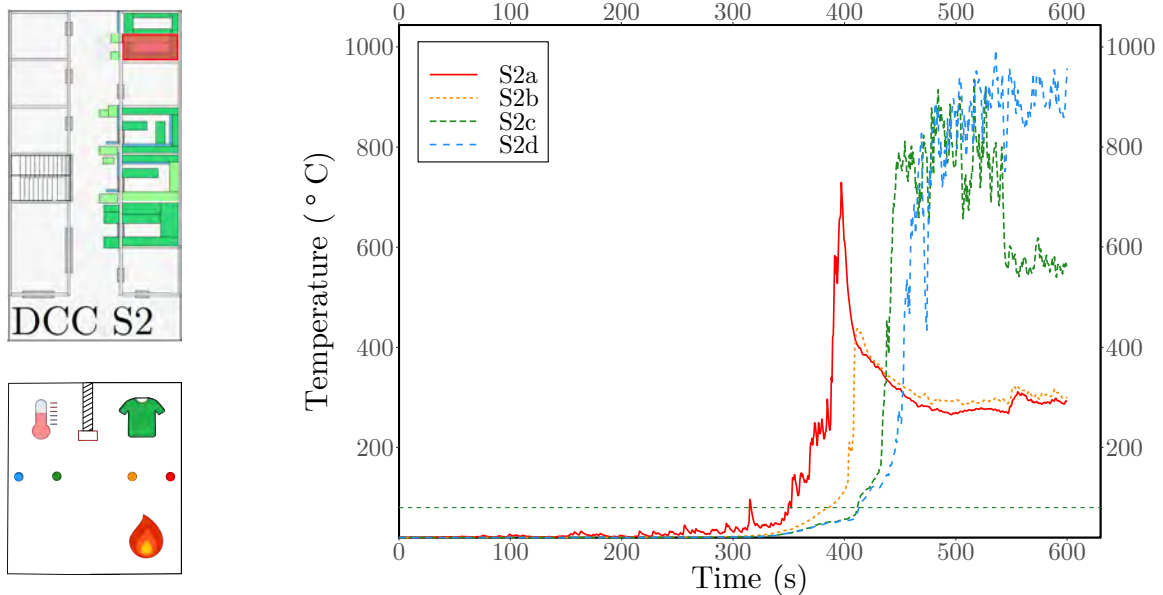
Fig. 3.13 Temperature distributions at positions S2a, S2b (inside the fire source) and S2c, S2d (outside the fire source) for air curtain at non-discharged condition for clothing fire scenario at fire source shop 2 (DCC_CS2).

Figure 3.13 shows the temperature distributions at positions S2a, S2b (inside the fire source) and S2c, S2d (outside the fire source) for DCC_CS2 simulation, clothing fire scenario at fire source shop 2 with non-discharged air curtain. The temperature inside the shop, for S2a and S2b thermocouple, remained below 100ºC, the upper limit
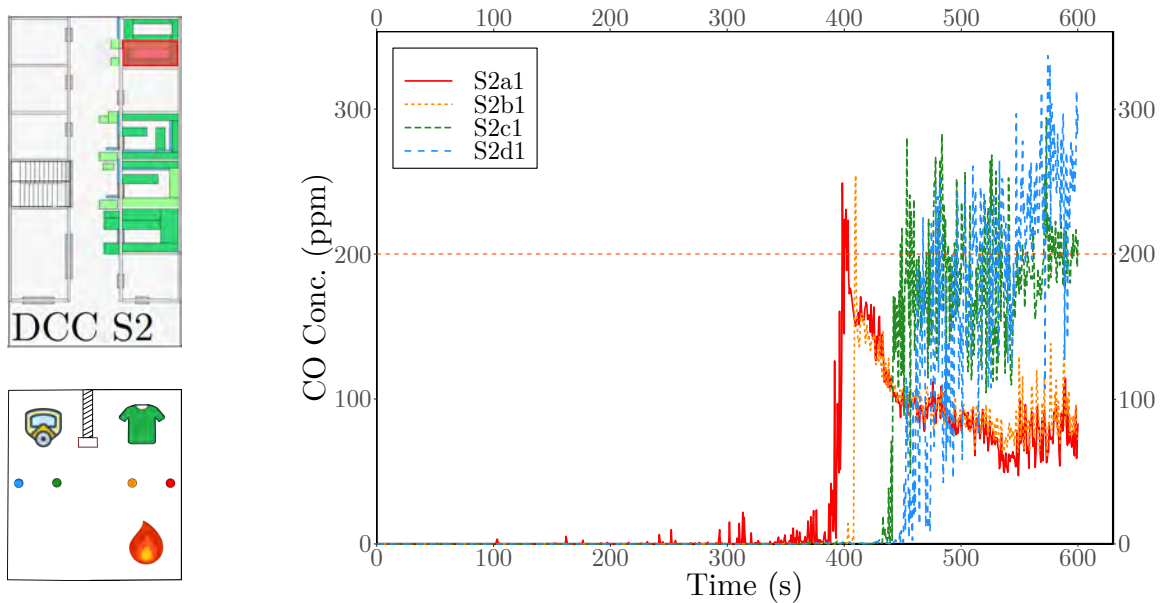
Fig. 3.14 CO concentration at positions S2a1, S2b1 (inside the fire source) and S2c1, S2d1 (outside the fire source) for air curtain at non-discharged condition for clothing fire scenario at fire source shop 2 (DCC_CS2).

of human temperature tenability, until 315s. After 350s the temperature begun to rise rapidly up to 400s to nearly 730ºC for S2a, the temperature for S2b raised shortly after S2a and peaked around 436ºC. The sudden drop in inside temperature and raise in outside temperature shortly after the peak indicated the movement of fire from inside the source to outside, on the corridor around 440s, where the temperature lines crossed. During the raise the thermocouple S2c peaked at 930ºC and S2d peaked at 950ºC. Although temperature of S2c dropped slightly at the end, the raise in temperature for outside thermocouple S2d continued gradually up to the end of simulation time. Thus, both the source shops the corridor temperature peaked around 1000ºC within 600s. This is an alarming finding as complete evacuation within 10 minutes of fire initiation may not be possible due to variety of reasons. CO concentration at positions S2a1, S2b1 (inside the fire source) and S2c1, S2d1 (outside the fire source) for DCC_CS2 is shown in Figure 3.14. Up to 400s all the CO devices showed negligible CO concentration in respect to lethal limit. For the inside CO devices S2a1 and S2b1 the 200 ppm line breached for the first time at around 400s and then dropped quickly to 100 ppm, indicating that the CO concentration will not be lethal inside the source during the simulation time. For S2c and S2d the CO concentration sharply crossed the 200 ppm mark at around 450s and 500s respectively and then gradually increased for the rest
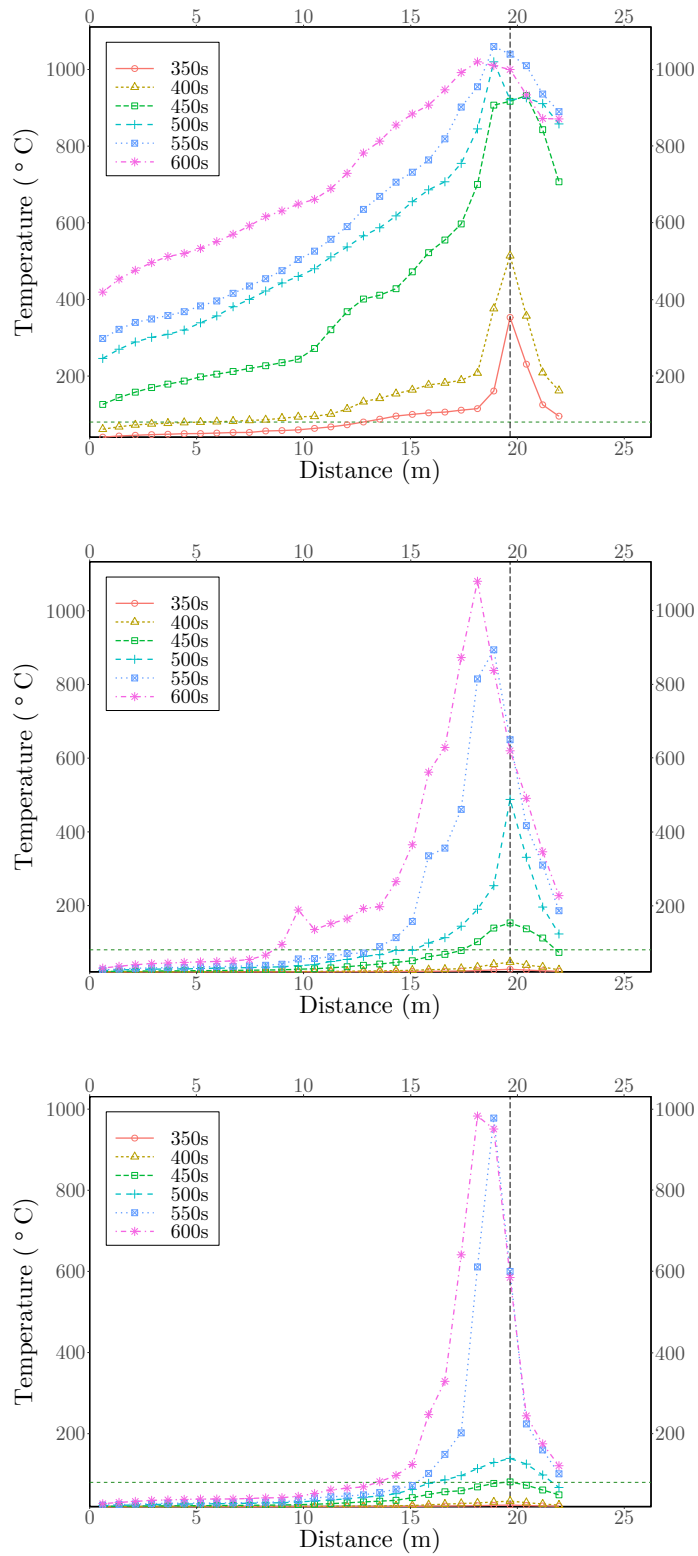
Fig. 3.15 Temperature distributions at 350s, 400s, 450s, 500s, 550s and 600s on the hallway for DCC_CS2, at 2.9 m height (top), at 1.524 m height (middle) and at 0.762 m height (bottom).
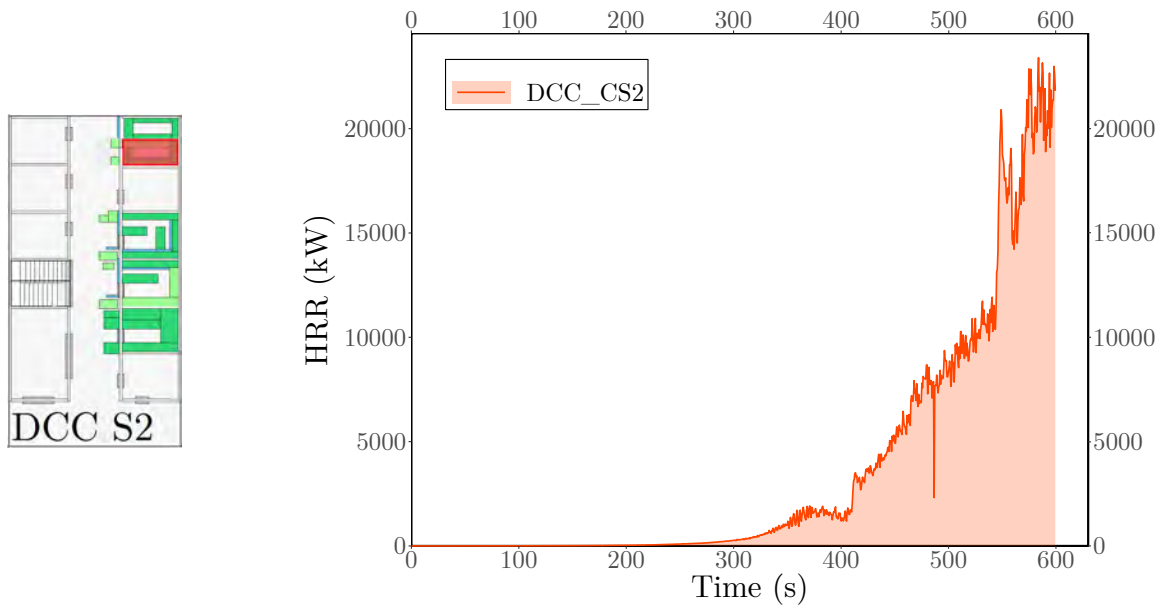
Fig. 3.16 Heat Release Rate (HRR) for clothing fire scenario at fire source shop 2 (DCC_CS2) without air curtain discharged.

of the simulation. The maximum CO concentration was 312 ppm for S2d at around 600s. Thus, as the CO concentration never reached the lethal limit for short exposure, for source 2 also, again temperature distribution played the vital role in successful evacuation in case of a fire hazard.

Figure 3.15 shows temperature distributions at 350s, 400s, 450s, 500s, 550s and 600s, on the hallway for DCC_CS2 simulation. The figure represents the temperature distribution at 29 thermocouple positions, on the corridor of the computation geometry, 0.61 m apart from one another, details of which are shown in figure 3.10. The top figure of figure 3.15, represents the temperature distributions at ceiling of the corridor, 2.9 m height from the floor. The middle figure shows the temperature distributions on the same locations for average human eye height, at 1.524 m height from the floor. And, the bottom figure shows the temperature distributions at human knee height, at 0.762 m from the floor. All the thermocouple distance shown in x-axis of figure 3.15 are measured taking the bottom left corner of figure 3.10 as the origin. This made the position of the source 2 at 19.65 m from the bottom end, which marked as a black dashed line in figure 3.15. The 100ºC, human tenability limit, was again marked as green horizontal dashed line. From the figure 3.15, it can be seen that, the temperature at 2.9 m, the ceiling of the corridor, was above 100ºC, at 5 m horizontal distance from the source shop at around 350s. At and above 450s the temperature at ceiling of the

total corridor was above human tenability limit, but luckily evacuees will not experience ceiling temperature, rather they have to endure the temperature around 1.524 m, the eye height, while running or walking during evacuation. In the middle figure of figure 3.15 thus, shows the temperature distribution at 1.524 m. The temperature was below 100°C in the whole corridor up to 400s, and at 5 m horizontally from the source shop the the temperature was below 100°C up to 550s. Thus, safe evacuation was possible up to 400s through the whole corridor, even crossing the source. At 550s as the fire started to burn intensely in source front, thus the spikes in temperature readings in front of the source, at eye height and even at 0.762 m, the knee height (from the bottom figure). So, it will not be possible to cross the source shop on the way to evacuation even by crawling from 550s. The temperature distributions on the corridor remained well below 100°C at 0.762 m, through out the simulation, except in front of the source after 550s. Even though at the tenability limit crossed at eye height at 600s up to 10 m from the source, the temperature remained below 100°C at knee height, thus, evacuation should be done by crawling rather than walking or running during prolong evacuation.

The heat release rate (HRR) curve for the DCC market source shop 2 for clothing fire scenario is shown in figure 3.16. The HRR curve slowly raised up to 400s and dropped a little like the source 1 HRR curve, indicating the movement of fire from inside of the source to the corridor due to lack of oxidizers. The curve then increased gradually up to 550s indicating the gradual fire growth on the corridor fuel stacks. The spike in HRR after 550s, indicate the intense burning in shop front discussed earlier. The maximum HRR observed here was around 23 MW at 600s. The area under the curve of figure 3.16 was calculated again by multiple-application Simpson's 1/3 rule, with $n = 1000$. The resulting total heat released was 2116.67 Tera Joule at a 331.4 TJ/m^2 of total heat released per unit area, after 600s.

3.1.1.4   Summary of the effects of the variation of fire source

To compare the flame generation from each source shop, firstly the area under both the HRR curves of DCC_CS1 and DCC_CS2, are presented in shades in figure 3.30 up to 600s for comparison. Although the area under the curve for DCC_CS1 was clearly larger than the area under the DCC_CS2 curve, meaning the total heat released in source 1 (4457.53 Tera Joule after 600s) was higher than source 2, additional calculation revealed some interesting findings. To get things in perspective, the comparison between the source 1 and 2 is provided in figure 3.18. During the design stage, to match the
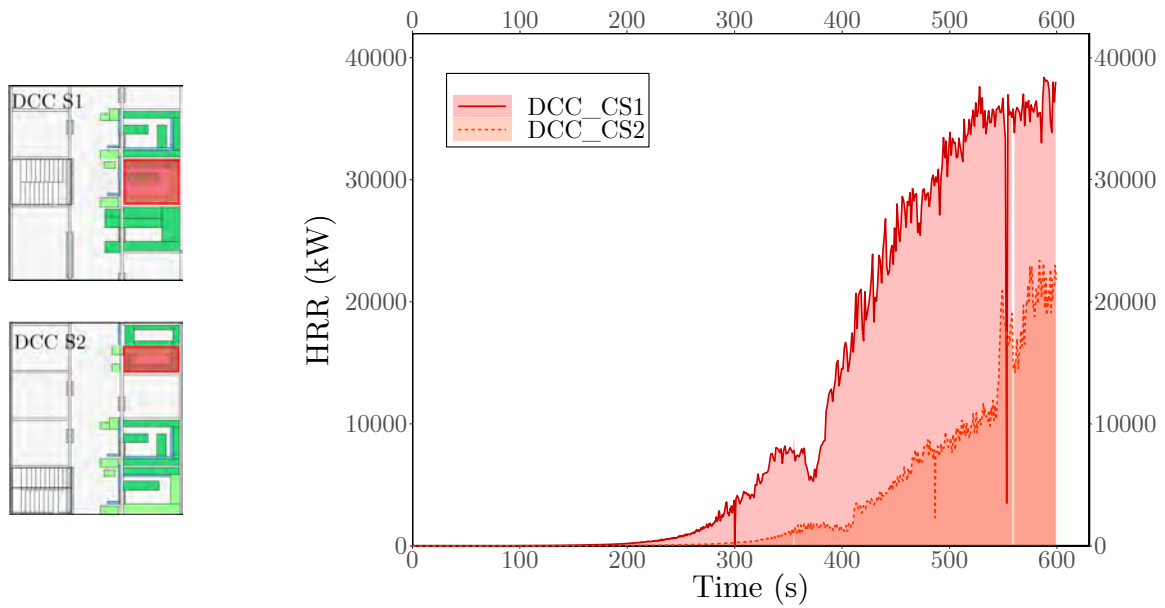
Fig. 3.17 Comparison of Heat Release Rates (HRRs) for clothing fire scenarios for DCC market at fire source shop 1 and 2 (DCC_CS1 & DCC_CS2) without air curtain discharged.
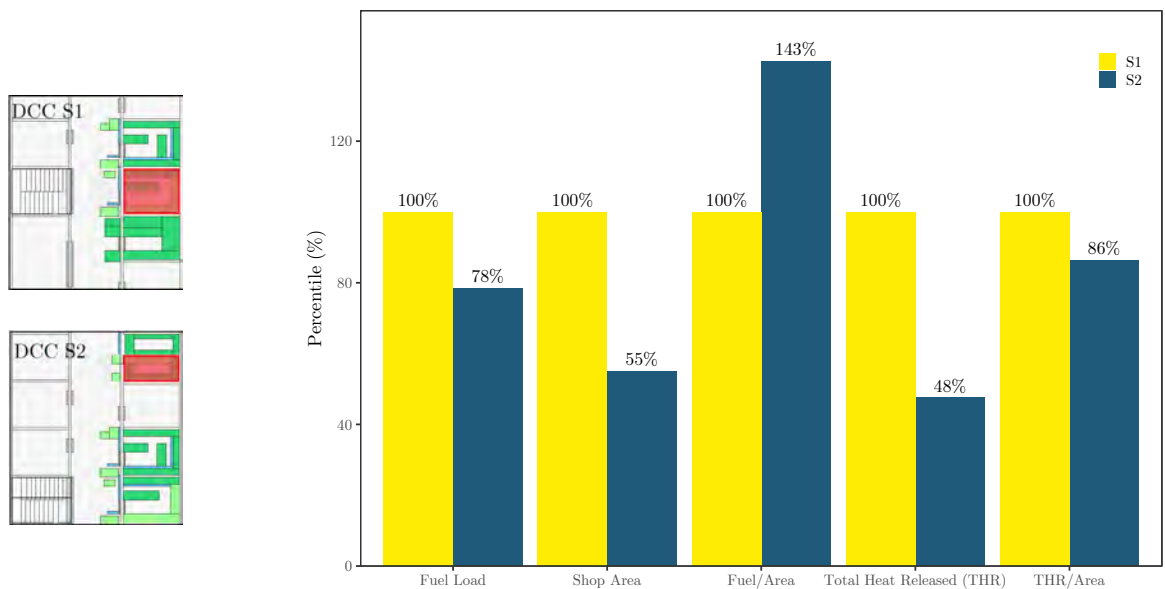

Fig. 3.18 Parametric comparison for clothing fire scenarios for DCC market at fire source shop 1 and 2 (DCC_CS1 & DCC_CS2) without discharging the air curtain.
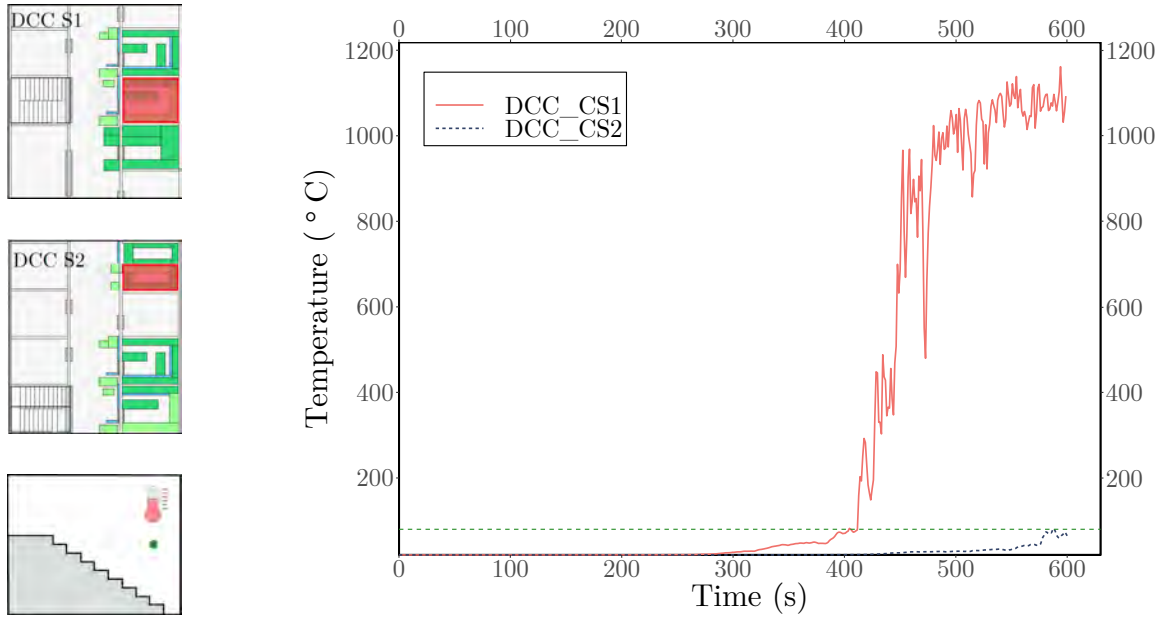
Fig. 3.19 Temperature distributions at staircase entrance for clothing fire scenario for DCC market at fire source shop 1 and 2 (DCC_CS1 & DCC_CS2) with air curtain at non-discharged condition. The path distance from source to staircase for source 1 and 2 is 4.28 m and 12.34 m respectively.

actual scenario, source shop 2 was designed with 78% fuel load in 55% area compared to source shop 1. Thus, yielding a 43% increase in fuel to area ratio for source shop 2 than source shop 1. Although source 2 had 78% fuel than source 1, the total heat released was only 48% of source 1, thus, total heat released per unit area of source 2 was 14% lower than source 1. This means at extreme fuel density, heat released during a fire incident decreases due to lack of oxidizers. Secondly the effect of the source variation on staircase environment during a fire hazard was analysed. Figure 3.19 and figure 3.20 represent temperature distribution and carbon monoxide concentration at staircase entrance for clothing fire scenario for DCC market at fire source shop 1 and 2 (DCC_CS1 & DCC_CS2) with air curtain at non-discharged condition. The path distance from source to staircase for source 1 and 2 is 4.28m and 12.34m respectively. And as the source shop 1 was just in front of the staircase heat and toxic gases reached far more quickly to the staircase than source shop 2. The temperature at staircase entrance crossed tenability limit within 400s when fire initiated at source shop 1, around the time fire came out of the source. Whereas, the temperature never crossed the tenability limit at staircase entrance for fire initiated from source 2 for the total simulation time of 600s. The picture on carbon monoxide concentration at staircase
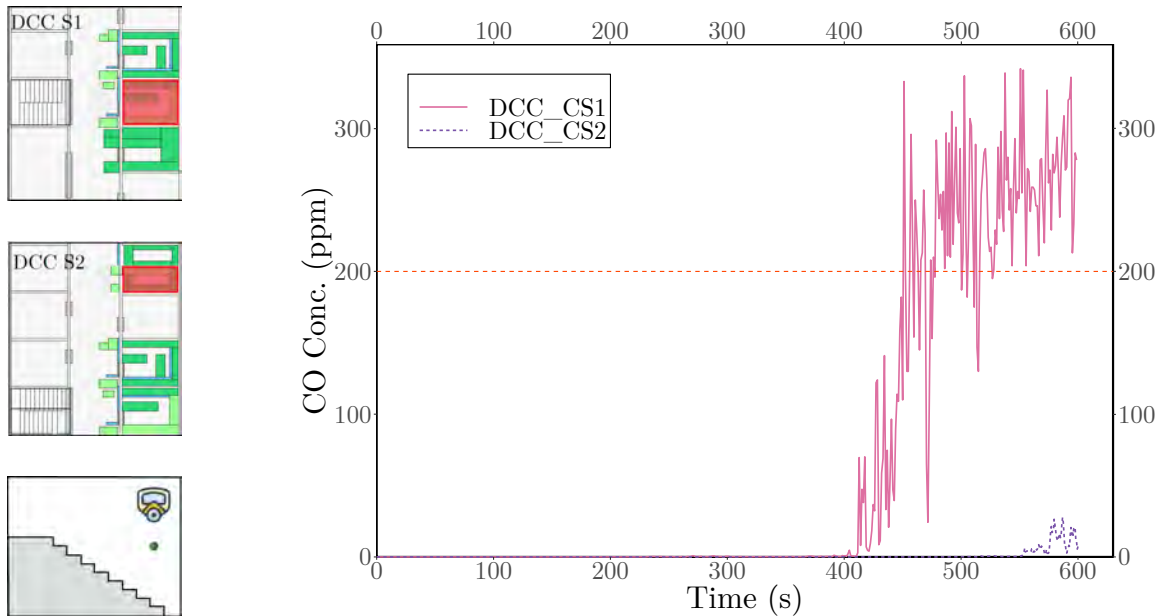
Fig. 3.20 CO concentration at at staircase entrance for clothing fire scenario for DCC market at fire source shop 1 and 2 (DCC_CS1 & DCC_CS2) with air curtain at non-discharged condition. The path distance from source to staircase for source 1 and 2 is 4.28 m and 12.34 m respectively.

entrance also remained the same, quickly reached 300 ppm at around 400s for source 1, but never reached a significant value for source shop 2 fire scenario.

3.1.1.5   Propagation of Fire and Smoke for furniture store fire

The fuel chosen for DCC market next round of simulation is furniture as in the ground floor of DCC market, most of the shops are furniture shops. Example of such a shop is shown in figure **??** Although in actual scenario, ground floor had different shop orientation than the first floor, simulation was continued with the previous computational geometry. five types of furniture were designed, non-assembled bed, almirah, sofa set, dining table and wardrobe. The wood was considered for this case was red oak with 150 kW/m² heat release rate per unit area (HRRPUA). The reason behind choosing red oak was that, the furniture found in DCC market were mainly made of Canadian red oak boards. The sources, igniters, number and position of shops with fuel were same as the clothing store as seen in figures 3.22a and 3.22b. For the source shop 1 actual fuel distribution was mimicked as per a photograph from the survey, other shops were designed as per typical shops found in ground floor on DCC market. The simulations with furniture as fuel for source shop 1 was named DCC_FS1

Fig. 3.21 Photographed furniture store in DCC market during the survey.

and for source shop 2 was named DCC_FS2 respectively. The fuel load in source 1 was 1906.7 kg yielding a fuel per unit area ratio of 164.2 kg/m^2. The source 2 had 829.6 kg fuel with 129.9 kg/m^2 fuel per unit area ratio.

Figure 3.23 shows flame and smoke propagation for DCC_FS1, for 100s, 200s, 300s, 400s, 500s and 600s of simulation time respectively from left to right. To no surprise the flame burns slowly and much less intensely than clothing fire and the smoke was much soot free than clothing fire too as seen from figure 3.23. This is because heat release rate of red oak wood considered here is nearly 10 times less than the heat release rate of cloths considered earlier. Also the soot yield and CO concentration also much lower than the clothing fire case. As the flame did not intensify much and smoke never really make any difference in the corridor visibility during 600s of simulation time, the simulation was then extended to 1800s i.e., 30 minutes. The flame and smoke propagation then for 800s, 1000s, 1200s, 1400s, 1600s and 1800s of simulation time are shown in figure 3.24 from left to right respectively. Surprisingly the flame stayed at the original position where it was initiated by the igniter even after 1800s of simulation time and the smoke formation inside the source was somewhat constant after 200s as the amount of new smoke generated was dispersed through the door and then from the open boundaries. And, during this dispersion of smoke through the corridor, visibility was never hampered due to low density of the generated smoke by wood fire.

The temperature distribution for DCC_FS1 inside the fire source and outside the fire source should provide conclusive evidence on the speculation made earlier on the corridor environment tenability. Thus, the figure 3.25 was plotted showing the temperature distributions for 1800s of simulation time at positions A, B (inside the fire source) and C, D (outside the fire source). Ambient temperature was set at 20ºC by default, and temperature at positions C and D remained nearly constant at that mark.
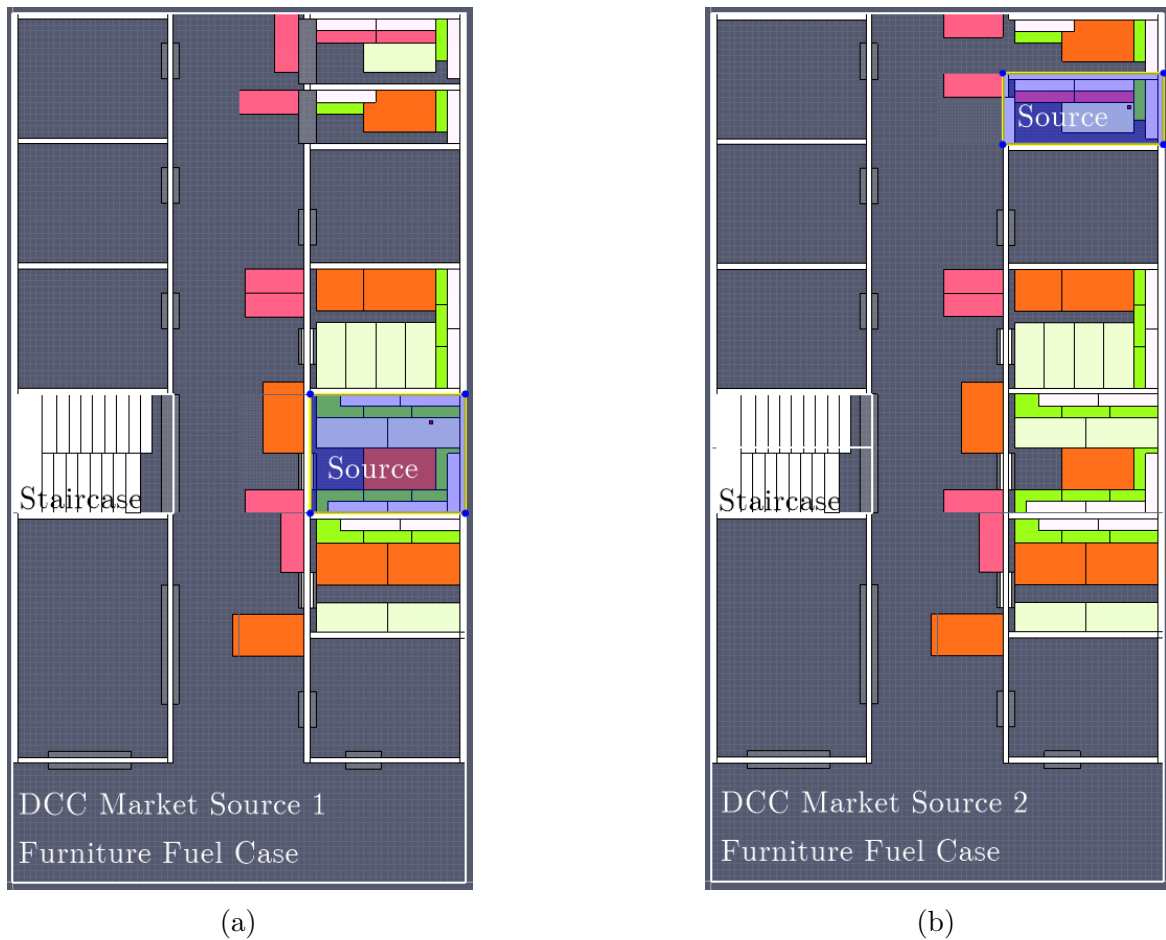
(a) (b)

Fig. 3.22 Furniture fuel distributions with source shops highlighted in blue for furniture source shop 1 (DCC_FS1) in (a) and furniture source shop 2 (DCC_FS2) in (b), for DCC market.

Fig. 3.23 Flame propagation through DCC market source shop 1, DCC_FS1, in case of furniture as fuel load. The figure shows both flame and smoke for 100s, 200s, 300s, 400s, 500s and 600s of simulation time respectively from left to right.

Fig. 3.24 Flame propagation through DCC market source shop 1, DCC_FS1, in case of furniture as fuel load. The figure shows both flame and smoke for 800s, 1000s, 1200s, 1400s, 1600s and 1800s of simulation time respectively from left to right.
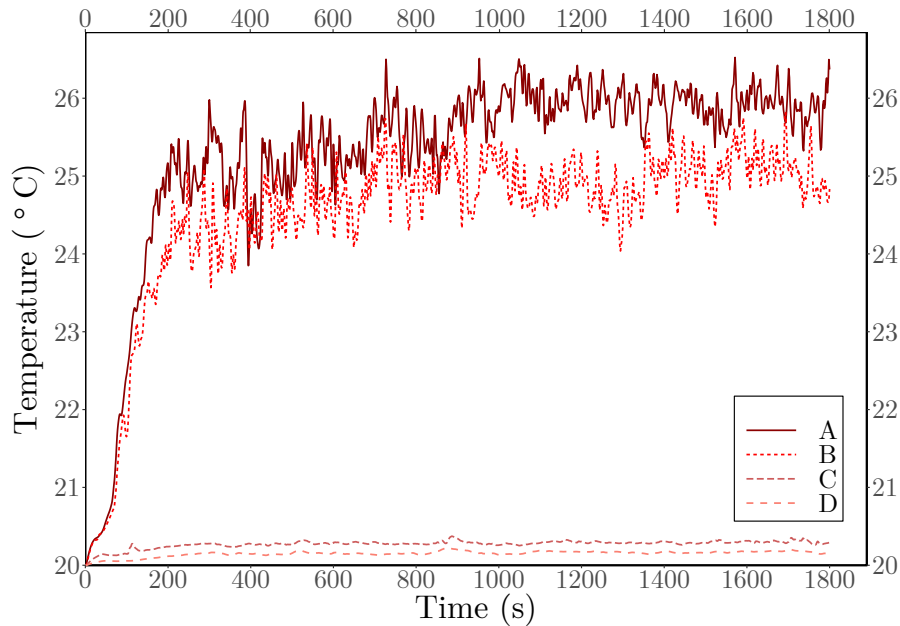

Fig. 3.25 Temperature distributions at positions A, B (inside the fire source) and C, D (outside the fire source) for air curtain at non-discharged condition for furniture fire scenario at fire source shop 1 (DCC_FS1).

Temperature inside the shop and near the door, position A and B, also varied within 25°C to 26°C i.e., increased only 5 6°C from the ambient condition. This increment should not hamper the evacuation process during such a fire hazard. Figure 3.26 shows the carbon monoxide concentration at positions A1, B1 (inside the fire source) and C1, D1 (outside the fire source) for total 1800s simulation time of DCC_FS1. As seen from the figure 3.26 the CO concentration did not increase at all outside the source and
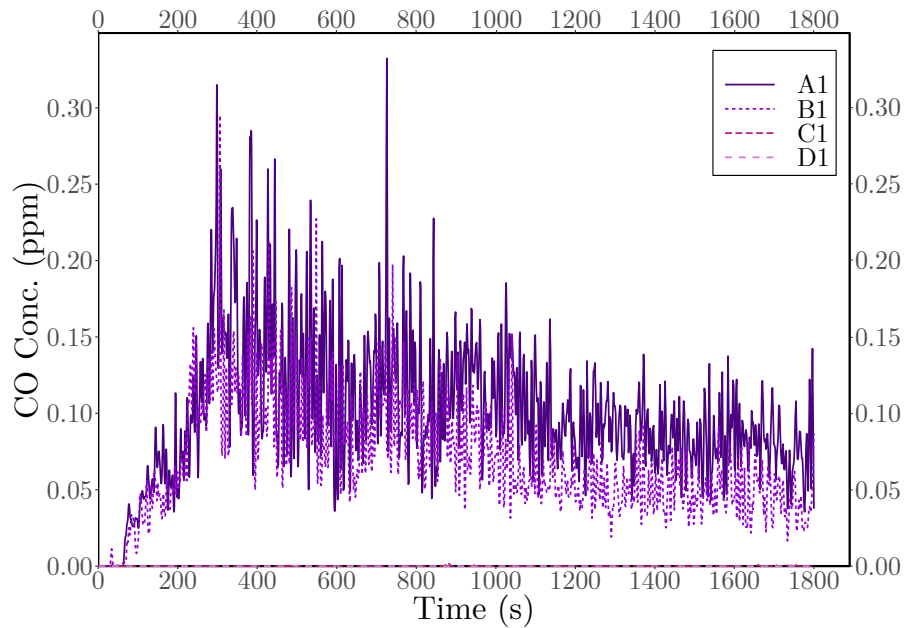
Fig. 3.26 CO concentration at positions A1, B1 (inside the fire source) and C1, D1 (outside the fire source) for air curtain at non-discharged condition for furniture fire scenario at fire source shop 1 (DCC_FS1).

Fig. 3.27 Flame propagation through DCC market source shop 2, DCC_FS2, in case of clothing as fuel load. The figure shows both flame and smoke for 100s, 200s, 300s, 400s, 500s and 600s of simulation time respectively from left to right.

increased nominally inside the source. Hence, impact of fire with furniture as fuel on corridor environment, seemed to be within the human tenability during the simulation time considered for the source shop 1 of DCC market.

For the fire at source shop 2 with furniture as fuel, the simulation was named DCC_FS2 and was performed for 600s. The flame and smoke propagation is shown in the figure 3.27 for 100s, 200s, 300s, 400s, 500s and 600s of simulation time respectively
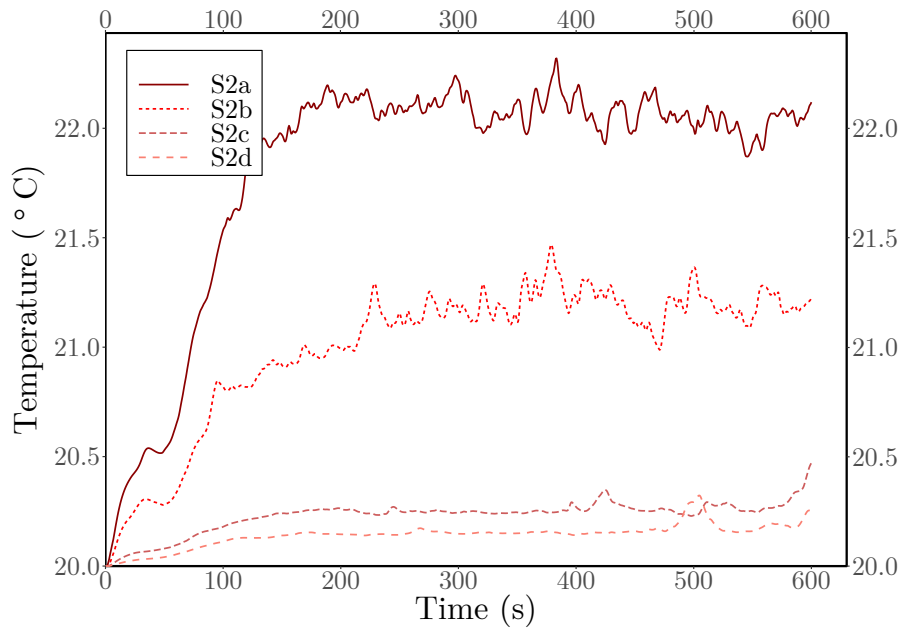
Fig. 3.28 Temperature distributions at positions S2a, S2b (inside the fire source) and S2c, S2d (outside the fire source) for air curtain at non-discharged condition for furniture fire scenario at fire source shop 2 (DCC_FS2).
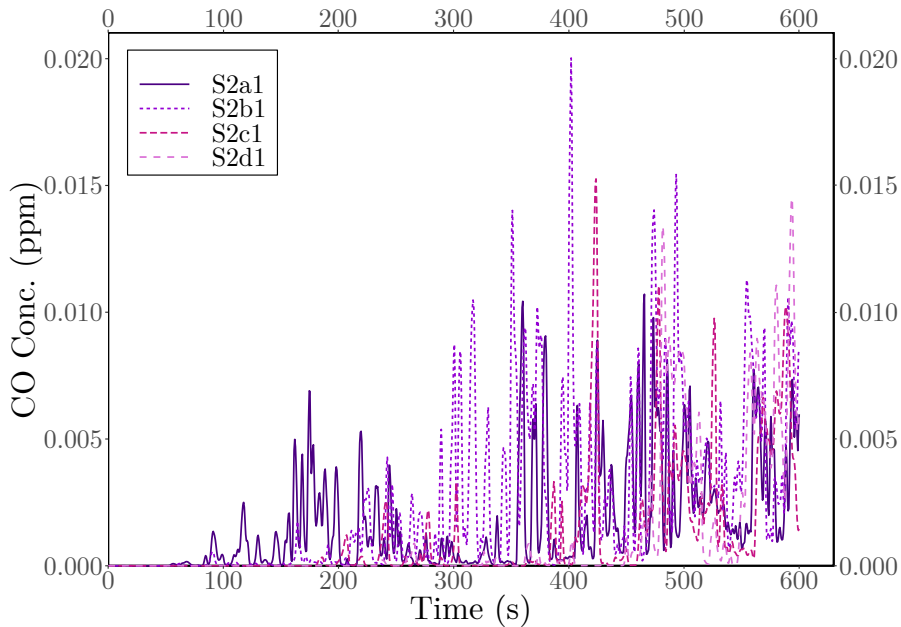

Fig. 3.29 CO concentration at positions S2a1, S2b1 (inside the fire source) and S2c1, S2d1 (outside the fire source) for air curtain at non-discharged condition for furniture fire scenario at fire source shop 2 (DCC_FS2).
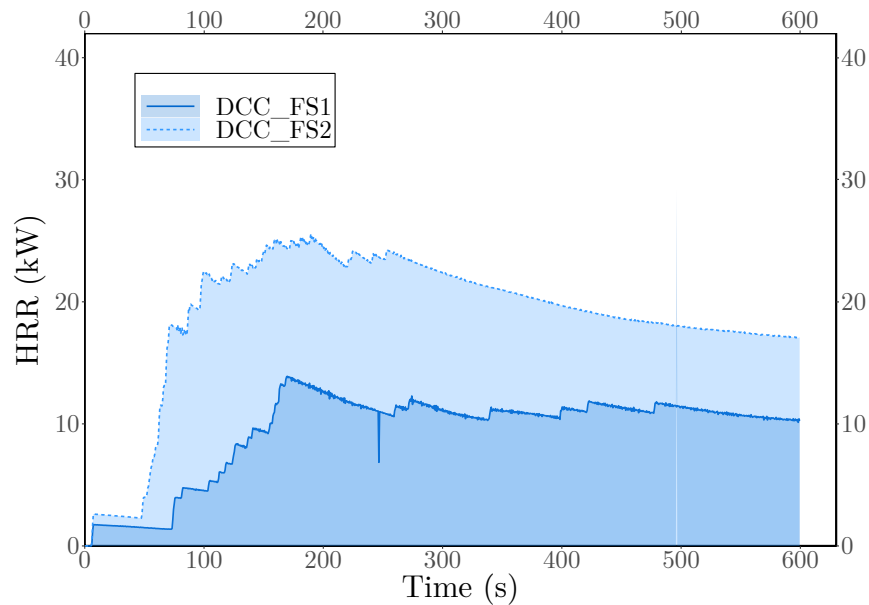
Fig. 3.30 Heat Release Rate (HRR) for furniture fire scenarios for DCC market at fire source shop 1 and 2 (DCC_FS1 & DCC_FS2), without air curtain discharged.

from left to right. Here again the fire was confined within the ignition zone without any outside factor affecting and the smoke did not hamper the visibility within and outside the source for the entire simulation time. Figure 3.28 shows the temperature distribution for positions S2a, S2b (inside the fire source), and S2c, S2d (outside the fire source), respectively for DCC_FS2. And, figure 3.29 shows the carbon monoxide concentration for positions S2a1, S2b1 (inside the fire source), and S2c1, S2d1 (outside the fire source), respectively for DCC_FS2. Once more, the temperature distribution and carbon monoxide concentration stayed well below the human tenability in both corridor and adjacent to the source door for the entire simulation time considered. Figure 3.30 shows the heat release rate curve for both sources for furniture fire on DCC market. The heat release rate was higher for source 2 in comparison with source 1 as the igniter at source 2 was placed at location where three furniture touched thus the increased HRR. However the HRR and total HRR was merely a fraction of what was observed for clothing fire scenario, 0.06% of clothing store fire.

3.1.1.6 Summary of the effect of the variation of fuel

Figure 3.31 shows the comparison of heat release rate of both fuel in two sources considered for DCC market. The extreme increment for clothing fuel scenario in both the sources after 200s indicated how quickly devastation could happen if fire generated from a clothing store instead of a furniture store for the same architectural configuration.
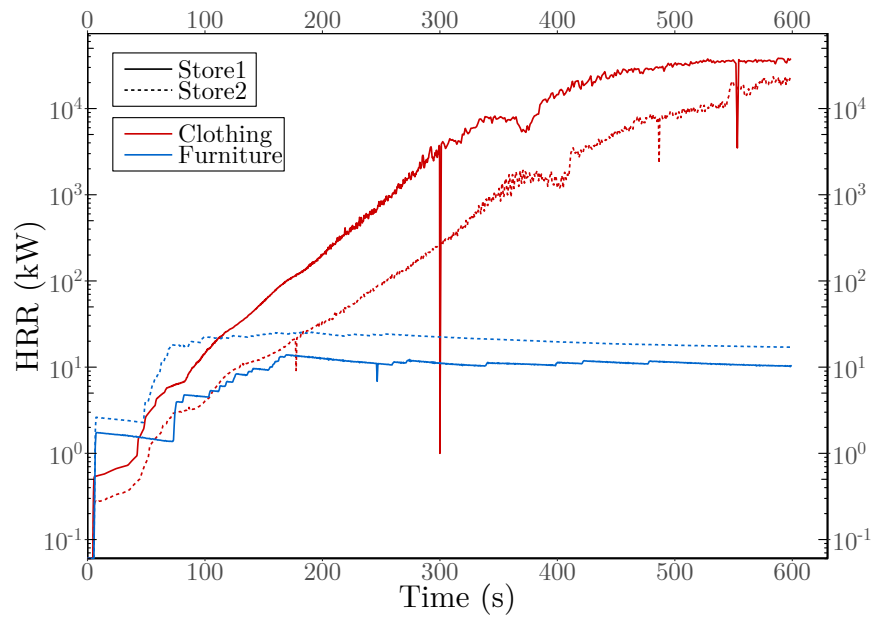

Fig. 3.31 Heat Release Rate (HRR) for clothing and furniture fire scenario at fire source shop 1 and 2 (DCC_CS1, DCC_CS2, DCC_FS1 & DCC_FS2) without air curtain discharged.

3.1.2 Shopping Mall-2: Co-operative market from Mirpur-1, Dhaka

3.1.2.1 Fire and smoke propagation for clothing store fire

CO-operative market from Mirpur-1 is a prominent market of that region, hosting mainly clothing stores in ground floor along with adjoining cosmetics and shoe shops sections. The main characteristics of this market was that, the shops were clustered in blocks with narrow corridor around them, which is a significant architectural difference from DCC market studied earlier. The long corridors of DCC market aided flame propagation along the corridor, the architectural design of this shopping mall might have a negative impact to flame propagation, thus aiding the evacuation process in case of a fire hazard originated a bit far from staircase. The computational geometry had 247 m^2 floor area with 11 shops on two corridors perpendicular to each other and 1 staircase. Five of those shops were designed with fuel and two source shops were chosen. Each shop had a wooden structure upon which the fuels were stocked, a unique configuration found only for this market during the survey. Figure 3.32 shows the 3D computational model of Co-Operative Market in PyroSim for clothing fire scenario. Temperature and carbon monoxide devices were placed in similar pattern as
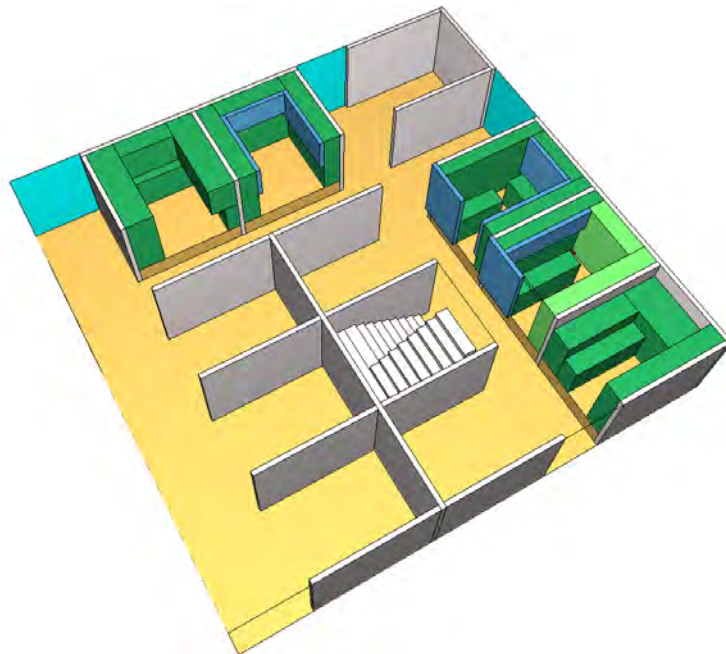

Fig. 3.32 The 3D computational model of Co-Operative Market in PyroSim. The shops are designed with clothing as fuel.

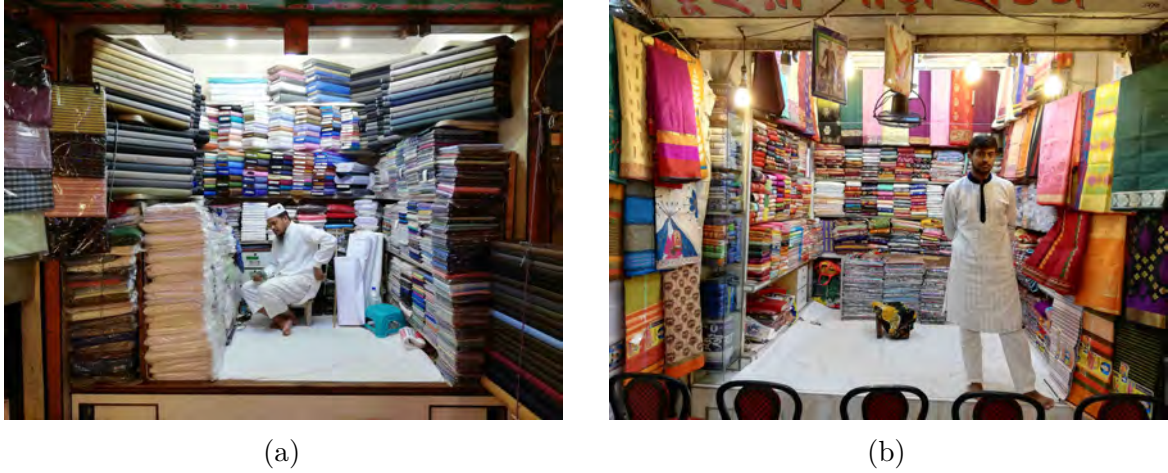(a)   (b)

Fig. 3.33 Photographed clothing stores in Co-Operative Market during the survey.

Table 3.5 Parameters of Co-Operative Market source shop 1 and 2.

Name	Source 1	Source 2
Simulation name	CoOp_CS1	CoOp_CS2
Fuel type	Clothing	Clothing
Heat Release Rate per unit area	1528 kW/m^2	1528 kW/m^2
Shop area	11.61 m^2	11.71 m^2
Path distance to staircase	2.3 m	14.6 m
Fuel load	3024.5 kg	6354.5 kg
Fuel load to shop area ratio	260.4 kg/m^2	542.7 kg/m^2
Simulation time	600s	600s
Total Heat Released	3907 Tera Joule	3127 Tera Joule
Total Heat Released per unit area	336.4 TJ/m^2	267 TJ/m^2

of DCC market in shops, corridors and staircase. Photographs of clothing stores in Co-Operative Market during the survey are shown in figure 3.33.

Figure 3.34 shows the top view of the computational model of Co-Operative Market in PyroSim for clothing fuel condition. Fire source shop 1 with cloths as fuel (CoOp_CS1) and fire source shop 2 with cloths as fuel (CoOp_CS2) are highlighted by blue rectangles in figure 3.34a and in figure 3.34b respectively. Yet again the sources were chosen as one in front of the staircase and one at furthermost from staircase within the computational geometry to ensure the architectural structure came in to play during flame propagation. Here both of the sources were of nearly same floor area, 11.61 m^2 for source 1 and 11.71 m^2 for source 2, according to the actual design of the shopping mall. The computational geometry was designed in PyroSim from data,
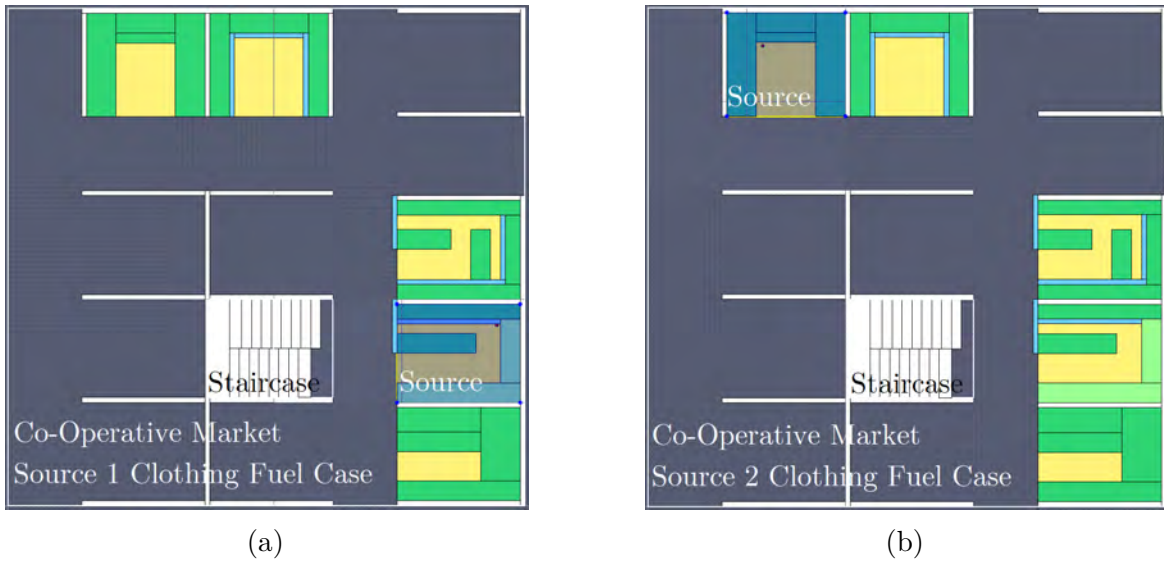
| (a) | (b) |

Fig. 3.34 Top view of the computational model of Co-Operative Market in PyroSim for clothing fuel condition. Fire source shop 1 (CoOp_CS1) and fire source shop 2 (CoOp_CS2) are highlighted by blue rectangles in (a) and (b) with clothing as fuel, respectively.
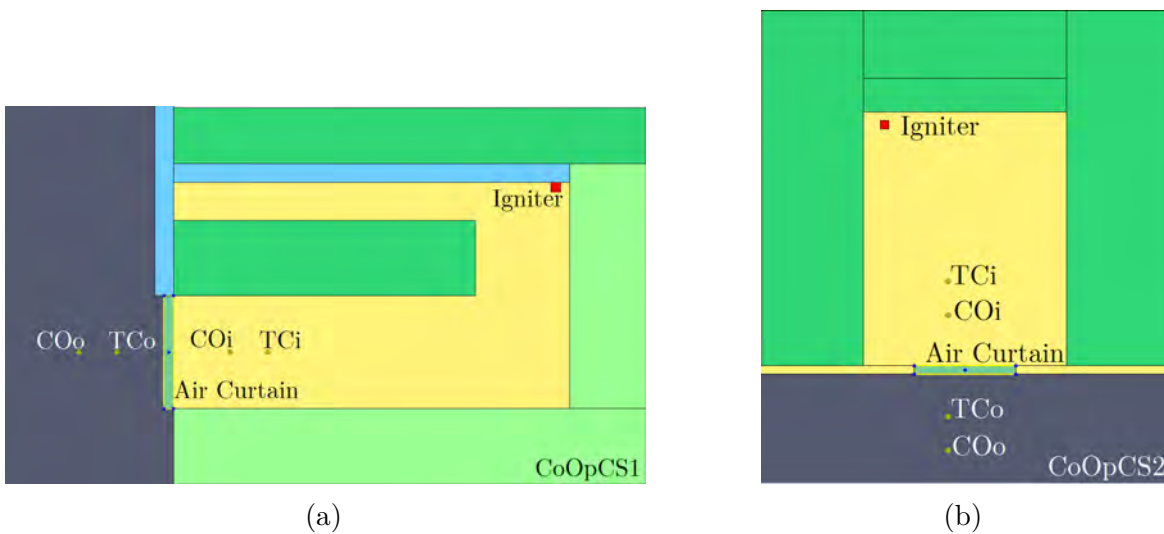

| (a) | (b) |

Fig. 3.35 Top view of the fire source shop 1 & 2 of Co-Operative Market (CoOp_S1) & (CoOp_S2), in PyroSim for clothing fuel condition. The respective positions of Igniter, Air curtain, Thermocouple (TCi and TCo) and CO devices (COi and COo) are highlighted.

notes and sketches taken during the survey as no CAD or manual drawing of floor plan was available for use. The floor and ceiling were designed as adiabatic and ends of the corridors and staircase top was designed as open boundary.

Fig. 3.36 Flame propagation through Co-Operative market source shop 1, CoOp_CS1, in case of clothing as fuel load. The top row shows the flame only, and bottom row shows both flame and smoke for 100s, 200s, 300s, 400s, 500s and 600s of simulation time respectively from left to right.

Fig. 3.37 Flame propagation through Co-Operative market source shop 2, i.e., for CoOp_CS2 simulation, in case of clothing as fuel load. The top row shows the flame only, and bottom row shows both flame and smoke for 100s, 200s, 300s, 400s, 500s and 600s of simulation time respectively from left to right.

The positions of the igniter, temperature and carbon monoxide measuring devices inside and outside of source and air curtain were shown in figure 3.51. Figure 3.35a shows the positions for fire source 1 and figure 3.35b shows the positions for fire source 2. For source shop 1 in Co-Operative market, the thermocouple TCi was placed 2.3 m horizontally left and 1.3 m vertically downward of the igniter in source 1. In source shop 2 the TCi was placed 0.62 m horizontally right and 1.37 m vertically downward of the igniter of source 2. The distance between TCi and TCo for both sources was 1.22 m and each CO devices were placed 0.31 m horizontally left of each thermocouple. The air curtains were placed at door of each source and thus in between the source inside outside measurement devices. The fuel load on source shop 1 of Co-Operative

Table 3.6 Flame and smoke propagation timeline for Co-Operative market for clothing fuel condition in source shop 1 and 2.

Event	Time (s)	
	CoOp_CS1	CoOp_CS2
Visible flame after ignition	55	55
Smoke came out of the source shop	75	70
Smoke filled source shop up to 1.524 m	125	-
Flame front came out of the shop	285	300
Fire spread to staircase inside	340	590
Smoke filled up the ceiling of the whole corridor	400	370
Fire came out of the source	440	600
Fire spread along the corridor	440	405
Fire violently burning in source shop front	450	460
Visibility lost at 1.524 m in total computational area	500	480
Fire spread to source adjacent shop insides	500	450
Fire spread to all shop insides	-	570
Fire sustains as enough fuel load still remains	600	600

market was 3024.5 kg, thus a 260.4 kg/m² fuel per unit area ratio. For source shop 2, the fuel load was 6354.5 kg, which made a 542.7 kg/m² fuel per unit area ratio for source shop 2, making it the largest fuel per unit area configuration. Table 3.5 shows the parameters for source shop 1 and 2.

Flame and smoke propagation for clothing store fire in Co-Operative market source shop 1 is shown in figure 3.36. The top row shows the flame only, and bottom row shows both flame and smoke for 100s, 200s, 300s, 400s, 500s and 600s of simulation time respectively from left to right. As of before, clothing fuel produces intense fire and vision obstructing smoke within a small period of time as evident from a quick overview from the figure 3.36. The fire was visible after 55s of ignition, and smoke came out of the source within 75s. Smoke filled up the shop up to 1.524 m from the floor around 125s. Flame front came out of the shop around 285s, and spread to the staircase at 340s. Flame again came out of the source due to pressure driven flow at 440s indicating flashover and fire burnt violently at 450s on corridor. Up to this point the flame propagation events closely followed DCC_CS1, except nearly 40s delay for flame front to came out of the shop, this was due to the low fuel per unit area ratio. After that, due to the bends in the corridors smoke spread to the perpendicular corridors slowly, and total corridor never fully covered in smoke up until 500s, thus nearly 100s after straight corridor of DCC market. The fire continued to burn up to
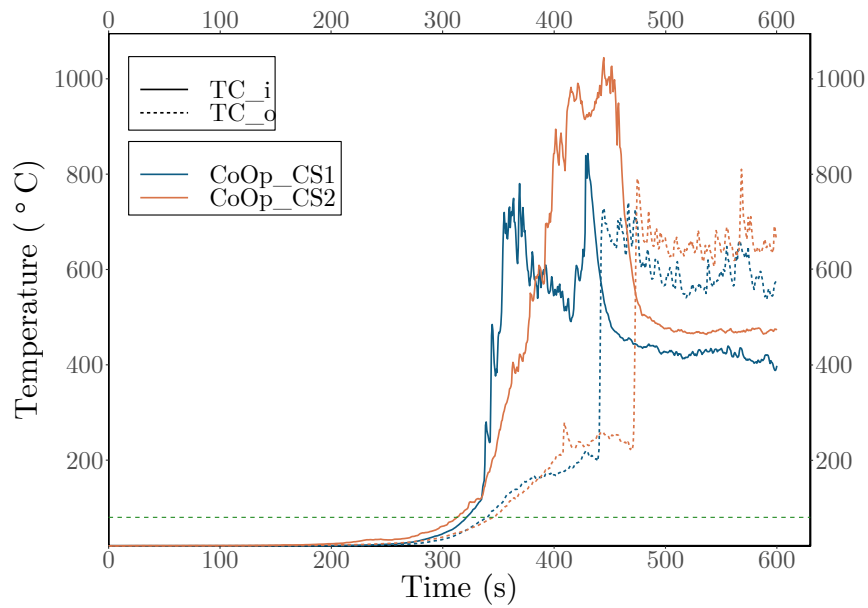
Fig. 3.38 Temperature distributions at positions TCi (inside the fire source) and TCo (outside the fire source) for air curtain at non-discharged condition for clothing fire scenario at Co-Operative market fire source shop 1 (CoOp_CS1) and fire source shop 2 (CoOp_CS2).
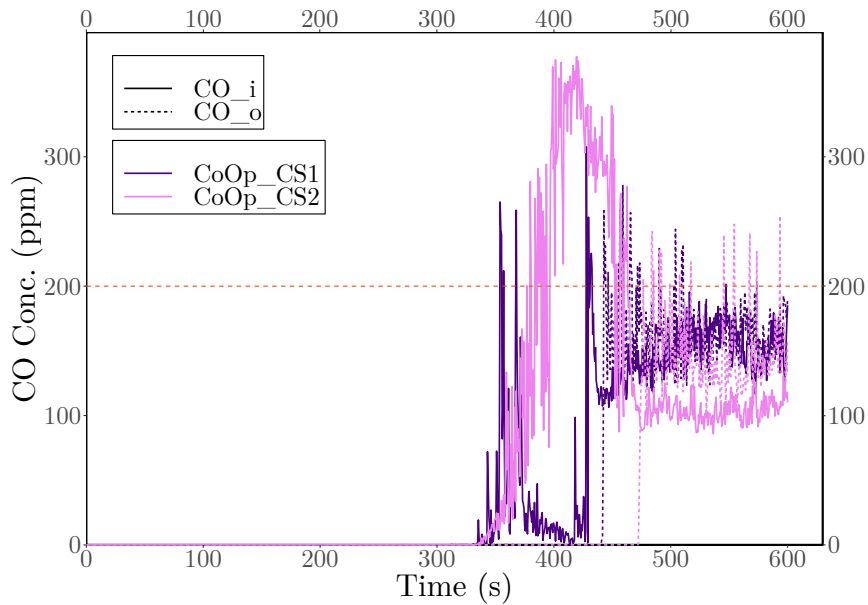

Fig. 3.39 Carbon monoxide concentration at positions COi (inside the fire source) and COo (outside the fire source) for air curtain at non-discharged condition for clothing fire scenario at Co-Operative market fire source shop 1 (CoOp_CS1) and fire source shop 2 (CoOp_CS2).

the end of simulation time due to availability of fuels. Figure 3.37 shows the flame and smoke propagation for clothing store fire in Co-Operative market source shop 2 for 100s, 200s, 300s, 400s, 500s and 600s of simulation time respectively from left to right. The flame again was visible after 55s and smoke came out of the shop a bit early at 70s as it faced no obstruction. And the smoke never fully filled up the source as it quickly moved to the corridor for this source, thus filled up the total ceiling of the computational area within 370s. The flame never came out of the source up until then end of the simulation, indicating there was ample oxidizers for the fuels to burn. Flame spread along the corridor at around 405s, 35s quicker than source 1. Flashover happened as the flame suddenly burnt violently at around 460s and visibility was lost at 1.524 m at around 480s. Fire engulfed the adjacent shops, corridors, and spread to total computational area at around 590s. It is evident that, fire originated at source 2 quickly spread in total computational area than source 1. This is because, the smoke and fire for source 2 needed to spread perpendicularly once to cover up the total area, whereas for source 1 they needed to move perpendicularly twice. Thus, fire originated at source 1, filled the total area with smoke a bit late, and flame never spread in the total computational area. Also, as the fuel per unit area was extremely higher than the rest of the scenarios considered, thus, generated fire was intense and burnt violently in total computation area than any other scenarios discussed earlier. Lastly, fire spread to staircase very late due to the large path distance between source and staircase. The flame and smoke propagation timeline for Co-Operative market for clothing fuel condition in source shop 1 and 2 is presented in table 3.6.

Figure 3.38 shows the temperature distributions at eye height, 1.524 m, for positions TCi (inside the fire source) and TCo (outside the fire source) for air curtain at non-discharged condition for clothing fire scenario at Co-Operative market fire source shop 1 (CoOp_CS1) and fire source shop 2 (CoOp_CS2). The temperature for TCi of CoOp_CS1 was below human tenability of 80ºC, the dashed green line in figure 3.38, up to 320s, and then increased rapidly up to 440s then dropped a little as the fire came out of the source shop at that time. The temperature peaked at 843ºC at 430s. And after 500s stayed nearly constant at above 400ºC for the rest of the simulation. The temperature outside the source 1, for TCo, increased steadily after 280s, stayed below 80ºC up to 340s, increased rapidly after that, and had a jump at 440s indicating the time when the fire came out of the shop, and remained near that mark until the end. For CoOp_CS2, temperature inside the source at TCi was below 80ºC up to 312s, and increased rapidly after that, going past the peak of CoOp_CS1, as it had more fuel load per unit area, reached 1044ºC at 445s. The temperature dropped at
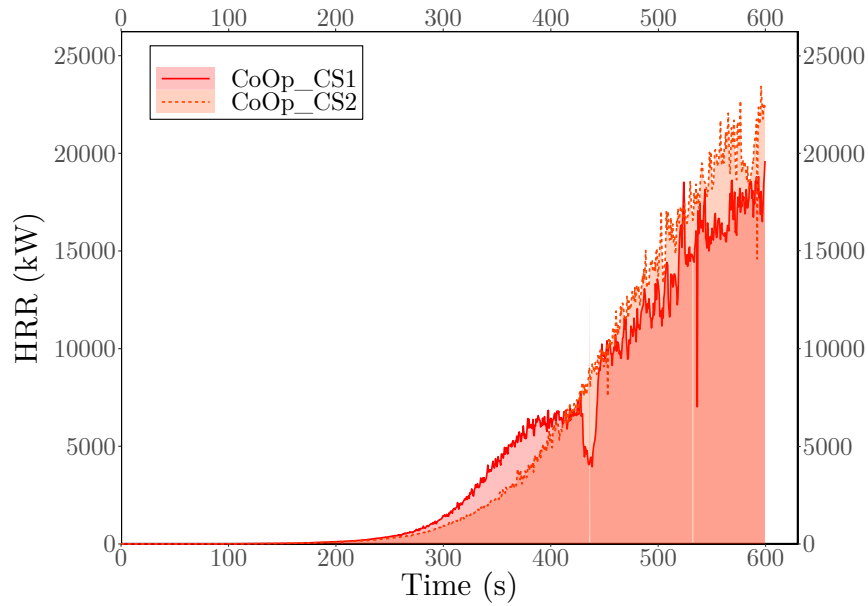
Fig. 3.40 Comparison of the Heat Release Rates (HRRs) for clothing fire scenarios for Co-Operative market at fire source shop 1 and 2 (CoOp_CS1 & CoOp_CS2) without air curtain discharged.
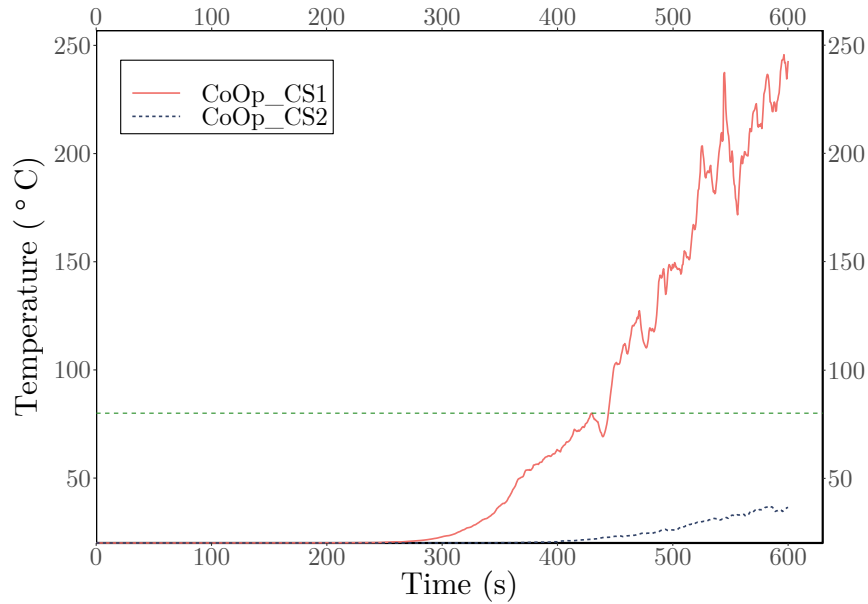

Fig. 3.41 Temperature distributions at staircase entrance for clothing fire scenario for Co-Operative market at fire source shop 1 and 2 (CoOp_CS1 & CoOp_CS2) with air curtain at non-discharged condition. The path distance from source to staircase for source 1 and 2 is 2.3 m and 14.6 m respectively.
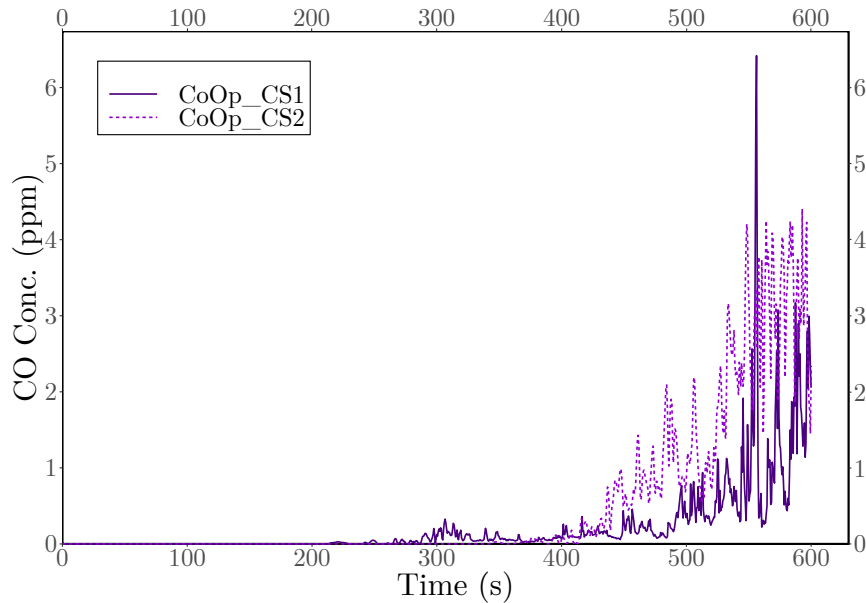
Fig. 3.42 CO concentration at at staircase entrance for clothing fire scenario for Co-Operative market at fire source shop 1 and 2 (CoOp_CS1 & CoOp_CS2) with air curtain at non-discharged condition. The path distance from source to staircase for source 1 and 2 is 2.3 m and 14.6 m respectively.

around 480s to 500ºC indicating the flashover event, and remain nearly constant up to the end of the simulation. The TCo for CoOp_CS2 increased steadily after 250s and stayed below 80ºC up to 345s. The jump in the temperature at around 475s to 791ºC again indicating the flashover event, the temperature than remained at that mark for the rest of the simulation. Figure 3.39 shows the carbon monoxide concentration at positions COi (inside the fire source) and COo (outside the fire source) for air curtain at non-discharged condition for clothing fire scenario at Co-Operative market fire source shop 1 (CoOp_CS1) and fire source shop 2 (CoOp_CS2). The significant jumps of all the curves in figure 3.39 mimicked the temperature curve as the followed the same events, but thankfully, lethal threshold for CO concentration for short exposure never reached.

Figure 3.40 shows heat release rate (HRR) for clothing fire scenarios for Co-Operative market at fire source shop 1 and 2 (CoOp_CS1 & CoOp_CS2). The dip in CoOp_CS1 HRR curve at around 440s indicate the oxygen deficiency at source and steady CoOp_CS2 HRR curve indicated that due to the open wall at shop front there was never any shortage of oxidizers for CoOp_CS2. For CoOp_CS1 total heat released was 3907 Tera Joule at 336.4 TJ/m^2 and for CoOp_CS2 total heat released was 3127 Tera Joule at 267 TJ/m^2. Here again although the fuel load for CoOp_CS2

was nearly twice the CoOp_CS1, total heat released was lower than CoOp_CS1 and thus, total heat released per unit area was lower. Thus, although CoOp_CS2 had extreme fuel load, like DCC_CS2, the total heat released not scaled as much even though CoOp_CS2 did not face any oxidizer shortage like DCC_CS2.

Figure 3.41 and figure 3.42 show the temperature distributions and CO concentrations at eye height, at staircase entrance, for clothing fire scenario for Co-Operative market at fire source shop 1 and 2 (CoOp_CS1 & CoOp_CS2) respectively. The path distance from source to staircase for source 1 and 2 is 2.3 m and 14.6 m respectively. Thus, due to smaller path distance the effect of the fire reached much quickly in staircase when originated at source 1 than source 2. The conditions in case of CoOp_CS1 breached human temperature tenability after 430s, and for CoOp_CS2 never crossed the tenability limit for the simulation time considered. The CO concentration for both cases never became lethal at staircase. Although this pattern agreed with the previously seen case of DCC market, the peak temperature at staircase in case of fire at Co-Operative market source shop 1 was only 242°C as the source front fire did not burnt with the extreme intensity which was observed for DCC_CS1 case.

3.1.2.2 Propagation of Fire and Smoke for furniture store fire

In the next step the Co-Operative market was designed with furniture fuel and investigated to observe if there was any change in conditions in this geometry with furniture fire. Figure 3.43 shows the top view of the computational model of Co-Operative Market in PyroSim for furniture fuel condition. Figure 3.43a and figure 3.43b show fire source shop 1 and fire source shop 2 positions in the geometry, highlighted in blue rectangles, respectively. The source were as seen from the figure 3.43 kept same as of clothing fire. The thermocouple and carbon monoxide positions were also kept same. Figure 3.44 and figure 3.45 show flame and smoke propagation through Co-Operative market in case of furniture as fuel load for 100s, 200s, 300s, 400s, 500s and 600s of simulation time respectively from left to right, for source shop 1 (named CoOp_FS1), and source shop 2 (named CoOp_FS2), respectively. A quick observation on both the figures 3.44 and 3.45, revealed that, once again furniture fire did not propagated much outside of the initiation zone and smoke also did not obstruct vision during total simulation time. Figure A.4 and figure 3.47 show the temperature distributions and carbon monoxide concentration at positions inside the fire source and outside the fire source, for CoOp_FS1 and CoOp_FS2. Once more, the change in the temperature and carbon monoxide concentration inside the source and outside the source were never
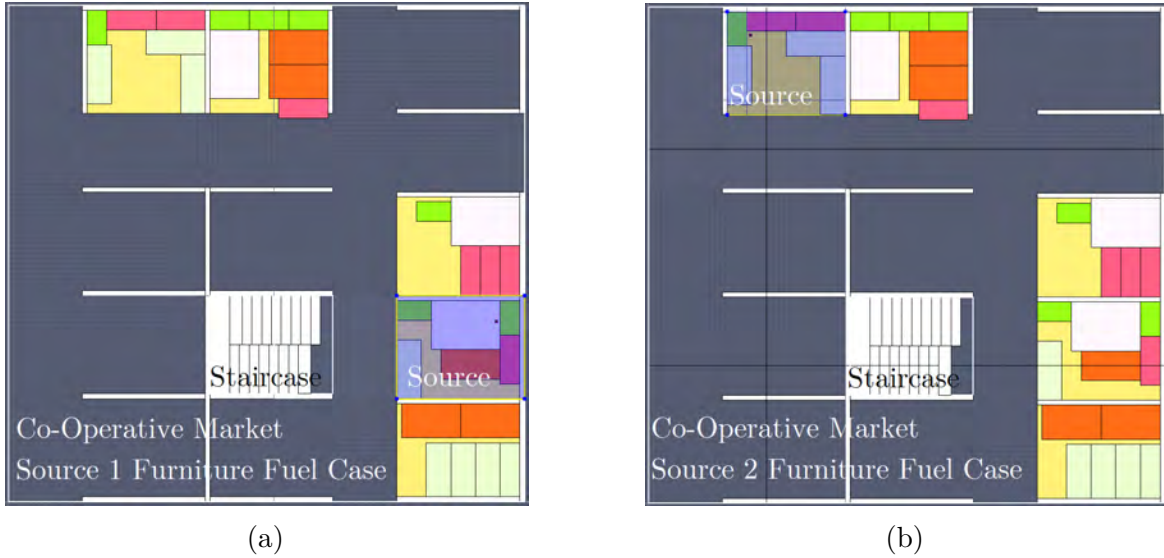
(a)   (b)

Fig. 3.43 Top view of the computational model of Co-Operative Market in PyroSim for furniture fuel condition. The positions of fire source shop 1 (CoOp_FS1) and fire source shop 2 (CoOp_FS2) are highlighted by blue rectangles in (a) and (b) respectively.

Fig. 3.44 Flame and smoke propagation through Co-Operative market source shop 1, CoOp_FS1, in case of furniture as fuel load. The figure shows both flame and smoke for 100s, 200s, 300s, 400s, 500s and 600s of simulation time respectively from left to right.

Fig. 3.45 Flame and smoke propagation through Co-Operative market source shop 2, CoOp_FS2, in case of clothing as fuel load. The figure shows both flame and smoke for 100s, 200s, 300s, 400s, 500s and 600s of simulation time respectively from left to right.

increased significantly during the time considered, thus the fuel was discarded from further geometric variations.
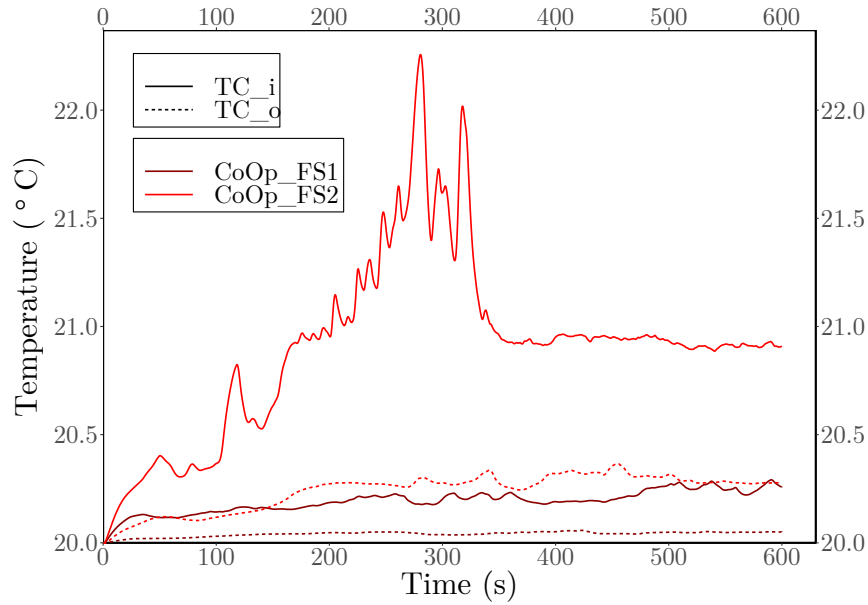
Fig. 3.46 Temperature distributions at positions TCi (inside the fire source) and TCo (outside the fire source) for air curtain at non-discharged condition for furniture fire scenario at Co-Operative market source 1 (CoOp_FS1) and source 2 (CoOp_FS2).
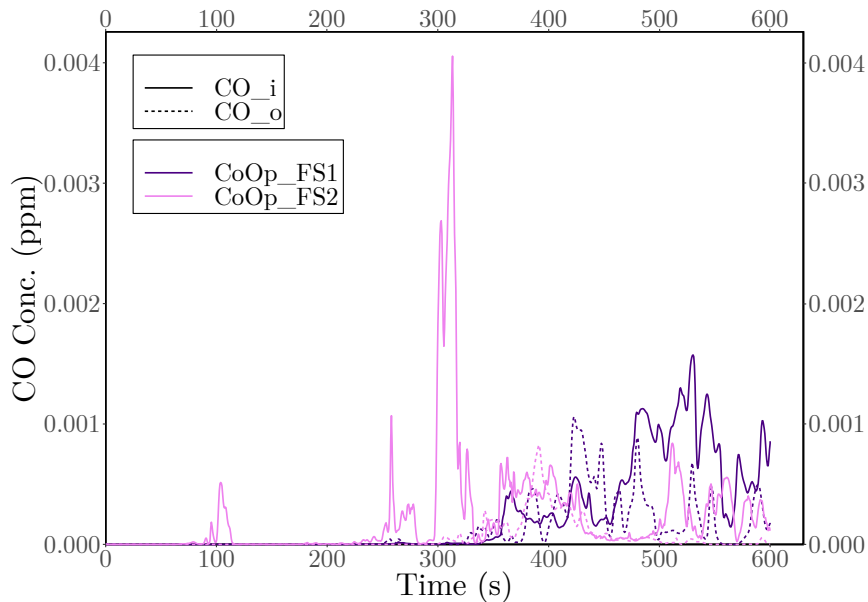

Fig. 3.47 Carbon monoxide concentration at positions COi (inside the fire source) and COo (outside the fire source) for air curtain at non-discharged condition for CoOp_FS1 and CoOp_FS2.

3.1.3 Shopping Mall-3: MultiPlan shopping complex from New Elephant Road, Dhaka

3.1.3.1 Fire and smoke propagation for clothing store fire

MultiPlan shopping complex on new elephant road is one of the prominent shopping complex in Dhaka. Although popular for computer related electronic products, up until recent redecoration, the ground floor of the market hosted clothing stores. Two characteristics of the MultiPlan shopping complex made it a choice to investigate in this study, one, it had a large open space in the middle surrounding the escalator and another was the fairly spacious fuel distribution, which was a rare occurrence for clothing store among the surveyed shopping malls. Figure 3.48 shows 3D computational model of MultiPlan shopping complex in PyroSim with clothing as fuel. The fuel distribution was again inspired by the photographs taken during the survey.
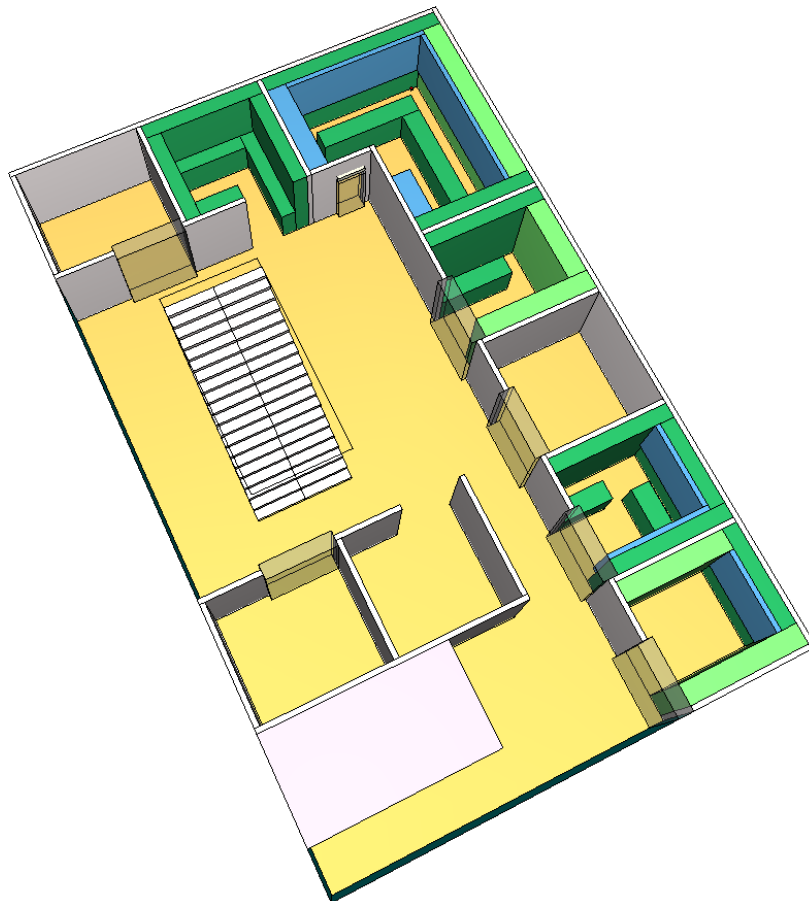

Fig. 3.48 The 3D computational model of MultiPlan shopping complex in PyroSim. The shops are designed with clothing as fuel.

(a)   (b)

Fig. 3.49 Photographed clothing stores in MultiPlan shopping complex during the survey.
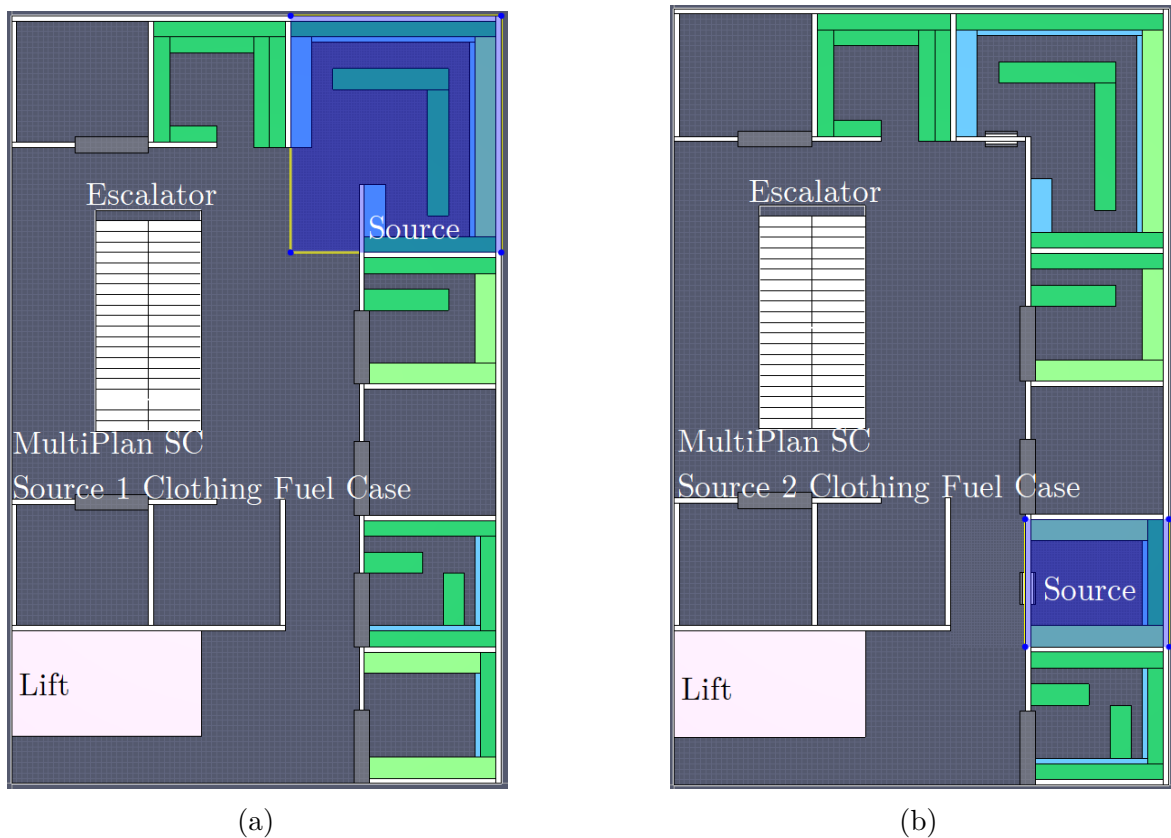

(a)   (b)

Fig. 3.50 Top view of the computational model of MultiPlan shopping complex in PyroSim for clothing fuel condition. Fire source shop 1 (MP_CS1) and fire source shop 2 (MP_CS2) are highlighted by blue rectangles in (a) and (b) with clothing as fuel, respectively.

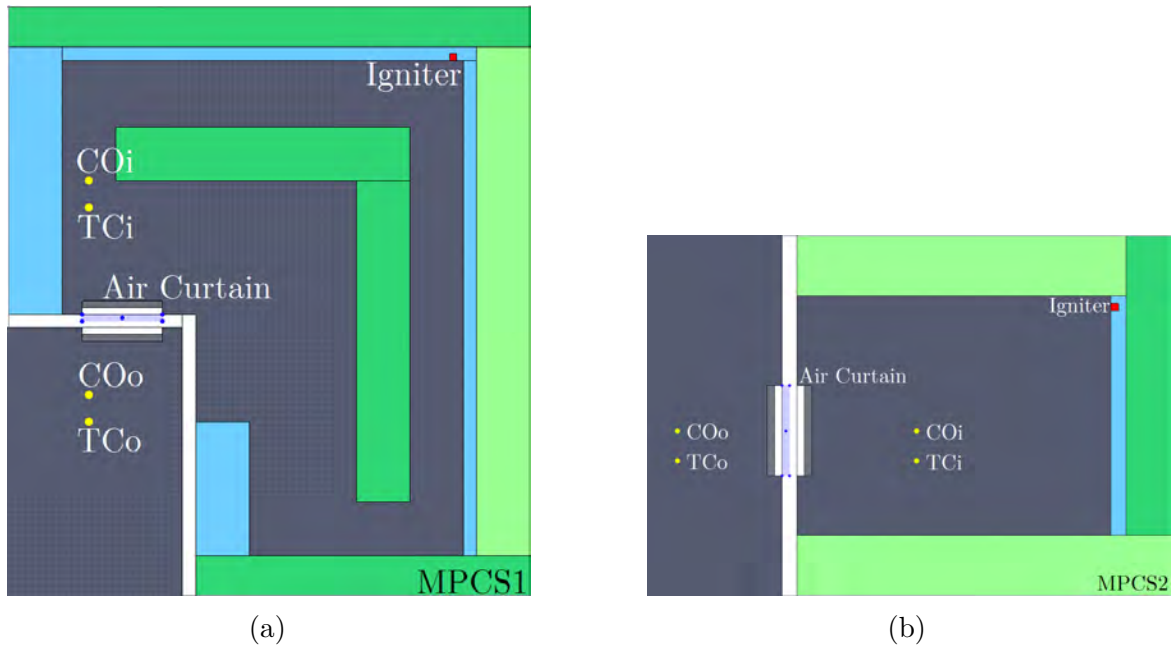(a)   (b)

Fig. 3.51 Top view of the fire source shop 1 & 2 of MultiPlan shopping complex (MP_CS1) & (MP_CS2), in PyroSim for clothing fuel condition. The respective positions of Igniter, Air curtain, Thermocouple (TCi and TCo) and CO devices (COi and COo) are highlighted.

Figure 3.49 shows such two actual clothing stores in MultiPlan shopping complex, and they clearly indicate the differences of fuel stacking from DCC market and Co-Operative market shops mentioned earlier. Two shops of 33 m² and 13.94 m² floor area were chosen as the source for this geometry. First source with 33m² floor area was near the staircase and in a corner to assist propagation along both corridors. And, second source with 13.94 m² floor area was at the end of the larger corridor. Figure 3.50 shows top view of the computational model of MultiPlan shopping complex in PyroSim for clothing fuel condition. Position of the fire source shop 1 (named MP_S1) and fire source shop 2 (named MP_S2) are highlighted by blue rectangles in figure 3.49a and figure 3.49b respectively. The respective positions of Igniter, Air curtain, Thermocouple (TCi and TCo) and CO devices (COi and COo) are highlighted in figure 3.51a and figure 3.51b for MP_S1 and MP_S2 respectively. For source shop 1 in MultiPlan shopping complex, the thermocouple TCi was placed 4.12 m horizontally left and 1.68 m vertically downward of the igniter in source 1. In source shop 2 the TCi was placed 1.98 m horizontally right and 1.53 m vertically downward of the igniter of source 2. The distance between TCi and TCo for source 1 and 2 were 3.66 m and 2.44 m respectively, and each CO devices were placed 0.31 m horizontally left of each

Table 3.7 Parameters of MultiPlan Shopping Complex source shop 1 and 2.

Name	Source 1	Source 2
Simulation name	MP_CS1	MP_CS2
Fuel type	Clothing	Clothing
Heat Release Rate per unit area	1528 kW/m^2	1528 kW/m^2
Shop area	33 m^2	13.94 m^2
Path distance to staircase	13 m	10.2 m
Fuel load	8342.1 kg	2697.6 kg
Fuel load to shop area ratio	252.6 kg/m^2	193.5 kg/m^2
Simulation time	600s	600s
Total Heat Released	3358 Tera Joule	4167 Tera Joule
Total Heat Released per unit area	101.7 TJ/m^2	299 TJ/m^2

Fig. 3.52 Flame propagation through MultiPlan shopping complex source shop 1, MP_CS1, in case of clothing as fuel load. The top row shows the flame only, and bottom row shows both flame and smoke for 100s, 200s, 300s, 400s, 500s and 600s of simulation time respectively from left to right.

thermocouple. The fuel load on source 1 was 8342.1 kg with 252.6 kg/m^2 fuel load per unit area ratio, and for source 2 was 2697.6 kg with 193.5 kg/m^2 fuel load per unit area ratio. For both source simulation was again performed for 600s. Table 3.7 shows the parameters for source shop 1 and 2.

Figure 3.52 shows the flame propagation for clothing fire in MultiPlan shopping complex source shop 1, MP_CS1, for 100s, 200s, 300s, 400s, 500s and 600s of simulation
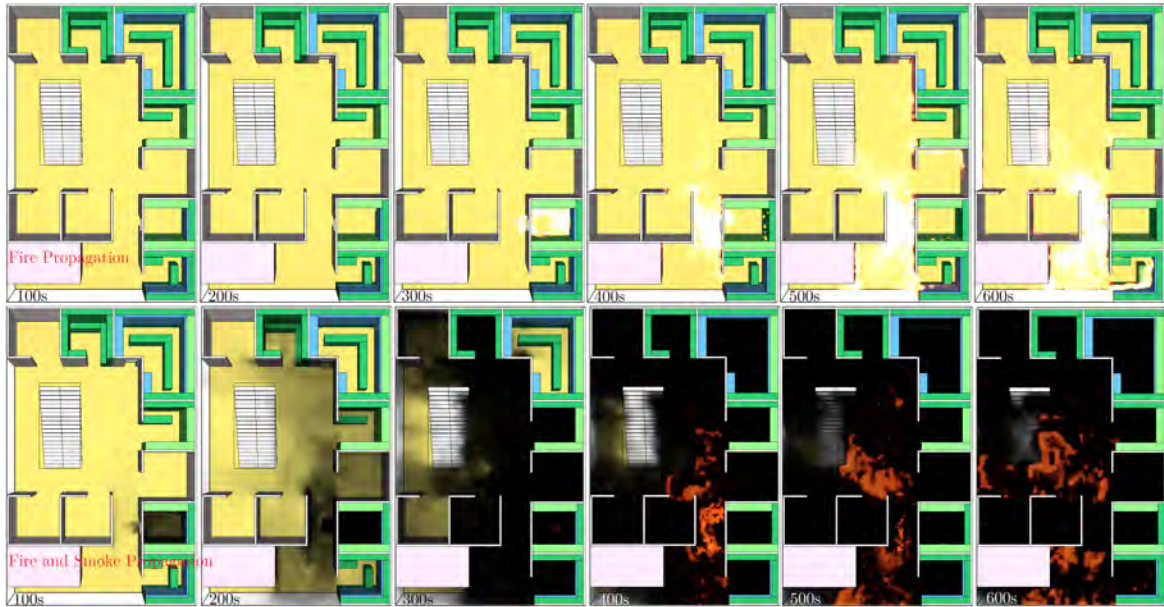
Fig. 3.53 Flame propagation through MultiPlan shopping complex source shop 2, MP_CS2, in case of clothing as fuel load. The top row shows the flame only, and bottom row shows both flame and smoke for 100s, 200s, 300s, 400s, 500s and 600s of simulation time respectively from left to right.

time respectively from left to right. The flame was again visible after 55s of ignition. And smoke came out of the source shop in about 80s. This slight delay was due to the large floor area of the source. And as it was also open in nearly an entire boundary, the visibility was lost up to 1.524 m due to smoke after nearly 400s, 25s after the flame front went out of the shop. The staircase was in an open space which also played an important role not to allow smoke build up inside the computation area. And at around 560s, visibility was lost at eye height for the entire computational area, i.e., nearly 150s after DCC_CS1. Also, nearly 80s after CoOp_CS2, and that geometry had perpendicular corridors to obstruct smoke propagation. The flame came out of the source at 375s, nearly 120s after DCC market source shop 1, which was also due to that fact that, MP_CS1 had a larger floor area. Fire spread to the staircase at around 450s, at that time the smoke filled up the source completely and cover the ceiling of the computational area. Fire came out of the source due to oxygen deficiency at 530s and burnt violently in front of the source at 540s, indicating the flashover event. Thus, the flashover, delayed for 150s than DCC_CS1, without any drastic difference in fuel load per unit area than DCC_CS1, and delayed for 100s than CoOp_CS1 at nearly same fuel load per unit area. Fire spread to the adjacent shop and along the corridor at 540s, i.e., during flashover and although flame was burning intensely up to

Table 3.8 Flame and smoke propagation timeline for MultiPlan Shopping Complex for clothing fuel condition in source shop 1 and 2.

Event	Time (s)	
	MP_CS1	MP_CS2
Visible flame after ignition	55	46
Smoke came out of the source shop	80	70
Smoke filled source shop up to 1.524 m	400	150
Flame front came out of the shop	375	265
Fire spread to staircase inside	450	460
Smoke filled up the ceiling of the whole corridor	450	390
Smoke filled up the source shop	450	315
Fire came out of the source	530	410
Fire spread along the corridor	540	
Fire violently burning in source shop front	540	430
Visibility lost at 1.524 m in total computational area	560	490
Fire spread to source adjacent shop insides	540	430
Fire spread to all shop insides	-	-
Fire sustains as enough fuel load still remains	600	600

600s, i.e., up to end of the simulation time considered for MP_CS1, fire never engulfed the entire computational area inside this time. In short, the larger floor area even with the same fuel load per unit area, showed resistance to flashover and a wide open space around the staircase ensured visibility for a longer period of time. Figure 3.53 shows the flame propagation in case of clothing fire in MultiPlan shopping complex source shop 2, MP_CS2, for 100s, 200s, 300s, 400s, 500s and 600s of simulation time respectively from left to right. The flame propagation events were similar to DCC_CS1 and CoOp_CS1, the small delay in each flame events were due to the fact that it had lower fuel load per unit area than those two scenarios. Having an open space in the middle in place of staircase was helpful to reduce the smoke accumulation to hinder visibility as it was evident once again in MP_CS2. Also, the flame propagation to extreme ends of the computational area also faced obstruction due to this open space as visible from MP_CS2. The flame and smoke propagation timeline for Co-Operative market for clothing fuel condition in source shop 1 and 2 is presented in table 3.8.

Figure 3.54 shows the temperature distributions at positions TCi (inside the fire source) and TCo (outside the fire source) for source shop 1 (MP_CS1) and source shop 2 (MP_CS2). The temperature inside the source 1 at position TCi was below human temperature tenability of 80°C for 384s, largest among all other source considered, the
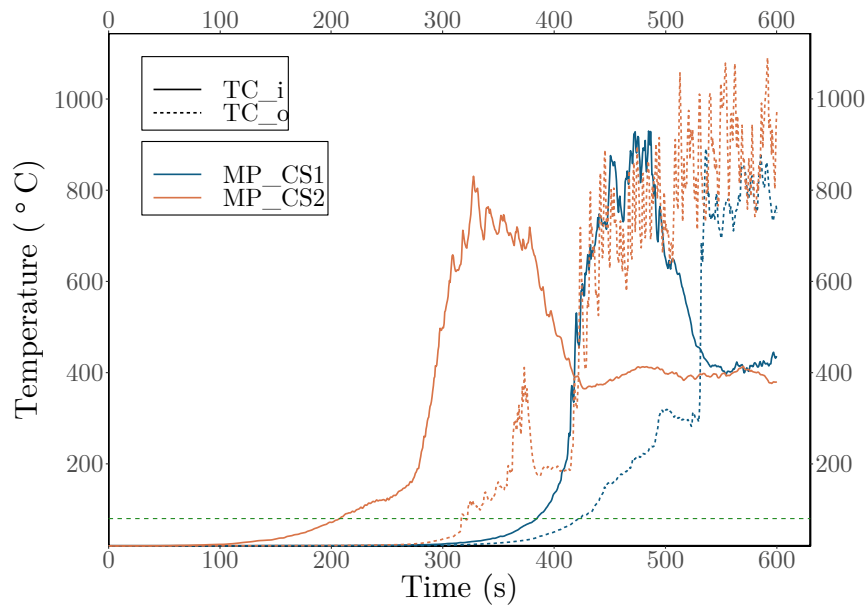
Fig. 3.54 Temperature distributions at positions TCi (inside the fire source) and TCo (outside the fire source) for air curtain at non-discharged condition for clothing fire scenario at MultiPlan shopping complex fire source 1 (MP_CS1) and fire source 2 (MP_CS2).
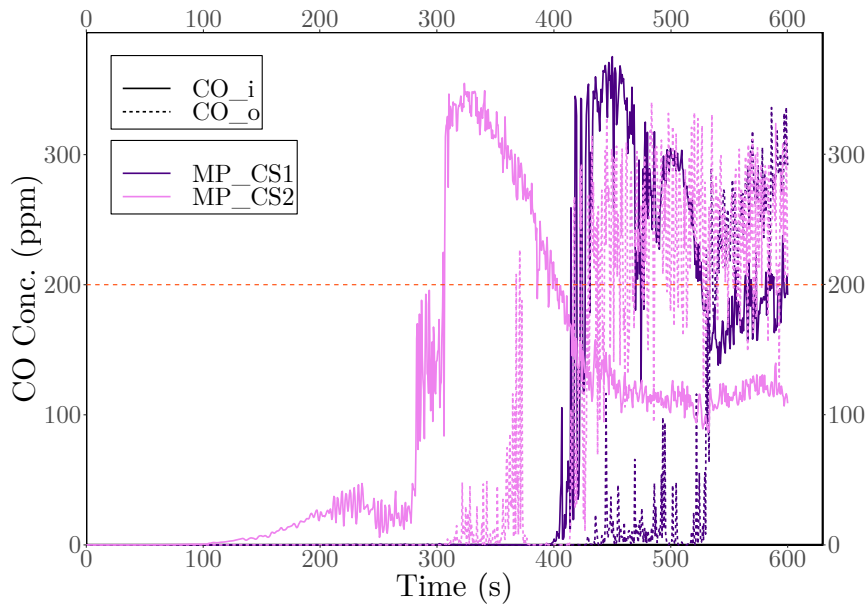

Fig. 3.55 Carbon monoxide concentration at positions COi (inside the fire source) and COo (outside the fire source) for air curtain at non-discharged condition for clothing fire scenario at MultiPlan shopping complex fire source 1 (MP_CS1) and fire source 2 (MP_CS2).
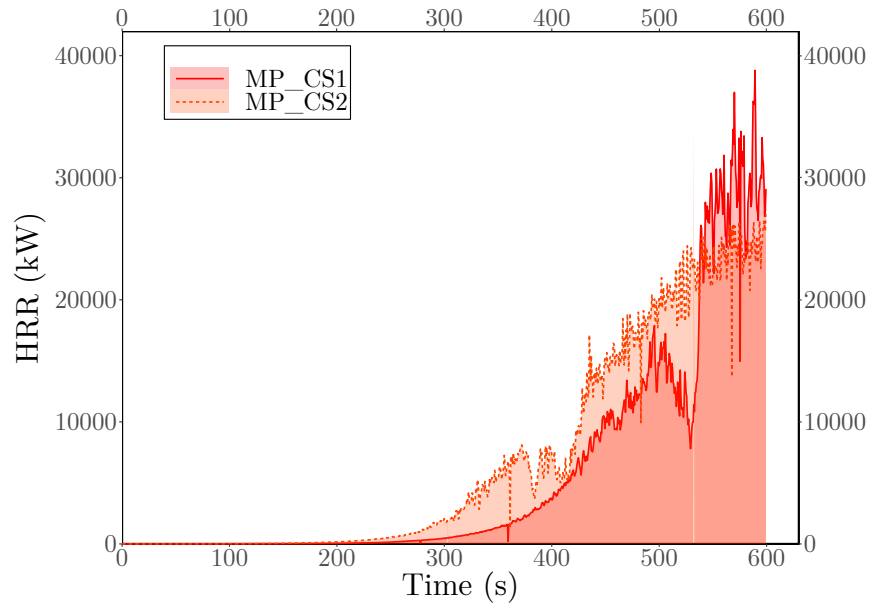
Fig. 3.56 Heat Release Rate (HRR) for clothing fire scenarios for MultiPlan shopping complex at fire source shop 1 and 2 (MP_CS1 & MP_CS2) without air curtain discharged.

temperature rapidly increased at around 410s and peaked at 929ºC at 484s, temperature dropped sharply after that indicating the oxidizer shortage inside the source and as fire came out of the source at 530s due to the pressure driven flow, temperature inside the source remained nearly constant at around 400s for rest of the simulation. Outside temperature at TCo for source 1 increased rapidly as fire came out of the source, the flashover and characterized by the cross-over of outside temperature curve with the inside one. And, as fire continued burning outside the source for the rest of the simulation temperature at TCo remained at around 800ºC with a peak of 830ºC at 577s. For source 2, the inside temperature remained below 80ºC for 207s and then raised steadily up to 280s. Rapid increment was observed after that, with a peak at 830ºC at 327s, then dropped to 400ºC due to oxidizer shortage. The outside curve closely followed the curve for source 1, but it was nearly 100s advanced in each step. In conclusion, the safe evacuation time for source shop 1 was nearly 150s more than DCC_CS1, and at least 60s or more for all other source considered, a clear indication of MP_CS1 to be a much preferable shop design in case of a fire hazard. Figure 3.55 shows carbon monoxide concentration at positions COi (inside the fire source) and COo (outside the fire source) for MP_CS1 and MP_CS2. Here again the oxidizer deficiency and the flashover events were visible, with the indication of the source 2 leading the steps by nearly 100s.
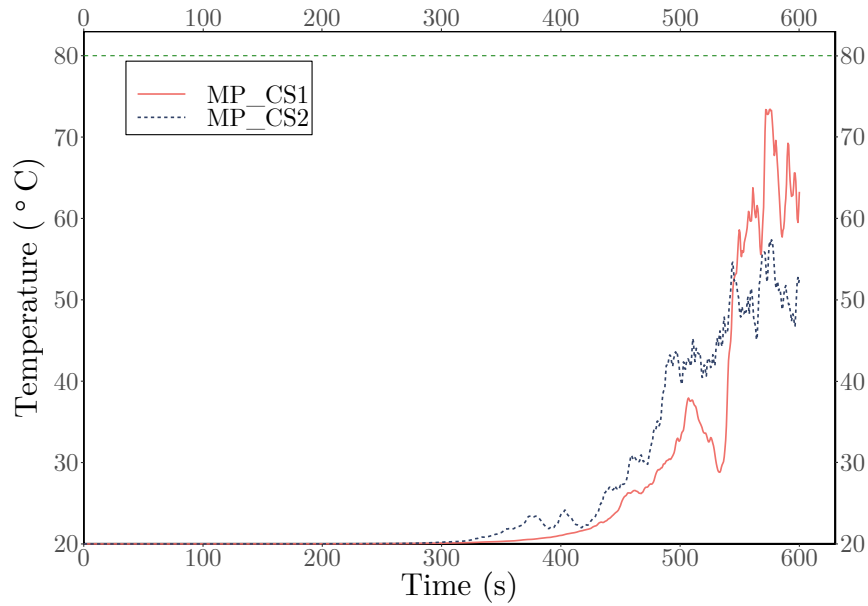
Fig. 3.57 Temperature distributions at staircase entrance for clothing fire scenario for MultiPlan shopping complex at fire source shop 1 and 2 (MP_CS1 & MP_CS2) with air curtain at non-discharged condition. The path distance from source to staircase for source 1 and 2 is 13 m and 10.2 m respectively.
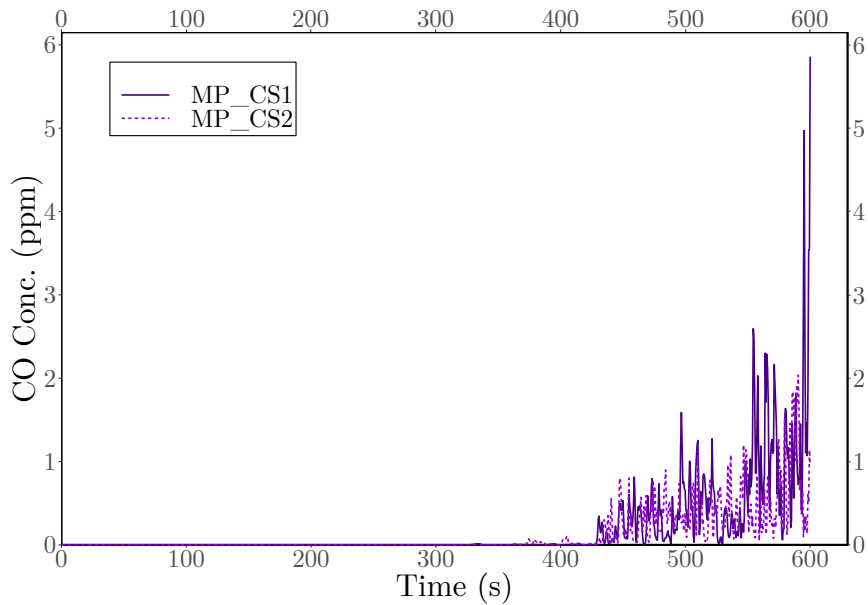

Fig. 3.58 CO concentration at at staircase entrance for clothing fire scenario for MultiPlan shopping complex at fire source shop 1 and 2 (MP_CS1 & MP_CS2) with air curtain at non-discharged condition. The path distance from source to staircase for source 1 and 2 is 13 m and 10.2 m respectively.

Figure 3.56 shows heat release rate (HRR) for clothing fire scenarios for MultiPlan shopping complex at fire source shop 1 and 2 (MP_CS1 & MP_CS2). The dip in the HRR curve at 530s for source 1 indicates the oxygen deficiency at source and subsequent flashover event due to pressure driven flow for MP_CS1, and event happened for MP_CS2 much earlier at around 410s. Using Simpson's 1/3 rule, the total heat released was 3358 Tera Joule for source shop 1, thus a 101.7 TJ/m^2 heat released per unit area, significantly lower than CoOp_CS1, at nearly same fuel load per unit area ratio. Thus, a shop with larger floor area with same fuel load per unit area ratio should be preferable for fire safety. The source 2 had 4167 Tera Joule total heat released at 299 TJ/m^2, nearly equivalent to other shops of similar size and fuel to area ratio. And lastly, the contribution of the wide space around the staircase is visible from figure 3.57 and figure 3.58, as the represent the temperature distributions and carbon monoxide concentration at staircase entrance for MP_CS1 and MP_CS2 respectively. For fire originated from either sources, the human tenability for temperature and CO concentration for short exposure, were never exceeded, making this geometry a safer one among all other geometries considered in this study.

3.1.3.2 Summary of the effect of the variation of architecture in different shopping malls

The flame propagation through three architectural variations with two sources in each variation, a total of six scenarios were discussed in above sections. In pursuit of finding a suitable architectural configuration to aid evacuation during a fire hazard, flame propagation along corridor to staircase, a crucial position during evacuation, was analyzed. Figure 3.59 shows the ratio of staircase temperature to source outside temperature in function of time for both sources of DCC market, Co-Operative market and MultiPlan Shopping Complex. The source outside temperature indicate the heat that came out of the source, thus eliminating the effect of the source in this analysis, and concerning with the propagation along the corridor only. Hence, the ratio here indicates the percentile of heat propagated through the corridor to the staircase entrance after it emerged from the source. The initially value of T_{stair}/T_{out} was observed as 1, as the temperature at source outside and at staircase entrance were same as the ambient temperature. The sudden dip in all the curves indicated that, the source outside temperature raised suddenly, meaning the heat begun to transfer from the source to the corridor. The filled circle in each line indicates the time at which human tenability limit was crossed at source outside. MP_CS1 being last reflect that, indeed it was the preferable source condition among the six source considered in this present study.
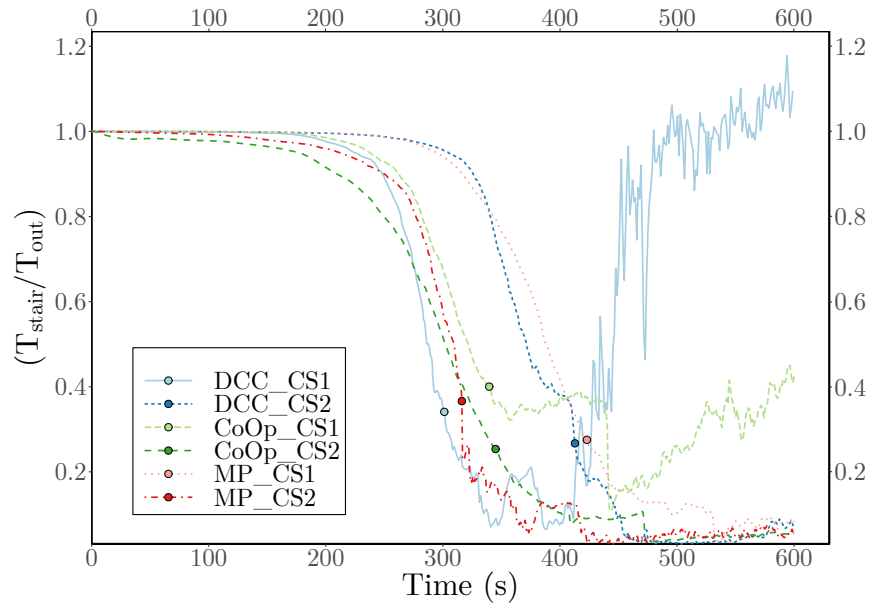
Fig. 3.59 Staircase temperature to source outside temperature ratio in function of time, for all geometric variations.

DCC_CS1 and CoOp_CS1 being the staircase front shop, transferred nearly 100% and 40% of the source emerged heat to staircase respectively. The percentile for DCC_CS1 went above 100% indicating that the fire was burnt more violently at staircase than at source front. And, DCC_CS2, CoOp_CS2 and MP_CS2 being furthest from staircase, transferred only 6~8% of the emerged heat to the staircase. However, in spite of being staircase front shop, due to the large wide space around the staircase, MP_CS1 transferred a maximum 12% of the emerged heat to the staircase. Thus, conclusion could be drawn as to include a wide space around the staircase for safer evacuation during a fire hazard.

3.2 Effects of Air Curtain on Fire and Smoke Propagation

The present study aimed to confine fire and smoke propagation through source shop door by installing an air curtain at source shop door, ergo, creating an aerodynamic sealing between the source and outside. For that reason, the effect of an air curtain, on fire and smoke propagation, was investigated for all the shopping mall fire scenarios discussed in previous section. The investigated air curtain was a single jet vertical air curtain (zero degree jet angle), with a cross section of 7.62 cm (jet width) × 91.4 cm (jet height), installed at source shop door at 2.13 m height from the floor. The velocity of the jet was taken as 10 m/s, which yielded a flowrate of 2500 m³/h. The parameters of the air curtain taken in this study closely resembled a commercially available off-the-self air curtain. The following sections discussed the effect of air curtain in confining heat and mass transfer from source shop for different geometric variations, fuel type and distribution variations, and air curtains position of installment variations. Table 3.9 provides an overview of the simulation cases covering these variations.

3.2.1 DCC Market from Gulshan-1

3.2.1.1 Clothing store fire with air curtain: Source shop 1

For the first case with air curtains, DCC source shop 1 with clothing as fuel was chosen to study the effect of air curtain at source shop door on flame and smoke propagation. The flame and smoke propagation, temperature, and carbon monoxide concentration at critical places during evacuation were compared for with and without air curtain case to observe the sealing property of air curtain. Figure 3.60 and 3.77 show flame propagation through DCC market source shop 1, in case of clothing as fuel load, with a vertical air curtain of 7.62 cm jet width and 10 m/s jet velocity, the simulation named DCC_CS1AC throughout this study. Due to the effect of air curtain injected air stream, the air inside the source gain sufficient movement and helped the combustion process inside the source, as a result the visible flame after ignition was at 42 seconds, 3 seconds earlier than no air curtain case. The air curtain contained stream of smoke out of the source for at least 25s more than no curtain case. Flame front came out of the source shop at around 265s, around 18s later than no curtain case. The full room involvement, the indication of already happened flashover event for no curtain case, DCC_CS1 was at 262s, whereas for the air curtain discharged case, DCC_CS1AC, was around at 280s. Smoke filled up the whole corridor at 350s, again nearly 50s later

Table 3.9 Summary of simulations conducted with a vertical air curtain at 2.13 m height.

| Case	Shopping mall	Source shop	Fuel type	Curtain position	Fuel Distribution	Curtain velocity (m/s)
1	DCC market	Source 1	Clothing	At source	Actual	0.0
2						10.0
3					Grid	0.0
4						10.0
5					Display	0.0
6						10.0
7				Staircase	Actual	10.0
8					Grid	10.0
9				Source & Stair	Actual	10.0
10					Grid	10.0
11			Furniture	At source	Actual	0.0
12						10.0
13		Source 2	Clothing	At source	Actual	0.0
14						10.0
15					Grid	0.0
16						10.0
17					Display	0.0
18						10.0
19				Staircase	Actual	10.0
20					Grid	10.0
21				Source & Stair	Actual	10.0
22					Grid	10.0
23			Furniture	At source	Actual	0.0
24						10.0
25	Co-Operative	Source 1	Clothing	At source	Actual	0.0
26						10.0
27					Grid	0.0
28						10.0
29				Source & Stair	Actual	10.0
30			Furniture	At source	Actual	0.0
31						10.0
32		Source 2	Clothing	At source	Actual	0.0
33						10.0
34					Grid	0.0
35				Staircase	Actual	10.0
36			Furniture	At source	Actual	0.0
37						10.0
38	Multiplan	Source 1	Clothing	At source	Actual	0.0
39						10.0
40					Grid	0.0
41					Display	0.0
42		Source 2	Clothing	At source	Actual	0.0
43						10.0

Fig. 3.60 Flame propagation through DCC market source shop 1, DCC_CS1AC, in case of clothing as fuel load, with a vertical air curtain of 7.62 cm jet width and 10 m/s jet velocity. The top row shows the flame propagation only, and bottom row shows both flame and smoke propagation for 50s, 100s, 150s, 200s, 250s and 300s of simulation time respectively from left to right.

than no curtain case. Flame spread to staircase at 370s, about 30s late compared no curtain case. Hence, the discharged air curtain jet could delay the fire events up to this point than no discharge case. But the events following did not match earlier sequence, and fire came out of the source shop after flashover 30s earlier than no curtain case. And, as the fire came out of the source shop, the air curtain case fire events proceeded aggressively than no curtain case. The comparative fire events for discharged and non-discharged case for DCC source shop 1 with clothing fuel is shown in table 3.10. These initial observation from smoke and flame propagation data from FDS revealed, although the injection and circulation of air, i.e., the oxidizer, improved the combustion process inside the source but the jet indeed provided aerodynamic sealing against smoke and fire propagation as expected up to certain point.

Figure 3.62 shows mean smoke temperature profiles at different positions or non-discharged and discharged cases for DCC market source shop 1 with clothing as fuel up to 250s of simulation time. The reason behind this specific amount of time was
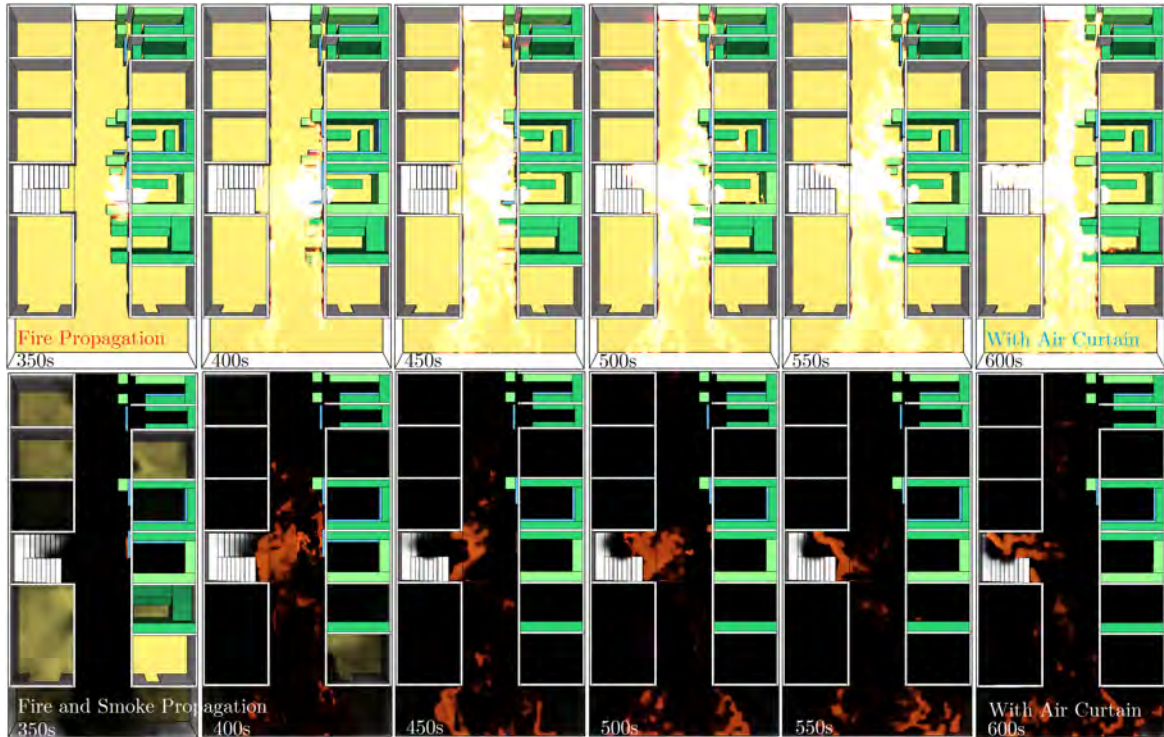
Fig. 3.61 Flame propagation through DCC market source shop 1, DCC_CS1AC, in case of clothing as fuel load, with a vertical air curtain of 7.62 cm jet width and 10 m/s jet velocity. The top row shows the flame propagation only, and bottom row shows both flame and smoke propagation for 350s, 400s, 450s, 500s, 550s and 600s of simulation time respectively from left to right.

to observe the effect of air curtain before flame came out of the source, as after that the effectiveness of air curtain declines. The top row shows mean temperature profile downstream (outside the source) of the air curtain at three positions, the bottom row shows mean temperature profile upstream (inside the source) of the air curtain at three positions. Inside the source, without air curtain the temperature profile showed clear contrast between upper smoke layer and lower layer. But with air curtain discharged, the motion of the jet created circulation inside the source, thus, the upper layer temperature reduced and lower layer temperature increased for at $x = -0.9144$ m and $x = -0.6096$ m. At $x = -0.3048$ m, the temperature profile had nearly 50ºC increased value for every instance. This confirmed that, verily combustion improved inside the source due to the air circulation as estimated by the flame propagation observations earlier. From the top row figures of figure 3.62, the upper smoke layer without air curtain was evidently blocked by air curtain jet at all sections. But as the jet momentum reduces downwards due to interaction with the smoke and ambient
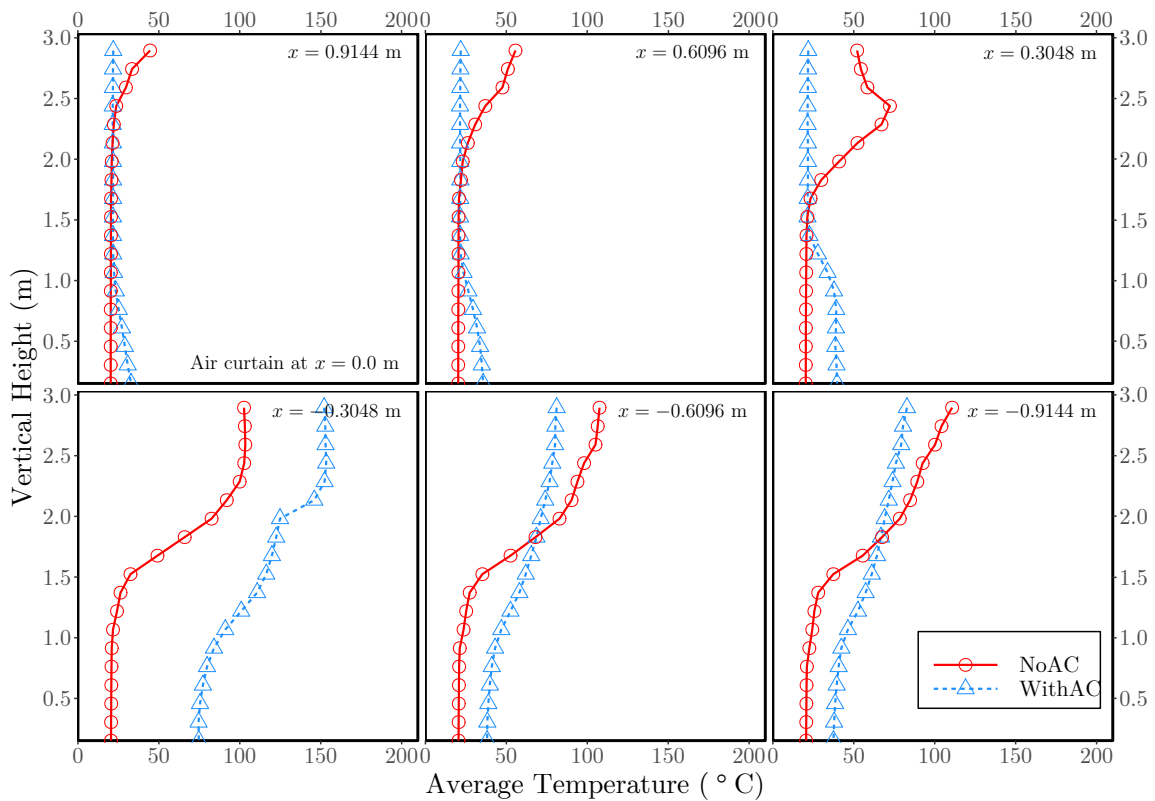
Fig. 3.62 Mean smoke temperature profiles up to 250s, at different positions downstream (top) and upstream (bottom) of the air curtain jet (air curtain at x=0) for non-discharged (DCC_CS1) and discharged (DCC_CS1AC) cases for DCC market source shop 1 with clothing as fuel.

air, the deflected hot smoke from upper layer escaped from lower segment of the door at around 1 m from the floor. The increase in lower layer temperature just after air curtain at $x = 0.3048$ m, was nearly 20°C, indicating considerable amount of heat and smoke could leak from bottom of the air curtain. An important observation could be made from these figures that, air curtain jet improved combustion inside the source but was also able to contain the increased temperature and the resultant combustion gas pressure, inside the source for considerable amount of time, i.e., for 250s with decent bottom leakage due to momentum reduction at jet front. The detailed understanding on effect of air curtain on evacuation required additional investigations on the temperature profile and carbon monoxide concentration in critical regions.

Table 3.10 Flame and smoke propagation timeline for DCC market for clothing fuel condition in source shop 1.

Event	Time (s)	
	No Air Curtain (DCC_CS1)	With Air Curtain (DCC_CS1AC)
Visible flame after ignition	45	42
Smoke came out of the source shop	80	105
Flame front came out of the shop	247	265
Smoke filled up the whole corridor	300	350
Fire spread to staircase inside	330	370
Fire came out of the source	390	360
Fire violently burning in source shop front	430	457
Fire fully engulfed the corridor	460	455
Fire spread to all adjacent shop insides	560	530

3.2.1.2 Effectiveness of Air Curtain

A well accepted measure of evaluating the aerodynamic sealing by air curtain is to measure its effectiveness. Effectiveness E of air curtain, is defined as the fraction of the exchange flow prevented by the air curtain compared to an unobstructed open door. The effectiveness E, could be measured by the equation (3.2), where, Q_a is the heat transfer through the door with the air curtain discharged and Q_{open} is the heat transfer through the door without the air curtain, respectively.

$$E = 1 - \frac{Q_a}{Q_{open}} \tag{3.2}$$

Figure 3.63 shows the effectiveness of air curtain measured with equation 3.2 for DCC market source shop 1 with clothing as fuel in function of time. The effectiveness was very low at early stages of fire, at around 2.3% at 200s. The air curtain's ability to contain the fire-induced heat inside the source shop was perceptible from the increased effectiveness at 250s to 43.7%. The maximum effectiveness about 55.8% was obtained at 300s. The effectiveness declined after that to 33.7% at 350s and further down to 3.3% at 400s, indicating that sufficient amount of heat escaped after 300s as fire came out of the source shop overcoming the jet momentum. Although at 300s the maximum effectiveness was obtained, the present study report air curtain effectiveness up to the time when flame came out of the source shop for no curtain condition. For DCC market source shop 1 the flame came out time was 247s, and effectiveness at that time was about 37.1%. This discards the extreme heat difference for a very short
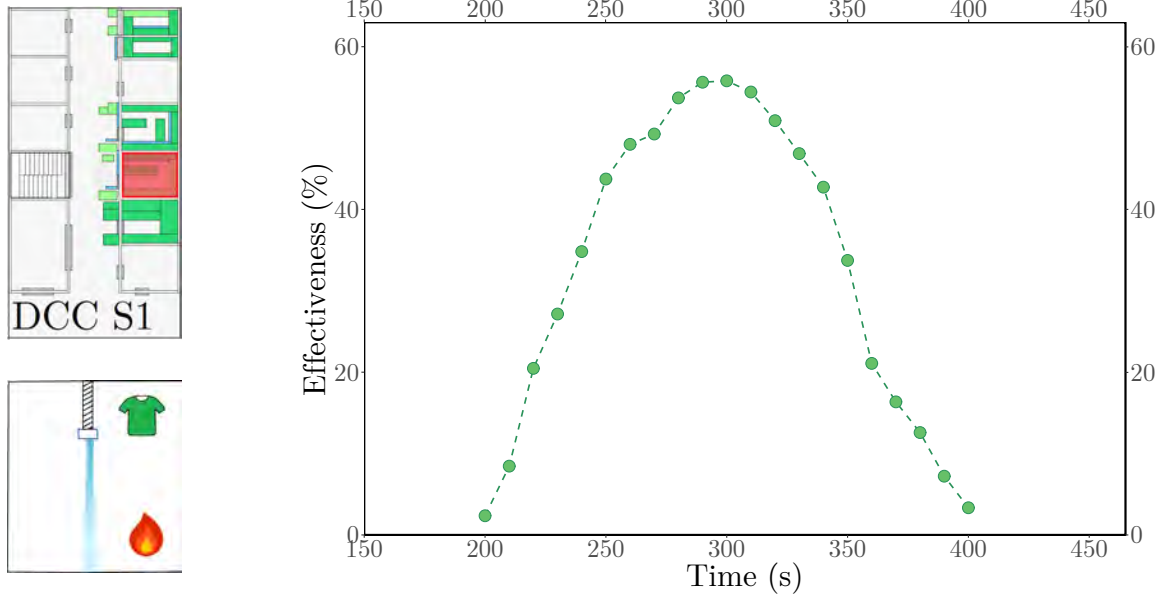
114

Fig. 3.63 Effectiveness of air curtain (7.62 cm jet width and 10 m/s jet velocity), in function of time for DCC_CS1AC.

time, when flame came out from the source shop for no curtain condition but stayed inside the source for air curtain discharged condition, i.e., the high effectiveness at 300s, unrealistically larger than any other time.
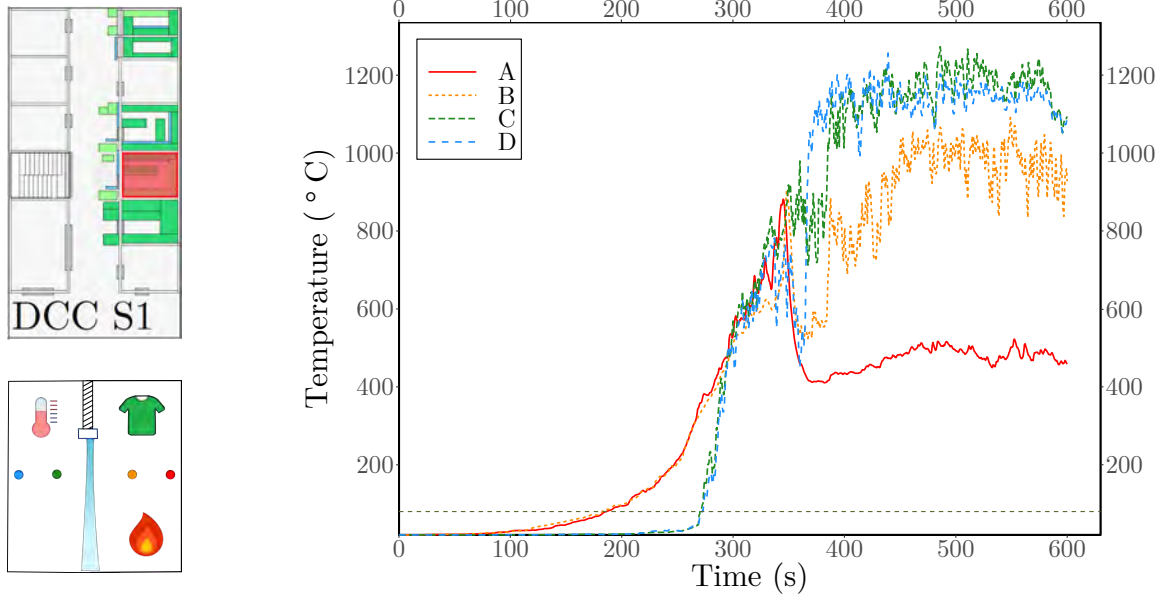
Figure 3.64 shows the temperature distributions at eye level (1.54 m), at positions A, B (inside the fire source) and C, D (outside the fire source) with air curtain discharged at 10 m/s, for DCC_CS1AC simulation case. With the introduction of air curtain, the temperature profile for these points divided into two distinct segment up to the flashover phase, rather than the gradual pattern seen for no curtain condition. This again provided convincing evidence that the curtain jet certainly contained the heat inside the source up to flashover. But the temperature at position D with air curtain discharged crossed the human tenability of 80°C at around 272s, around 35s earlier than no curtain case, as without the curtain the temperature was below the human tenability up to 307s. Figure 3.65 shows the temperature distributions at eye level (1.54 m), at positions A (inside the fire source) and D (outside the fire source), for air curtain at non-discharged condition compared with air curtain discharged case (at 10 m/s). And from this figure 3.65 is was evident that, source outside temperature at position D, with air curtain discharged (blue curve) crossed the human tenability earlier than non-discharged case (red curve).

Fig. 3.64 Temperature distributions at eye level (1.54 m) for positions A, B (inside the fire source) and C, D (outside the fire source) with air curtain discharged at 10 m/s, for DCC_CS1AC.
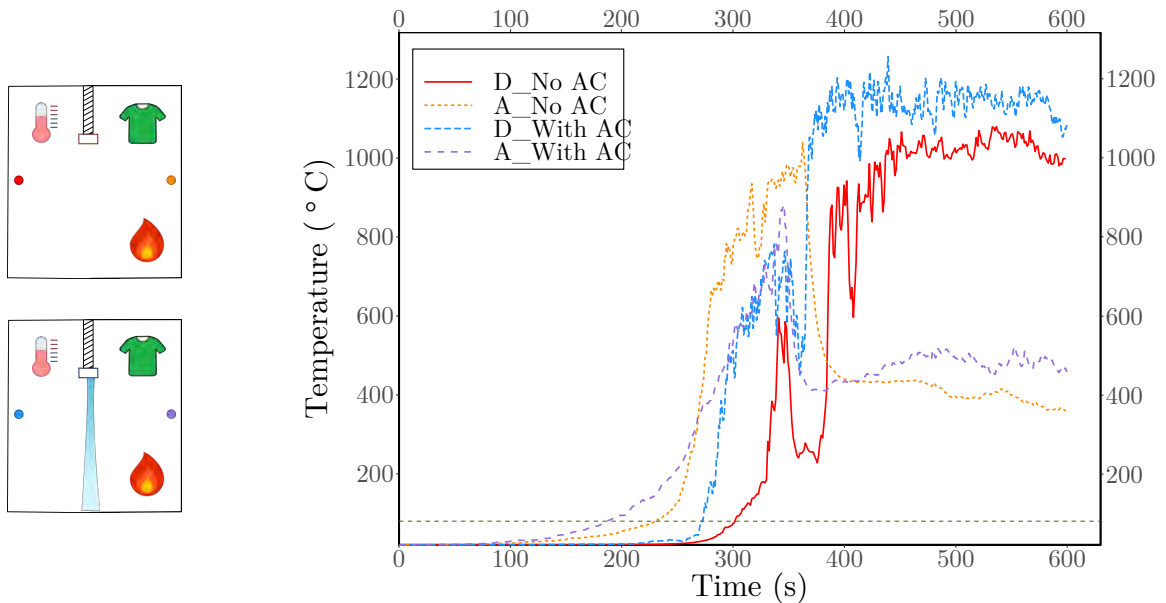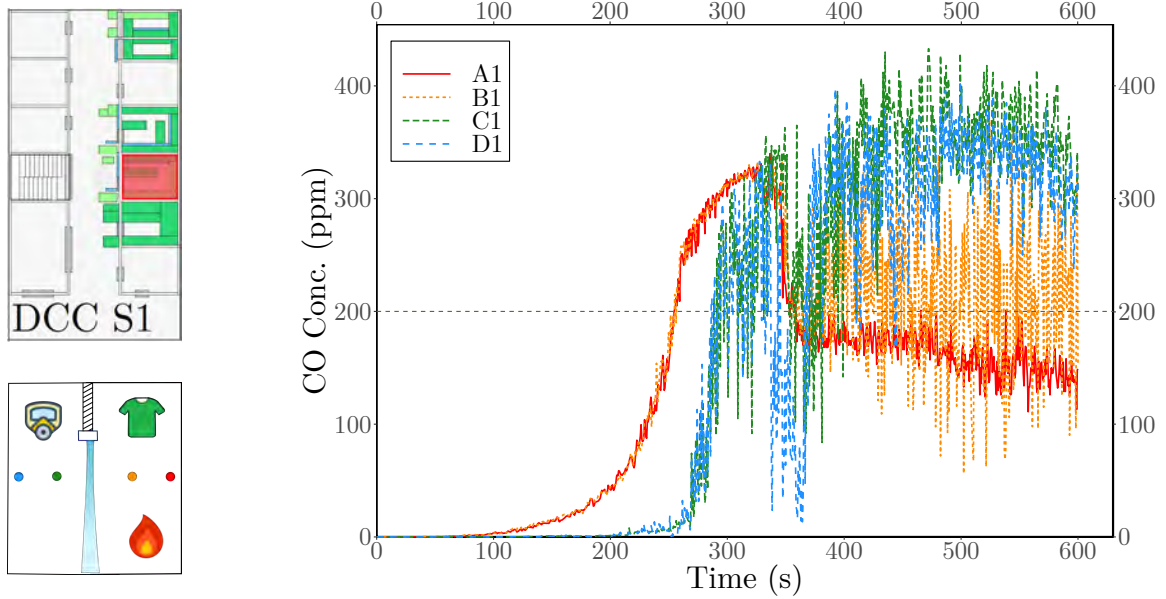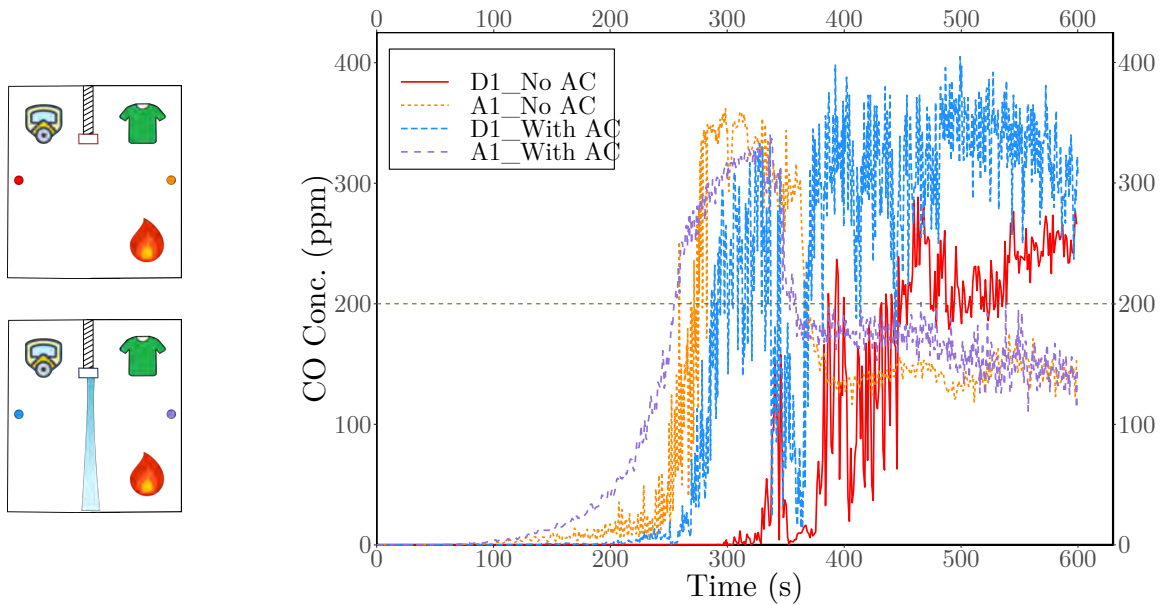

Fig. 3.65 Temperature distributions at eye level (1.54 m) for positions A (inside the fire source) and D (outside the fire source), for air curtain at non-discharged condition compared with air curtain discharged at 10 m/s, for DCC_CS1 and DCC_CS1AC.

Fig. 3.66 CO concentration at eye level (1.54 m) for positions A1, B1 (inside the fire source) and C1, D1 (outside the fire source) with air curtain discharged at 10 m/s, for DCC_CS1AC.

Fig. 3.67 CO concentration at eye level (1.54 m) for positions A1, (inside the fire source) and D1 (outside the fire source), for air curtain at non-discharged condition compared with air curtain discharged at 10 m/s, for DCC_CS1 and DCC_CS1AC.

117
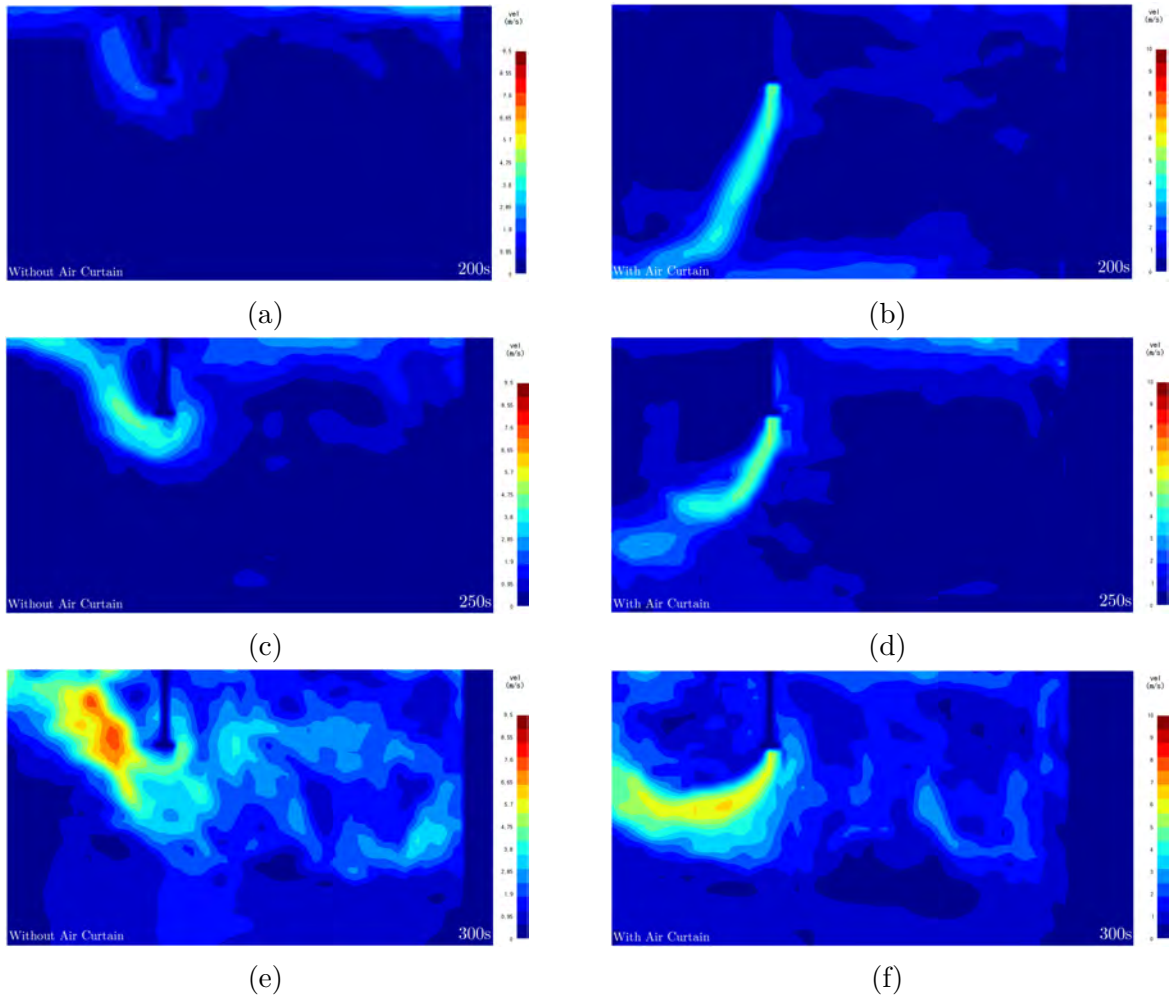
Fig. 3.68 Velocity contours for a vertical plane passing through the points A and D of DCC market source shop 1. Figure (a), (c), and (e) show the velocity contours at 200s, 250s and 300s for air curtain at non-discharged condition. Figure (b), (d), and (f) show the velocity contours at 200s, 250s and 300s for air curtain discharged at 10 m/s.

The carbon monoxide concentration curves at eye level (1.54 m) for positions A1, B1 (inside the fire source) and C1, D1 (outside the fire source) with air curtain discharged at 10 m/s, for DCC_CS1AC was plotted in figure 3.66. The CO concentration was well below the lethal concentration for short exposure, and again two distinct regions of concentration before and after air curtain were seen. And, the comparison of CO concentration at eye level (1.54 m) for position A1, (inside the fire source) and D1 (outside the fire source), for air curtain discharged and non-discharged condition is shown in figure 3.67. Observations from figure 3.66 and figure 3.67 again justify that, although air curtain could contain the increased smoke pressure inside the source, the source outside position D1 experienced increased CO while air curtain was discharged
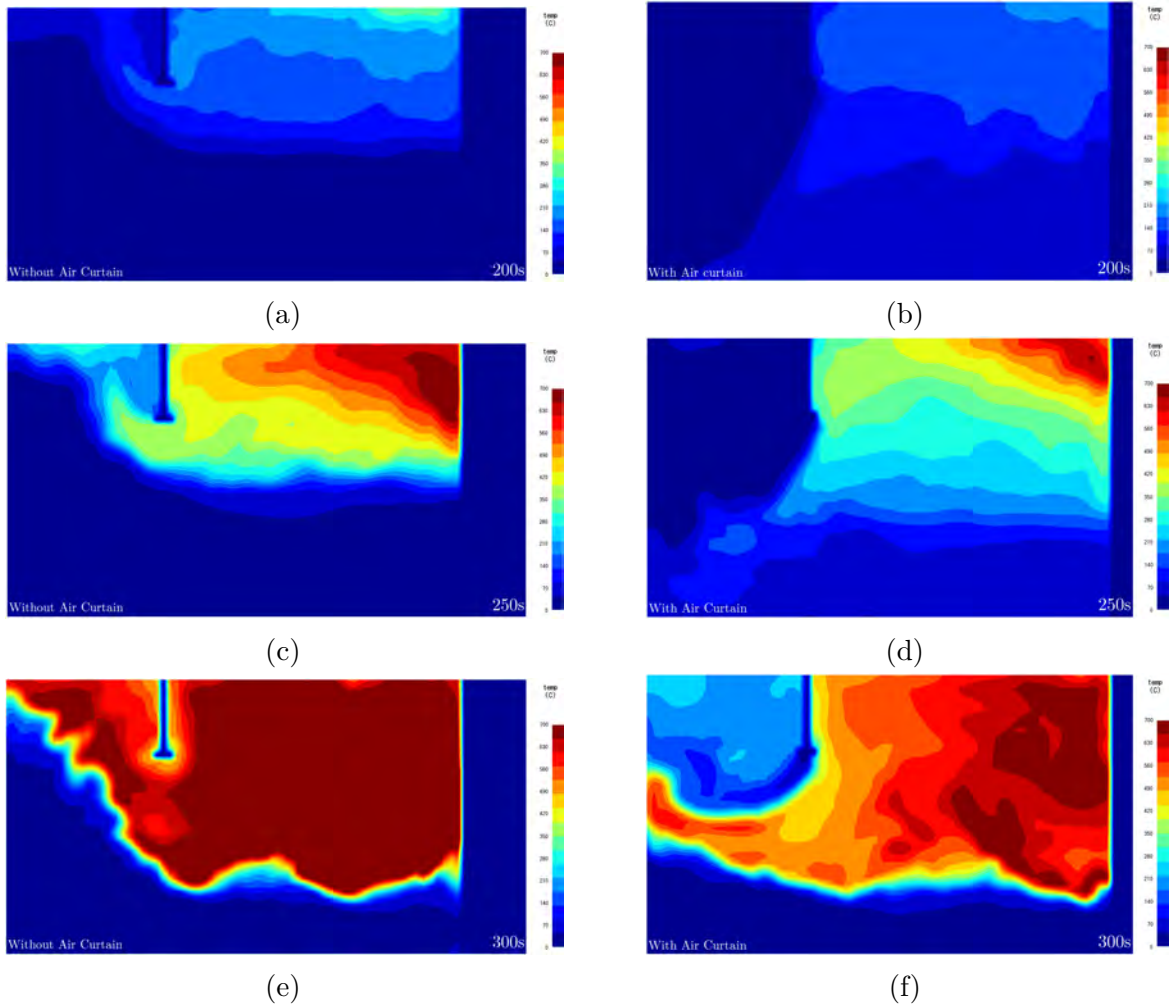
Fig. 3.69 Temperature contours for a vertical plane passing through the points A and D of DCC market source shop 1. Figure (a), (c), and (e) show the temperature contours at 200s, 250s and 300s for air curtain at non-discharged condition. Figure (b), (d), and (f) show the temperature contours at 200s, 250s and 300s for air curtain discharged at 10 m/s.

than non-discharged condition. This discrepancy between the effectiveness data and temperature profiles of discharged and non-discharged at eye level might baffle an oblivious observant but there was a rational explanation to this phenomenon.

Figure 3.68 shows velocity contours for a vertical plane passing through the points A and D of DCC market source shop 1. Figure 3.68a, 3.68c, and 3.68e show the velocity contours at 200s, 250s and 300s for air curtain at non-discharged condition. Figure 3.68b, 3.68d, and 3.68f show the velocity contours at 200s, 250s and 300s for air curtain discharged at 10 m/s. The figure 3.68 clearly portraits the difference in smoke movement with and without air curtain. Without the curtain hot smoke
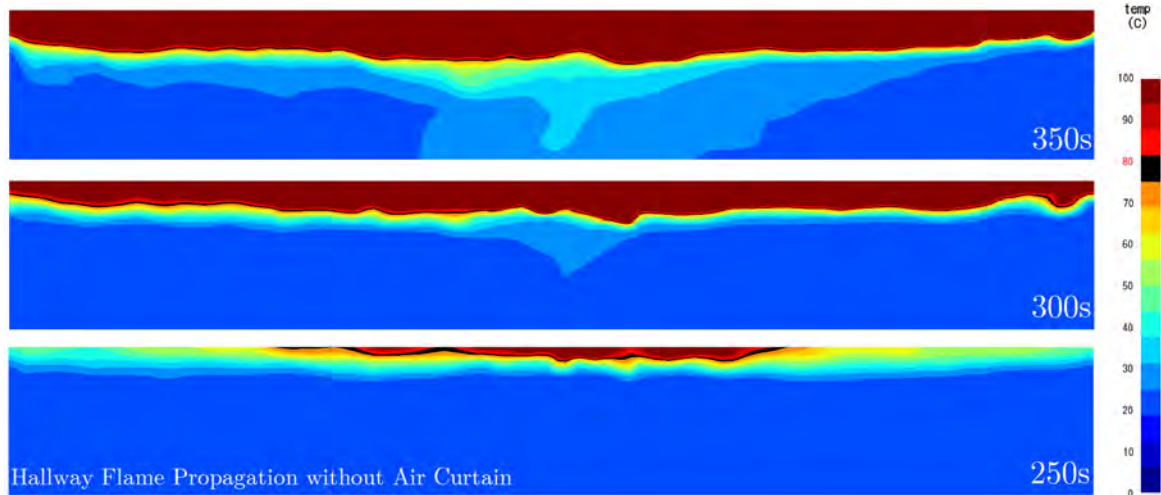
Fig. 3.70 Temperature contours at 250s, 300s and 350s for a vertical plane passing through the middle of the hallway width for air curtain at non-discharged condition. The hallway is 21.94 m long with the source shop at about in middle of the hallway. Human temperature tenability, 80ºC is highlighted with black color.
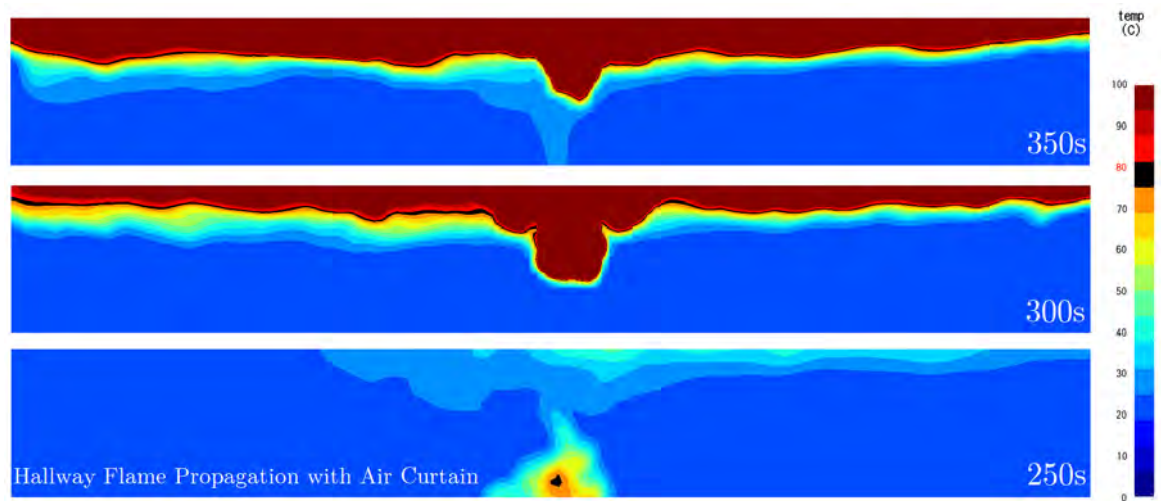

Fig. 3.71 Temperature contours at 250s, 300s and 350s for a vertical plane passing through the middle of the hallway width for air curtain discharged at 10 m/s. Human temperature tenability, 80ºC is highlighted with black color.

layer accumulate at ceiling agreeing well with the characteristics of smoke buoyancy. The air at bottom remained virtually motionless. The hot smoke then escaped the room through the door and accumulate at hallway ceiling. When the air curtain was discharged, the curtain jet introduced a motion in the bottom fluid layer of the source along with the natural buoyant flow of the smoke. Although the injection was vertical, at 250s the air curtain's stream was pushed outwards by the increased fluid pressure.

This increment in pressure was caused by the fluid expansion due to the heat release rate of the fire inside the store. The combined jet and smoke then pass through around the middle of the jet length, nearly at eye level from the floor. Thus, although air curtain did confine most of the heat up to this point, the escaped heat did pass through the eye level and was reflected at the thermocouple reading at eye level on figure 3.65. Figure 3.69 Temperature contours for a vertical plane passing through the points A and D of DCC market source shop 1. Figure 3.69a, 3.69c, and 3.69e show the temperature contours at 200s, 250s and 300s for air curtain at non-discharged condition. Figure 3.69b, 3.69d, and 3.69f show the temperature contours at 200s, 250s and 300s for air curtain discharged at 10 m/s. The temperature profile for non-discharged case again justify the movement of hot smoke layer were indeed over the eye height and due to the jet motion temperature profile for discharged case was more involved and passed through eye height from the floor after deflecting by curtain jet.

Figure 3.70 and 3.71 show the temperature contours at 250s, 300s and 350s for a vertical plane passing through the middle of the hallway width for air curtain discharged at 10 m/s and non-discharged conditions. The hallway is 21.94 m long with the source shop at about in middle of the hallway. Human temperature tenability, 80ºC is highlighted with black color. From figure 3.70 it is evident that, the escaped heat from the source came out just below the source door and accumulated at the ceiling and propagated along the ceiling. But as seen from figure 3.71, the heat escaped from the source, firstly came out from the bottom of the source door after being deflected by the curtain jet (at 250s), then at eye level (at 300s) when the smoke pressure begun to overcome the jet momentum and lastly at extreme smoke pressure came out just below the door like no curtain case (at 350s). The cumulative findings from these contours of figure indicated that, the path of the heat flow from source to hallway changed due to curtain jet. Thus, although much of the heat is confined with air curtain, the escaped heat follows a new path, under the curtain jet, and an increment in eye level temperature profile at position D with air curtain was observed. This proposal further strengthens up by the comparative ceiling temperature and CO concentration profile at position D as seen from figure 3.72 and 3.73.

The discrepancy in the air curtain effectiveness and the eye level temperature profile for discharged and non-discharged case now had a valid explanation for the temperature rise at eye level with air curtain, but yet to prove the effectiveness of implementing an air curtain in case of evacuation. According to the earlier claim, if only the path was altered and sufficient heat was confined by air curtain jet, there should be a point in the corridor where the hot smoke layer again moves up to the ceiling and eye level
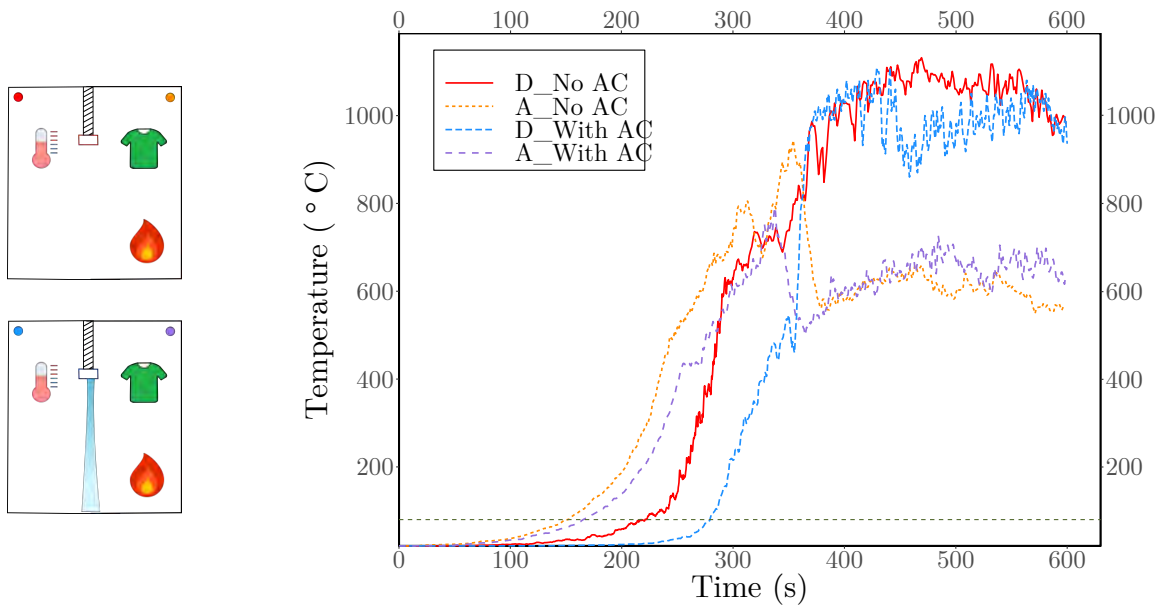
Fig. 3.72 Temperature distributions at ceiling level (2.9 m) for positions A (inside the fire source) and D (outside the fire source), for air curtain at non-discharged condition compared with air curtain discharged at 10 m/s, for DCC_CS1 and DCC_CS1AC.
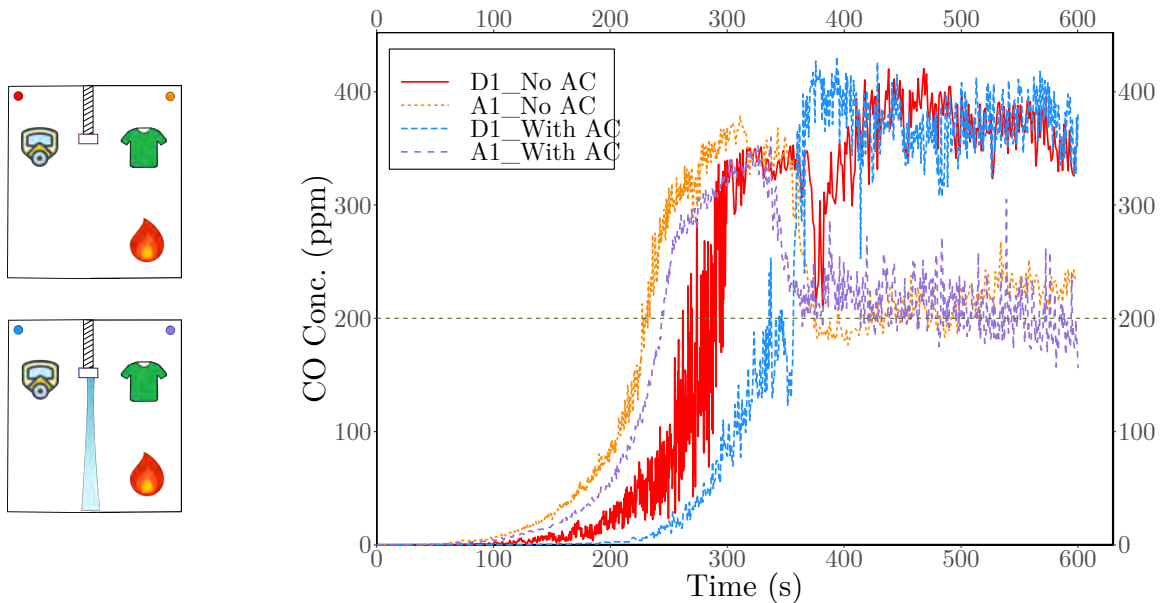

Fig. 3.73 CO concentration at ceiling level (2.9 m) for positions A1, (inside the fire source) and D1 (outside the fire source), for air curtain at non-discharged condition compared with air curtain discharged at 10 m/s, for DCC_CS1 and DCC_CS1AC.
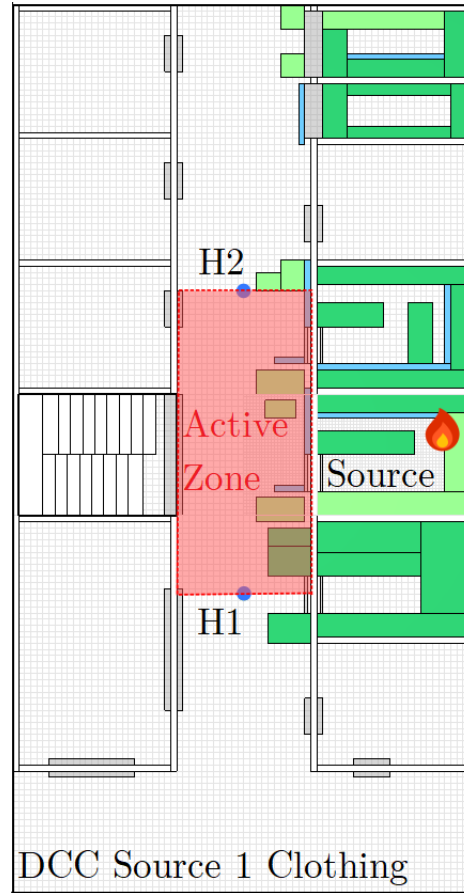
Fig. 3.74 Top view of DCC market showing the air curtain induced active zone due to jet deflected smoke path for source shop 1 (DCC_CS1AC).

temperature should be below the air curtain non-discharged condition. This will suffice the claim of air curtain effectiveness mentioned earlier and if the recovery length is small and time to cross tenability limit is high enough, the successful evacuation might also be assumed. By comparing the hallway temperature at eye level on both sides, pleasantly there were two borderline points on both sides of the hallway where with air curtain discharged, the eye level temperature reached tenability limit after the non-discharged condition. And, beyond that borderline points the delay on crossing tenability limit with air curtains were longer than non-discharged condition. Thus, an area of active zone was defined where the effect of air curtain was detrimental to evacuation compared to non-discharged condition. Although time required to reach the tenability limit within the active zone was greater than 4.5 minutes (270s). Figure 3.74 shows the active zone marked in red and the position of the borderline point H1 and H2 for DCC market source shop 1. The length of the hallway affected was 4.5 m upwards towards the point H2 and 3.048 m downwards towards the point H1, a
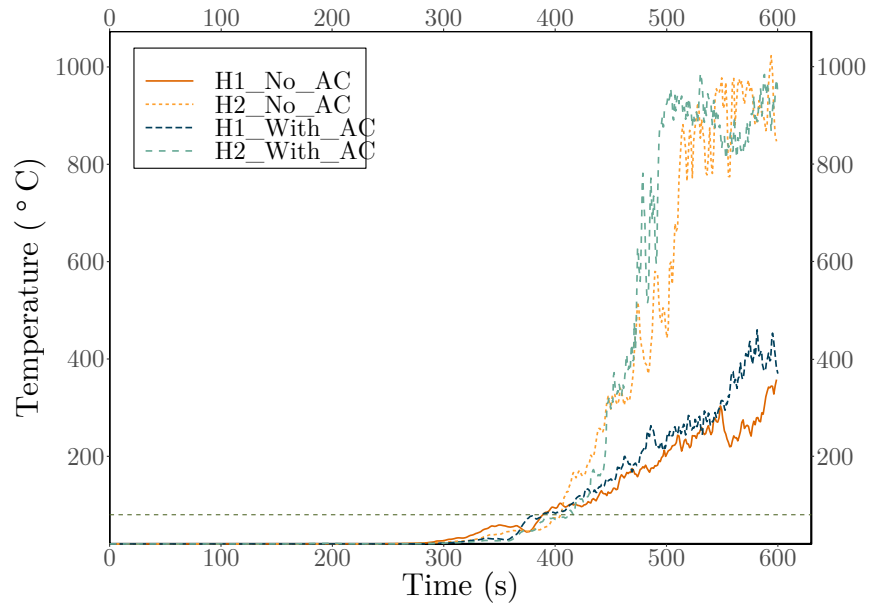
Fig. 3.75 Temperature profile at H1 and H2, the borderline of the active zone for DCC market source shop 1, with air curtain discharged at 10 m/s and without air curtain discharged.
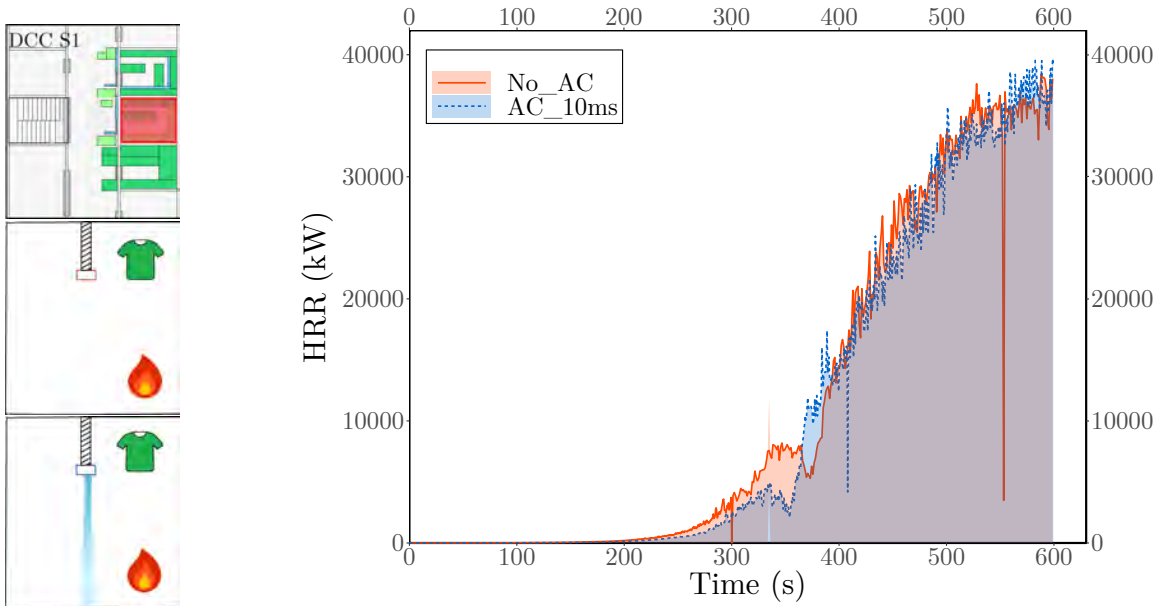

Fig. 3.76 Comparisons of Heat release rate (HRR) curves for DCC market fire source shop 1 with clothing as fuel, for air curtain discharged at 10 m/s and air curtain at non-discharged condition.

total of 7.548 m around the source, which should be evacuated within 4.5 minutes of time in normal conditions. Figure 3.75 shows the temperature profile at H1 and H2, the borderline of the active zone for DCC market source shop 1, with air curtain discharged at 10 m/s and without air curtain discharged. The tenability limit crossed at the borderlines of the active zone at around 400s for both point and for both cases. The jet circulation improved the combustion process inside the shop as seen from the flame propagation pictures, but as the heat release rate (HRR) curves of figure 3.76 suggest, the heat released with air curtain was lower than the non-discharged condition up to 360s, where the fire came out of the source shop due to lack of oxidizers. And, although the fire came out early, the total heat released remained lower for the rest of the simulation than the non-discharged condition. Thus, the common intuition of increasing the flammability of the fuels by blowing air towards the source is not justified. And, after considering all the strengths and weaknesses of air curtains in details, it might be safe to say that, introducing air curtain to confine heat and mass transfer in case of a fire could be a realistic alternative.

3.2.1.3 Clothing store fire with air curtain: Source shop 2

Air curtain was introduced for source shop 2 of DCC market in the next phase to observe effectiveness of air curtains for different source and fuel load. Also, this would reveal air curtains ability on fire and smoke confinement from the staircase for a reasonably distant source shop fire scenario. The flame and smoke propagation through DCC market source shop 2, DCC_CS2AC, in case of clothing as fuel load, with a vertical air curtain of 7.62 cm jet width and 10 m/s jet velocity is shown in figure 3.77. Analyzing the flame propagation for this source shop it was again evident that, circulation of air inside the source by the air curtains jet aided the combustion process as the visible flame was 5 seconds earlier than that of no curtain condition. And, the jet again able to withstand the improved combustion for longer period of time than the no curtain case as the smoke after 25 seconds of the no curtain condition, same as the DCC_CS1AC case. The smoke filled up the corridor 40s later than no curtain, but flashover event occurred 15 seconds earlier and flame came out of the shop 23 seconds
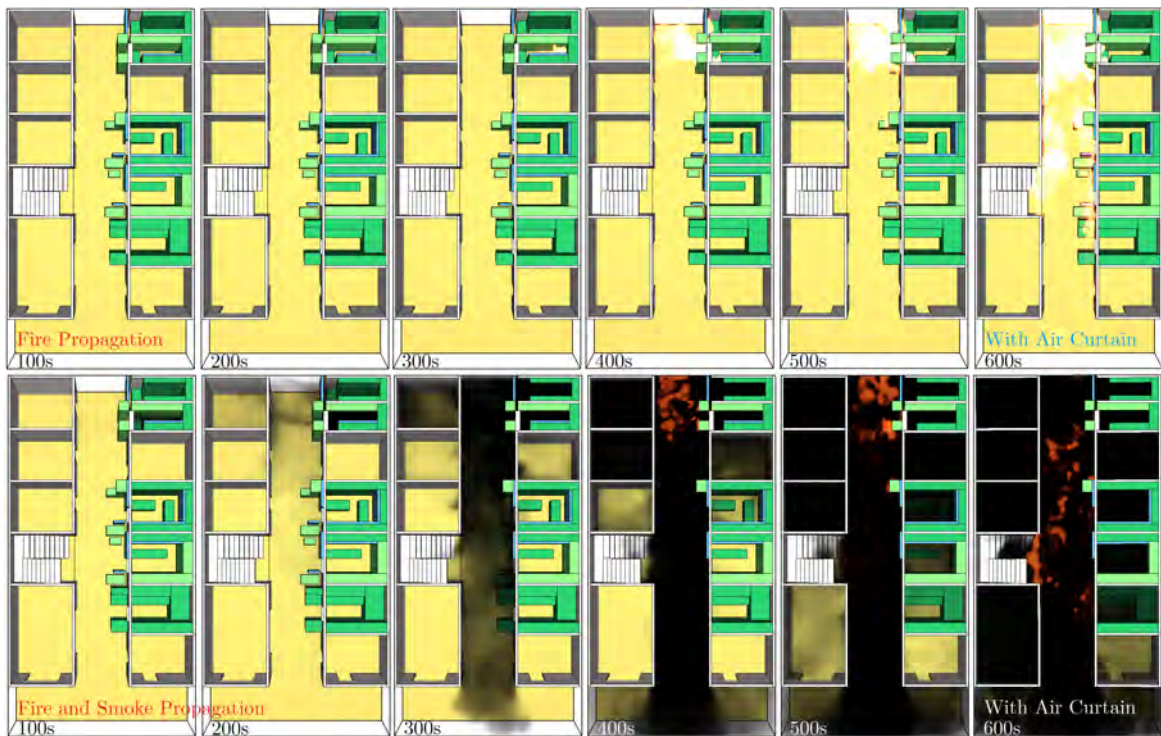

Fig. 3.77 Flame propagation through DCC market source shop 2, DCC_CS2AC, in case of clothing as fuel load, with a vertical air curtain of 7.62 cm jet width and 10 m/s jet velocity. The top row shows the flame propagation only, and bottom row shows both flame and smoke propagation for 100s, 200s, 300s, 400s, 500s and 600s of simulation time respectively from left to right.

Table 3.11 Flame and smoke propagation timeline for DCC market for clothing fuel condition in source shop 2.

Event	Time (s)	
	No Air Curtain (DCC_CS2)	With Air Curtain (DCC_CS2AC)
Visible flame after ignition	60	55
Smoke came out of the source shop	75	100
Smoke filled up the whole corridor	300	340
Flame front came out of the shop	333	310
Fire spread to adjacent shop	410	380
Fire spread to staircase inside	430	480
Fire came out of the source	440	-
Fire intensely burning in source shop front	550	540
Fire spread to all shop front fuels	560	580

earlier. The source 2 was a small one and the air curtain was placed at 3 m instead of 2.13 m, the jet strength thus reduced earlier than source 1 case, and the much widened jet plume offered increased circulation of oxidizers and thus improving the combustion process, evidence of which was visible as the fire never came out of the source shop due to shortage of oxidizers up to 600s. And, as the fire remained inside the source for longer period of time the flame spread to adjacent shop, staircase, and all shop fronts were delayed considerably. The details of the fire events are presented in table 3.11.
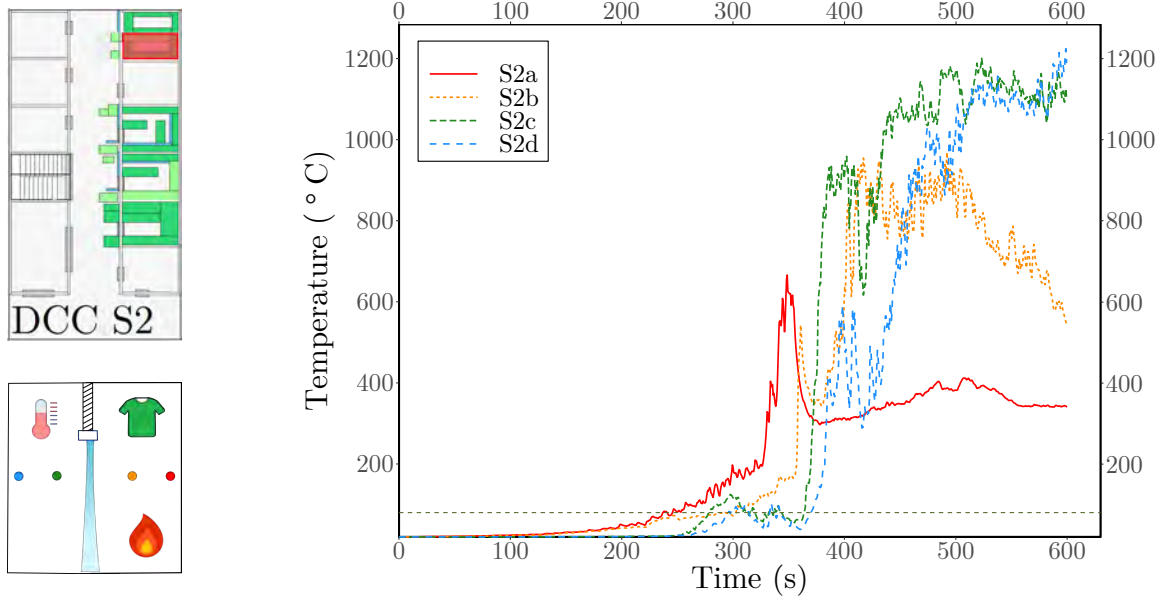
Temperature distributions at eye level (1.54 m) for positions S2a, S2b (inside the fire source) and S2c, S2d (outside the fire source) with air curtain discharged at 10 m/s, for DCC_CS2AC is presented in figure 3.78. Comparing the inside and outside temperature it could be deduced that, air curtain could hold the increased temperature inside source for considerable amount of time, nearly 100s for this case. But again, while comparing with the non-discharged case shown in figure 3.79, the eye level temperature with air curtains crossed the human tenability, the green dashed line in figure 3.79, nearly 117s earlier than the non-discharged case. Figure 3.80 portraits CO concentration at eye level (1.54 m) for positions S2a1, S2b1 (inside the fire source) and S2c1, S2d1 (outside the fire source) with air curtain discharged at 10 m/s, for DCC_CS2AC. And, figure 3.81 shows CO concentration at eye level (1.54 m) for positions S2a1, (inside the fire source) and S2d1 (outside the fire source), for air curtain at non-discharged condition compared with air curtain discharged at 10 m/s, for DCC_CS2 and DCC_CS2AC. Although in both figures the lethal concentration

Fig. 3.78 Temperature distributions at eye level (1.54 m) for positions S2a, S2b (inside the fire source) and S2c, S2d (outside the fire source) with air curtain discharged at 10 m/s, for DCC_CS2AC.
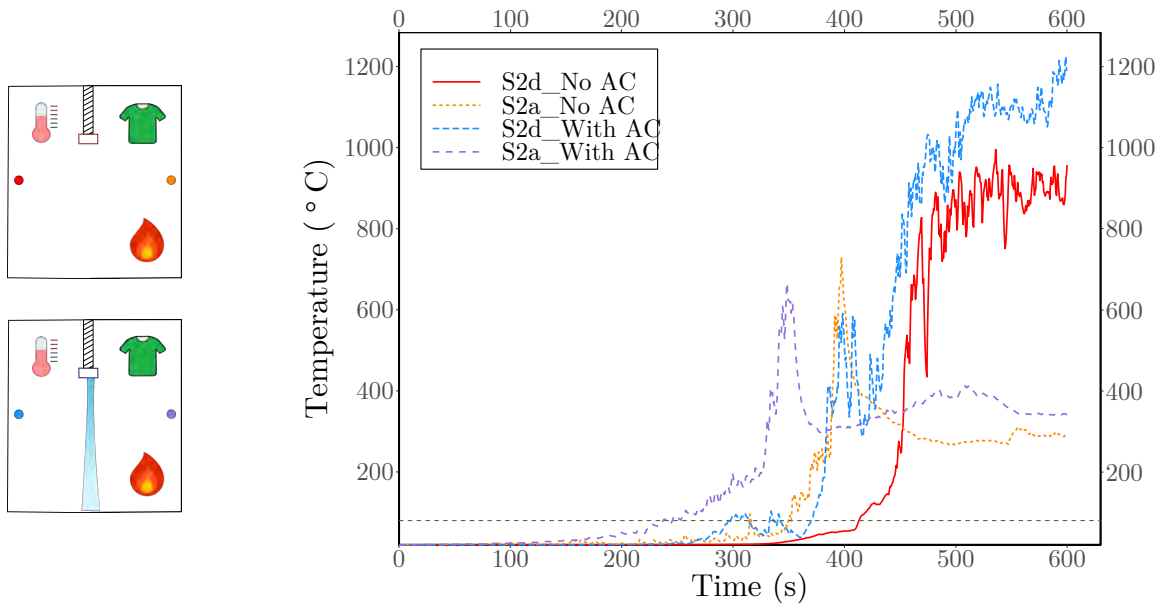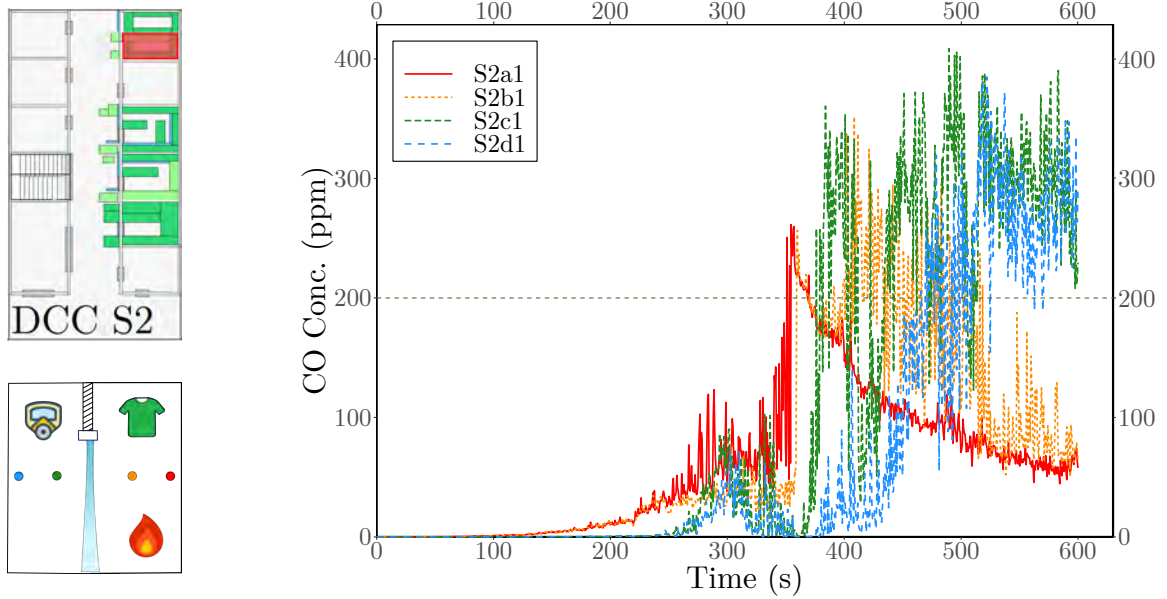

Fig. 3.79 Temperature distributions at eye level (1.54 m) for positions S2a (inside the fire source) and S2d (outside the fire source), for air curtain at non-discharged condition compared with air curtain discharged at 10 m/s, for DCC_CS2 and DCC_CS2AC.

Fig. 3.80 CO concentration at eye level (1.54 m) for positions S2a1, S2b1 (inside the fire source) and S2c1, S2d1 (outside the fire source) with air curtain discharged at 10 m/s, for DCC_CS2AC.
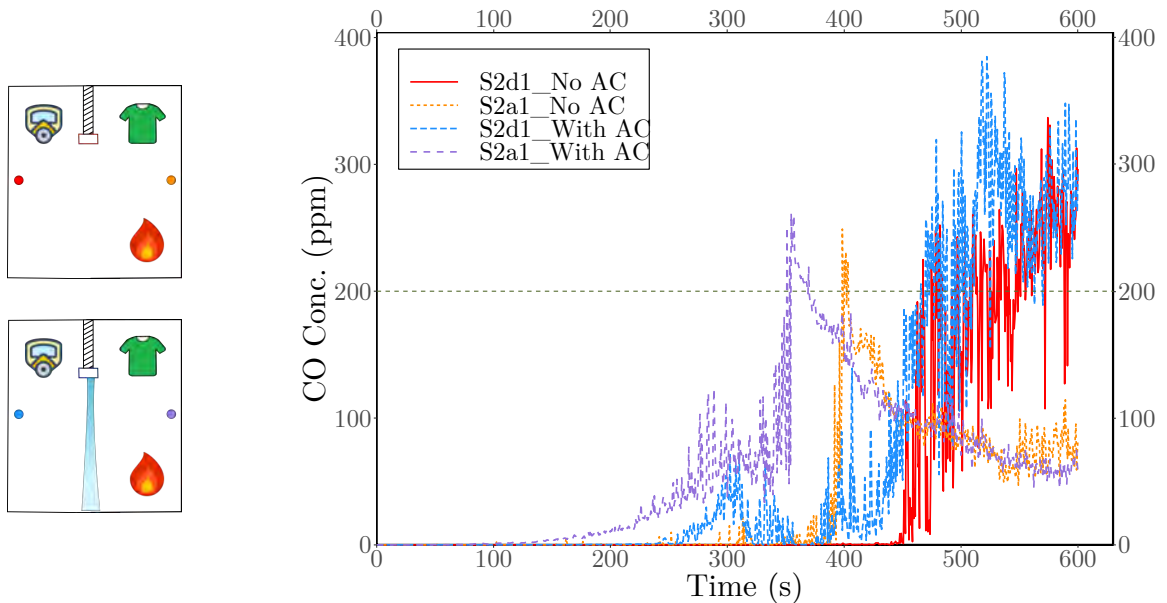

Fig. 3.81 CO concentration at eye level (1.54 m) for positions S2a1, (inside the fire source) and S2d1 (outside the fire source), for air curtain at non-discharged condition compared with air curtain discharged at 10 m/s, for DCC_CS2 and DCC_CS2AC.
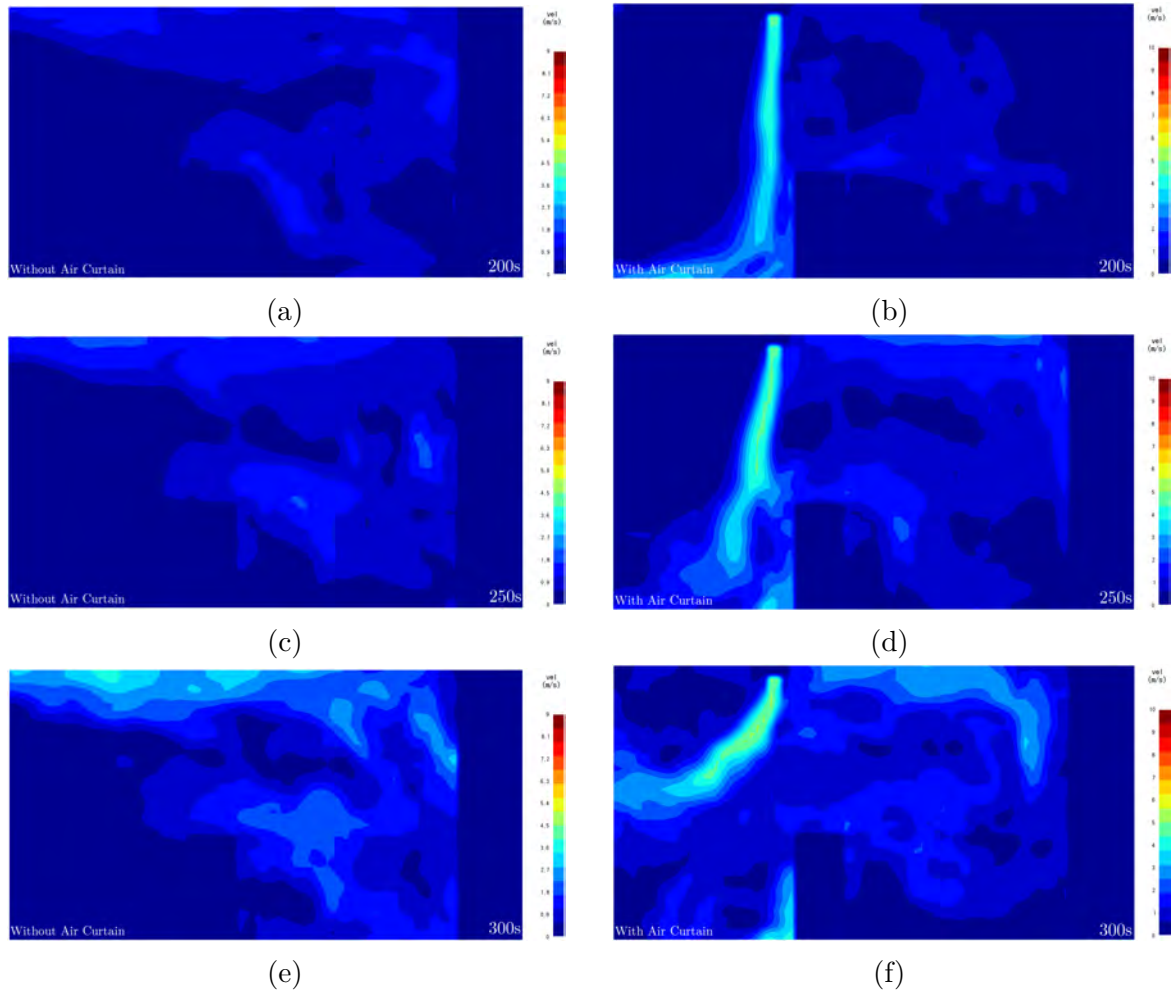
Fig. 3.82 Velocity contours for a vertical plane passing through the points S2a and S2d of DCC market source shop 2. Figure (a), (c), and (e) show the velocity contours at 200s, 250s and 300s for air curtain at non-discharged condition. Figure (b), (d), and (f) show the velocity contours at 200s, 250s and 300s for air curtain discharged at 10 m/s.

for short term exposure was never attained, air curtain again performed poorly when compared to the non-discharged case.

Figure 3.82 shows velocity contours for a vertical plane passing through the points S2a and S2d of DCC market source shop 2. Figure 3.82a, 3.82c, and 3.82e, show the velocity contours at 200s, 250s and 300s for air curtain at non-discharged condition. Figure 3.82b, 3.82d, and 3.82f show the velocity contours at 200s, 250s and 300s for air curtain discharged at 10 m/s. The smoke layer without air curtain maintaining the laws of buoyant flow stacked at ceiling and propagated through there. And with air curtain again the smoke layer deflected by air curtain jet and escaped the source at eye height as seen from figure 3.82f. The temperature contours for a vertical plane passing
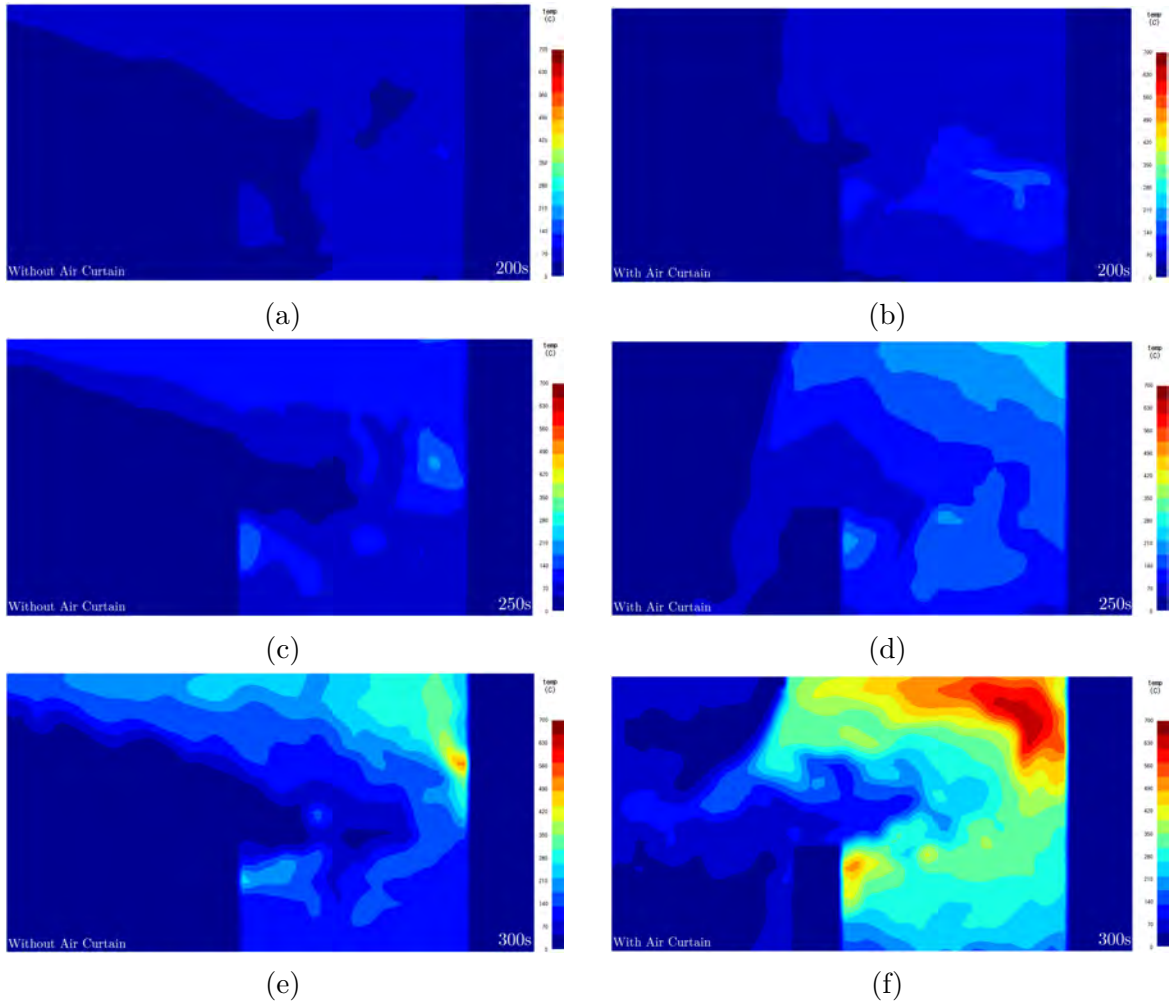
Fig. 3.83 Temperature contours for a vertical plane passing through the points S2a and S2d of DCC market source shop 1. Figure (a), (c), and (e) show the temperature contours at 200s, 250s and 300s for air curtain at non-discharged condition. Figure (b), (d), and (f) show the temperature contours at 200s, 250s and 300s for air curtain discharged at 10 m/s.

through the points S2a and S2d of DCC market source shop 1 is shown in figure 3.83. Figure 3.83a, 3.83c, and 3.83e show the temperature contours at 200s, 250s and 300s for air curtain at non-discharged condition. Figure 3.83b, 3.83d, and 3.83f show the temperature contours at 200s, 250s and 300s for air curtain discharged at 10 m/s. The temperature contours along with the conformation of the smoke layer path mentioned earlier, and the more distributed temperature contours shows evidence of improved combustion due to circulation of source air.

Figure 3.84 and 3.85 show the temperature contours at 250s, 300s and 350s for a vertical plane passing through the middle of the hallway width for air curtain at
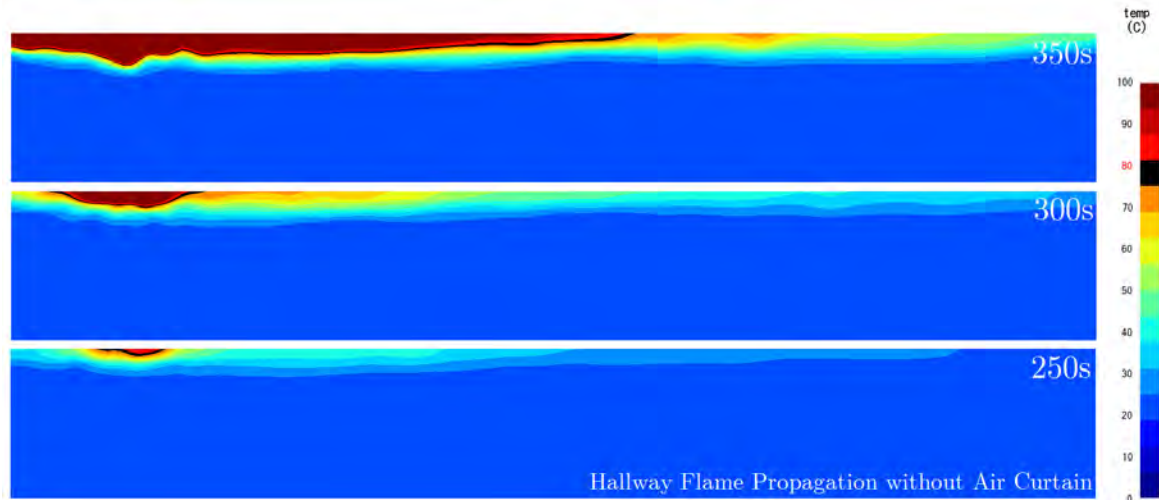
Fig. 3.84 Temperature contours at 250s, 300s and 350s for a vertical plane passing through the middle of the hallway width for air curtain at non-discharged condition. The hallway is 21.94 m long with the source shop at about 19.67 m from the right in the hallway. Human temperature tenability, 80ºC is highlighted with black color.
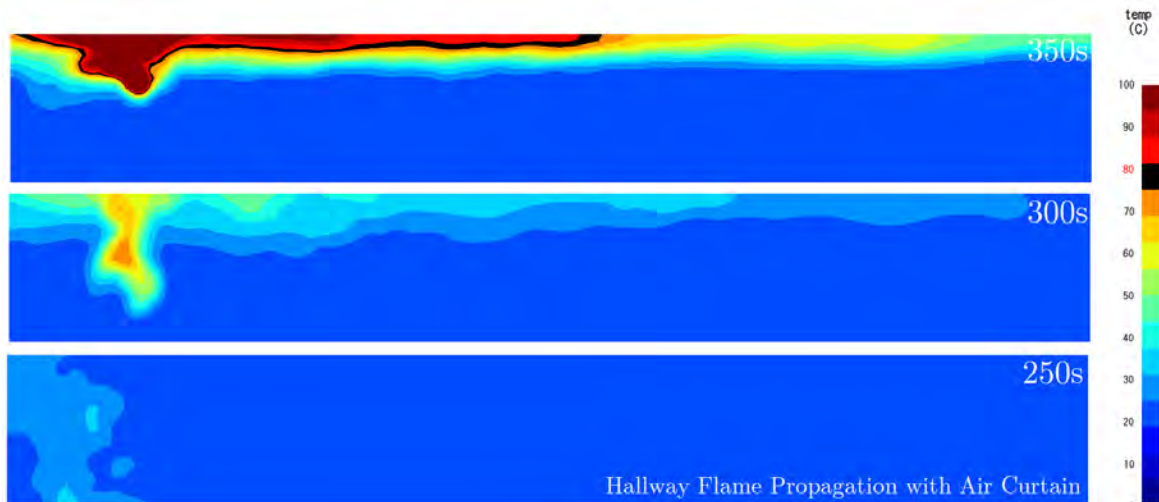

Fig. 3.85 Temperature contours at 250s, 300s and 350s for a vertical plane passing through the middle of the hallway width for air curtain discharged at 10 m/s. Human temperature tenability, 80ºC is highlighted with black color.

non discharged condition and discharged at 10 m/s condition. Human temperature tenability, 80ºC is highlighted with black color. These figures conclusively indicated the smoke layer path from the source to the hallway. For non-discharged condition of figure 3.84 the hot smoke came out of the source from the door top and accumulated in the ceiling thus the lower temperature reading at eye level just in front of the source shop.
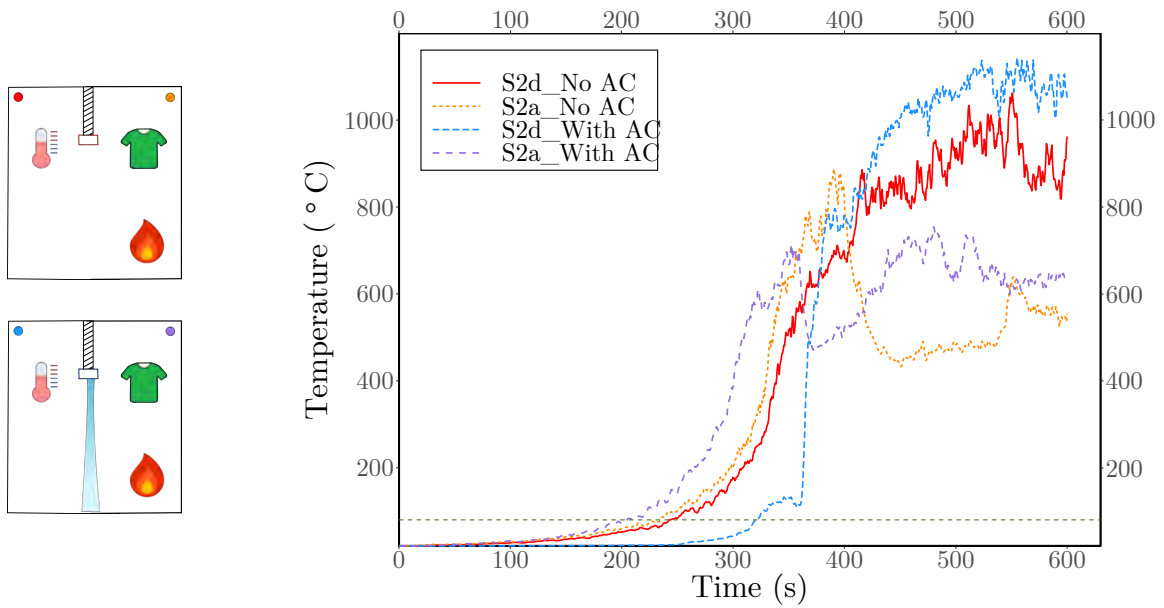
Fig. 3.86 Temperature distributions at ceiling level (2.9 m) for positions S2a (inside the fire source) and S2d (outside the fire source), for air curtain at non-discharged condition compared with air curtain discharged at 10 m/s, for DCC_CS2 and DCC_CS2AC.
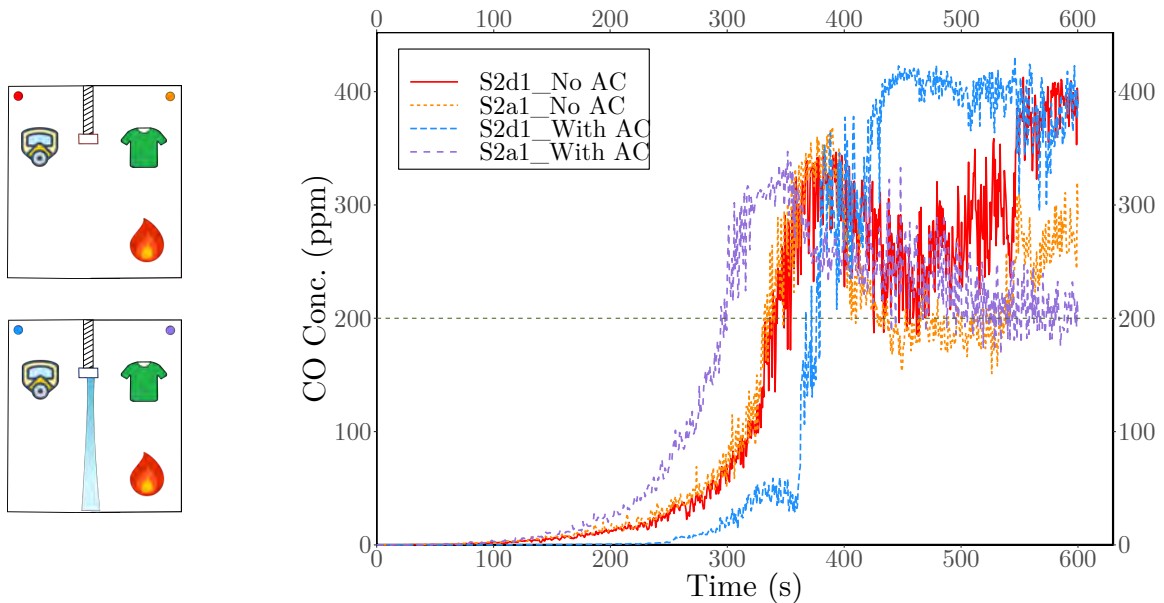

Fig. 3.87 CO concentration at ceiling level (2.9 m) for positions Sa1, (inside the fire source) and Sd1 (outside the fire source), for air curtain at non-discharged condition compared with air curtain discharged at 10 m/s, for DCC_CS2 and DCC_CS2AC.
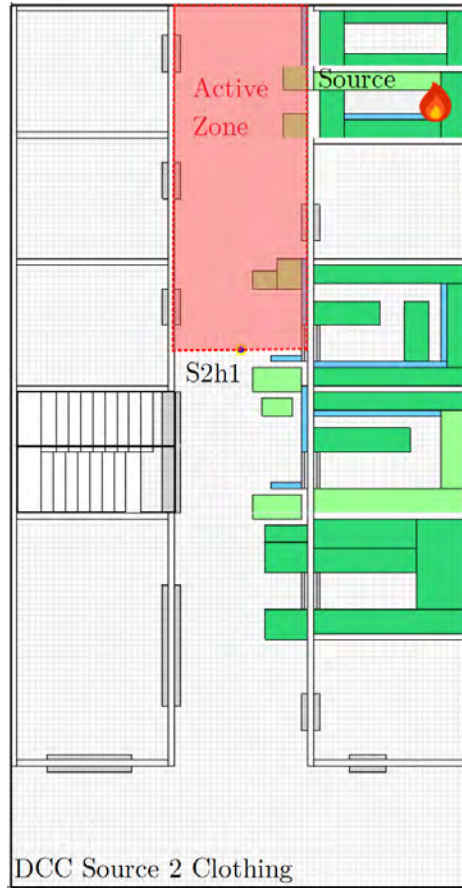
Fig. 3.88 Top view of DCC market showing the air curtain induced active zone due to jet deflected smoke path for source shop 2 (DCC_CS2AC).

And, in case of the air curtain discharged condition, smoke layer was deflected by the jet and came out of the source under the jet plume initially, as the smoke momentum increased the smoke's escape path moved upwards, and accumulated in ceiling completing the buoyant flow mechanics. Thus, as the leaked heat totally channeled through a path overlapping the eye level thermocouple, the eye level temperature profile at position S2d crossed the tenability limit earlier. Figure 3.86 shows the temperature distributions at ceiling level (2.9 m) for positions S2a (inside the fire source) and S2d (outside the fire source), for air curtain at non-discharged condition compared with air curtain discharged at 10 m/s, for DCC_CS2 and DCC_CS2AC. And, figure 3.87 shows the CO concentration at ceiling level (2.9 m) for positions Sa1, (inside the fire source) and Sd1 (outside the fire source), for air curtain at non-discharged condition compared with air curtain discharged at 10 m/s, for DCC_CS2 and DCC_CS2AC. From these figures it can be seen that the temperature and CO concentration at ceiling level (2.9 m) for air curtain discharged condition, were indeed less than the non-discharged case.
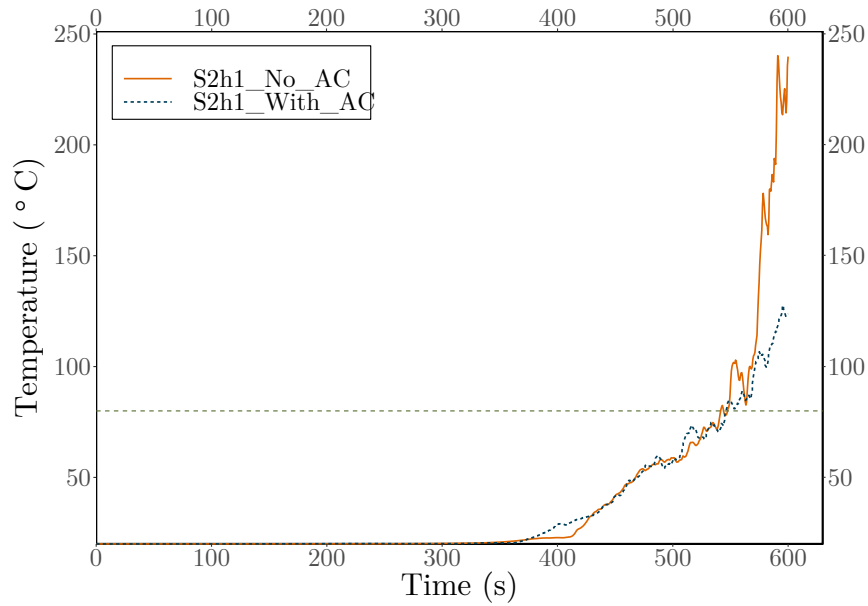
Fig. 3.89 Temperature profile at S2h1, the borderline of the active zone for DCC market source shop 2 at one end, with air curtain discharged at 10 m/s and without air curtain discharged.
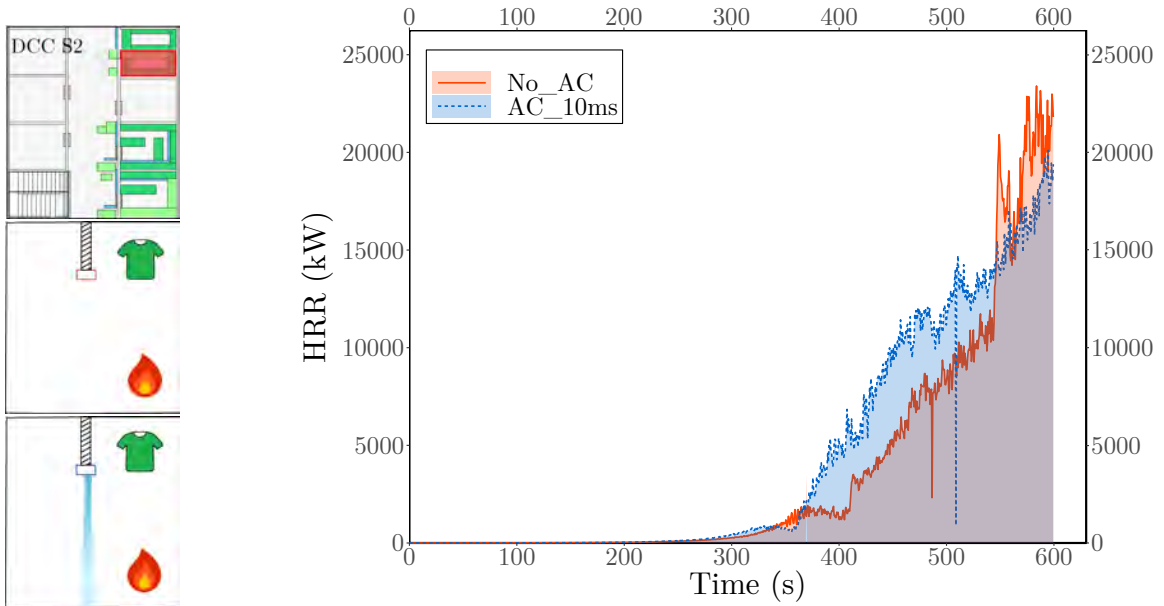

Fig. 3.90 Comparisons of Heat release rate (HRR) curves for DCC market fire source shop 2 with clothing as fuel, for air curtain discharged at 10 m/s and air curtain at non-discharged condition.

Thus, here again should be an active zone like the source shop 1, after which the air curtains effect was positive through out the total domain.

After observing the eye level thermocouples on the corridor placed at 0.76 m apart from each other, a downstream point S2h1 was found at 6.09 m from the source towards the staircase where the effect of air curtain was always positive in comparison to non-discharged case. As, the source was nearly at the end of the corridor, no such points could be obtained for the other direction. Figure 3.88 shows top view of DCC market with the air curtain induced active zone due to jet deflected smoke path for source shop 2 (DCC_CS2AC). In the active zone crossed the human temperature tenability at source front nearly at 300s, although this is essentially the middle portion of the active zone, due to the low area of the zone, it is safe to assume that, evacuation will be possible before this time from the furthest corners of the zone even before this point crosses the tenability limit. And, from the figure 3.89, it can be seen that, the tenability limit crossed at point S2h1 at 547s with air curtain discharged and at 541s with non-discharged condition. As, mentioned earlier it should be possible without exception to evacuated the 6 m corridor with in 9 minutes. The heat release rate curve for air curtain discharged and non-discharged condition is shown in figure 3.90 for DCC market source shop 2. The improved combustion did increased the total heat released for the source, but the increment was after 350s, and thus should started after successful evacuation from the source. Thus, conclusion could be drawn as, although the combustion was improved, flashover was earlier due to air curtain jet, the corridor was safe for longer period of time with air curtain, which should aid the evacuation process.

3.2.1.4 Summary of the effect of air curtains on fire source location

The temperature and CO concentration at staircase with and without air curtain for both DCC market source shop were presented in figure 3.91 and 3.92 respectively. For source shop 1, the temperature tenability with air curtain crossed later than no curtain case and for the source shop 2, the tenability never crossed with air curtain. The situation is similar for CO concentration too. Thus, installing an off-the-self air curtain at source shop proved to be beneficial for evacuation through staircase for both near source and far source fire scenarios for typical shopping malls of Bangladesh even with the actual, extremely dense fuel arrangements.
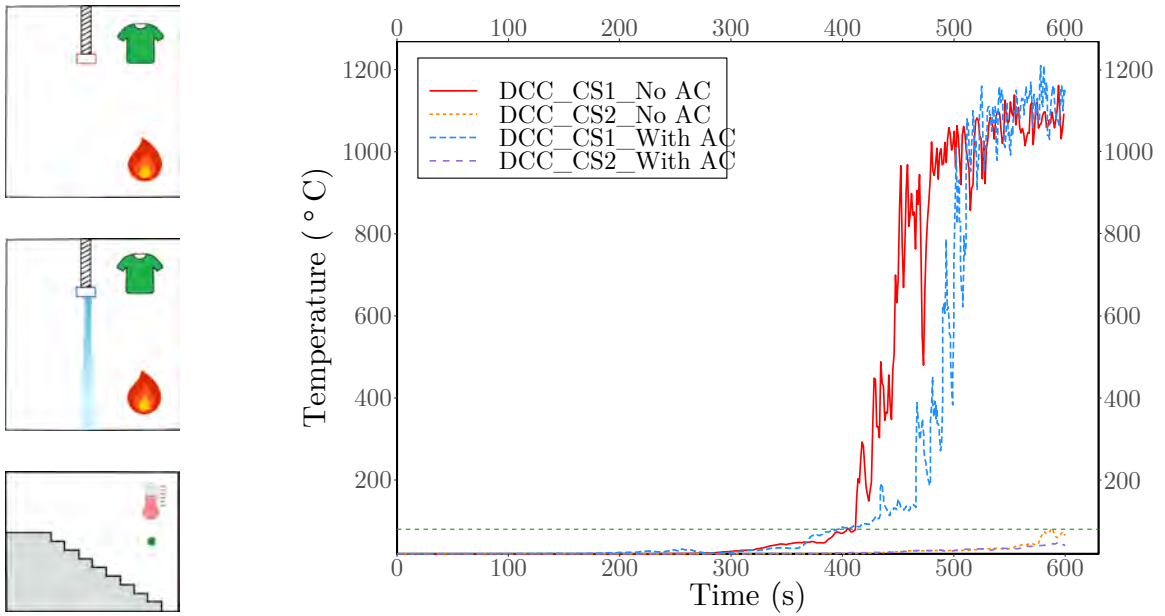
Fig. 3.91 Temperature distributions at staircase for air curtain at discharged and non-discharged condition for clothing fire scenario for DCC market.
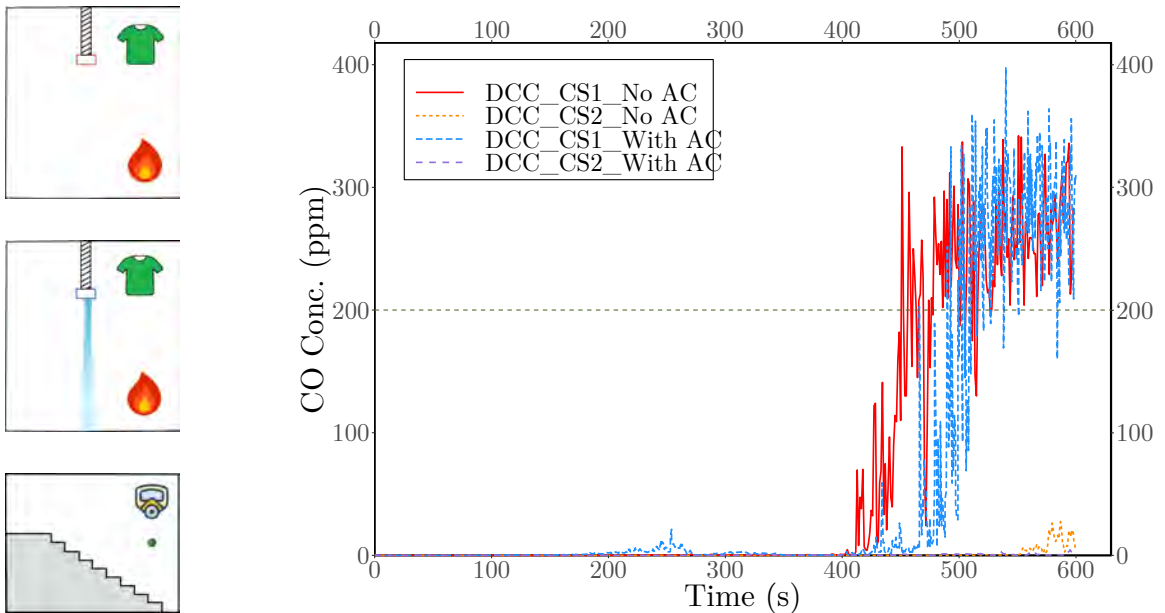

Fig. 3.92 CO concentration at staircase for air curtain at discharged and non-discharged condition for clothing fire scenario for DCC market.

3.2.1.5 The effects of the variation of fuel distribution

The fuel distribution observed during the survey at different shopping malls were extremely dense and only matched with book store, greeting card shop and storage area of the study Zalok and Hadjisophocleous (2007), conducted for Ottawa and Gatineau cities of Canada. Due to this extremely dense fuel distribution the heat released from a fire originated in a typical shopping mall became disastrous rapidly. A solution to this problem was to implement standard fuel distribution in high heat release rate per unit area (HRRPUA) fuel load hosting shops. One of the standard fuel distributions was Grid type fuel distribution, where fuel loads are placed in aisles leaving freely moving space in between them, typically seen in super shops. This study investigated the standard Grid type fuel distribution with 'Rack' type cloth arrangements up to 1.524 m. Placing 'Display' type cloth arrangements with standard Grid distribution, Display distribution was obtained and investigated in this present study. The reason behind the Display distribution was to observe the effect of fuel loads in a shop, case of a fire scenario, as Display distribution has extremely low fuel load compare to actual case.

Figure 3.93 shows the top view of DCC market, with different distributions of clothing fuel considered in the next phase of our investigation. For better understanding
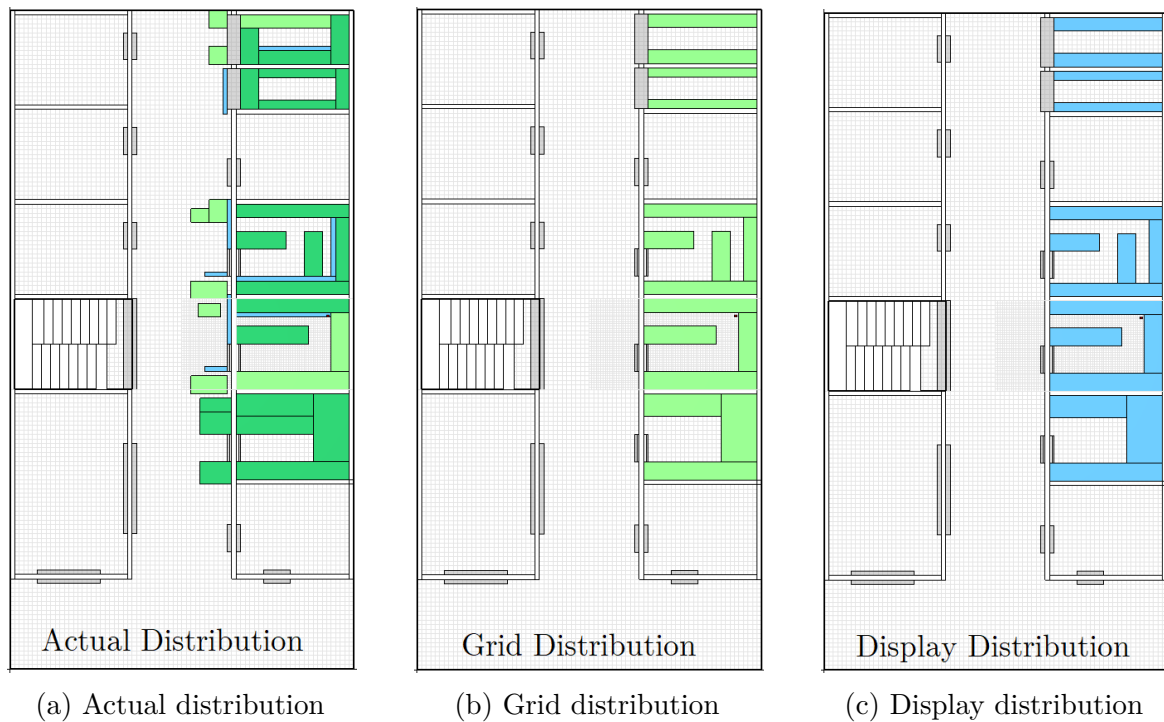

(a) Actual distribution	(b) Grid distribution	(c) Display distribution

Fig. 3.93 Top view of DCC market showing clothing fuel arrangement for different fuel distribution considered.
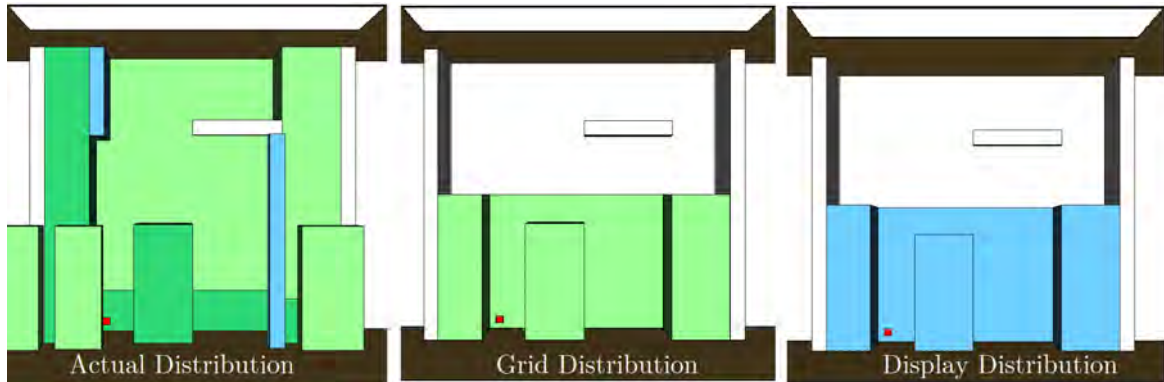
Fig. 3.94 Front view of DCC market source shop 1 showing clothing fuel arrangement for different fuel distribution considered.

Table 3.12 Comparison between different fuel distribution for DCC source shop 1 with clothing as fuel. The shop area was 11.61 m².

Name	Description	Clothing in kg (%)	Fuel Load (kg/m²)	Total heat released (TJ)	THR/A (TJ/m²)
Actual	Actual fuel arrangement as seen during survey	4104.15 (100)	353.41	4457.53	383.8
Grid	Standard 'Grid' type distribution with 'Rack' fuel	763.44 (18.6)	65.74	1725.72	148.60
Display	'Grid' type distribution with 'Display' fuel	190.87 (4.65)	16.43	1590.08	136.92

of the source shop condition, figure 3.94 shows the front view of DCC market source shop 1 only, in different distributions of clothing fuel. In the Actual distribution shown in figure 3.93a, the fuel load was 4104.15 kg of cloths, implementing the Grid type distribution as in figure 3.93b the fuel load reduced to 763.44 kg of cloths, i.e., about 18.6% of Actual condition. While arranging the fuels in Display distribution as seen from the figure 3.93c, the fuel load reduced to 190.87 kg of cloths, a mere 4.6% of the Actual condition present in a typical clothing store of Bangladesh. Details of these arrangements are shown in table 3.12. For Grid and Display type distribution the fuel were stored up to 1.524 m height, instead of up to ceiling height, as seen in actual scenario during survey. Observing the flame propagation without air curtain for the fuel distribution variations revealed that, flashover delayed for nearly 88s, smoke and flame came out of the source nearly 20s and 63s after for Grid distribution compared to Actual distribution. Interestingly, the fire events for Display distribution was nearly similar to Grid distribution except the flame came out 5s earlier than Grid distribution. The fire events for three types of fuel distribution are given in table 3.16. Figure 3.95

Table 3.13 Comparison between different fuel arrangements and air curtain parameters for DCC source shop 1 with clothing as fuel.

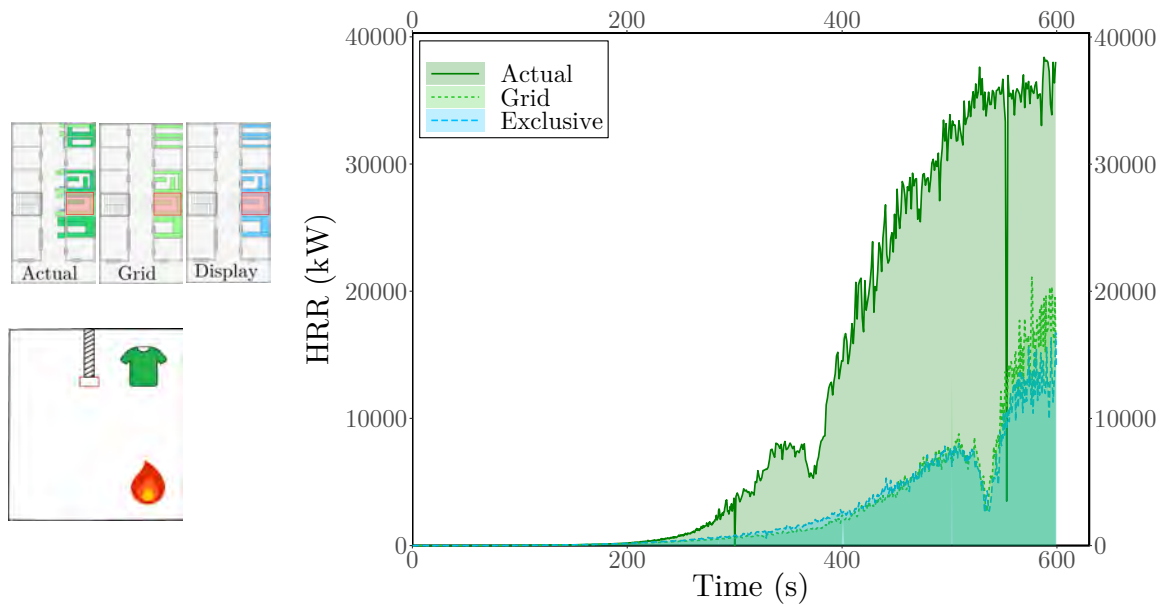| Fuel Distribution	Air curtain	Smoke confinement	Flame confinement	Flashover
Actual	No Curtain	80s	247s	262
Grid	No Curtain	100s	310s	350s
Display	No Curtain	100s	295s	350s

Fig. 3.95 Heat release rate (HRR) curve for DCC market source shop 1 for different fuel distribution considered, keeping air curtain at non-discharged condition.

shows the heat release rate (HRR) curve for DCC market source shop 1 for different fuel distribution considered, keeping air curtain at non-discharged condition. And surprisingly, the heat release rate curve for Grid distribution and Display distribution were nearly identical. The total heat released in 600s of simulation time were also similar, as for Grid type distribution was 1725.72 TJ and for Display distribution was 1590.08 TJ respectively. The similar HRR of Grid and Display distribution indicated that, although fuel load was nearly one third for Display distribution compared to Grid type, better burning was achieved due to the availability of excess oxidizers for Display distribution.

The average smoke layer velocity for different fuel and fuel distribution at the door of DCC market source shop 1 in vertical direction is shown in figure 3.96. The average
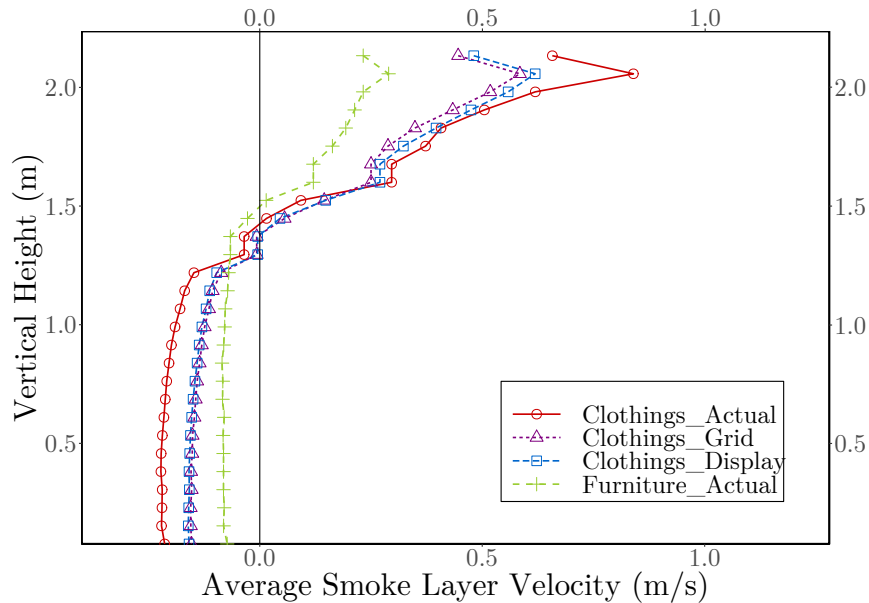
Fig. 3.96 Average smoke layer velocity for different fuel and fuel distribution at the door of DCC market source shop 1.

smoke layer velocity of Grid distribution and Display distribution were also similar and lower than the Actual distribution case. For furniture fire the smoke layer velocity was the smallest. Figure 3.97 shows the temperature distributions at eye level (1.54 m) for position D (outside the fire source) for clothing fire scenario at DCC market fire source shop 1 with different fuel distribution variations. Figure 3.98 shows CO concentration at eye level (1.54 m) for position D1 (outside the fire source) for clothing fire scenario at DCC market fire source shop 1 with different fuel distribution variations. The temperature and CO concentration raise at position D for Grid and Display were once more identical. Thus, Grid type distribution was preferable due to the low heat release rate, 38.7% of Actual condition, in case of fire hazard at comparatively higher amount of fuel, 18.6% of Actual fuel load. Whereas Display distribution produce 35.6% heat of Actual condition with a mere 4.65% of Actual load.

Figure 3.99 shows the heat release rate (HRR) curve for DCC market source shop 1 with Grid type fuel distribution for air curtain discharged at 10 m/s and air curtain at non-discharged condition (DCC_CS1ACG vs. DCC_CS1G). And, figure 3.100 shows the heat release rate (HRR) curve for DCC market source shop 1 with Display type fuel distribution for air curtain discharged at 10 m/s and air curtain at non-discharged condition (DCC_CS1ACD vs. DCC_CS1D). These figures indicated that with introduction of air curtain in Grid and Display fuel distribution made no drastic change in heat release rate as these fire scenarios were not under-ventilated.
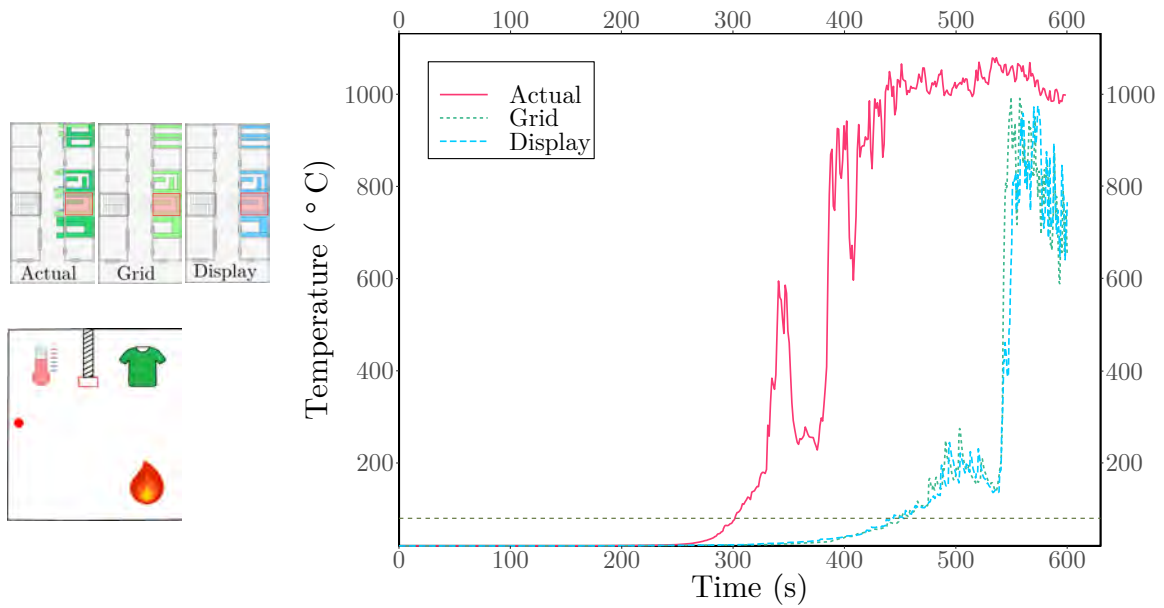
Fig. 3.97 Temperature distributions at eye level (1.54 m) for position D (outside the fire source) for clothing fire scenario at DCC market fire source shop 1 with different fuel distribution variations.
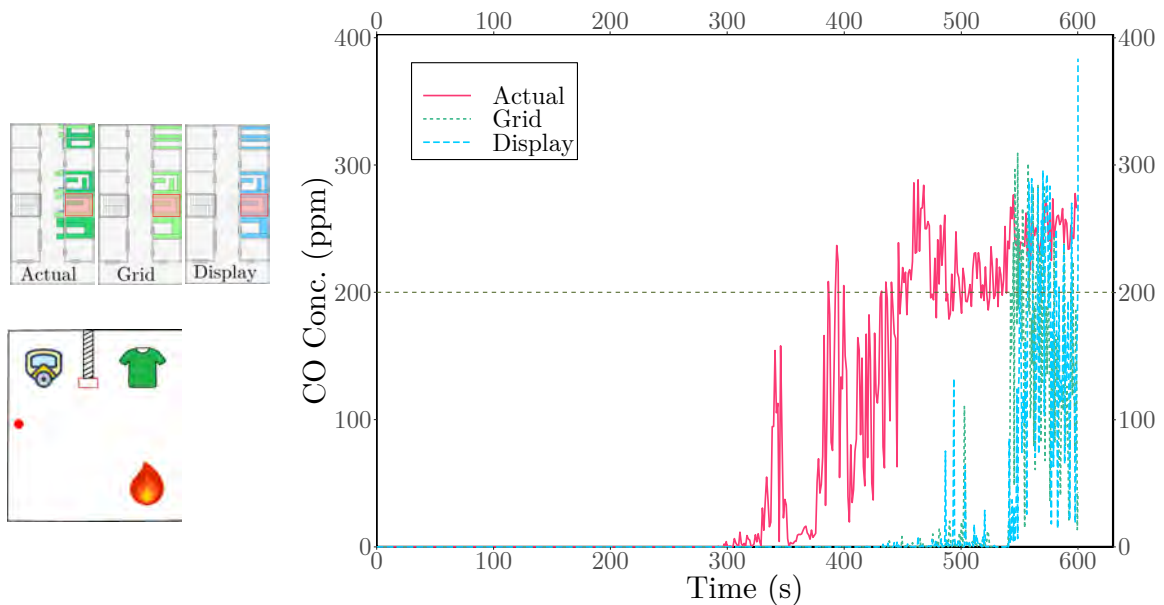

Fig. 3.98 CO concentration at eye level (1.54 m) for position D1 (outside the fire source) for clothing fire scenario at DCC market fire source shop 1 with different fuel distribution variations.

Fig. 3.99 Heat release rate (HRR) curve for DCC market source shop 1 with Grid type fuel distribution for air curtain discharged at 10 m/s and air curtain at non-discharged condition (DCC_CS1ACG vs. DCC_CS1G).
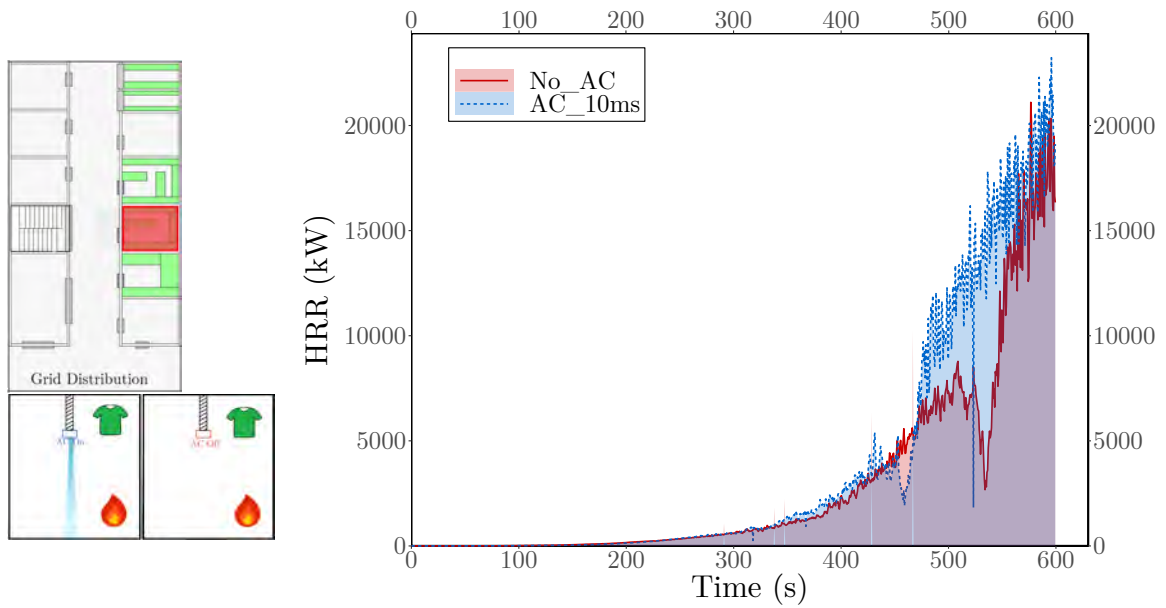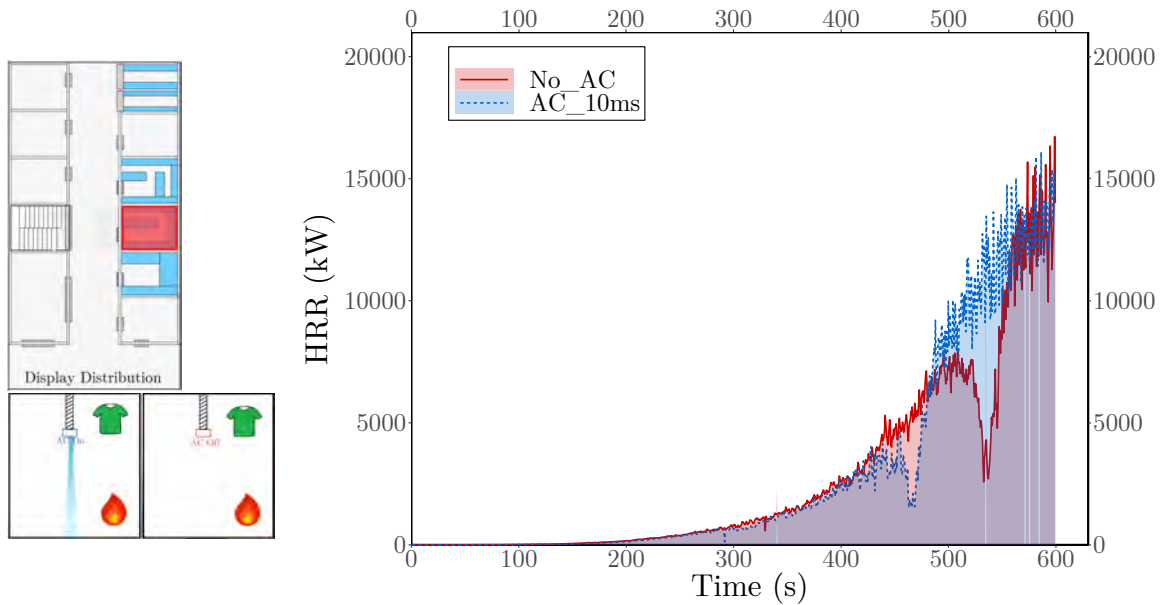

Fig. 3.100 Heat release rate (HRR) curve for DCC market source shop 1 with Display type fuel distribution for air curtain discharged at 10 m/s and air curtain at non-discharged condition (DCC_CS1ACD vs. DCC_CS1D).
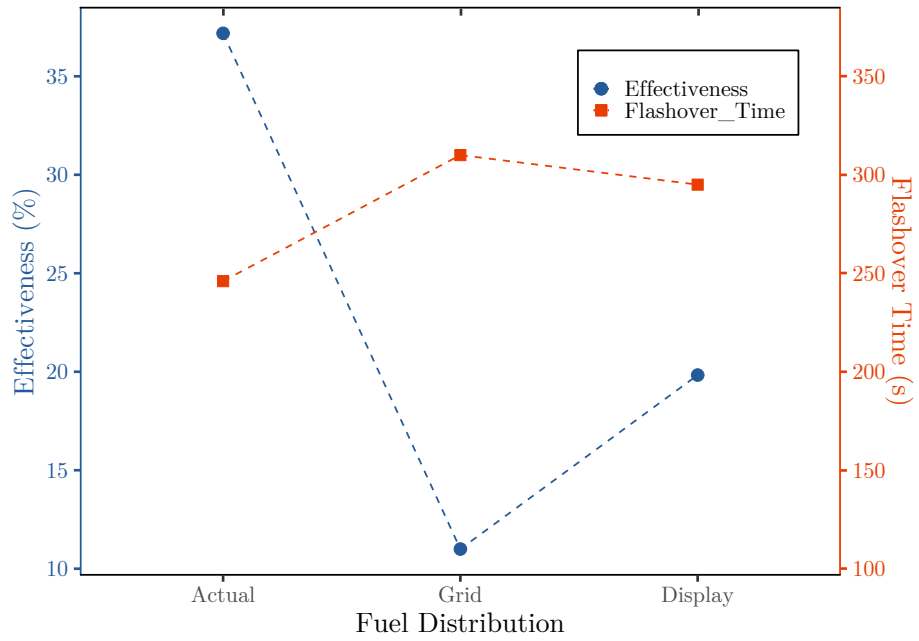
Fig. 3.101 Effectiveness and flashover time for no curtain condition of different fuel distribution of DCC market source shop 1.

Fig. 3.102 Temperature distribution at eye level (1.54 m) in staircase for DCC market source shop 1 for different fuel distribution with a vertical single jet air curtain discharged at 10 m/s.

Fig. 3.103 Heat release rate (HRR) curve for DCC market source shop 2 for for different fuel distribution considered, keeping air curtain at non-discharged condition.

Fig. 3.104 Temperature distribution at eye level (1.54 m) in staircase for DCC market source shop 2 for different fuel distribution with a vertical single jet air curtain discharged at 10 m/s.

Thus, air curtains could be safely introduced to confine the heat and mas inside the source. Figure 3.101 shows effectiveness and no curtain condition flashover time for different fuel distribution of DCC market source shop 1. The effectiveness for a particular distribution was calculated up to the no curtain flashover time for that particular distribution. The single jet vertical air curtain at 10 m/s jet velocity was less effective whi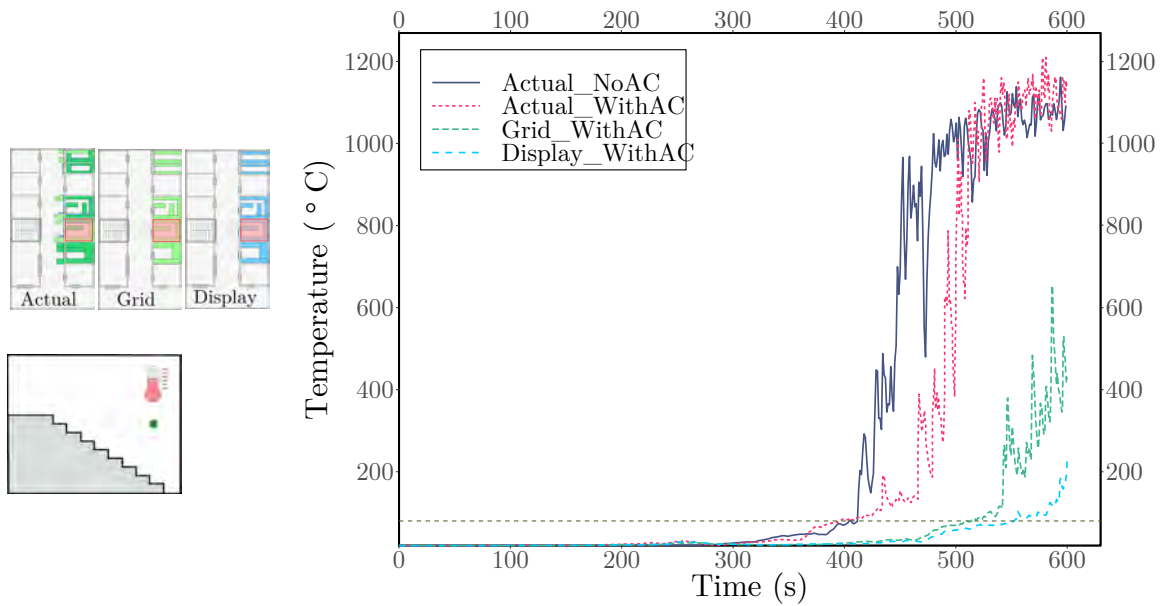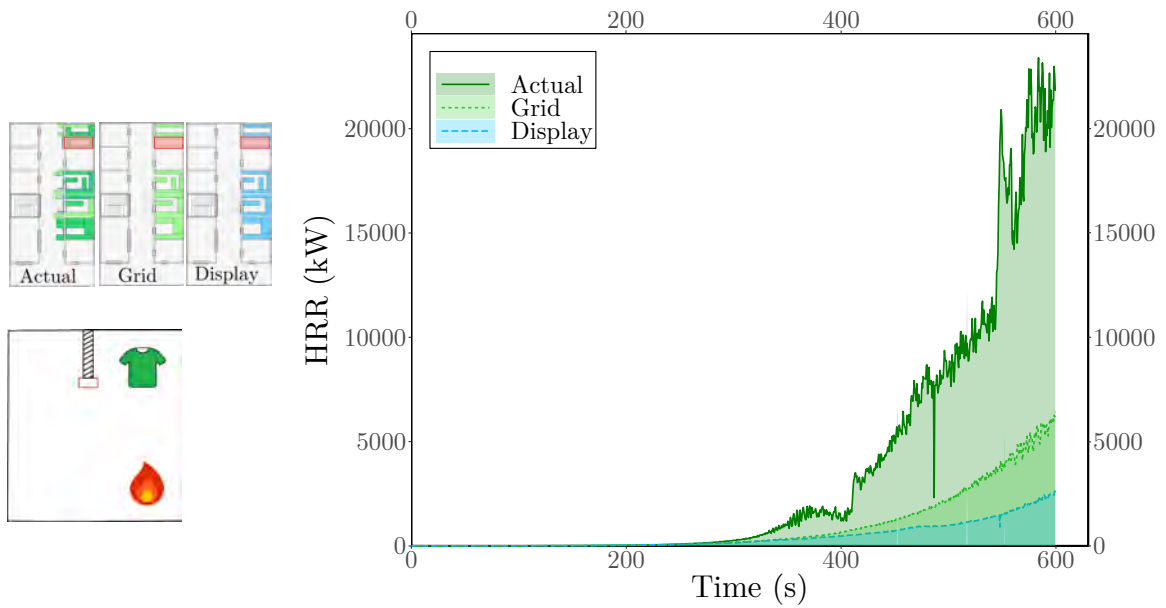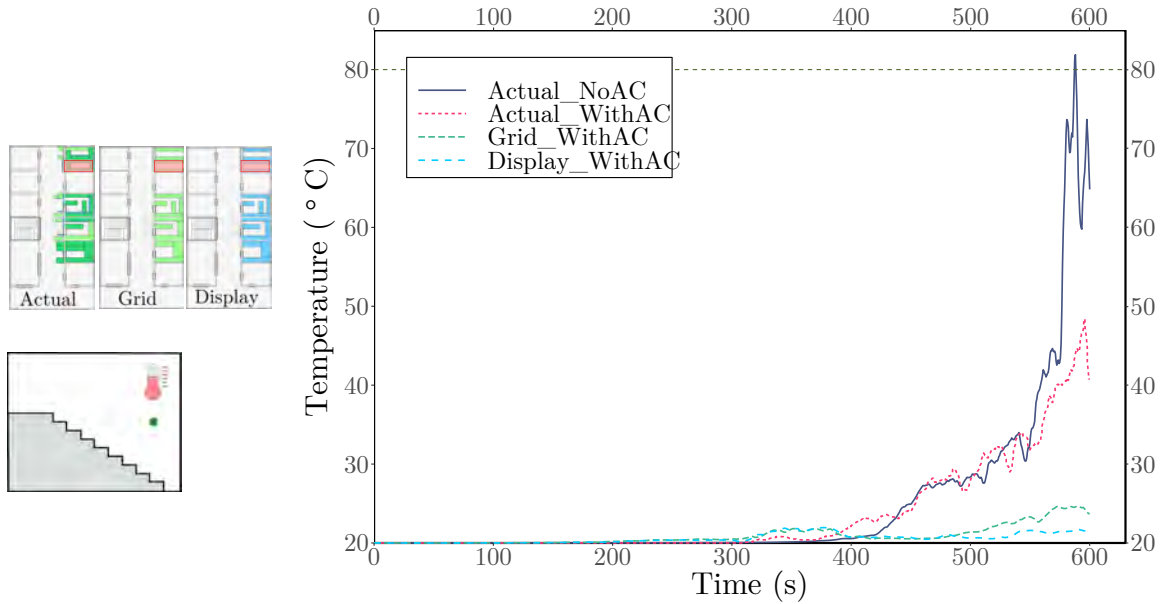le used against at Grid type fuel distribution. Figure 3.102 shows the temperature distribution at eye level (1.54 m) in staircase for DCC market source shop 1 for different fuel distribution with a vertical single jet air curtain discharged at 10 m/s. As expected from the earlier flame propagation data, the temperature tenability at staircase crossed much later for Grid and Display type fuel distribution than Actual one, and the peak temperature for Display distribution was considerably lower than other two distributions.

The heat release rate (HRR) curve for DCC market source shop 2 for different fuel distribution considered, keeping air curtain at non-discharged condition is shown in figure 3.103. Although not identical like source shop 1, the Grid and Display distribution for source shop 2 again produced much lower HRR profile than Actual distribution. And as seen from figure 3.104, the effect of the fire at source 2 was not felt at staircase for the total simulation time considered, for Grid and Display distribution.

3.2.1.6   Summary of the effects of the variations of fuel distribution

The DCC market source 1 and source 2 fuel distribution variation results indicated that, considering the amount of fuel that can be stored and lower heat release rate in case of a fire hazard, the Grid type fuel distribution should be implemented in higher heat release rate per unit area fuel hosting shops to avoid devastating fire hazards.

3.2.1.7 Air Curtain with Furniture Fuel in the DCC market

As the furniture fuel had low heat release rate as seen from the flame propagation section, introduction of air curtain virtually made no difference in the temperature and heat release rate for the furniture fire scenarios. Figure 3.105 shows temperature distributions at eye level (1.54 m) for positions A (inside the fire source) and D (outside the fire source), for air curtain at non-discharged condition compared with air curtain discharged at 10 m/s, for DCC_FS1 and DCC_FS1AC, i.e., for source shop 1. The outside temperature was unchanged while temperature inside the source raised about 10°C due to the air curtain jet circulation. But in all positions the temperature remained below the human tenability limit of 80°C.

The total heat released was also increased slightly with air curtain's introduction as seen from the heat release rate (HRR) curve for air curtain at discharged and non-discharged case in figure 3.106. The situation was similar for source shop 2 also, as from figure 3.107, which illustrates the temperature distributions at eye level (1.54 m) for positions S2a (inside the fire source) and S2d (outside the fire source), for air curtain at non-discharged condition compared with air curtain discharged at 10 m/s, for DCC_FS2 and DCC_FS2AC, the outside temperature remained nearly unchanged

Fig. 3.105 Temperature distributions at eye level (1.54 m) for positions A (inside the fire source) and D (outside the fire source), for air curtain at non-discharged condition compared with air curtain discharged at 10 m/s, for DCC market furniture fire source shop 1, (DCC_FS1 vs. DCC_FS1AC).

147
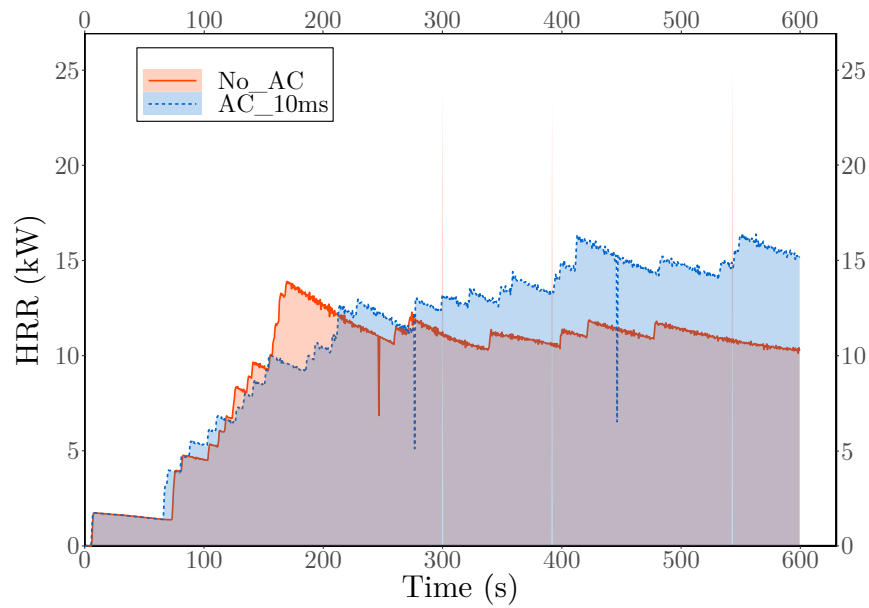
Fig. 3.106 Comparisons of Heat release rate (HRR) curves for DCC market fire source shop 1 for air curtain discharged at 10 m/s and air curtain at non-discharged condition for furniture fuel.
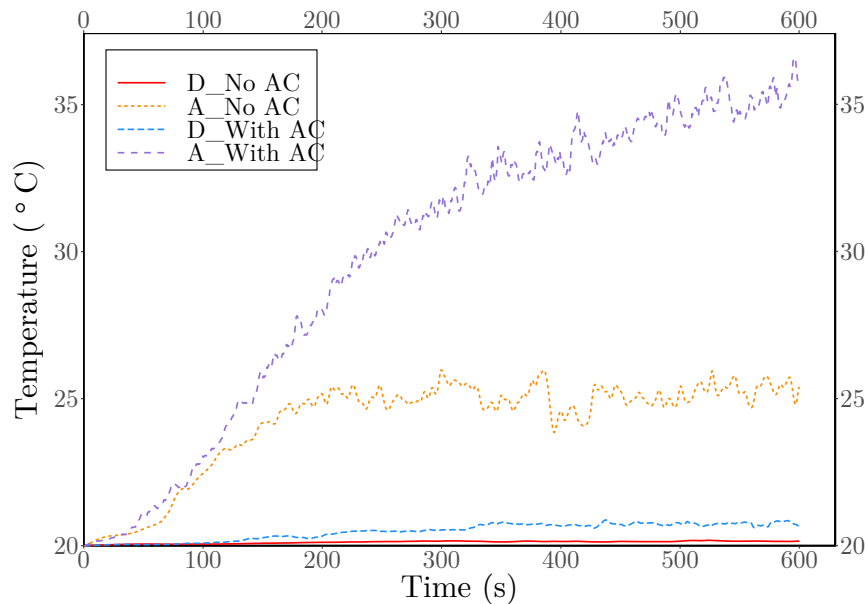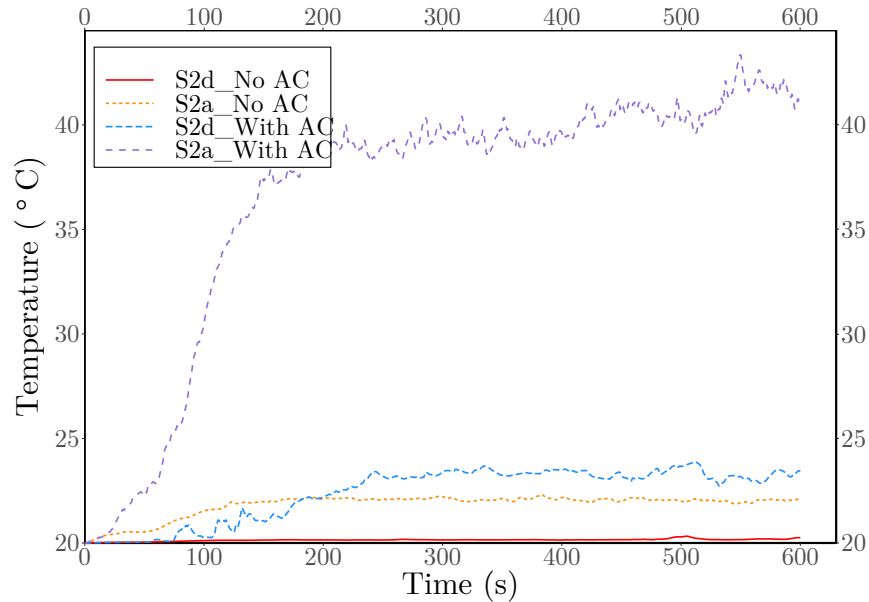

Fig. 3.107 Temperature distributions at eye level (1.54 m) for positions S2a (inside the fire source) and S2d (outside the fire source), for air curtain at non-discharged condition compared with air curtain discharged at 10 m/s, for DCC market furniture fire source shop 2, (DCC_FS2 vs. DCC_FS2AC).
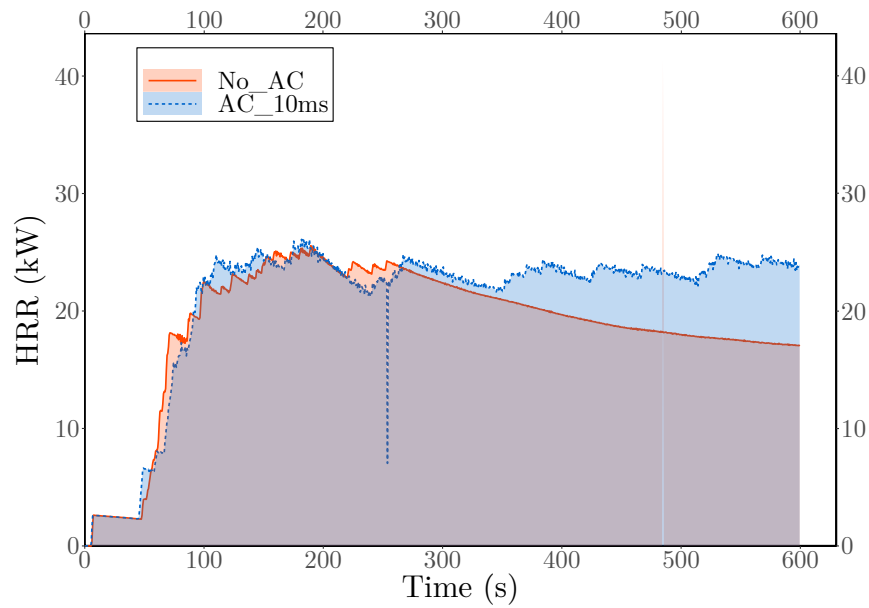
Fig. 3.108 Heat release rate (HRR) curve for DCC market source shop 1 for air curtain discharged at 10 m/s and air curtain at non-discharged condition for furniture fuel.

and inside temperature raised about 15ᵒC. The heat release curve of figure 3.108 shows similar HRR curve pattern for air curtain discharged and non-discharged condition for DCC market source shop 2 with furniture fire scenario. In short, a shopfront air curtain for low HRR fuel should not harm the evacuation process, as seen within the bounds of the present study.

3.2.1.8 Air curtain at the Staircase

Air curtain could confine the fire generated heat and smoke inside the source for a considerable amount of time for variety of fuel and fuel distributions, as seen from the previous sections. Thus, installing air curtain at staircase front, an important location during a fire incident for evacuation, was only logical. In this next segment air curtain was studied for its ability to confine the smoke and heat from a fire incident outside the staircase, ergo, isolating the staircase. Different combinations of air curtain location and fuel distributions were studied for finding the optimum solution for DCC market source shop 1 and source shop 2. The temperature distribution at eye level (1.54 m) in staircase for a single jet air curtain with air curtain's installation position variation for DCC market source shop 1 with clothing as fuel in Actual distribution is shown in figure 3.109. For this case the temperature tenability at staircase breached nearly at the same time, at around 400s for all configurations. Observing the figure 3.110, which represents the temperature distribution at eye level (1.54 m) in staircase for a single jet air curtain with air curtain's installation position variation for DCC market source shop 2 with clothing as fuel in Actual distribution, decision could be made on
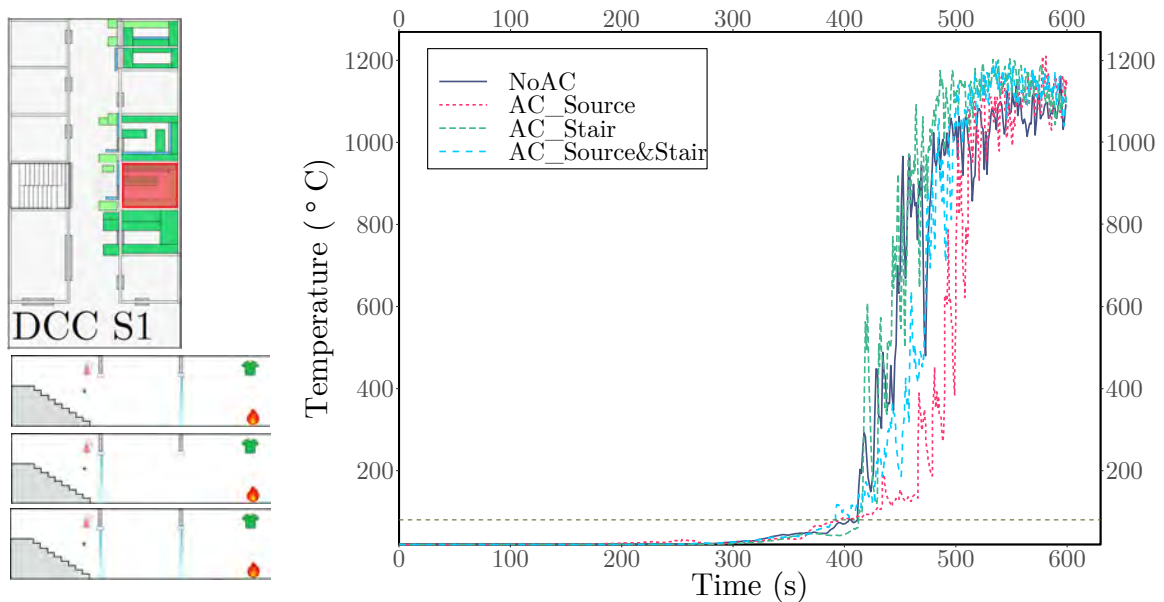

Fig. 3.109 Temperature distribution at eye level (1.54 m) in staircase for a single jet air curtain with air curtain's installation position variation for DCC market source shop 1 with clothing as fuel in Actual distribution.

Fig. 3.110 Temperature distribution at eye level (1.54 m) in staircase for a single jet air curtain with air curtain's installation position variation for DCC market source shop 2 with clothing as fuel in Actual distribution..

air curtain position variation. Air curtain at source and stair case provided the best results than other conditions.

Now as the fuel distribution was changed to Grid from Actual, as in figure 3.111, which illustrates the temperature distribution at eye level (1.54 m) in staircase for a single jet air curtain with air curtain's installation position variation for DCC market source shop 1 with clothing as fuel in Grid distribution, no curtain condition seemed to performed better than others. And for this near stair source case, air curtain at both source and stair case provide similar results with air curtain at source only case. However, from figure 3.112, the temperature distribution at eye level (1.54 m) in staircase for a single jet air curtain with air curtain's installation position variation for DCC market source shop 2 with clothing as fuel in Grid distribution, shows that air curtain at source and staircase performed better than other conditions in case of a far source from staircase. The reason behind this finding, where no curtain performed better again with respect to air curtain, also related to the defected hot smoke path by air curtain as discussed earlier while explaining 'active zone'. Figure 3.113 show the smoke and fire propagation for DCC market source shop 1 with clothing in 'Grid' distribution for simulation time of 100s, 150s, 200s, 250s, and 300s from left to right. Figure 3.113a shows the FDS figures for no curtain condition and figure 3.113b shows
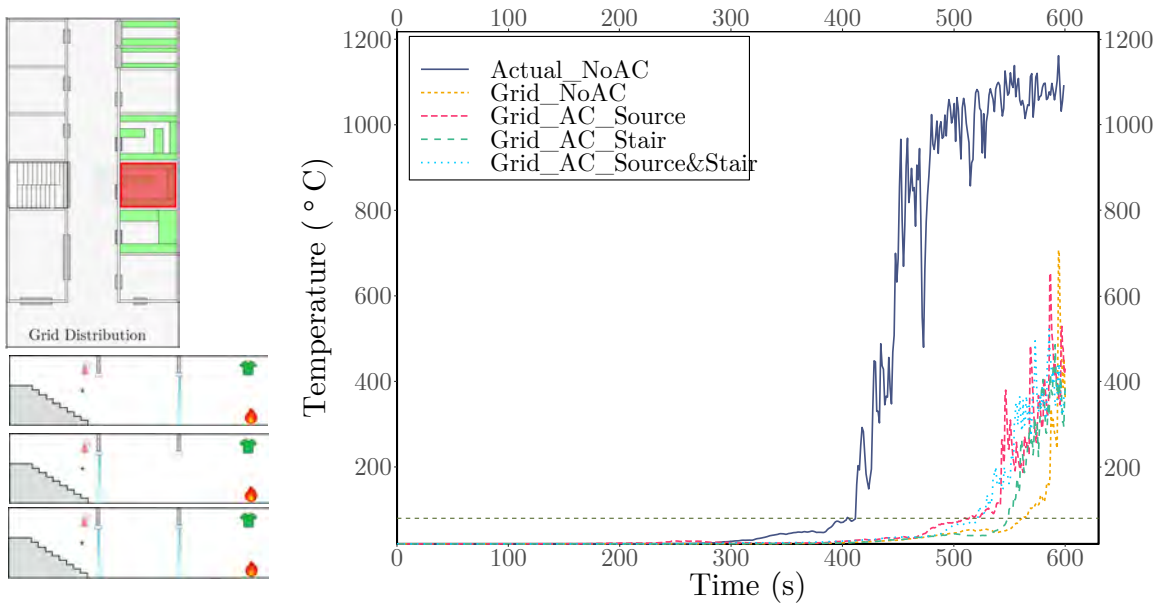
Fig. 3.111 Temperature distribution at eye level (1.54 m) in staircase for a single jet air curtain with air curtain's installation position variation for DCC market source shop 1 with clothing as fuel in Grid distribution.
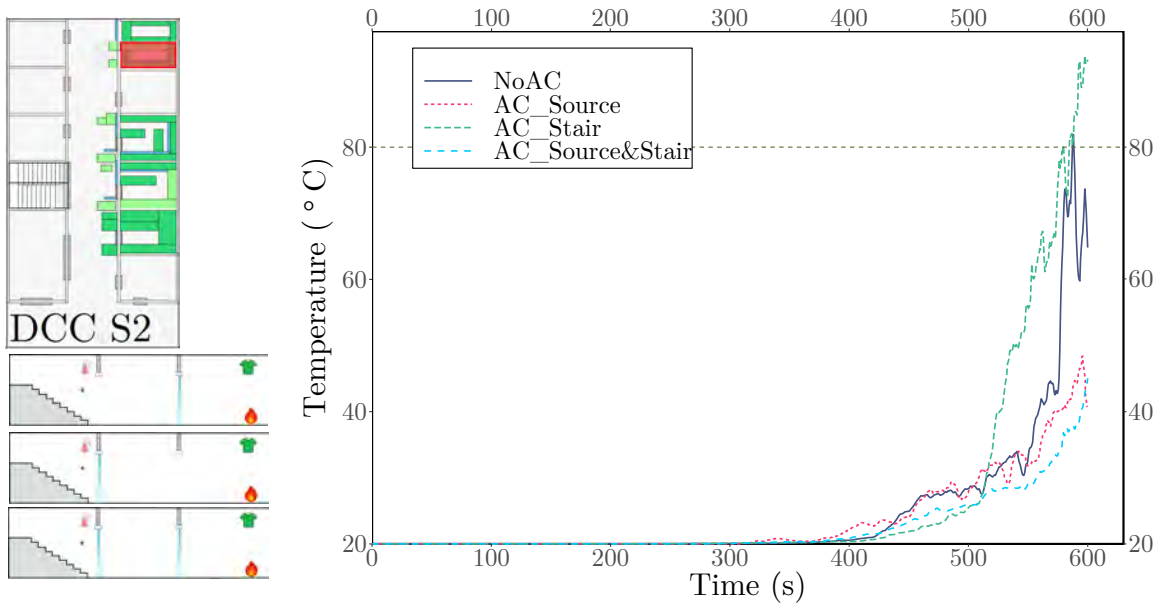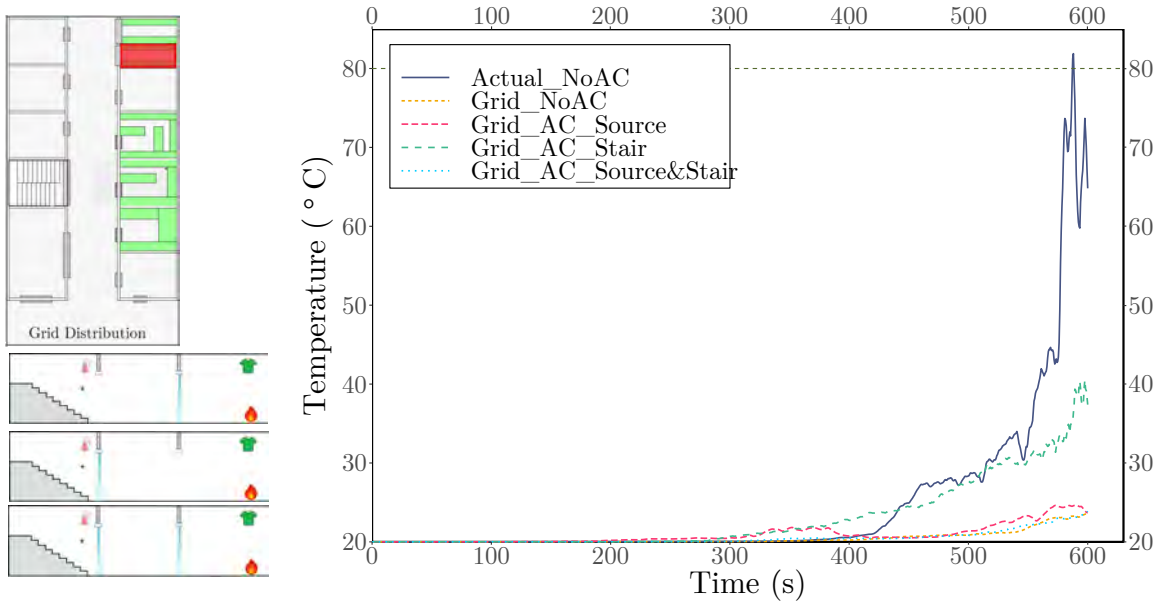

Fig. 3.112 Temperature distribution at eye level (1.54 m) in staircase for a single jet air curtain with air curtain's installation position variation for DCC market source shop 2 with clothing as fuel in Grid distribution.
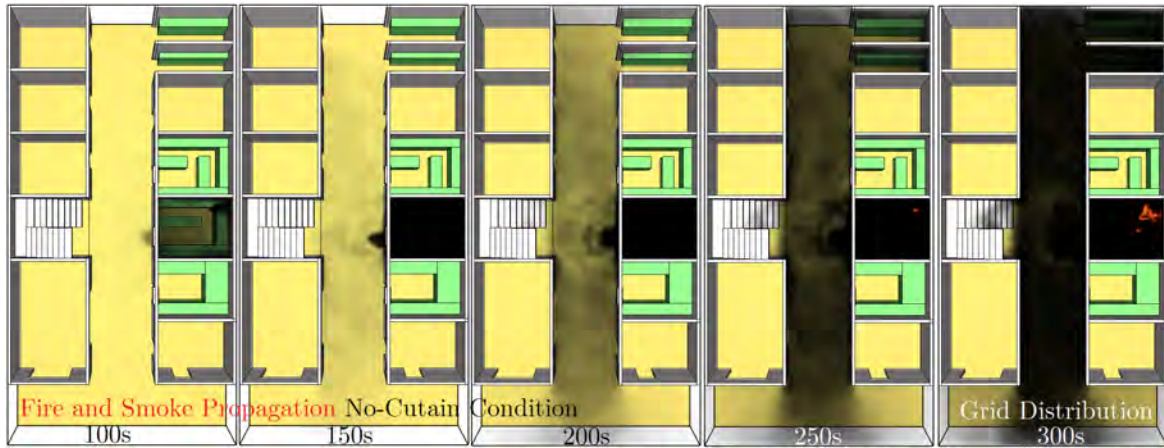
(a) Without Air curtain
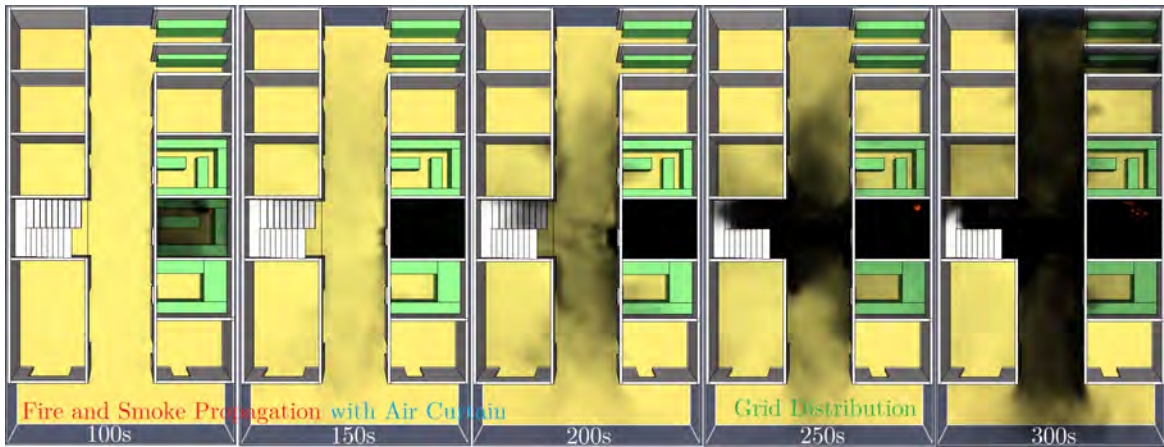
(b) With Air curtain

Fig. 3.113 Top view of Co-Operative market showing the air curtain induced active zone due to jet deflected smoke path for source shop 1 (left) and source shop 2 (right).

the FDS figures with air curtain discharged. From the figure 3.113, it is apparent that, with air curtain the smoke is confined within the source instead of dispersing along the hallway like no-curtain case up to 200s. But, when the fluid pressure inside the shop overcomes the air curtain jet momentum, the pressurized hot smoke is forced directly to shopfront area (the staircase in this case). This in turn increases the staircase eye level temperature for air curtain discharged case, than no-curtain case. Nevertheless, as air curtain certainly provides smoke and fire confinement as seen from earlier sections, placing a shopfront air curtain should be beneficial irrespective of the staircase location. Moreover, air curtains might be beneficial at staircase front during evacuation as seen from this particular analysis. And air curtains at source shops and air curtains at the staircase together should enhanced the isolation of staircase during any fire hazard.

3.2.2 Shopping Mall-2: Co-Operative Market from Mirpur-1, Dhaka

A vertical single jet air curtain with 7.62 cm jet width and 10 m/s jet velocity was introduced at Co-Operative Market source shop 1 and source shop 2 with clothing as fuel, in the next phase of the investigation. Like DCC market, Co-Operative market was also investigated for two source within the geometry, two fuel types, variation of fuel distributions and variation of air curtain placement position.

Figure 3.114 shows the temperature distributions at positions TCi (inside the fire source) and TCo (outside the fire source) for air curtain discharged and non-discharged condition for clothing fire scenario at Co-Operative market fire source shop 1 (CoOp_CS1AC vs. CoOp_CS1). And, figure 3.115 shows the temperature distributions at positions TCi (inside the fire source) and TCo (outside the fire source) for air curtain discharged and non-discharged condition for clothing fire scenario at Co-Operative market fire source shop 2 (CoOp_CS2AC vs. CoOp_CS2). For both cases again the source outside temperature at eye level (1.54 m) for air curtain cases crossed human temperature tenability earlier than non-discharged condition. Thus, here again an active zone should be identified after which the effect of the air curtain is positive
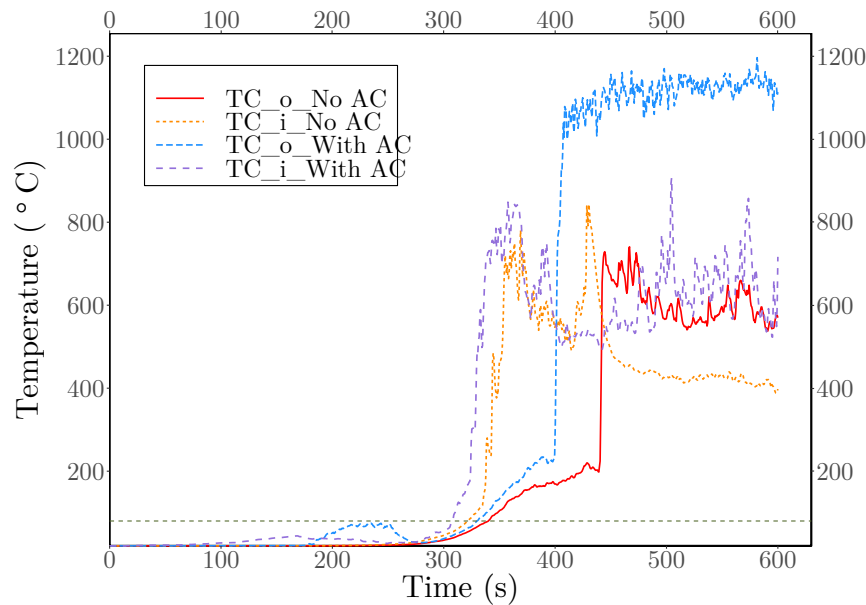
Fig. 3.114 Temperature distributions at eye level (1.54 m) for positions TCi (inside the fire source) and TCo (outside the fire source) for air curtain discharged and non-discharged condition for clothing fire scenario at Co-Operative market fire source shop 1 (CoOp_CS1AC vs. CoOp_CS1).
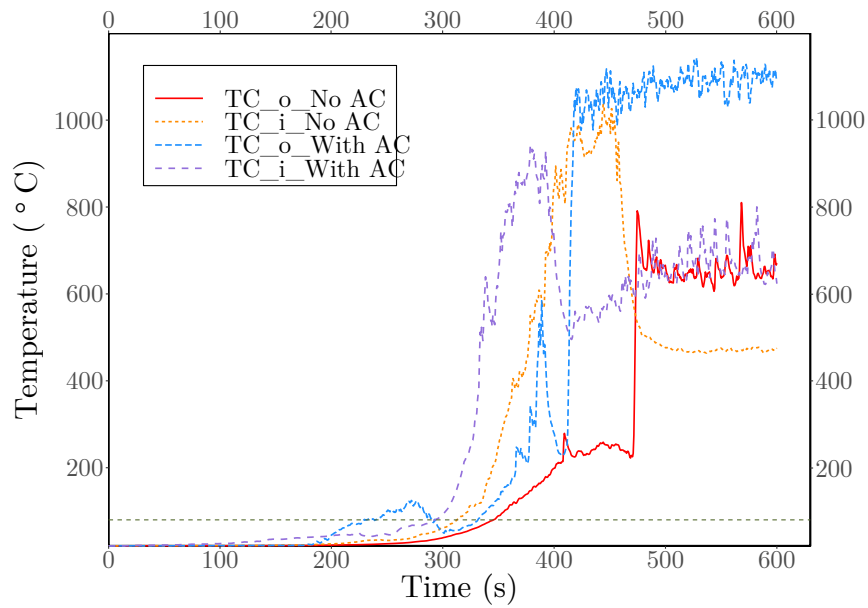
Fig. 3.115 Temperature distributions at eye level (1.54 m) for positions TCi (inside the fire source) and TCo (outside the fire source) for air curtain discharged and non-discharged condition for clothing fire scenario at Co-Operative market fire source shop 2 (CoOp_CS2AC vs. CoOp_CS2).
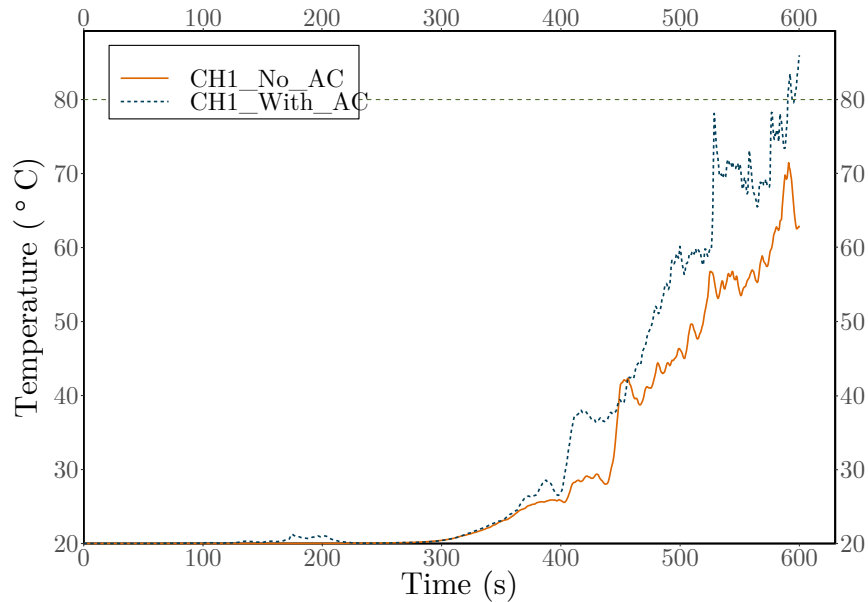
Fig. 3.116 Temperature profile at eye level (1.54 m) for CH1, the borderline of the active zone for Co-Operative market source shop 1 at one end, with air curtain discharged at 10 m/s and without air curtain discharged.
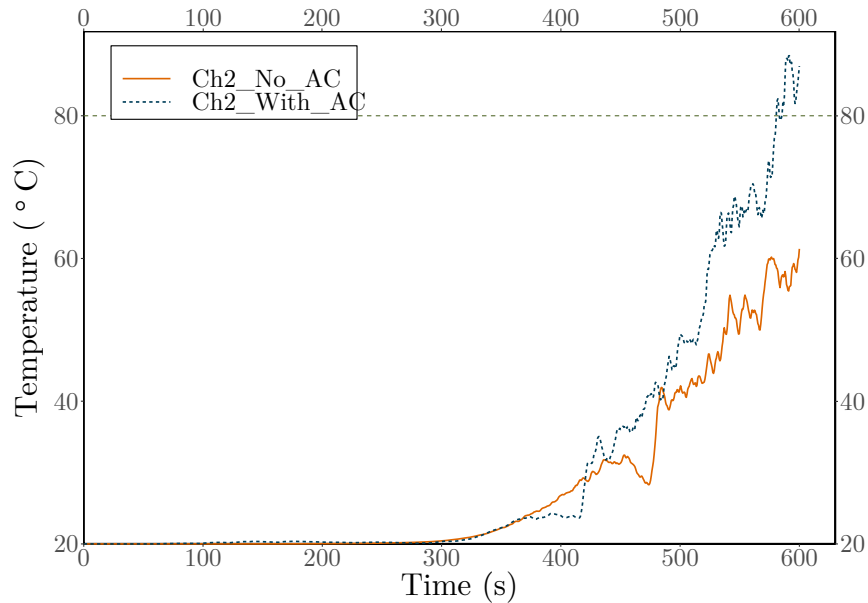
Fig. 3.117 Temperature profile at eye level (1.54 m) for Ch2, the borderline of the active zone for Co-Operative market source shop 2 at one end, with air curtain discharged at 10 m/s and without air curtain discharged.

through out the simulation. Figure 3.116 and figure 3.117 show the temperature profile at eye level (1.54 m) for CH1, the borderline of the active zone for Co-Operative market source shop 1 at north end, and temperature profile at eye level (1.54 m) for Ch2, the borderline of the active zone for Co-Operative market source shop 2 at east end, respectively.

Figure 3.120a and figure 3.120b show the air curtain induced active zone due to jet deflected smoke path for Co-Operative market source shop 1 (left) and source shop 2 (right). The active zone for this architectural variation, i.e., for Co-Operative market was different than DCC market although the shop size and fuel distributions were comparable. The narrow corridor might be a reason behind this long active zone, additional data is needed to confirm this hypothesis. Figure 3.118 and figure 3.119 show heat release rate (HRR) curve for Co-Operative market source shop 1 and source shop 2 for air curtain discharged at 10 m/s and air curtain at non-discharged condition respectively. The HRR were slightly higher for air curtain discharged case indicating better combustion as more oxidizers were available, the increment was not alarming as the fire was not an under-ventilated one, and was only after 400s.

Figure 3.121 illustrates temperature distributions at staircase for air curtain at discharged and non-discharged condition for clothing fire scenario for Co-Operative market source shop 1 for different fuel distribution and air curtain position variation.
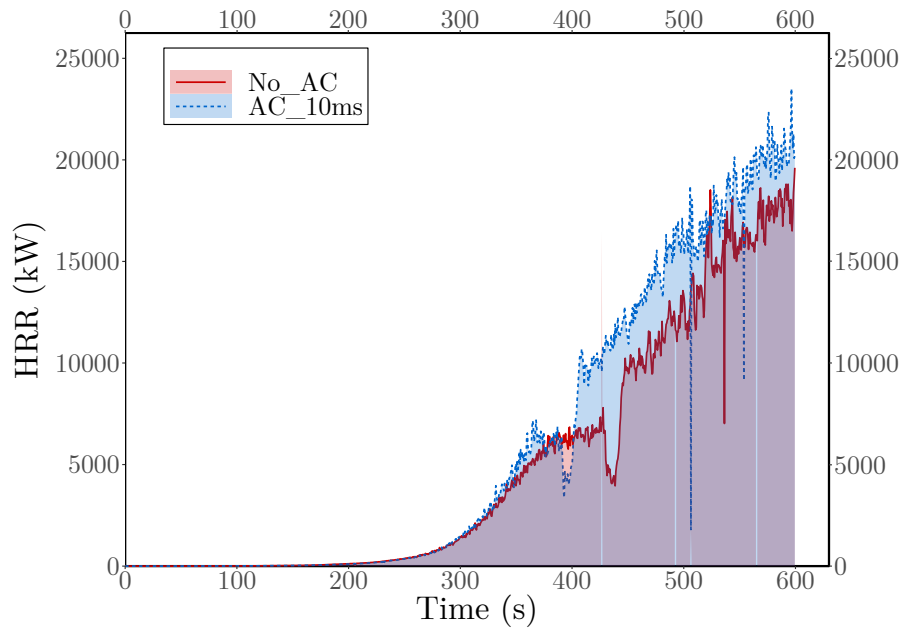
Fig. 3.118 Heat release rate (HRR) curve for Co-Operative market source shop 1 for air curtain discharged at 10 m/s and air curtain at non-discharged condition (CoOp_CS1AC vs. CoOp_CS1).
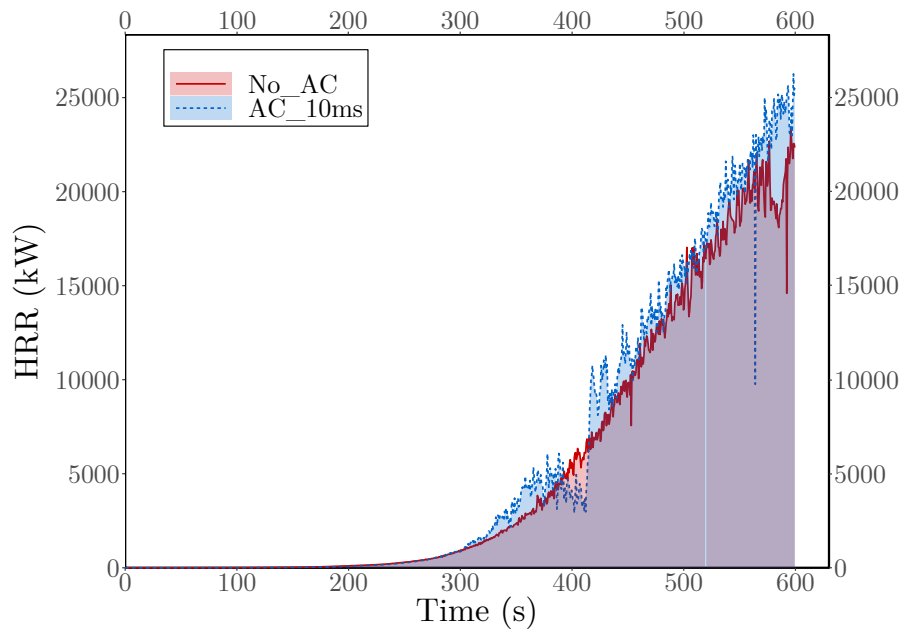
Fig. 3.119 Heat release rate (HRR) curve for Co-Operative market source shop 2 for air curtain discharged at 10 m/s and air curtain at non-discharged condition (CoOp_CS2AC vs. CoOp_CS2).

(a) CoOp_CS1AC

(b) CoOp_CS2AC
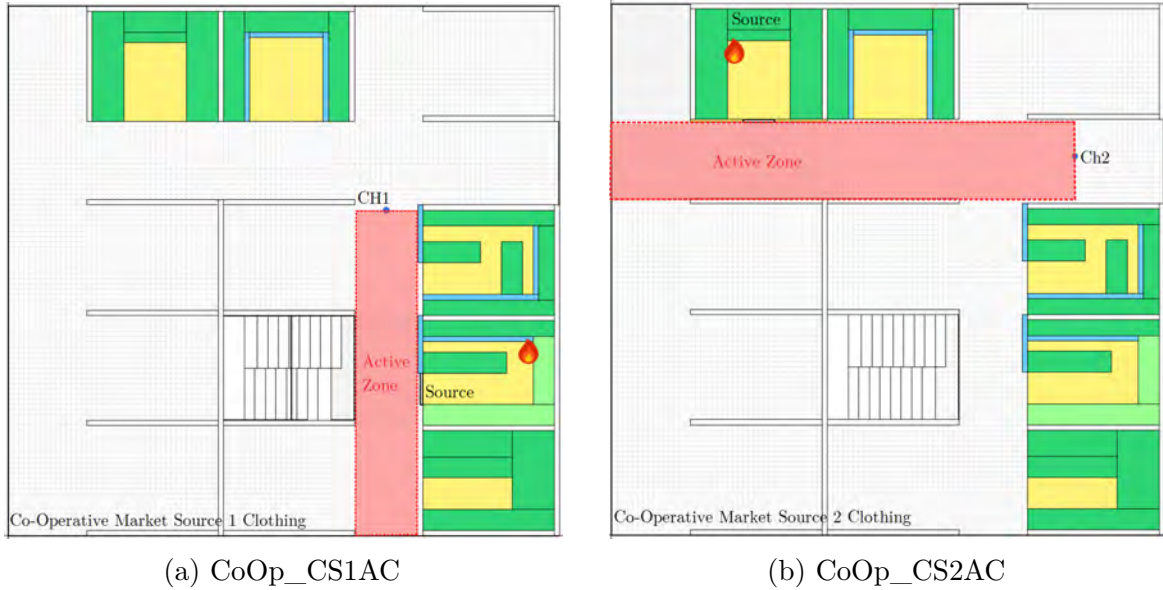
Fig. 3.120 Top view of Co-Operative market showing the air curtain induced active zone due to jet deflected smoke path for source shop 1 (left) and source shop 2 (right).
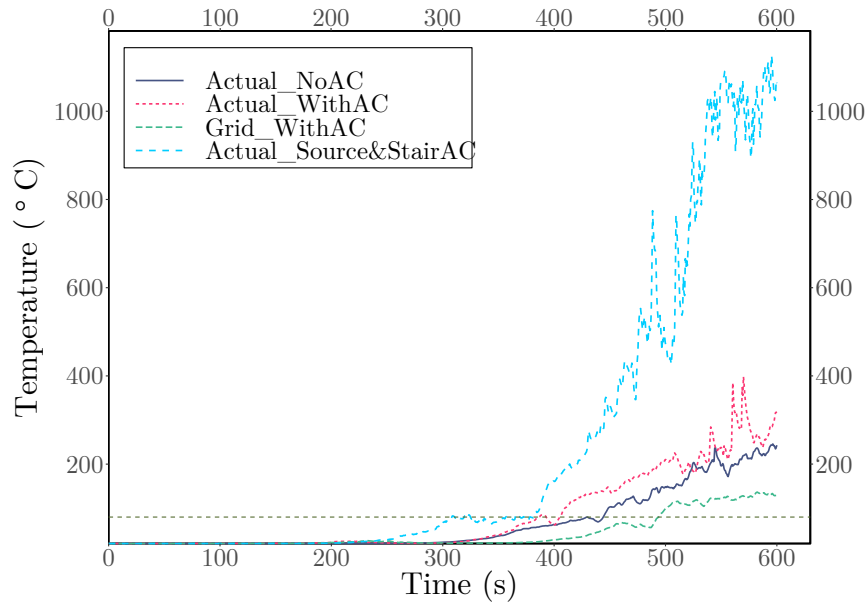
Fig. 3.121 Temperature distributions at staircase for air curtain at discharged and non-discharged condition for clothing fire scenario for Co-Operative market source shop 1 for different fuel distribution and air curtain position variation.

Here again Grid type fuel distribution with air curtain at source provided the utmost time for evacuation. The air curtain at source and actual fuel distribution crossed the tenability earlier at staircase due to shift in heat path due to deflection by curtain jet

and staircase being inside the active zone. The extreme increase in temperature for the case when air curtain installed both at source and staircase, was due to the fact that, staircase air curtain was inside the active zone and the re-circulation of air further assisted the heat transfer for this case. The furniture fire scenario with air curtain discharged for Co-Operative market follows similar pattern of furniture fire scenario of DCC market, slight increase in inside temperature and HRR but virtually unchanged outside temperature. Supporting curves are attached in Appendix A.

3.2.3 Shopping Mall-3: MultiPlan Shopping Complex from New Elephant Road, Dhaka

MultiPlan Shopping Complex provided good outcome during the flame and smoke propagation study without air curtains. Thus, with air curtains the architectural design of this shopping complex was expected to perform better again than other two shopping malls. MultiPlan Shopping Complex was also investigated for two source within the geometry, two fuel types, variation of fuel distributions and variation of air curtain placement position. Initially, A vertical single jet air curtain with 7.62 cm jet width and 10 m/s jet velocity was introduced at source shop 1 and source shop 2 door with
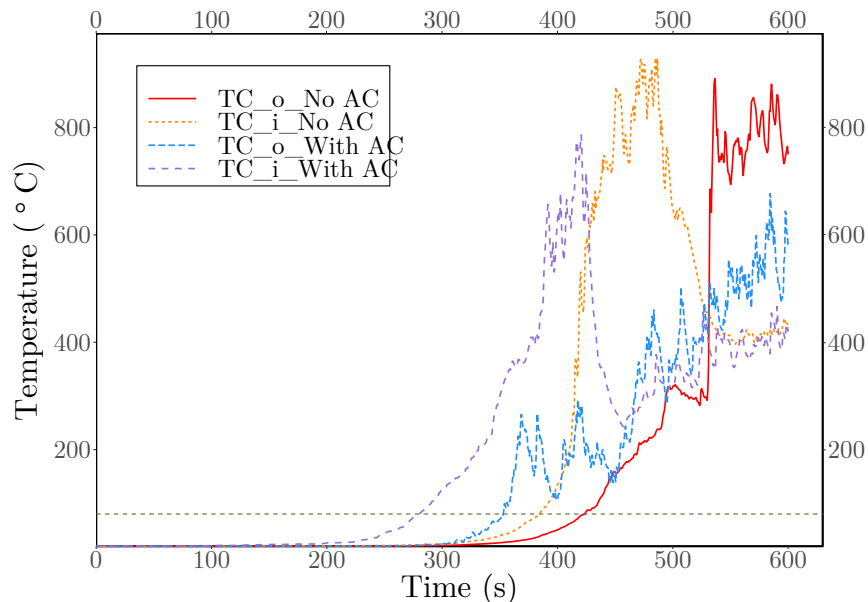
Fig. 3.122 Temperature distributions at eye level (1.54 m) for positions TCi (inside the fire source) and TCo (outside the fire source) for air curtain discharged and non-discharged condition for clothing fire scenario at MultiPlan Shopping Complex fire source shop 1 (MP_CS1AC vs. MP_CS1).
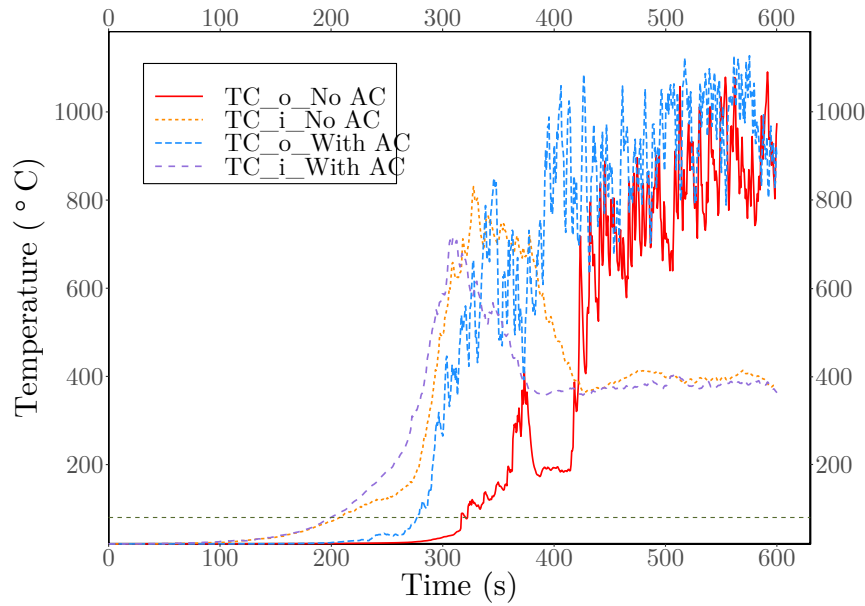
Fig. 3.123 Temperature distributions at eye level (1.54 m) for positions TCi (inside the fire source) and TCo (outside the fire source) for air curtain discharged and non-discharged condition for clothing fire scenario at MultiPlan Shopping Complex fire source shop 2 (MP_CS2AC vs. MP_CS1).

clothing as fuel. Figure 3.122 shows the temperature distributions at eye level (1.54 m) for positions TCi (inside the fire source) and TCo (outside the fire source) for air curtain discharged and non-discharged condition for clothing fire scenario at MultiPlan Shopping Complex fire source shop 1 (MP_CS1AC vs. MP_CS1). Figure 3.123 shows the temperature distributions at eye level (1.54 m) for positions TCi (inside the fire source) and TCo (outside the fire source) for air curtain discharged and non-discharged condition for clothing fire scenario at MultiPlan Shopping Complex fire source shop 2 (MP_CS2AC vs. MP_CS1). Like all other cases here again the source outside temperature at eye level (1.54 m) for air curtain cases crossed human temperature tenability earlier than non-discharged condition.

But surprisingly while searching for the borderline of the active zone again in case of MP_CS1AC, i.e., MultiPlan Shopping Complex source shop 1, the thermocouple immediately next to the source outside thermocouple on both sides showed lower temperature than non-discharged condition for total 600s of simulation time. The thermocouple positions named MH1 and MH2 and the temperature profiles for these two points for air curtain discharged and non-discharged condition were plotted in figure 3.124. For MultiPlan Shopping Complex source shop 2, the active zone was nearly 12 m in total, twice the size of the active zone for DCC_CS1AC. Again additional data
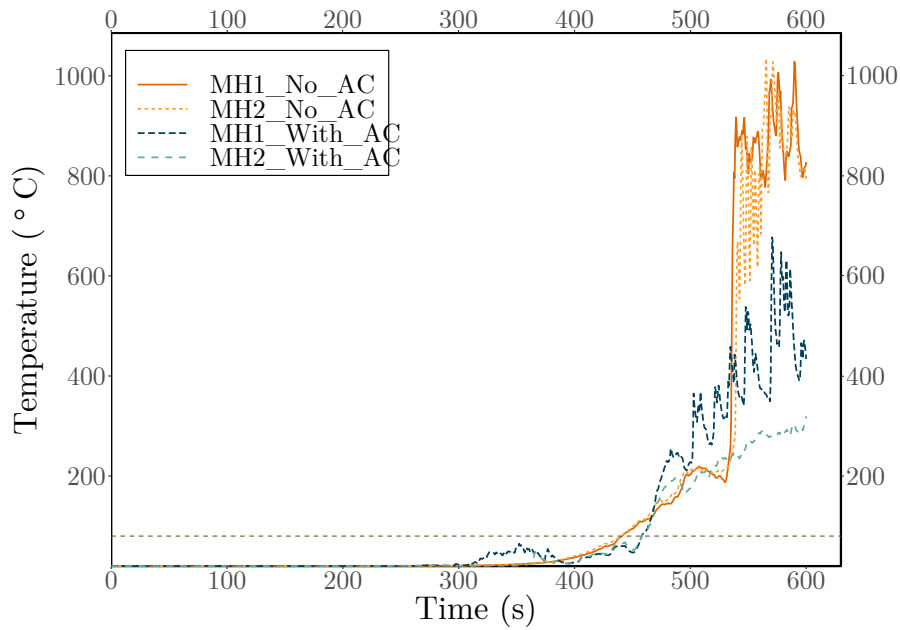
Fig. 3.124 Temperature profile at eye level (1.54 m) for MH1 and MH2, the borderline of the active zone for MultiPlan Shopping Complex source shop 1, with air curtain discharged at 10 m/s and without air curtain discharged.
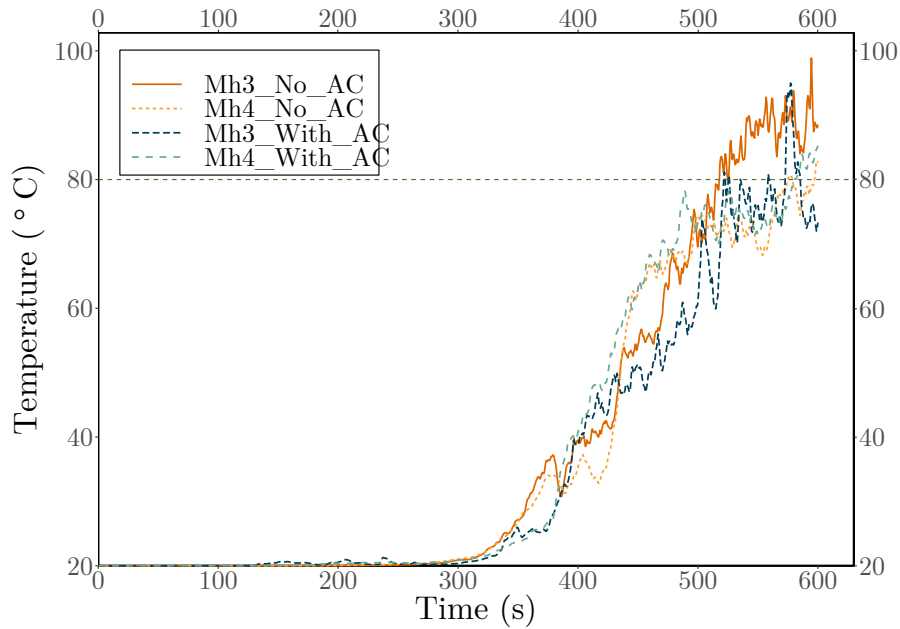
Fig. 3.125 Temperature profile at eye level (1.54 m) for Mh3 and Mh4, the borderline of the active zone for MultiPlan Shopping Complex source shop 2, with air curtain discharged at 10 m/s and without air curtain discharged.

(a) MP_CS1AC

(b) MP_CS2AC
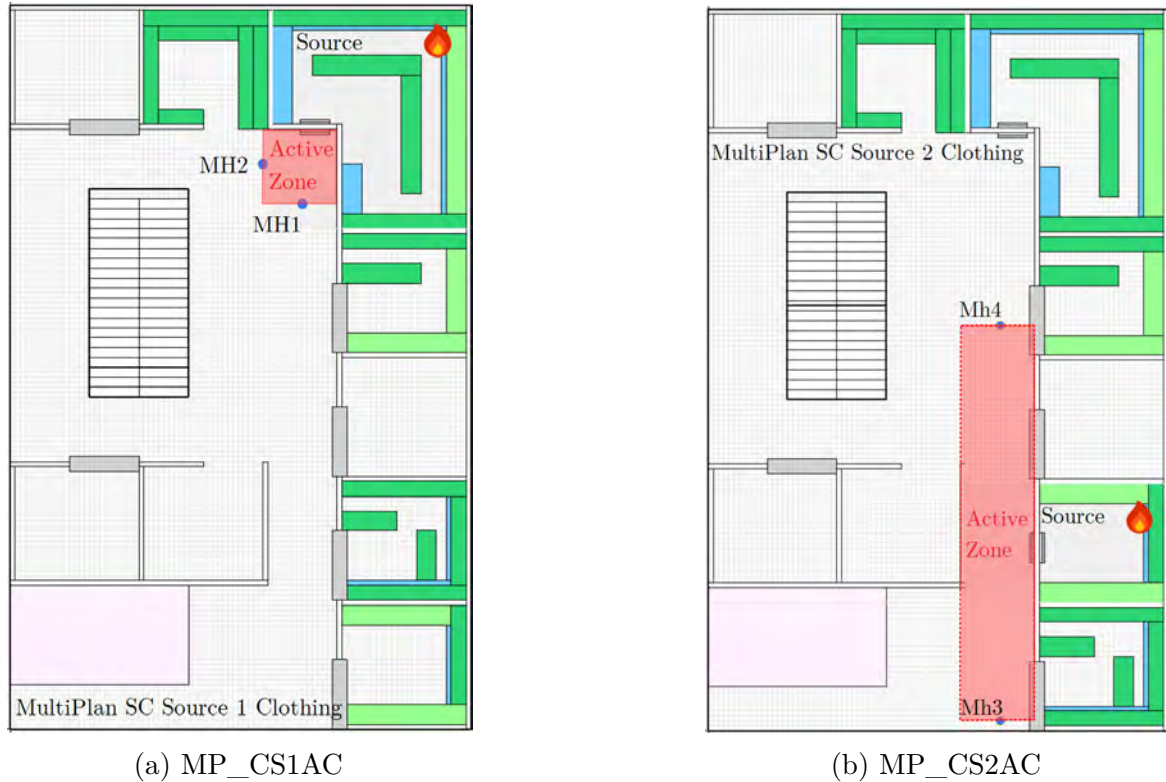
Fig. 3.126 Top view of MultiPlan Shopping Complex showing the air curtain induced active zone due to jet deflected smoke path for source shop 1 (left) and source shop 2 (right).

is needed for confirming the exact reason for different active zone size. Figure 3.125 shows the temperature profile at eye level (1.54 m) for Mh3 and Mh4, the borderline of the active zone for MultiPlan Shopping Complex source shop 2, with air curtain discharged at 10 m/s and without air curtain discharged. The active zones for both source shops are shown in figure 3.126.

Figure 3.127 and figure 3.128 show the heat release rate (HRR) curve for MultiPlan Shopping Complex source shop 1 and source shop 2 for air curtain discharged at 10 m/s and air curtain at non-discharged condition respectively. Interestingly with air curtain discharged the HRR was lower for MultiPlan Shopping Complex source shop 1 within the simulation time of 600s. The HRR curve for source shop 2 with air curtain discharged was nearly similar with non-discharged condition.

For MultiPlan Shopping Complex source shop 1, different fuel type variations were also investigated as this source shop has significantly larger area. Figure 3.129 shows the heat release rate (HRR) curve for MultiPlan Shopping Complex source shop 1 for for different fuel distribution considered, keeping air curtain at non-discharged
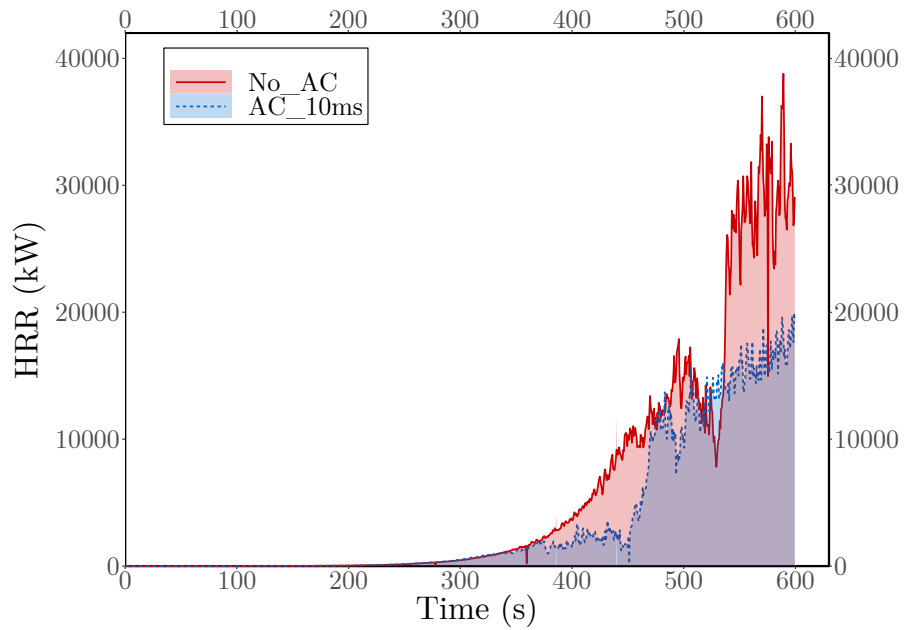
Fig. 3.127 Heat release rate (HRR) curve for MultiPlan Shopping Complex source shop 1 for air curtain discharged at 10 m/s and air curtain at non-discharged condition (MP_CS1AC vs. MP_CS1).
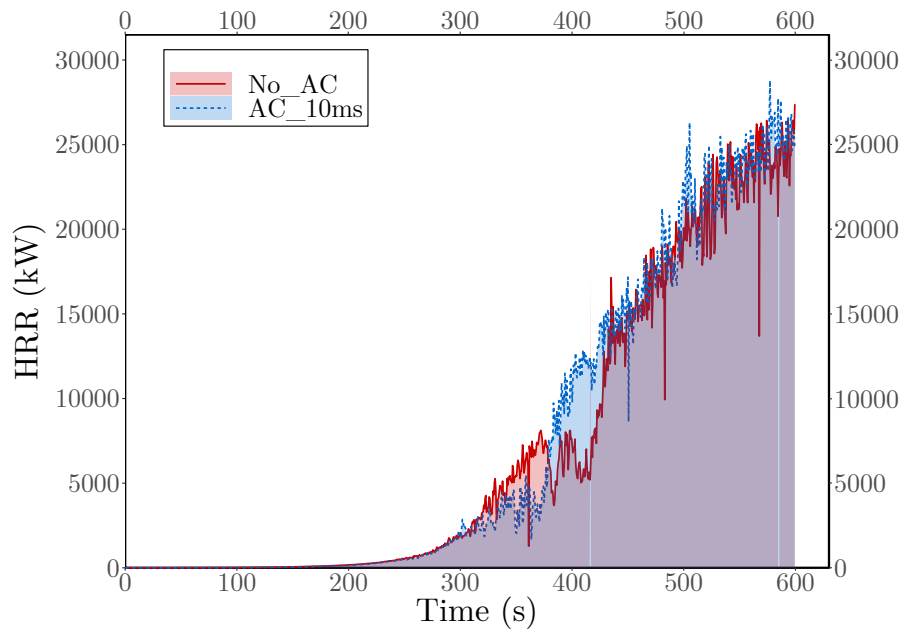
Fig. 3.128 Heat release rate (HRR) curve for MultiPlan Shopping Complex source shop 1 for air curtain discharged at 10 m/s and air curtain at non-discharged condition (MP_CS1AC vs. MP_CS1).
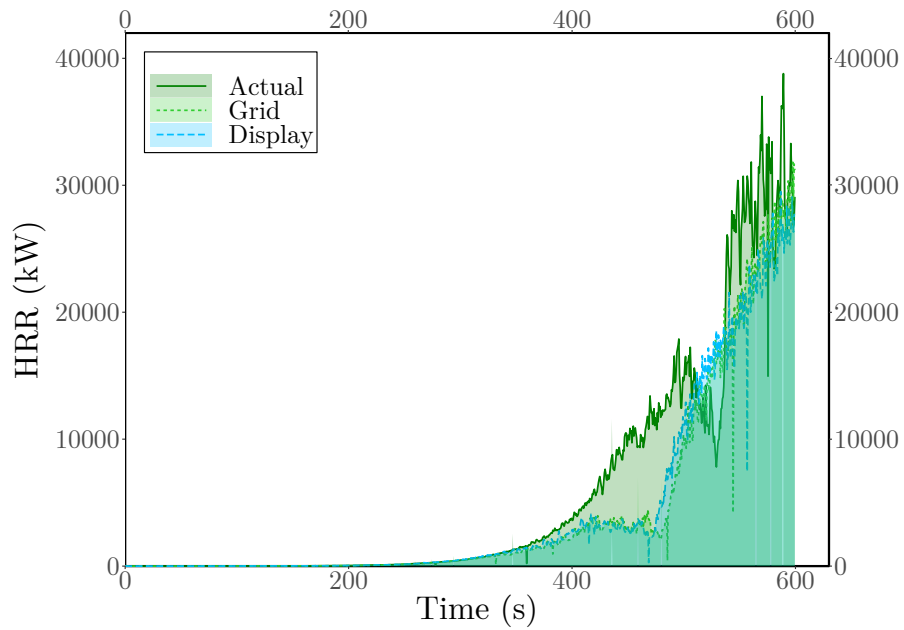
Fig. 3.129 Heat release rate (HRR) curve for MultiPlan Shopping Complex source shop 1 for for different fuel distribution considered, keeping air curtain at non-discharged condition.
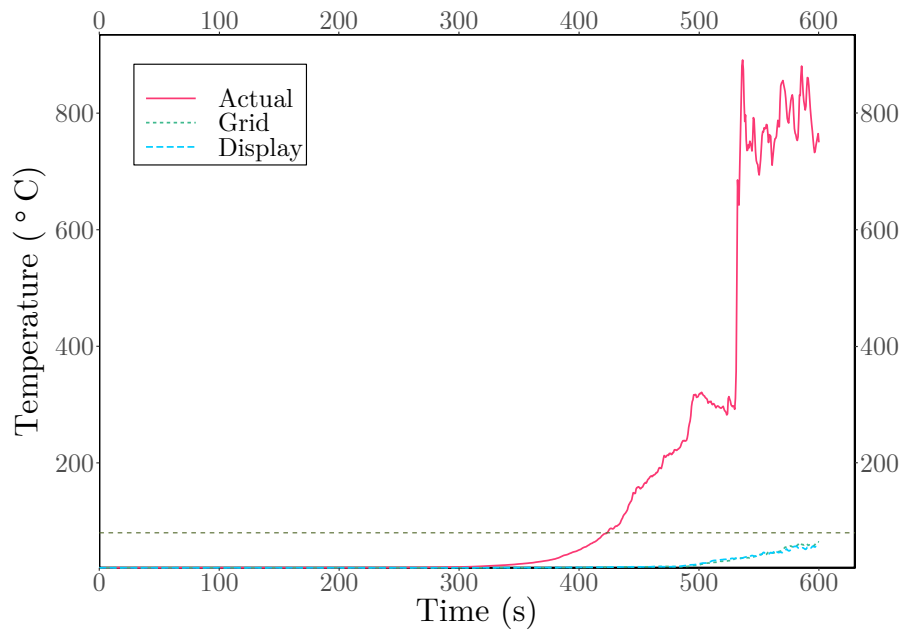
Fig. 3.130 Temperature distributions at eye level (1.54 m) for TCo (outside the fire source) for clothing fire scenario at MultiPlan Shopping Complex fire source shop 1 with different fuel distribution variations.

condition. Here again like DCC market source shop 1, the heat release rate for Grid type fuel distribution and Display fuel distribution were similar. The similar HRR of Grid and Display distribution indicated that, although fuel load was nearly one third for Display distribution compared to Grid type, better burning was achieved due to the availability of excess oxidizers for Display distribution. Thus, it can be concluded that, from DCC market source shop 1, 2, and MultiPlan Shopping Complex source shop 1,, the heat release rate of Grid type fuel distribution and Display fuel distribution were comparable independent of source shop size. Figure 3.130 shows the temperature distributions at eye level (1.54 m) for TCo (outside the fire source) for air curtain non-discharged condition for clothing fire scenario at MultiPlan Shopping Complex fire source shop 1 with different fuel distribution variations. Here again the Grid and Display distribution provided similar temperature profile, much lower than the actual distribution case, in fact the temperature for Grid and Display distribution case never crossed the human tenability limit for total simulation time. This again indicated that, Grid type distribution was preferable due to the low heat release rate in case of fire hazard at comparatively higher amount of fuel.

3.3 Effects of the Parametric Variation of Air curtain

Air curtain installed at source shop door, was able to confine the fire generated heat and smoke inside source shop for certain amount of time, and aid the evacuation process, depending on the fuel load and fuel arrangements, as previous investigations suggested. The air curtain studied matched the parameters of a commercially available off-the-self air curtain. To further increase the air curtains effectiveness to confine heat and mass transfer due to pressure generated inside the source after initiation of a fire hazard, the air curtain operating parameters were thoroughly analyzed to find optimum operating condition. Air curtain's jet velocity, jet angle, flow rate and number of jets with distance between consecutive jets were varied strategically with realistic values. The resulting cases are presented in table 3.14.

Table 3.14 Overview of simulations conducted with air curtain's parametric variations. The fire was simulated at DCC market source shop 1 with clothing fuel in actual distribution and air curtain at source shop door.

Case	Jet width (cm)	Number of jet	Pitch ratio	Jet angle	Velocity of jet (m/s)	Flowrate (m^3/h)
1(previous)	7.62	1	Zero	0	10	2500
44					9	2250
45					8	2000
46					7	1750
47					6	1500
48					5	1250
49					4	1000
50					3	750
51	7.62	1	Zero	15	10	2500
52				30	10	2500
53				45	10	2500
54				60	10	2500
55	7.62	2	One	0	10	5000
56			Two	0	10	5000
57			Three	0	10	5000
58			Four	0	10	5000
59	7.62	1	Zero	0	5	1250
60	15.24	1	Zero	0	5	2500
61	15.24	1	Zero	0	10	5000
62	30.48	1	Zero	0	5	5000
63(optimum)	7.62	1	Zero	30	9	2250

3.3.1 Variation of Jet Velocity

The air curtain's jet velocity was varied from 3 m/s to 10 m/s at a step size of 1 m/s, for obtaining optimum jet velocity. Increasing the velocity monotonously will not produce effective sealing as momentum ratio R plays the pivoting role determining the effectiveness of air curtain. The momentum ratio R is the ratio of the vertically downward air curtain momentum to the horizontal smoke layer momentum as defined in equation 3.3.

$$R = \frac{\rho_j A_j V_j^2}{\rho_s A_s V_s^2} \tag{3.3}$$

Here, ρ_j, V_j and A_j are density, velocity and area of the air curtain jet respectively, and ρ_s, V_s and A_s are density, velocity and area of the upper smoke layer respectively. The other operating air curtain parameters were fixed at, single jet with zero jet angle and 7.62 cm jet width. As flowrate is directly proportional to the jet velocity as fixed cross-sectional area were considered, flowrate varied with jet velocity. The effect of air curtain's jet velocity on the temperature outside the source shop at ceiling level (2.9 m) for position D, for jet velocity of 3 m/s to 10 m/s at a step size of 1 m/s, for a single jet vertical air curtain of 7.62 cm jet width, is shown in Figure 3.131. The effect of jet

Fig. 3.131 Temperature at ceiling level (2.9 m) for position D (outside the fire source) for a single jet vertical air curtain of 7.62 cm jet width, discharged at velocities ranged from 3 m/s to 10 m/s with 1 m/s step size.

Fig. 3.132 CO concentration distribution at ceiling level (2.9 m) for position D1 (outside the fire source) for a single jet vertical air curtain of 7.62 cm jet width, discharged at velocities ranged from 3 m/s to 10 m/s with 1 m/s step size.

velocity on CO concentration at ceiling level (2.9 m) for position D1, for jet velocity of 3 m/s to 10 m/s at a step size of 1 m/s, is shown in Figure 3.132. The temperature and CO concentration was measured at ceiling level (2.9 m) due to the fact that, the sealing effect was visible at ceiling level, and not in eye level as discussed on length in previous sections. As at low air curtain velocity the momentum ratio R was low, air curtains with 3 m/s and 4 m/s jet velocity were not effective in confining the heat and mass transfer. Increasing the air curtain jet velocity increase the momentum ratio, i.e., the air curtain jet was able to resist the smoke and heat flow through the door due to the pressure generated inside the source, as heat was increased as combustion progressed. At 5 m/s injection velocity there was considerable temperature reduction at the position D and the reduction in temperature was proportional to the increase in injection velocity to 10 m/s, the highest velocity considered in this study.

Although the ceiling level (2.9 m) temperature and CO concentration decreased as velocity increased, the total sealing effect through the open door might not be reflected on only one thermocouple. For getting the total sealing effect, the effectiveness of air curtain should be measured as a function of jet velocity as done in figure 3.139. The highest effectiveness, about 40% was observed at 9 m/s jet velocity, thus, considered optimum operating velocity. As mentioned earlier highest effectiveness was not gained
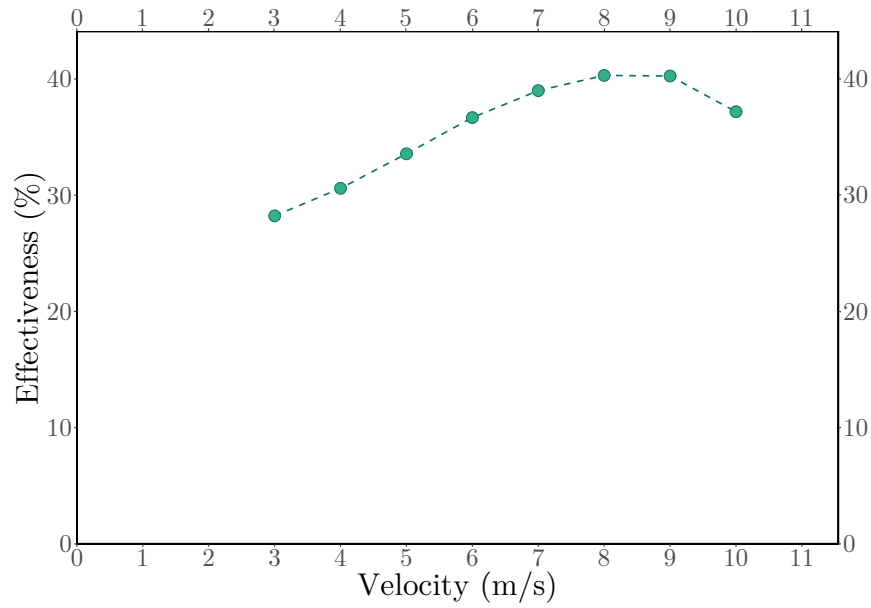
Fig. 3.133 The Effectiveness of a single jet vertical air curtain of 7.62 cm jet width, in function of jet velocity.
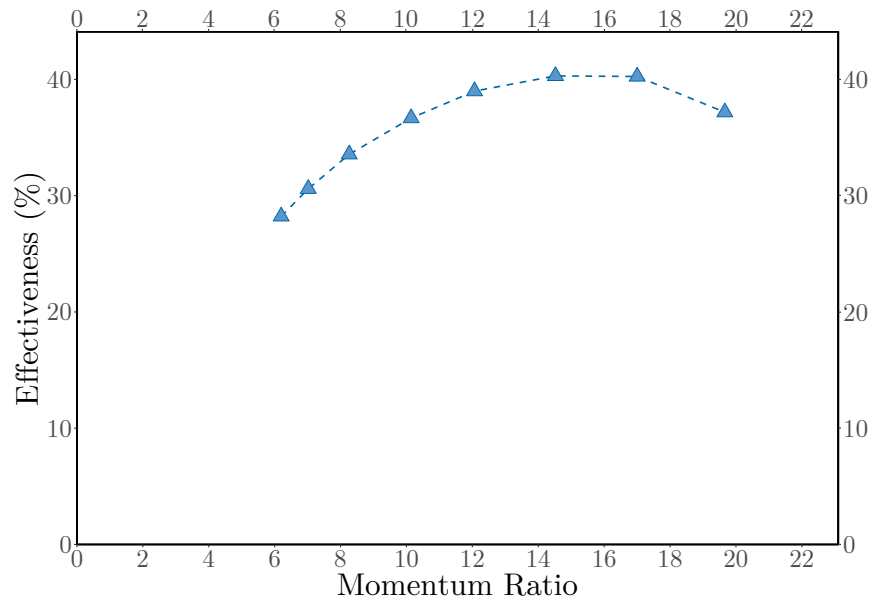
Fig. 3.134 The Effectiveness of a single jet vertical air curtain of 7.62 cm jet width, in function of momentum ratio.

with highest velocity as momentum ratio comes into play. Figure 3.134 shows the Effectiveness of a single jet vertical air curtain of 7.62 cm jet width, in function of momentum ratio. As reported by Yu et al. (2016), for small R values, the sealing effect

169

increased as R increased, and at higher values of R the sealing effect was diminishing as the impinging curtain jet pushes smoke and heat downstream. Here again the 9 m/s velocity was considered optimum as at higher R, more fresh air will be injected towards the source.

3.3.2 Variation of Jet Angle

The variation of temperature outside the source-store at ceiling level (2.9 m) for position D with jet angle variation for a single jet air curtain with fixed flow velocity of 10 m/s and 7.6 cm flow channel width, are shown in Figure 3.135. The jet angle of the air curtain was varied from 0º to 60º, inclined towards the fire source, with 15º step size. Air curtain while injected at 15º showed no improvement over the 0º injection angle, i.e., when air curtain injected vertically. The 30º, 45º and 60º injection angle were more effective at delaying the temperature increase, for about 15s for 30º, and 22s for 45º and 60º injection angle. CO concentration at ceiling level (2.9 m) for position D1 and for the same operating conditions and the same angle variations of air curtain jet are presented in Figure 3.136. The 30º, 45º and 60º jet angle cases were again effectively confined the CO particles i,e., the smoke, for increased amount of time than
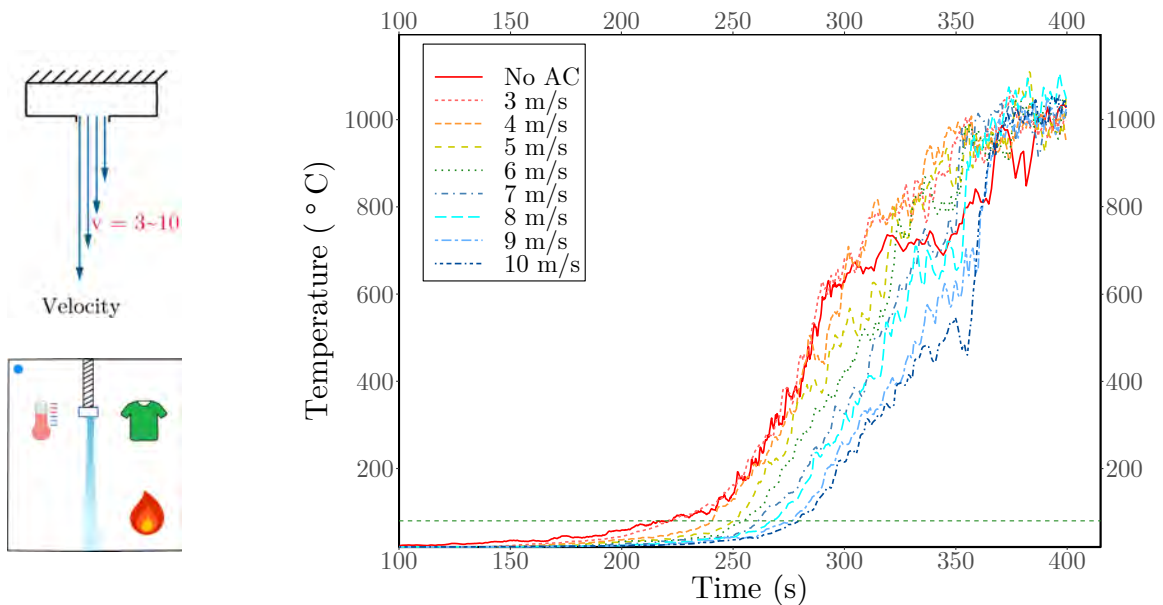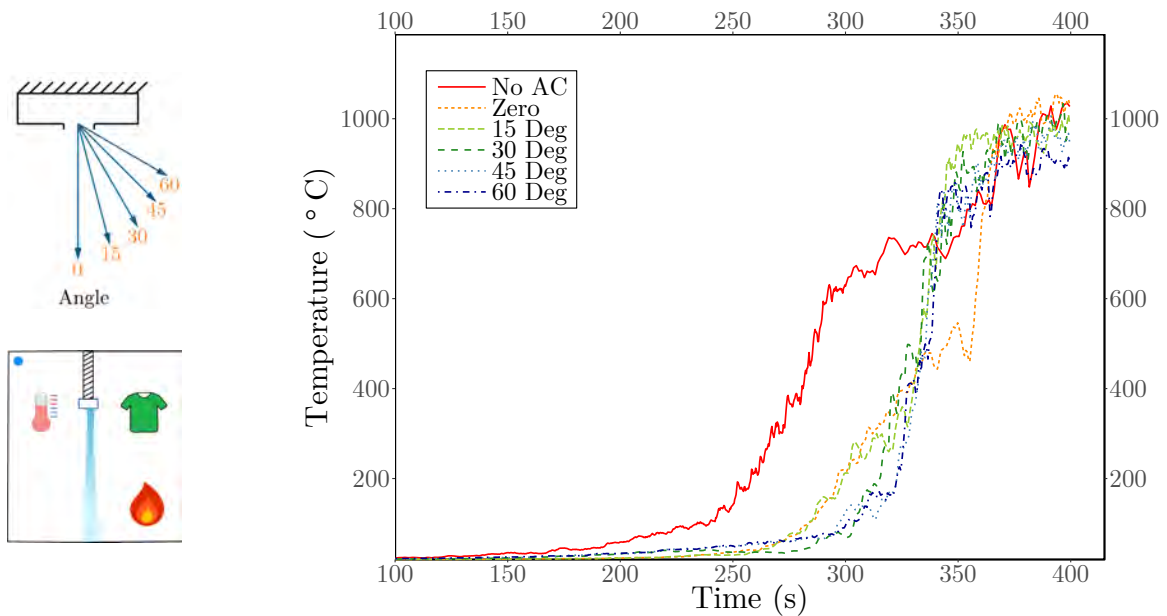

Fig. 3.135 Temperature at ceiling level (2.9 m) for position D (outside the fire source) for a single jet air curtain of 7.62 cm jet width, discharged at 10 m/s jet velocity, and at 0º to 60º jet angle with 15º step size.

170
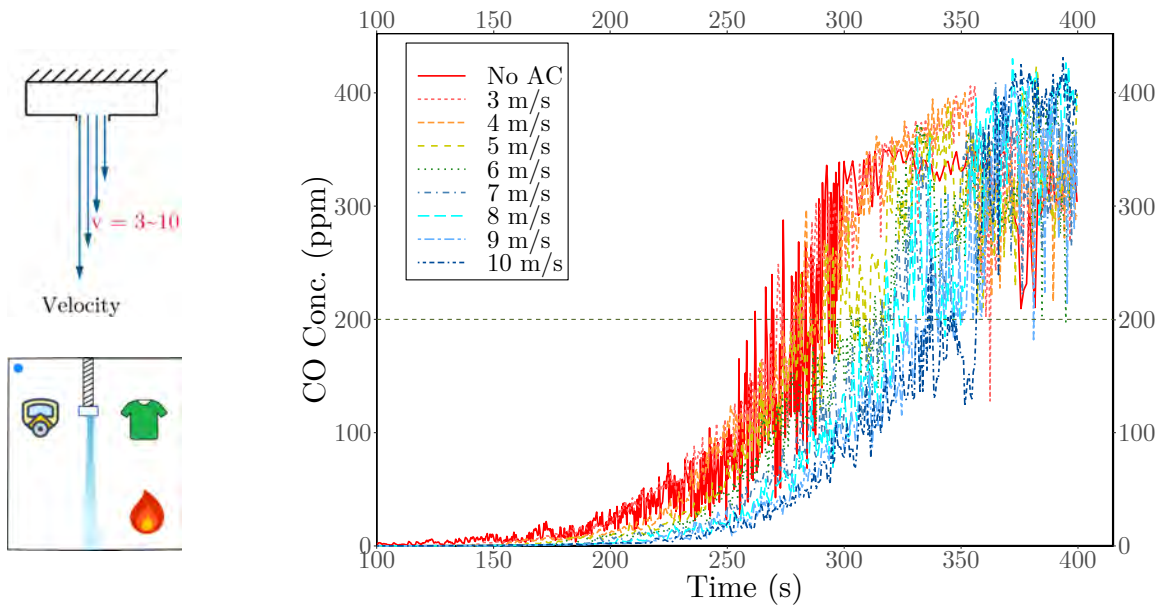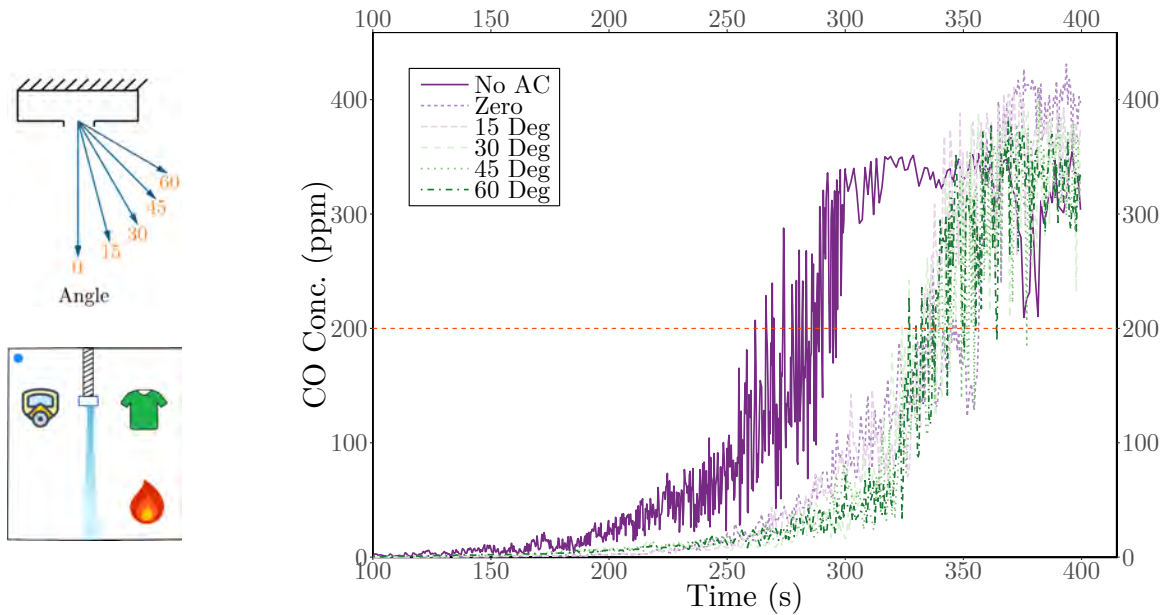
Fig. 3.136 CO concentration at ceiling level (2.9 m) for position D1 (outside the fire source)for a single jet air curtain of 7.62 cm jet width, discharged at 10 m/s jet velocity, and at 0º to 60º jet angle with 15º step size.

the 0º and 15º jet angle cases. Thus varying the jet angle proved to be effective from 30º to 60º for both heat and smoke confinement.

Figure 3.137 represents the velocity contours for a 2D vertical plane through AD, in the middle of fire source store door, intersecting the thermocouples at positions A, B, C, and D, with air curtain (for discharge at 10 m/s) and without air curtain at 250s simulation time. From Figure 3.137a, it was observed that, when air curtain was not discharged, the smoke escapes the room through the door and accumulated at the ceiling, agreeing well with the characteristics of smoke buoyancy as discussed in details earlier. The fluids in bottom of the store remained nearly motionless. The velocity contours at 250s with 10 m/s air curtain velocity for the plane AD is shown in Figure 3.137b. Due to the air curtain's impinging jet, the circulation of fluids inside the store was visible in this figure 3.137b. Although the injection was vertical initially, at 250s the air curtain's stream was pushed outwards by the increased fluid pressure. This increment in pressure was caused by the fluid expansion due to the heat release rate of the fire inside the store. The Figure 3.137c shows the velocity contours at AD plane, for 30º jet angle configuration. As the velocity stream was initially inclined towards the fire source, and smoke accumulated at ceiling first, the resulting interaction of the fluid forces made the stream nearly vertical at 250s. Thus, even at 250s the
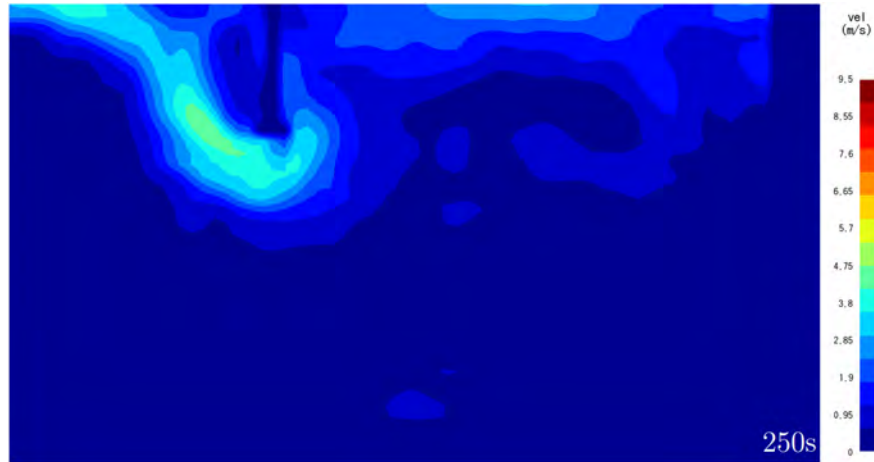
(a) Velocity contours for a 2D vertical plane through AD, without air curtain at 250s.
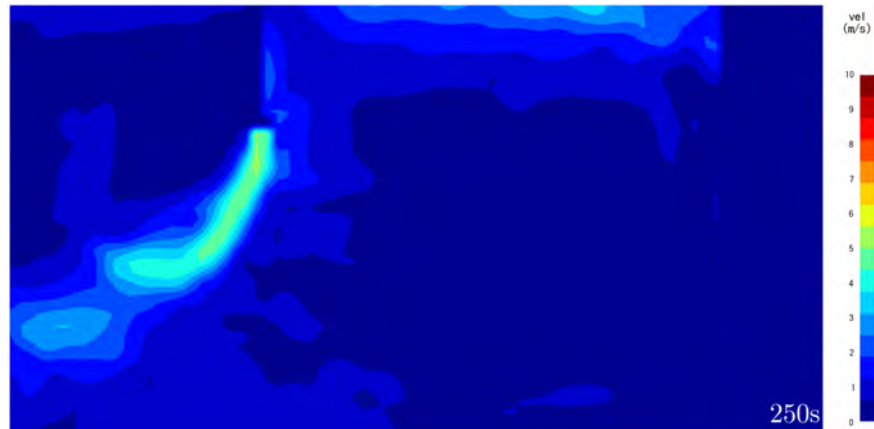
(b) Velocity contours for a 2D vertical plane through AD, with air curtain discharge at 10 m/s at 250s.
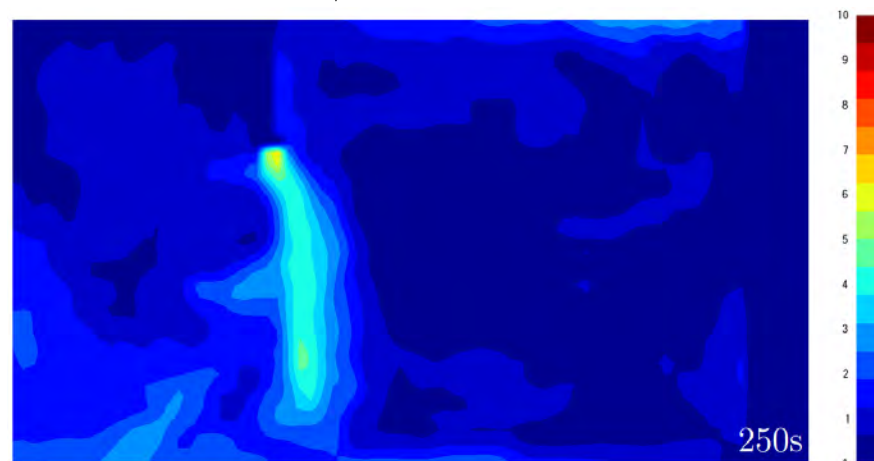
(c) Velocity contours for a 2D vertical plane through AD, with the air curtain discharged at 10 m/s injection velocity and 30º injection angle at 250s.

Fig. 3.137 Velocity contours for a 2D vertical plane through AD, at the middle of the fire source store door.
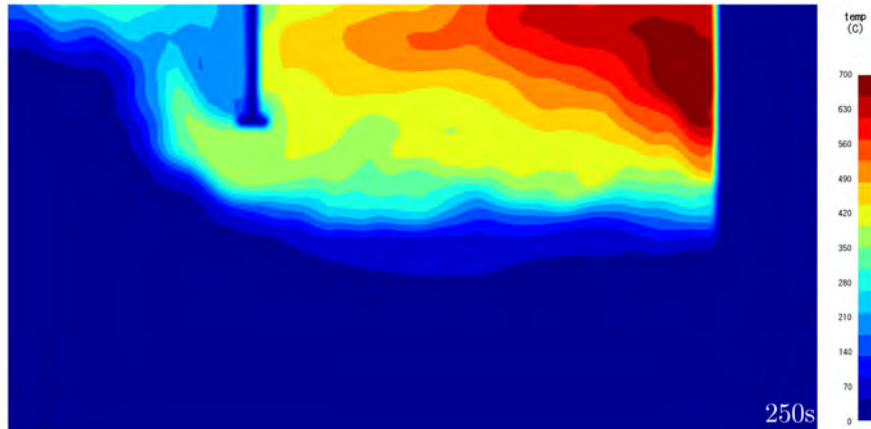
(a) Temperature contours for a 2D vertical plane through AD, without air curtain at 250s.
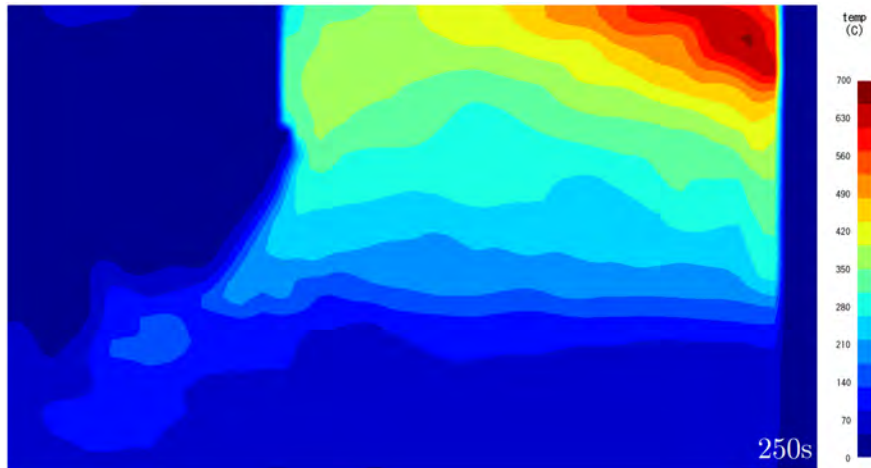
(b) Temperature contours for a 2D vertical plane through AD, with air curtain discharge at 10 m/s at 250s.
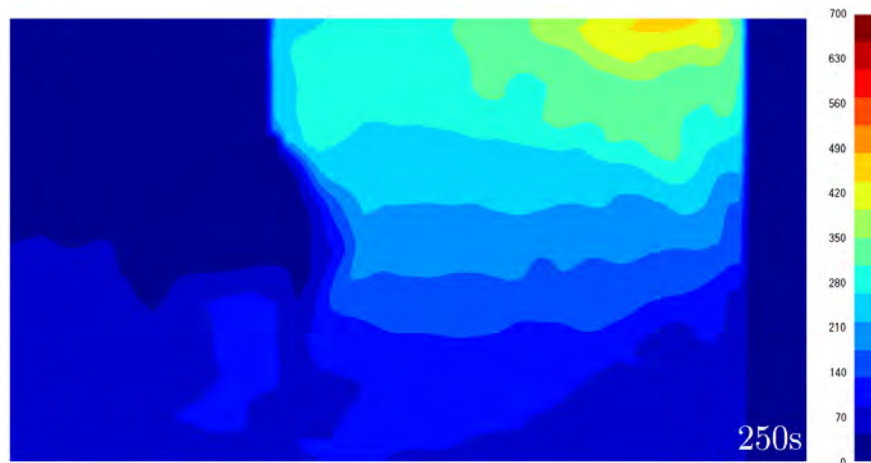
(c) Temperature contours for a 2D vertical plane through AD, with the air curtain discharged at 10 m/s jet velocity and 30° jet angle at 250s.

Fig. 3.138 Temperature contours for a 2D vertical plane through AD, at the middle of the fire source store door.
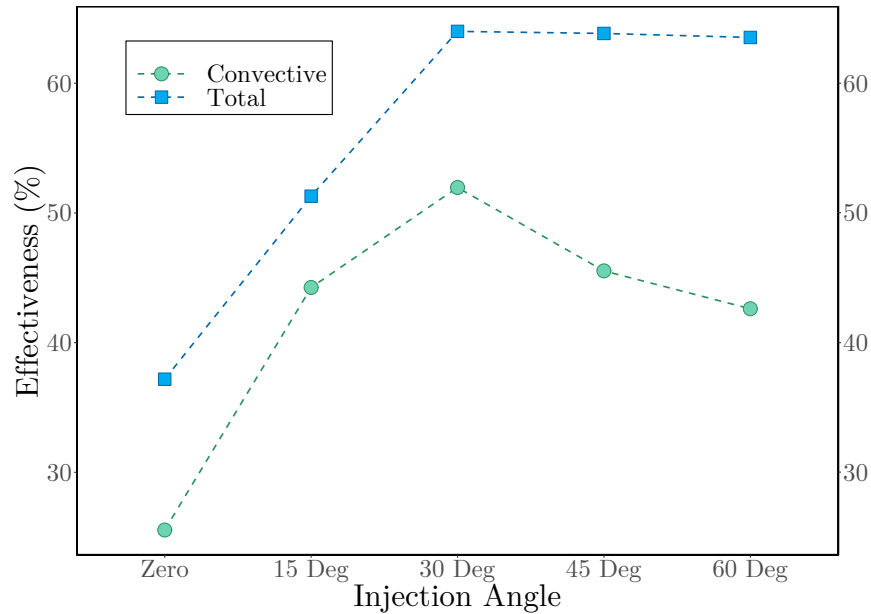
Fig. 3.139 The total and convective effectiveness of air curtains at 7.62 cm flow channel width and 10 m/s jet velocity in function of jet angle.

air curtain was able to retain the propagation of heat and smoke outside the store, except the bottom leakages mentioned in previous sections. The figure 3.138 shows the temperature contours for a 2D vertical plane through AD, at the middle of the fire source store door, with air curtain discharge at 10 m/s and without air curtain discharged at 250s simulation time. Heat accumulated in ceiling and escaped through the door for air curtain non-discharged case as seen in figure 3.138a. As a vertical air curtain was discharged in figure 3.138b, the temperature profile was distributed in larger area and heat escaped at eye level. For the 30° jet angle configuration of figure 3.138c, the temperature distribution was even more distributed and escaped heat was minimum among the three cases seen in figure 3.138 at 250s.

To observe the effect of the angle variations more explicitly, the effectiveness E was calculated for the investigated jet angles. The convective heat flux and the radiative heat flux was calculated at the door of the source store with and without the air curtain. Although air curtain, discharged at 10 m/s, was effective in confining the fire and smoke inside the store for about 50s more than non-discharged case, it was unable to control the fire at the flashover phase. The flashover defined as the phase when fire spreads rapidly throughout the space, resulting total involvement of the enclosed area. Due to the extreme fluid pressure at this phase, air curtain failed to confine the spread of fire, and fire came out of the store to the hall way. Including flashover phase in effectiveness calculation for air curtain will greatly over shadow air curtain's

contribution before flashover phase. Thus, the effectiveness was evaluated up to 247s, when flashover was observed for the non-discharged air curtain configuration. Both the total effectiveness and the convective-only effectiveness of a single jet air curtain with 7.62 cm flow channel width and 10 m/s jet velocity are calculated and presented in function of jet angle in Figure 3.139. The 30º jet angle case provides the best total and convective only effectiveness among the investigated jet angles. The total effectiveness was about 64% and convective-only effectiveness was about 51% for the 30º jet angle configuration. Thus, 30º was considered the optimum jet angle for air curtain jet.

3.3.3   Variation of Jet Width

Instead of a single jet design, many manufactures provide a twin jet configuration air curtain, and thus the configuration was put in to test for finding the optimum jet to jet distance. A dimensionless parameter named pitch ratio, p, was defined as the ratio of jet to jet distance to jet width as clarified in equation 3.4.

$$p = \frac{\text{jet to jet distance}}{\text{jet width}} \tag{3.4}$$

The pitch ratio variations studied here was zero (single jet), 1, 2, 3 and 4 to find the optimum pitch ratio for curtain jets, the flow width increased to 15.24 cm as two jets was considered, the jet velocity was 10 m/s and jet was vertical. The temperature at ceiling level (2.9 m) for position D, and CO concentration at ceiling level (2.9 m) for position D1, for air curtains in twin jet configuration in 0, 1, 2, 3, and 4 pitch ratios, are plotted in function of time in Figure 3.140 and Figure 3.141, respectively. There were two 7.62 cm flow channels and the jet velocity was 10 m/s at 0º jet angle. From both of the Figure 3.140 and 3.141 it was evident that the twin jet configuration was less effective at sealing the heat and smoke transfer at all pith ratios when compared to the zero pitch ratio, i.e., at single jet configuration.

3.3.4   Variation of Flowrate

The volume flowrate, jet width and jet velocities are related by the continuity equation of fluid dynamics for in-compressible flow. At fixed flowrate of fan, the jet velocity and width of jet could be changed and tuned for optimum configuration. Thus, for the optimum operating condition, three flowrates of 1250, 2500 and 5000 m³/h, with three flow width of 7.62 cm, 15.24 cm, and 30.48 cm, and two flow velocities of 5 m/s and 10 m/s are investigated systematically. The temperature at ceiling level (2.9 m) for
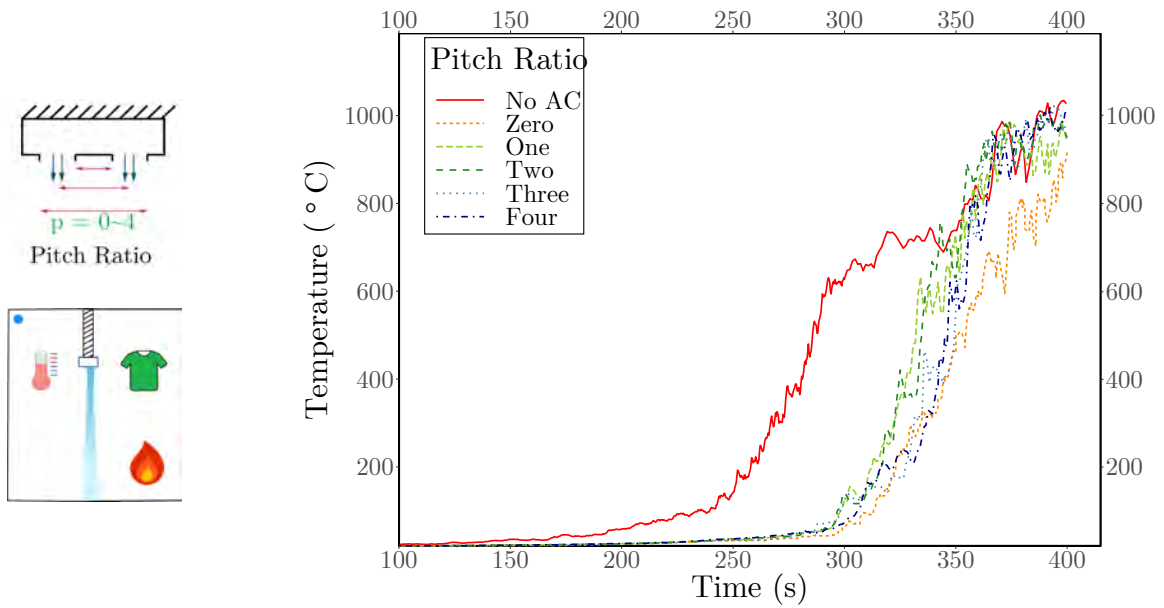
Fig. 3.140 Temperature at ceiling level (2.9 m) for position D (outside the fire source) for a 15.24 cm channel width vertical air curtain at 10 m/s jet velocity for 0, 1, 2, 3, and 4 pitch ratios.
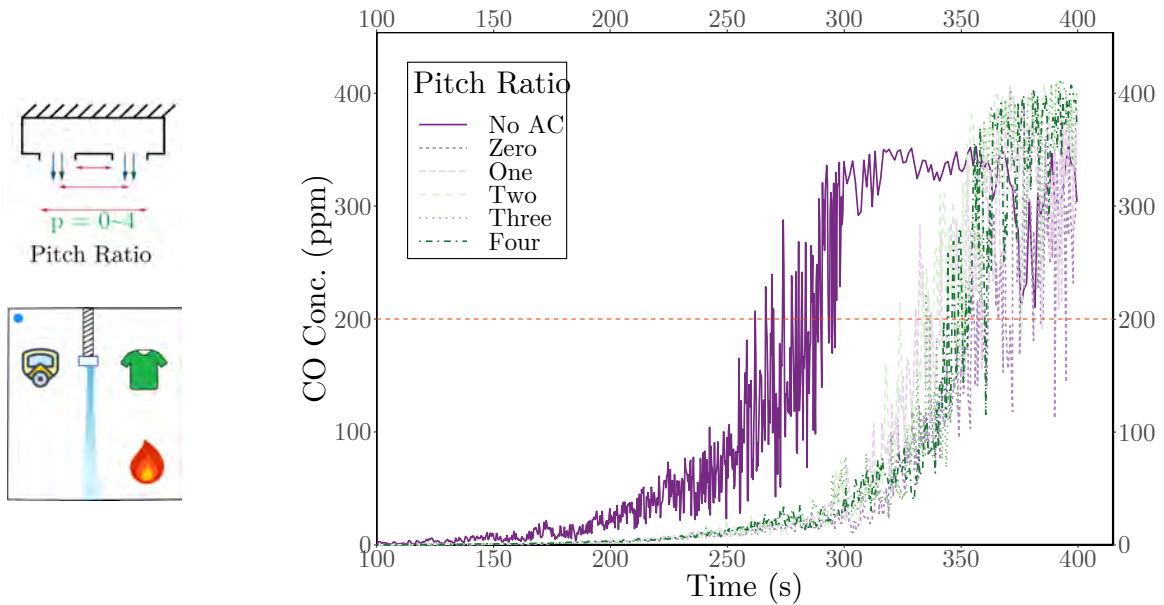
Fig. 3.141 CO concentration at ceiling level (2.9 m) for position D1 (outside the fire source) for a 15.24 cm channel width vertical air curtain at 10 m/s jet velocity for 0, 1, 2, 3, and 4 pitch ratios.
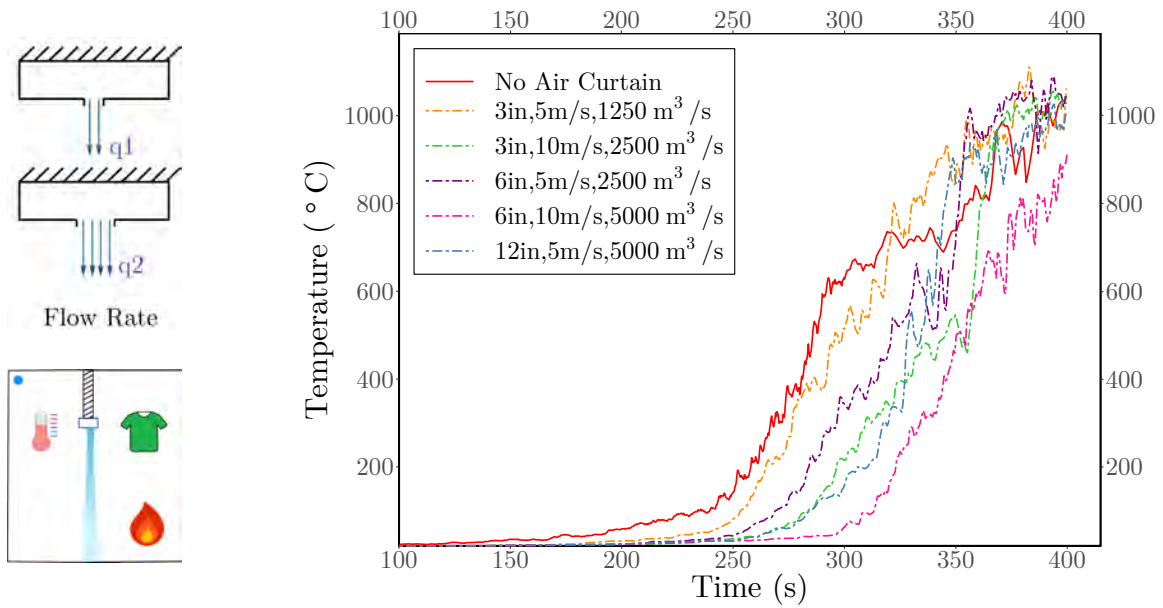
Fig. 3.142 Temperature at ceiling level (2.9 m) for position D (outside the fire source) for air curtain discharged at 1250, 2500 and 5000 m^3/h at different channel width and injection velocity.

position D for air curtains at different flow channel width and velocities at same flow rate for three different flow rates are shown in Figure 3.142. The increase in velocity reducing the channel width for a certain flow rate was seen to be beneficial for the heat confinement.

3.3.5 Optimum Air Curtain Operating Parameters

The sealing performance of a single jet air curtain with 7.62 cm channel width, at 9 m/s jet velocity and 30º jet angle at the door of fire source store was investigated in the next phase of this study. The parameters for this air curtain were taken as the best performing ones, from the previous results. The combined effects of these different best performing air curtain parameters were found had constructive influence in between them. This air curtain configuration had an effectiveness of 59.4%, sufficient improvement over an off-the-self air curtain which could provide about 37.1% effectiveness. This improvement in sealing the heat and smoke inside the fire source store could ensure more safe evacuees for a typical fire incident in context of Bangladesh. Figure 3.143 shows the velocity and temperature contours for AD plane with a single jet air curtain operating with optimum parameters. From figure 3.143a and figure 3.143b
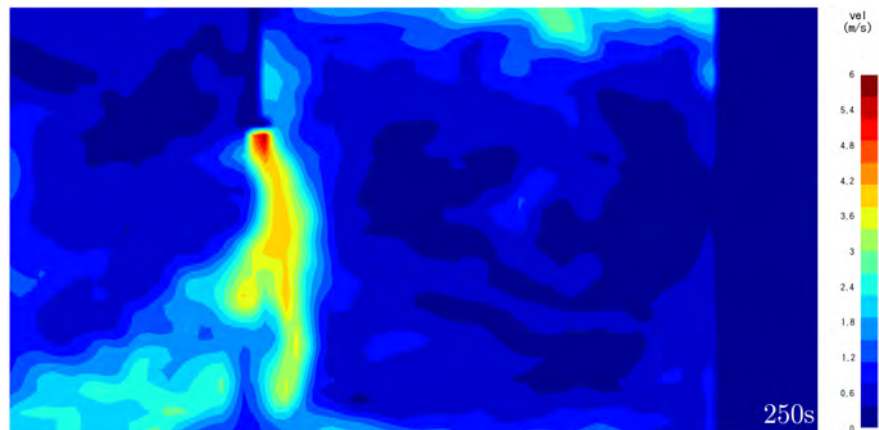
(a) Velocity contours for a 2D vertical plane through AD plane with the air curtain discharged at 9 m/s injection velocity and 30º injection angle at 250s.
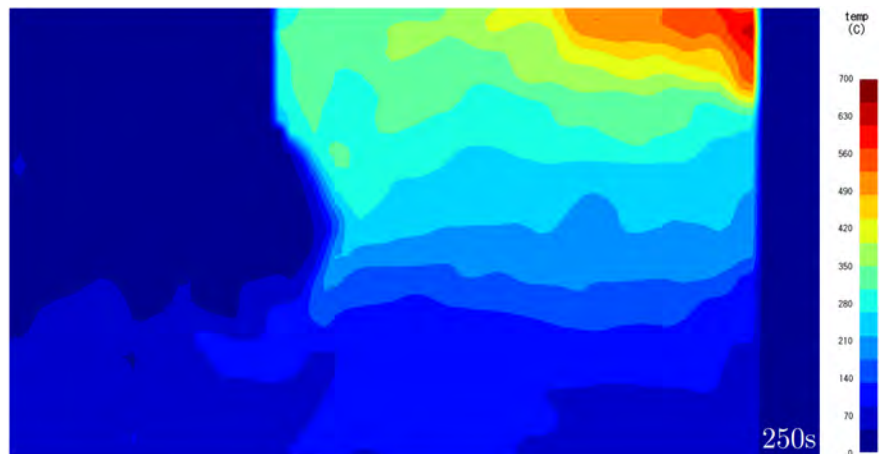
(b) Temperature contours for a 2D vertical plane through AD plane with the air curtain discharged at 9 m/s injection velocity and 30º injection angle at 250s.

Fig. 3.143 Velocity and temperature contours for AD plane with a single jet air curtain operating with optimum parameters.

it is seen that, the curtain jet was nearly vertical at 250s thus providing better sealing even on the eve of flashover, and the temperature profile was also evenly distributed with lower heat escaping from under the curtain jet. Although 10 m/s jet velocity with 30º jet angle had slightly better effectiveness, the amount of fresh air is more at higher velocities, which could be disastrous for under ventilated fire, thus the lower jet velocity was preferred.

3.3.6   Ideal Fuel Distribution and Optimum Air Curtain Case

The results of fuel distribution variation and air curtain's parametric variations were put to together to provide even more evacuation friendly shopping mall configuration in case of a fire hazard in a typical shopping mall of Bangladesh. The actual fuel distributions typically present in shopping malls of Bangladesh are extremely dense due to compact stacking of combustibles. The proposed Grid configuration with air curtain at optimum parameters at source and staircase could provide more evacuation time. Thus additional investigations were carried out with different fuel distribution and air curtain configurations. The new investigated case details are provided in table 3.15. Air curtain in optimum condition provided better effectiveness about 22% at 247s, better flame and smoke confinement, for about 11s and 5 s respectively, and delayed flashover for 14s than an off-the-self one. Using an off-the-self air curtain with Grid fuel distribution also provided better flame and smoke confinement but had lower effectiveness. Operating at optimum condition, air curtain could provide about 33.4% effectiveness at 310s with Grid type fuel distribution. Comparing with no air curtain with actual fuel distribution, air curtain operating at optimum condition with Grid type fuel distribution could delay the flashover for nearly 100s, confine smoke and fire for nearly 50s and 63s more respectively and release only 20% of heat at 247s. The details of these investigations as documented in table 3.16.

The installing positions of the air curtain operating at optimum condition were varied again for both Actual and Grid type distribution. Figure 3.144 shows the temperature distribution at eye level (1.54 m) in staircase for a single jet air curtain at optimum parameters with air curtain's installation position variation for DCC market source shop 1 with clothing as fuel. CO concentration at eye level (1.54 m) in staircase for a single jet air curtain at optimum parameters with air curtain's installation position

Table 3.15 Overview of miscellaneous simulations conducted by a single jet air curtain. The fire was simulated at DCC market source shop 1 with clothing as fuel.

Case	Curtain position	Fuel Distribution	Jet width (cm)	Jet angle	Velocity of jet (m/s)	Flowrate (m^3/h)
64	Source & Stair	Actual	7.62	30	9	2250
65	Source	Grid	7.62	30	9	2250
66	Source& Stair	Grid	7.62	30	9	2250
67	All shops	Grid	7.62	0	10	2500
68	No Curtain	Actual & Hallway free	0	0	0	0

Table 3.16 Comparison between different fuel arrangements and air curtain parameters for DCC source shop 1 with clothing as fuel.

Fuel Distribution	Air curtain Parameter	Smoke confinement	Flame confinement	Flashover	Effectiveness (%)
Actual	No Curtain	80s	247s	262	0
Actual	Off-the-self	+25s	+18s	+18s	37.1
Actual	Optimum	+30s	+29s	+32s	59.4
Grid	No Curtain	100s	310s	350s	0
Grid	Off-the-self	+45s	-5s	+10s	11
Grid	Optimum	+30s	+0s	+10s	33.4
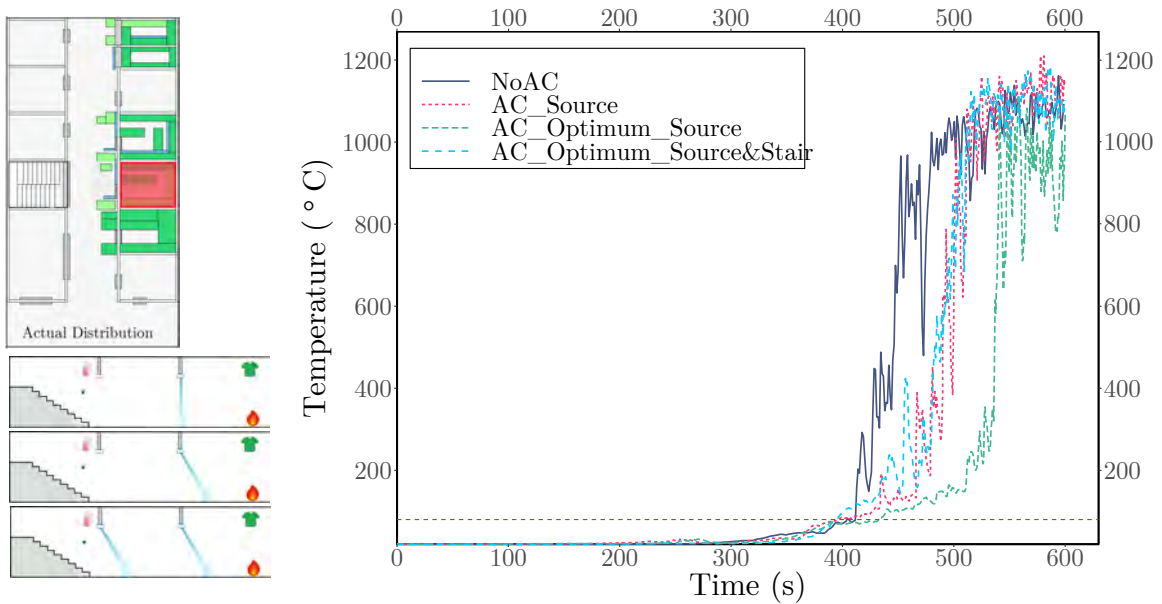
Fig. 3.144 Temperature distribution at eye level (1.54 m) in staircase for a single jet air curtain at optimum parameters with air curtain's installation position variation for DCC market source shop 1 with clothing as fuel in Actual distribution.

variation for DCC market source shop 1 with clothing as fuel in Actual distribution is shown in figure 3.145. For Actual fuel distribution air curtain at optimum condition at source only provided better temperature profile than optimum air curtain both source and staircase as the staircase was too close to the active zone as discussed in details earlier. Figure 3.146 shows the temperature distribution at eye level (1.54 m) in staircase for a single jet air curtain at optimum parameters with air curtain's installation position variation for DCC market source shop 1 with clothing as fuel in
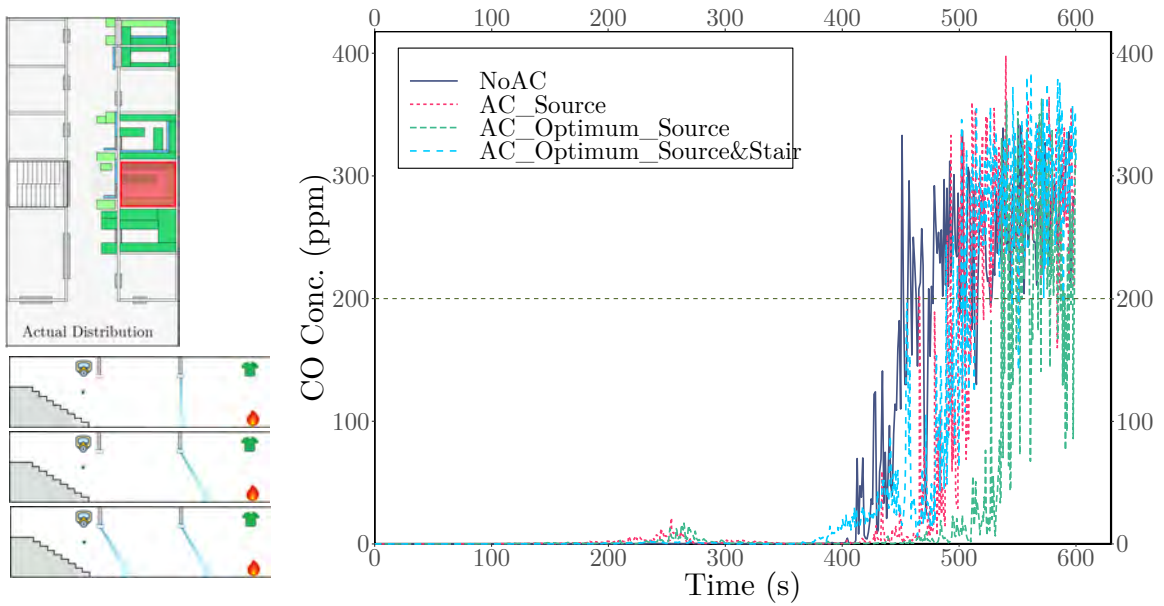
Fig. 3.145 CO concentration at eye level (1.54 m) in staircase for a single jet air curtain at optimum parameters with air curtain's installation position variation for DCC market source shop 1 with clothing as fuel in Actual distribution.
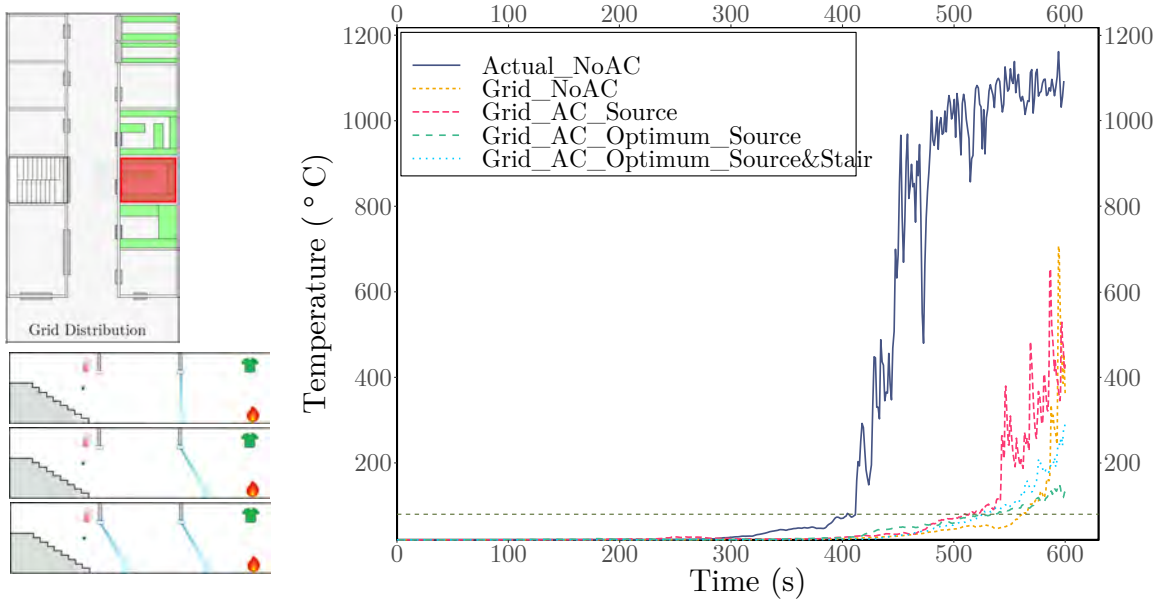
Fig. 3.146 Temperature distribution at eye level (1.54 m) in staircase for a single jet air curtain at optimum parameters with air curtain's installation position variation for DCC market source shop 1 with clothing as fuel in Grid distribution.
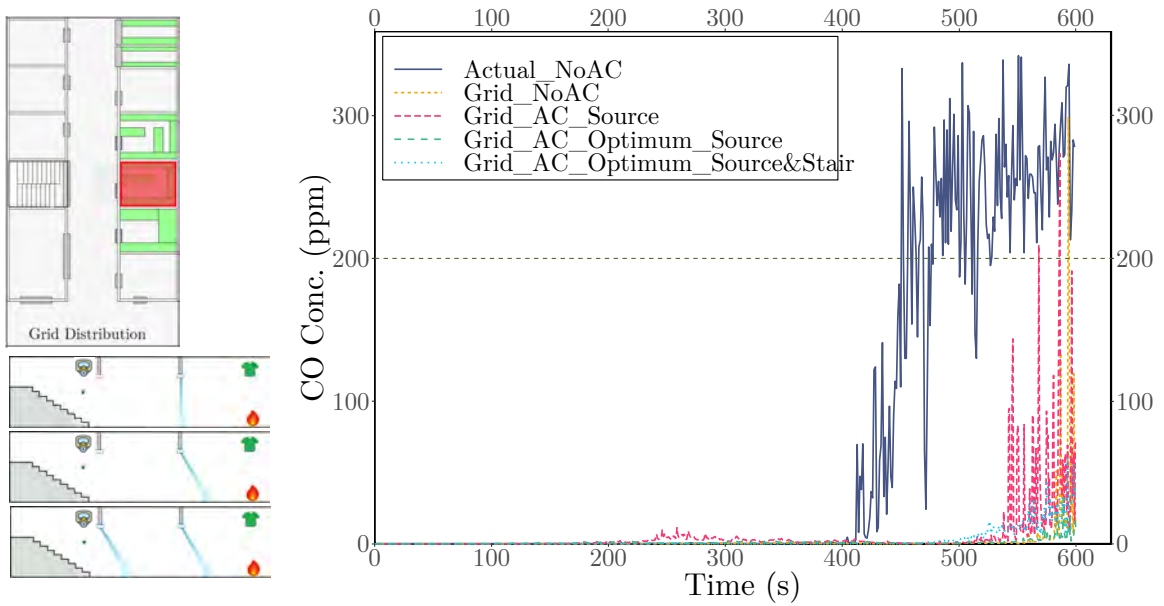
Fig. 3.147 CO concentration at eye level (1.54 m) in staircase for a single jet air curtain at optimum parameters with air curtain's installation position variation for DCC market source shop 1 with clothing as fuel in Grid distribution.

Grid distribution. CO concentration at eye level (1.54 m) in staircase for a single jet air curtain at optimum parameters with air curtain's installation position variation for DCC market source shop 1 with clothing as fuel in Grid distribution is shown in figure 3.147. For Grid type fuel distribution, the cases with optimum air curtain at source, and optimum air curtain at both source and staircase, performed effectively and could resist the temperature tenability for at least 120s more than that of the no air curtain case with actual distribution. The results conclusively indicated that, improved evacuation was possible with air curtain at both source and staircase, if staircase was after the active zone, induced by the air curtain jet.

3.3.7 Miscellaneous Case Studies

3.3.7.1 Case study 1: No Fuel in the Hallway

From the observation of flame propagation during no air curtain condition in DCC market source shop 1 with clothing as fuel for no air curtain case, it was concluded that, flame propagates faster due to available fuel load in hallway after fire came out of the source shop. Thus, to verify the claim made earlier, another simulation was performed with no fuel loads in hallway for DCC source shop 1 with no air curtain. The top view of the computation geometry with two points inside two nearby shops labelled as 'as1' and 'as2', where comparisons of temperature profile were made, is shown in figure 3.148. And the temperature profile inside adjacent shops was compared for no fuel in hallway with actual condition of DCC_CS1. The only difference between these two fuel distributions was the fuel free hallway. Figure 3.149 and figure 3.150 show the temperature distribution at eye level (1.54 m) inside adjacent shops at position 'as1' and 'as2' respectively, for fire in DCC market source shop 1 with no clothing in hallway vs DCC_CS1. And, as expected these figures clearly indicated that, the absence of fuel in hallway lessen the impact of fire inside adjacent shops. The temperature for both
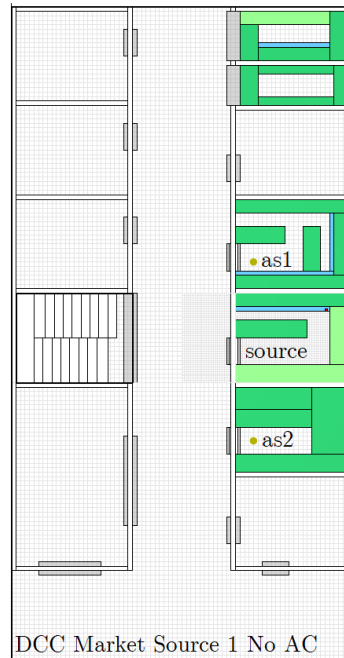
Fig. 3.148 Top view of DCC market in no fuel for hallway case with two points inside two nearby shops labelled as 'as1' and 'as2', where comparisons of temperature profile were made.
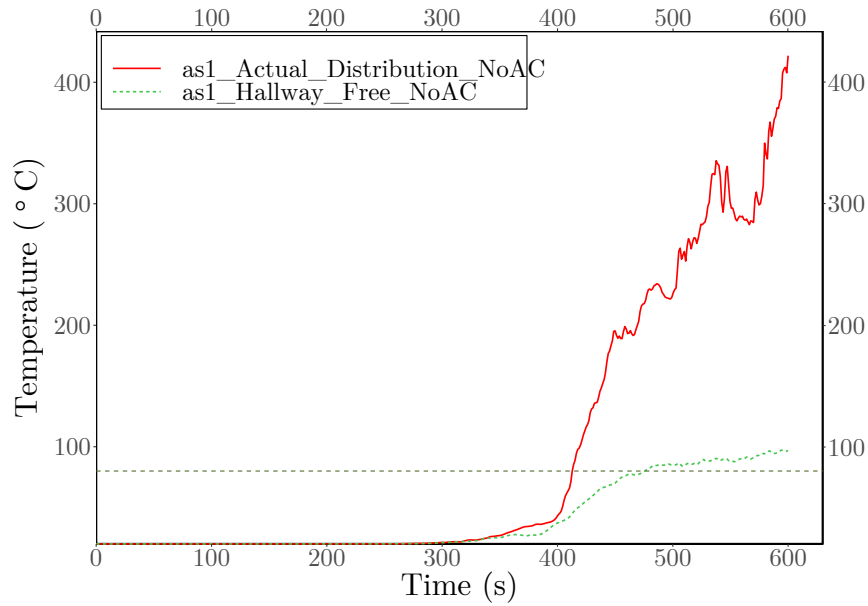
Fig. 3.149 Temperature distribution at eye level (1.54 m) inside adjacent shop at position 'as1' for fire in DCC market source shop 1 with no clothing in hallway vs DCC_CS1.
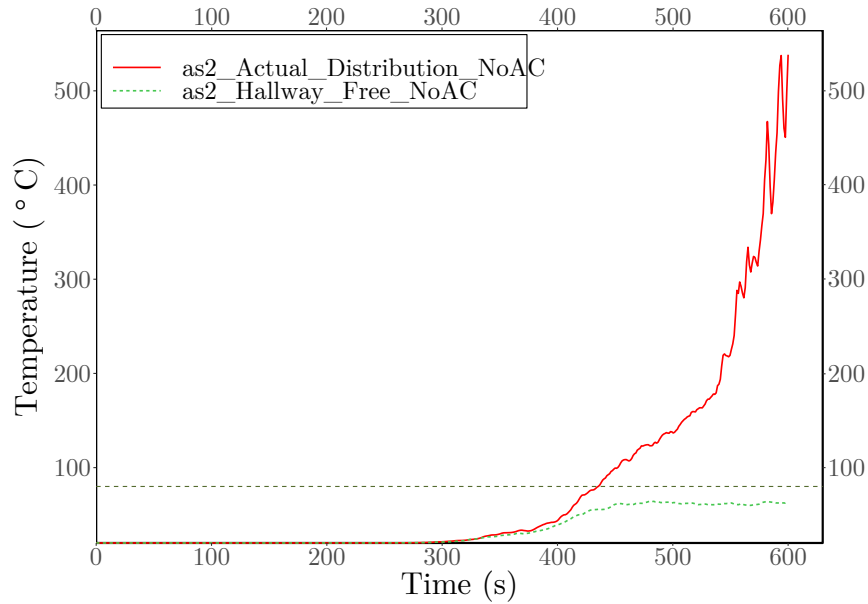
Fig. 3.150 Temperature distribution at eye level (1.54 m) inside adjacent shop at position 'as2' for fire in DCC market source shop 1 with no clothing in hallway vs DCC_CS1.

positions were significantly lower for fuel free hallway case, and 'as2' even remained below the tenability for total simulation time.

3.3.7.2 Case study 2: Air Curtain at All Shops

The generation of an active zone when air curtain was discharged, could induced a threat to actual effectiveness of air curtains in evacuation, if all shops had air curtains installed and all air curtains produced another active zone in front of the installation position by adding further swirl to the escaped heat flow from the fire source. Thus, air curtains were installed in source shop and at four adjacent shop doors, sequentially two on each side, on both sides of the source shop to investigate their combined effect on hallway temperature profile in case of any fire incident. Figure 3.151 shows top view of DCC market for air curtain installed at all shop front case, the 'Grid' type fuel distribution was considered here. The temperature distribution at eye level (1.54 m) in hallway for all shop case was then compared against no air curtain case (DCC_CS1) and source only air curtain case (DCC_CS1AC). Figure 3.152 shows the temperature profile comparison in hallway for the three mentioned cases at 500s of simulation time, the black vertical dashed line at 10.5 m shows the position of source shop. The temperature for no curtain case was low at eye height as the escaped heat flow did not cross the eye height thermocouple as it went past just under the door frame and to the ceiling. The all shop air curtain case was seen to perform better than source only case.
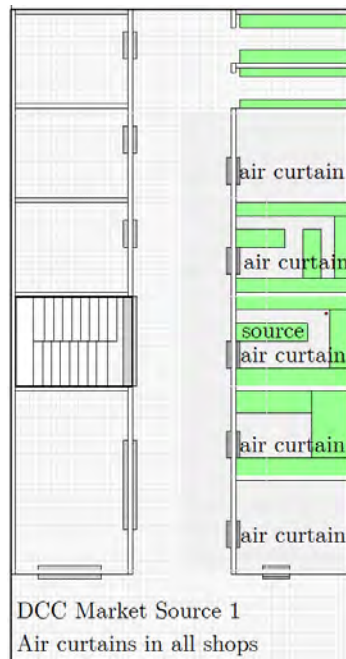
Fig. 3.151 Top view of DCC market in 'Grid' type fuel distribution with clothing for air curtain installed at all shop front case.

185
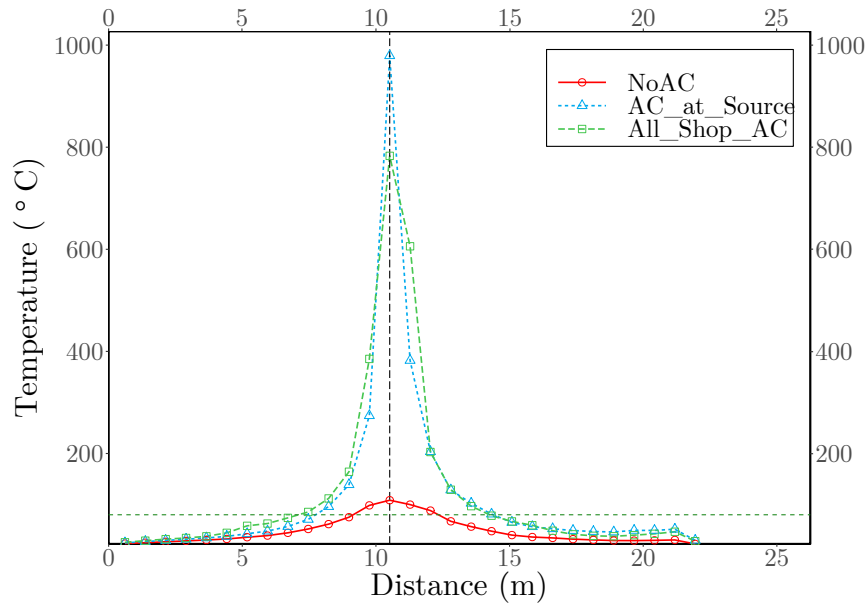
Fig. 3.152 Temperature distribution at eye level (1.54 m) in hallway for fire in DCC market source shop 1, having air curtains at all shop door compared with DCC_CS1 and DCC_CS1AC at 500s of simulation time. The black vertical dashed line at 10.5 m shows the position of source shop.
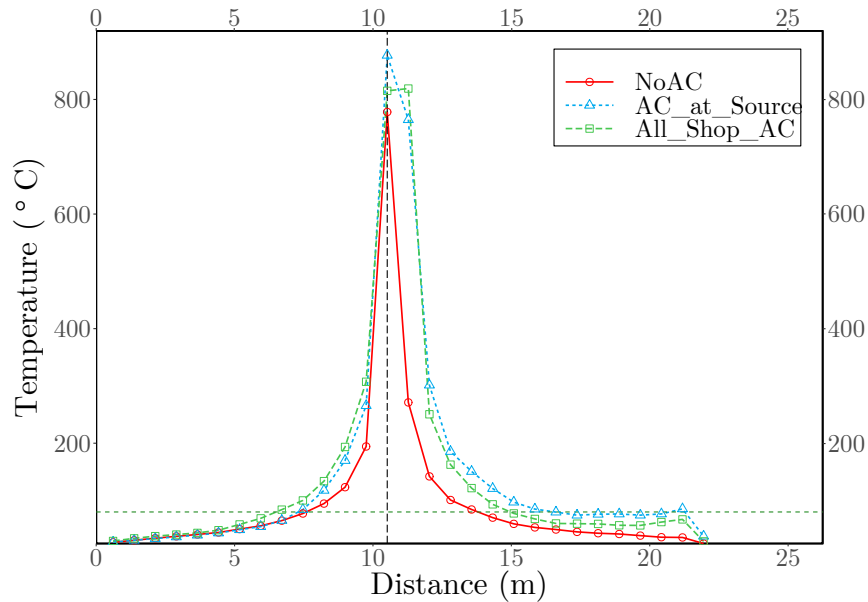
Fig. 3.153 Temperature distribution at eye level (1.54 m) in hallway for fire in DCC market source shop 1, having air curtains at all shop door compared with DCC_CS1 and DCC_CS1AC at 550s of simulation time.
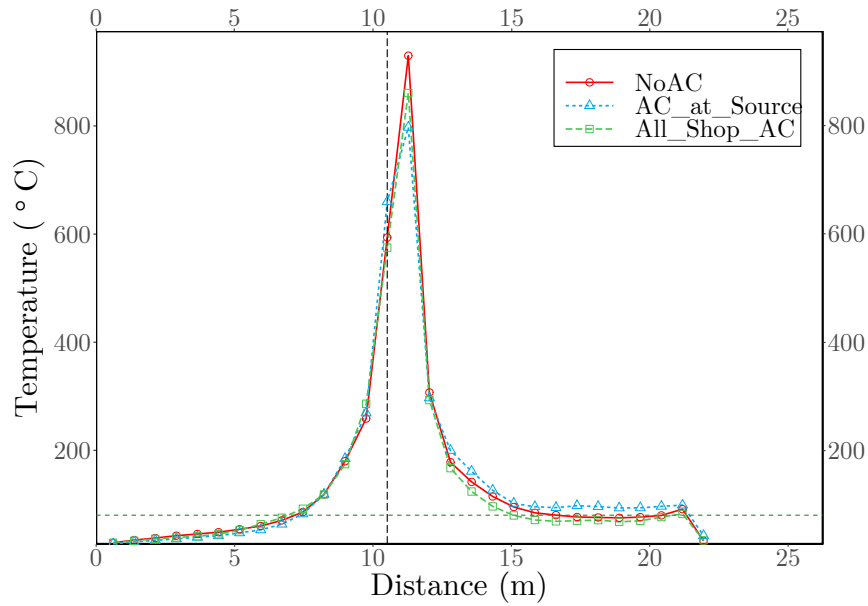
Fig. 3.154 Temperature distribution at eye level (1.54 m) in hallway for fire in DCC market source shop 1, having air curtains at all shop door compared with DCC_CS1 and DCC_CS1AC at 600s of simulation time.

Figure 3.153 shows the hallway temperature comparison at 550s, and at this time the no curtain case also had increased temperature profile and again all shop case provided better hallway temperature profile than source only air curtain. In figure 3.154, temperature comparison at 600s, the all shop air curtain condition provided better hallway temperature condition than both no air curtain and source only air curtain case, and it was the only condition that could provide human tenable temperature within 10 m (5 m in each side) of source. Hence, if the number of air curtains increased it will further aid the evacuation process, as additional air curtains did not increase the source air curtains active zone rather somewhat suppress it with supplementary jets. Thus, this investigation with all shop air curtain case provided conclusive evidence of air curtains being beneficial during evacuation process.

3.3.8 Proposed Guideline

After analyzing the 68 fire scenarios considered in this present study, a guideline for fuel distribution, fuel arrangements and use of air curtain as an aerodynamic sealing is proposed for typical shopping malls in context of Bangladesh.

(a) Shop just in front of staircase should preferably contain fuels with lower heat released rate per unit area (HRRPUA), if possible.

(b) High HRRPUA fuel shops like clothing store, shoe store, etc., should follow the Grid type fuel arrangement.

(c) Hallways of high HRRPUA fuel shops should be free of shop front fuel stacks.

(d) Air curtains might be installed at high HRRPUA fuel shop doors for confining fire and smoke in case of a fire hazard.

(e) Air curtain might be installed at staircase to provide better evacuation in case of a fire hazard.

(f) Air curtain with the proposed optimum parameters might provide better smoke and fire sealing compared to an off-the-self air curtain.

Chapter 4

Conclusion

4.1 Conclusion

In this study, the effectiveness of air curtain to act as a fire and smoke propagation barrier is examined in case of typical shopping mall fires in Bangladesh. The present study report first such analysis on the potential applicability of air curtains as a heat and smoke barrier in case of shopping mall fires. The effect of air curtains with strategic variations of the location and operating parameters of the air curtains is analyzed numerically from an evacuation perspective. Three different designs of shopping malls with distinct geometric and architectural features, two fuel types, and three distinct fuel arrangements are examined to imitate the diversities present in actual shopping malls. A total of 68 different configurations were studied to determine the optimum location and operating parameters of the air curtain to confine fire and smoke and to aid the evacuation process. The major findings are as follows:

- Air curtain jet could confine the heat and mass transfer through the open door effectively and delay the flashover process sufficiently. An off-the-self air curtain at fire source shop door, could confine up to 37.1% of fire generated heat, and delay smoke and fire propagation outside the source and flashover event for at least 18s for typical shopping malls of Bangladesh, even against the actual, extremely dense fuel arrangements. The shopfront air curtain also proved to be beneficial, for evacuation process through staircase, a critical location during evacuation, for both near source (from staircase) and far source fire scenarios.

- Although placing air curtain at fire source shop door alters the heat and mass escape path through the door, air curtain installed only at source or only at staircase, enables more time at human tenable condition at staircase, than no air

curtain case. Air curtain installed at shopfront and at staircase together, offers the safest scenario at staircase.

- Alternative to the Actual fuel distribution present in typical shopping malls, the standard 'Grid' type fuel distribution was suggested, as the reduction in storage capacity was favorable for both heat release rate and business aspect.

- Parametric study of air curtain revealed that, evacuation process might be improved by operating air curtain at optimum conditions. An air curtain with 7.62 cm channel width in single jet configuration, operated at 9 m/s jet velocity and 30º jet angle, is the optimum configuration, as obtained within the parametric space of this study.

- By arranging fuel loads inside shop with 'Grid' type distribution and installing air curtain at source and staircase in optimum operating parameters, a maximum of 59.4% heat confinement at source and about 120s increment in safe evacuation time through staircase could be achieved.

- A guideline for fuel distribution, fuel arrangement and air curtain installation in case of a typical shopping mall in context of Bangladesh is proposed.

In summary, the use of air curtain at the shopfront and at the staircase would benefit evacuation process in case of typical shopping mall fire incident. Reducing the amount of fuel present in typical shops and rearranging them strategically, together with the optimum air curtain configuration, will further assist the safe evacuation. The findings of this study would help to identify the desired air curtain characteristics required to ensure adequate prevention against fire-smoke propagation for different stores in typical shopping malls having a wide range of combustible materials.

4.2   Future Recommendations

The present study reports the effectiveness and applicability of air curtains as a barrier to smoke and fire propagation in case of typical shopping malls fires in Bangladesh. There are certain scopes for future work, which are proposed below:

- The present study analyzed each air curtain's operating parameters separately, keeping all other parameters constant. In future endeavors study of multiple parametric variations at once might be beneficial.

- Air curtain's ability to confine the heat and mass transfer in fire source level of a multi-level shopping mall might be an auspicious venture.

- Detailed investigation on so called 'Active zone' mentioned in this study is needed to reveal its dependence on fuel load and shopping malls architectural design.

References

Ahmed, R. and Safi, M. (2019), ''the builders don't care': Dhaka reels from another deadly blaze', The Guardian, 29 March 2019[Online]. Available at https://www.theguardian.com/world/2019/mar/29/builders-dont-care-dhaka-reacts-another-deadly-blaze-bangladesh. [Accessed 23 August 2019].

Alam, M. J. and Baroi, G. N. (2004), 'Fire hazard categorization and risk assessment for dhaka city in gis framework', *J. Civ. Eng.(IEB)* **32**(1), 35–45.

Alarie, Y. (2002), 'Toxicity of fire smoke', *Critical reviews in toxicology* **32**(4), 259–289.

Bahman, A., Rosario, L. and Rahman, M. M. (2012), 'Analysis of energy savings in a supermarket refrigeration/hvac system', *Applied Energy* **98**, 11–21.

Bangladesh Shongbad Shongstha (2017), 'Fire causes tk 430cr loss in one year: Fire chief', The Daily Star Online, 22 July 2017[Online]. Available at https://www.thedailystar.net/country/bangladesh-fire-~-1437073. [Accessed 22 August 2019].

Bei, P., Liwei, C. and Chang, L. (2012), 'An experimental study on the burning behavior of fabric used indoor', *Procedia Engineering* **43**, 257–261.

Bengtsson, L.-G. (2001), *Enclosure fires*, Swedish Rescue Services Agency.

Besserre, R. and Delort, P. (1997), 'Recent studies prove that the main cause of death during urban fires is poisoning by smoke', *Urgences Medicales* **2**(16), 77–80.

BFSCDA Annual Fire Report (2019), Technical Report 1, Bangladesh Fire Service and Civil Defense Authority, Dhaka, Bangladesh.

BNBC (2015), Bangladesh national building code, Technical Report 1, Housing and Building Research Institute, (HBRI), Dhaka, Bangladesh.

Chapter 6 - Solid-fuel firing (1982), *in* I. DRYDEN, ed., 'The Efficient Use of Energy (Second Edition)', second edition edn, Butterworth-Heinemann, pp. 64 – 92.
URL: *http://www.sciencedirect.com/science/article/pii/B9780408012508500155*

Cox, G. and Kumar, S. (2002), 'Modelling enclosure fires using cfd', *SFPE Handbook of Fire Protection Engineering, 3rd edn. Quincy, MA, USA: National Fire Protection Association* pp. 194–218.

Deardorff, J. W. (1980), 'Stratocumulus-capped mixed layers derived from a three-dimensional model', *Boundary-Layer Meteorology* **18**(4), 495–527.

Elicer-Cortés, J., Demarco, R., Valencia, A. and Pavageau, M. (2009), 'Heat confinement in tunnels between two double-stream twin-jet air curtains', *International Communications in Heat and Mass Transfer* **36**(5), 438–444.

Fan, C., Ji, J., Gao, Z., Han, J. and Sun, J. (2013), 'Experimental study of air entrainment mode with natural ventilation using shafts in road tunnel fires', *International Journal of Heat and Mass Transfer* **56**(1-2), 750–757.

Felis, F., Pavageau, M., Elicer-Cortés, J. C. and Dassonville, T. (2010), 'Simultaneous measurements of temperature and velocity fluctuations in a double stream-twin jet air curtain for heat confinement in case of tunnel fire', *International Communications in Heat and Mass Transfer* **37**(9), 1191–1196.

Foster, A., Swain, M., Barrett, R., D'agaro, P. and James, S. (2006), 'Effectiveness and optimum jet velocity for a plane jet air curtain used to restrict cold room infiltration', *International journal of refrigeration* **29**(5), 692–699.

Frank, D. and Linden, P. F. (2014), 'The effectiveness of an air curtain in the doorway of a ventilated building', *Journal of Fluid Mechanics* **756**, 130–164.

Gao, R., Li, A., Hao, X., Lei, W. and Deng, B. (2012), 'Prediction of the spread of smoke in a huge transit terminal subway station under six different fire scenarios', *Tunnelling and Underground Space Technology* **31**, 128–138.

Gawad, A. A., Khalid, A. A. and Radhwi, M. N. (2015), 'Fire dynamics simulation and evacuation for a large shopping center (mall): Part i, fire simulation scenarios', *American Journal of Energy Engineering* **3**, 52–71.

Gettleman, J. (2019), 'Scores dead in bangladesh fire: 'this isn't about poverty, it's about greed'', The New York Times, 21 February 2019[Online]. Available at https://www.nytimes.com/2019/02/21/world/asia/bangladesh-fire.html. [Accessed 23 August 2019].

Goldstein, M. (2008), 'Carbon monoxide poisoning', *Journal of Emergency Nursing* **34**, 538–542.

Gorbett, G. E., Pharr, J. L. and Rockwell, S. (2016), *Fire dynamics*, Pearson.

Gross, D. and Robertson, A. (1958), 'Self-ignition temperatures of materials from kinetic-reaction data', *Journal of Research of the National Bureau of Standards* **61**(5), 413–417.

Grosshandler, W. L. (1993), 'Radcal: a narrow-band model for radiation', *Calculations in a Combustion Environment, NIST Technical Note* **1402**.

Gupta, S., Pavageau, M. and Elicer-Cortes, J.-C. (2007), 'Cellular confinement of tunnel sections between two air curtains', *Building and Environment* **42**(9), 3352–3365.

Guyonnaud, L., Solliec, C., De Virel, M. D. and Rey, C. (2000), 'Design of air curtains used for area confinement in tunnels', *Experiments in Fluids* **28**(4), 377–384.

Hasan, M. K., Rabbi, A. R. and Mahmud, A. H. (2017), 'Fire partially destroys gulshan market', Dhaka Tribune, 04 January 2017[Online]. Available at https://www.dhakatribune.com/bangladesh/dhaka/2017/01/04/fire-partially-destroys-gulshan-market. [Accessed 22 August 2019].

Hietaniemi, J., Kallonen, R. and Mikkola, E. (1999), 'Burning characteristics of selected substances: production of heat, smoke and chemical species', *Fire and materials* **23**(4), 171–185.

Hu, L., Zhou, J., Huo, R., Peng, W. and Wang, H. (2008), 'Confinement of fire-induced smoke and carbon monoxide transportation by air curtain in channels', *Journal of hazardous materials* **156**(1-3), 327–334.

Hurley, M. J., Gottuk, D. T., Hall Jr, J. R., Harada, K., Kuligowski, E. D., Puchovsky, M., Watts Jr, J. M., Wieczorek, C. J. et al. (2015), *SFPE handbook of fire protection engineering*, Springer.

Islam, M. M. and Adri, N. (2008), 'Fire hazard management of dhaka city: addressing issues relating to institutional capacity and public perception', *Jahangirnagar Planning Review* **6**(6), 56–67.

Islam, M. Z. and Hossain, K. M. (2018), 'Fire hazards in dhaka city: An exploratory study on mitigation measures', *IOSR Journal of Environmental Science, Toxicology and Food Technology* **12**(5), 46–56.

Ji, J., Wan, H., Li, K., Han, J. and Sun, J. (2015), 'A numerical study on upstream maximum temperature in inclined urban road tunnel fires', *International Journal of Heat and Mass Transfer* **88**, 516–526.

Johansson, P. and Van Hees, P. (2000), 'Development of a test procedure for sandwich panels using iso 9705 philosophy. nordtest project 1432-99'.

Khan, E., Ahmed, M. A., Khan, E. and Majumder, S. (2017), 'Fire emergency evacuation simulation of a shopping mall using fire dynamic simulator (fds)', *Journal of Chemical Engineering* **30**(1), 32–36.
URL: *https://www.banglajol.info/index.php/JCE/article/view/34795*

Krajewski, G. and Węgrzyński, W. (2015), 'Air curtain as a barrier for smoke in case of fire: Numerical modelling', *Bulletin of the Polish Academy of Sciences Technical Sciences* **63**(1), 145–153.

Lawton, E. B. and Howell, R. H. (1995), Energy savings using air curtains installed in high-traffic doorways, Technical report, American Society of Heating, Refrigerating and Air-Conditioning Engineers . . . .

Lecaros, M., Elicer-Cortés, J., Fuentes, A. and Felis, F. (2010), 'On the ability of twin jets air curtains to confine heat and mass inside tunnels', *International Communications in Heat and Mass Transfer* **37**(8), 970–977.

Luo, N., Li, A., Gao, R., Tian, Z., Zhang, W., Mei, S., Feng, L. and Ma, P. (2013), 'An experiment and simulation of smoke confinement and exhaust efficiency utilizing a modified opposite double-jet air curtain', *Safety science* **55**, 17–25.

Luo, N., Li, A., Gao, R., Zhang, W. and Tian, Z. (2013), 'An experiment and simulation of smoke confinement utilizing an air curtain', *Safety science* **59**, 10–18.

Luo, N., Li, A., Leng, B., Xu, L. and Liu, X. (2017), 'Smoke confinement with multi-stream air curtain at stairwell entrance', *Procedia Engineering* **205**, 337–344.

Magnussen, B. F. and Hjertager, B. H. (1977), On mathematical modeling of turbulent combustion with special emphasis on soot formation and combustion, *in* 'Symposium (international) on Combustion', Vol. 16, pp. 719–729.

McDermott, R. J., Forney, G. P., McGrattan, K. and Mell, W. E. (2010), 'Fire dynamics simulator version 6: Complex geometry, embedded meshes, and quality assessment', *National Institute of Standards and Technology, NIST* .

McGrattan, K., Hostikka, S., McDermott, R., Floyd, J. and Vanella, M. (2018), 'Fire dynamics simulator technical reference guide volume 1: mathematical model', *NIST special publication* **1018-1**(1), 189.

McGrattan, K., Hostikka, S., McDermott, R., Floyd, J., Weinschenk, C. and Overholt, K. (2013), 'Fire dynamics simulator user's guide', *NIST special publication* **1019**(6).

National Fire Protection Association (2013), *NFPA 921: Guide for Fire & Explosion Investigations*, Technical Committee on Fire Investigations.

National Fire Protection Association (2017), *NFPA 130, Standard for Fixed Guideway Transit and Passenger Rail Systems*, National Fire Protection Association.

Pavageau, M., Nieto, E. and Rey, C. (2001), 'Odour and voc confining in large enclosures using air curtains', *Water science and technology* **44**(9), 165–171.

Poh, W. and Engineer, P. F. (2010), 'Tenability in building fires: Limits and design criteria', *Fire Australia* pp. 24–26.

Prothom Alo (2019), 'Mirpur slum fire hurts woman, burns hundreds of shanties', Prothom Alo, 12 March 2019[Online]. Available at https://en.prothomalo.com/bangladesh/news/172421/Mirpur-slum-fire-hurts-woman-burns-hundreds-of. [Accessed 23 August 2019].

Rabbi, A. R. (2016), 'Bashundhara mall fire under control', Dhaka Tribune, 21 August 2016[Online]. Available at https://www.dhakatribune.com/bangladesh/2016/08/21/fire-erupts-bashundhara-city. [Accessed 22 August 2019].

Rahman, M. S. (2010), 'The only solution', *Forum* .

Rehm, R. G. and Baum, H. R. (1978), 'The equations of motion for thermally driven, buoyant flows', *Journal of Research of the NBS* **83**(297-308), 2.

Ryder, N. L., Schemel, C. F. and Jankiewicz, S. P. (2006), 'Near and far field contamination modeling in a large scale enclosure: Fire dynamics simulator comparisons with measured observations', *Journal of hazardous materials* **130**(1-2), 182–186.

Ryder, N. L., Sutula, J. A., Schemel, C. F., Hamer, A. J. and Van Brunt, V. (2004), 'Consequence modeling using the fire dynamics simulator', *Journal of hazardous materials* **115**(1-3), 149–154.

Shen, C., Shao, X. and Li, X. (2017), 'Potential of an air curtain system orientated to create non-uniform indoor thermal environment and save energy', *Indoor and Built Environment* **26**(2), 152–165.

Shen, T.-S., Huang, Y.-H. and Chien, S.-W. (2008), 'Using fire dynamic simulation (fds) to reconstruct an arson fire scene', *Building and environment* **43**(6), 1036–1045.

Shih, Y.-C., Yang, A.-S. and Lu, C.-W. (2011), 'Using air curtain to control pollutant spreading for emergency management in a cleanroom', *Building and Environment* **46**(5), 1104–1114.

Smagorinsky, J. (1963), 'General circulation experiments with the primitive equations: I. the basic experiment', *Monthly weather review* **91**(3), 99–164.

The Daily Star (2009), 'Blaze at bashundhara city', The Daily Star Online, 14 March 2009[Online]. Available at https://www.thedailystar.net/news-detail-79603. [Accessed 22 August 2019].

The Daily Star (2019*a*), '211 tin-shed shops of dncc market completely razed in fire', The Daily Star Online, 30 March 2019[Online]. Available at https://www.thedailystar.net/city/news/fire-breaks-out-gulshan-1-dncc-market-1722427. [Accessed 22 August 2019].

The Daily Star (2019*b*), 'Banani fire: Death toll rises to 25', The Daily Star Online, 29 March 2019[Online]. Available at https://www.thedailystar.net/city/news/banani-fire-death-toll-rises-25-1722037. [Accessed 23 August 2019].

The Guardian (2019), 'Bangladesh fire leaves 10,000 homeless after blaze razes slum', The Guardian, 18 August 2019[Online]. Available at https://www.theguardian.com/world/2019/aug/18/bangladesh-fire-leaves-10000-homeless-after-blaze-razes-slum. [Accessed 23 August 2019].

Tran, H. C. and White, R. H. (1992), 'Burning rate of solid wood measured in a heat release rate calorimeter', *Fire and materials* **16**(4), 197–206.

UNB (2019), 'High court on chawkbazar fire: Not accident but negligence', Dhaka Tribune, 26 February 2019[Online]. Available at https://www.dhakatribune.com/bangladesh/court/2019/02/26/high-court-on-chawkbazar-fire-not-accident-but-negligence/. [Accessed 22 August 2019].

United News of Bangladesh (2019), 'Fire incidents in bangladesh triple over 22 years', Dhaka Tribune, 26 February 2019[Online]. Available at https://www.dhakatribune.com/bangladesh/nation/2019/02/26/fire-incidents-in-bangladesh-triple-over-22-years. [Accessed 22 August 2019].

Viegas, J. C. and Cruz, H. (2019), 'Air curtains combined with smoke exhaust for smoke control in case of fire: Full-size experiments', *Fire Technology* **55**(1), 211–232.

Wahlqvist, J. and Van Hees, P. (2013), 'Validation of fds for large-scale well-confined mechanically ventilated fire scenarios with emphasis on predicting ventilation system behavior', *Fire Safety Journal* **62**, 102–114.

Wang, L. (2013), 'Investigation of the impact of building entrance air curtain on whole building energy use', *Arlington Heights, IL, USA: Air Movement and Control Association* .

Yu, L.-X., Beji, T., Zadeh, S. E., Liu, F. and Merci, B. (2016), 'Simulations of smoke flow fields in a wind tunnel under the effect of an air curtain for smoke confinement', *Fire Technology* **52**(6), 2007–2026.

Yu, L.-X., Liu, F., Beji, T., Weng, M.-C. and Merci, B. (2018), 'Experimental study of the effectiveness of air curtains of variable width and injection angle to block fire-induced smoke in a tunnel configuration', *International Journal of Thermal Sciences* **134**, 13–26.

Zalok, E. and Hadjisophocleous, G. (2007), Characterizing of design fires for clothing stores, *in* 'Proceedings of the 5th International Seminar on Fire and Explosion Hazards', Vol. 23, pp. 328–337.

Zhiyin, Y. (2015), 'Large-eddy simulation: Past, present and the future', *Chinese journal of Aeronautics* **28**(1), 11–24.

Appendix A

Additional Figures

Fig. A.1 Temperature distributions at positions A, B (inside the fire source) and C, D (outside the fire source) for air curtain at non-discharged condition for clothing fire scenario at fire source shop 1 (DCC_CS1).
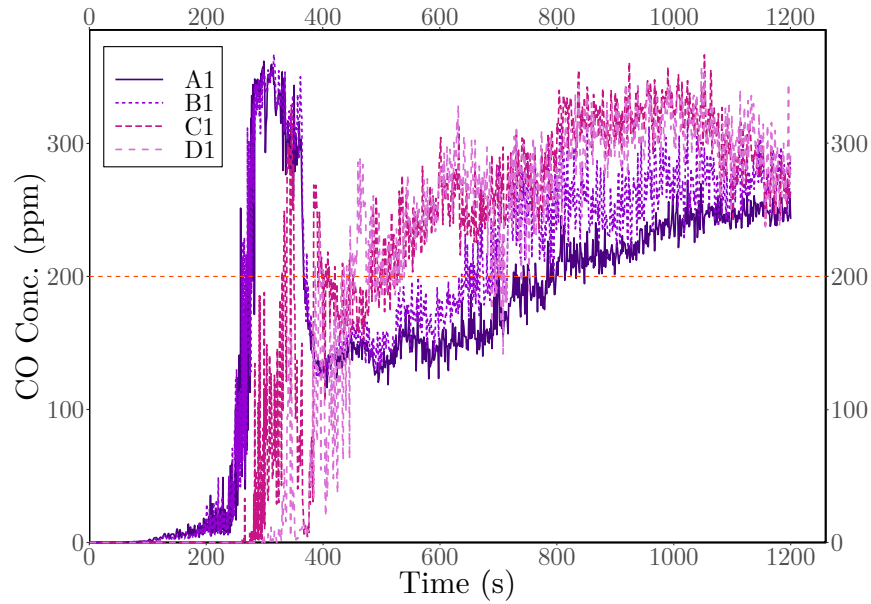
Fig. A.2 CO concentration at positions A1, B1 (inside the fire source) and C1, D1 (outside the fire source) for air curtain at non-discharged condition for clothing fire scenario at fire source shop 1 (DCC_CS1).
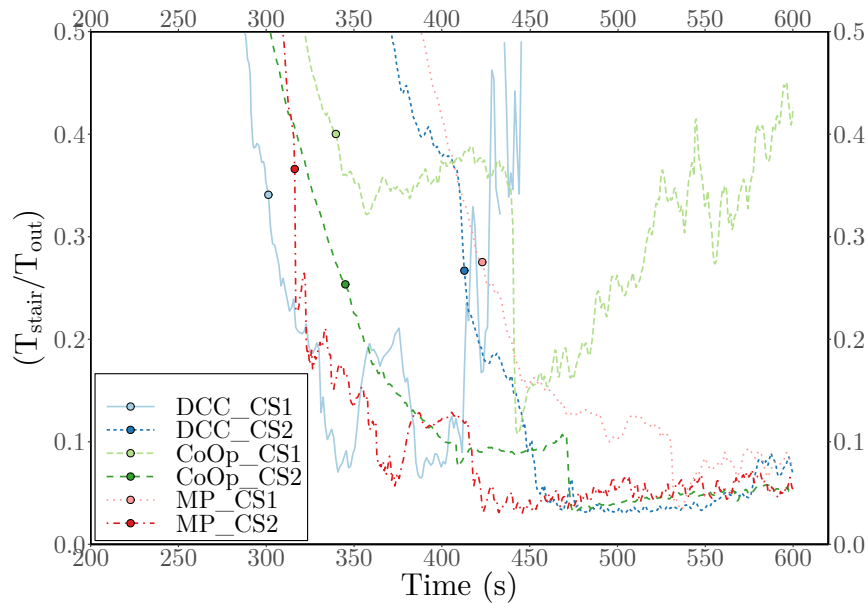
Fig. A.3 Staircase temperature to source outside temperature ratio in function of time, for all geometric variations (more close view).
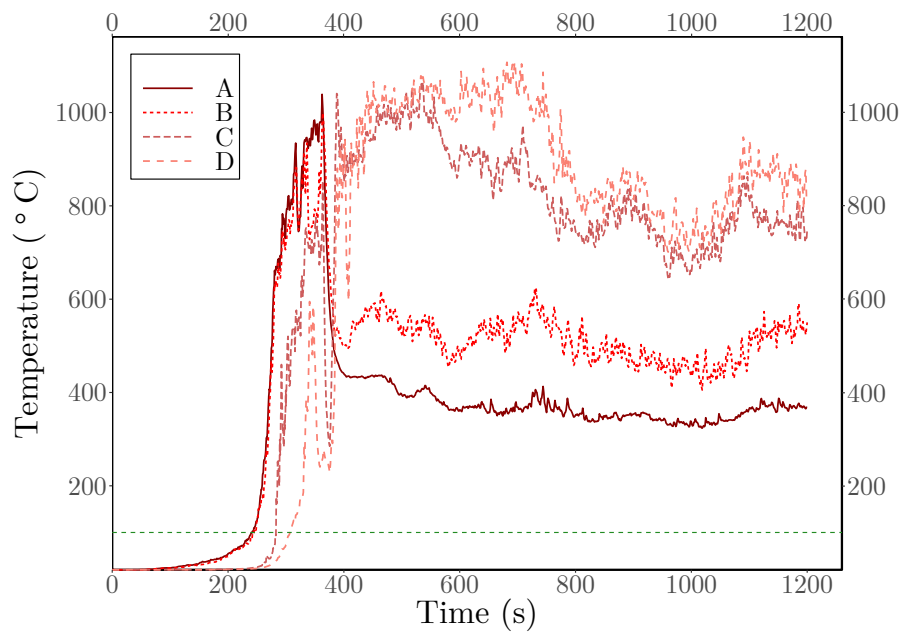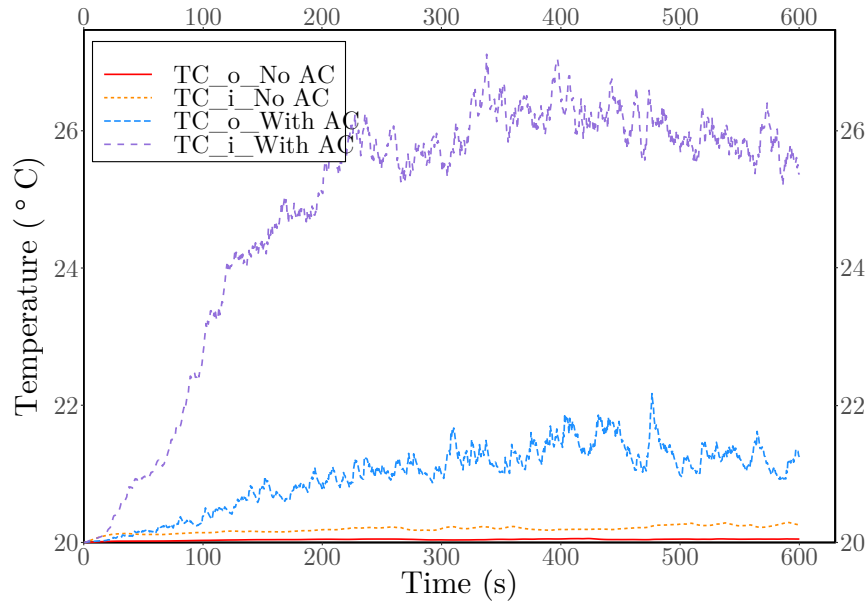
Fig. A.4 Temperature distributions at positions TCi (inside the fire source) and TCo (outside the fire source) for air curtain at discharged and non-discharged condition for furniture fire scenario at Co-Operative market source 1 (CoOp_FS1 vs. CoOp_FS1AC).
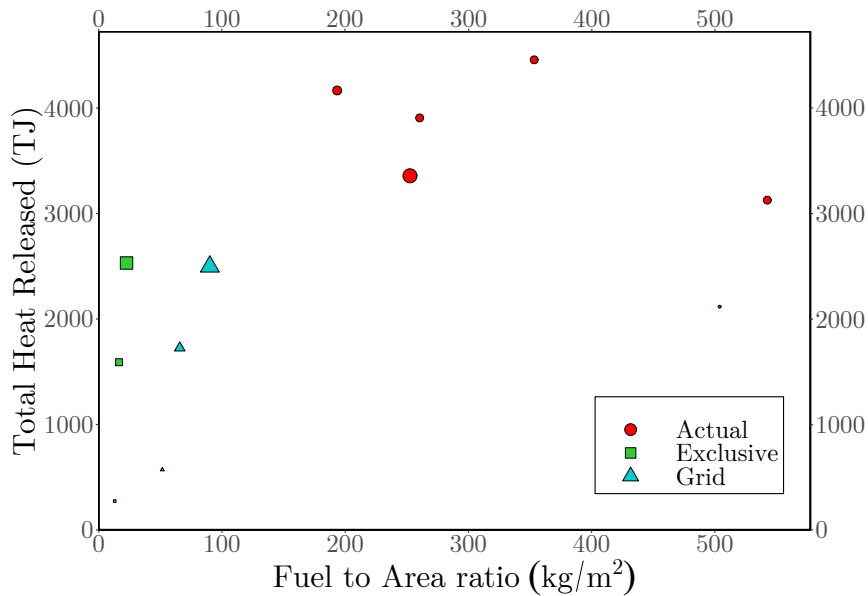
Fig. A.5 Total Heat Released vs. fuel to Area ratio for all fuel distribution in all geometry.

Appendix B

Sample FDS Code

B.1 Shopping Mall-1 Air curtain Discharged Case

```
01C_AC_S1_100.fds
Genearted by PyroSim - Version 2018.3.1210

&HEAD CHID='01C_AC_S1_100'/
&TIME T_END=1200.0/
&DUMP RENDER_FILE='01C_AC_S1_100.gel', COLUMN_DUMP_LIMIT=.TRUE., DT_RESTART=300.0, DT_SL3D=0.25/
&RADI PATH_LENGTH=0.1/

&MESH ID='DCC First Floor-a-a', IJK=38,62,20, XB=0.0,5.7912,0.0,9.4488,0.0,3.048/
&MESH ID='DCC First Floor-a-b', IJK=38,62,20, XB=5.7912,11.5824,0.0,9.4488,0.0,3.048/
&MESH ID='DCC First Floor-b-b-a', IJK=38,40,40, XB=5.7912,8.6868,9.4488,12.4968,0.0,3.048/
&MESH ID='DCC First Floor-b-b-b', IJK=38,40,40, XB=8.6868,11.5824,9.4488,12.4968,0.0,3.048/
&MESH ID='DCC First Floor-c-b', IJK=38,64,20, XB=5.7912,11.5824,12.4968,22.2504,0.0,3.048/
&MESH ID='DCC First Floor-b-a-merged', IJK=38,84,20, XB=0.0,5.7912,9.4488,22.2504,0.0,3.048/


&REAC ID='POLYURETHANE',
      FYI='NFPA Babrauskas',
      FUEL='REAC_FUEL',
      C=6.3,
      H=7.1,
      O=2.1,
      N=1.0,
      AUTO_IGNITION_TEMPERATURE=5.684342E-14,
      CO_YIELD=0.0369,
      SOOT_YIELD=0.1,
      EPUMO2=1.31E4/

&PROP ID='TC_Celling35ft props',
      BEAD_DIAMETER=9.99998E-4,
      BEAD_DENSITY=8908.000003,
      BEAD_SPECIFIC_HEAT=0.439999/
&PROP ID='TC_Eye35ft props',
      BEAD_DIAMETER=9.99998E-4,
      BEAD_DENSITY=8908.000003,
      BEAD_SPECIFIC_HEAT=0.439999/
&PROP ID='TC_Celling33ft props',
      BEAD_DIAMETER=9.99998E-4,
      BEAD_DENSITY=8908.000003,
      BEAD_SPECIFIC_HEAT=0.439999/
&PROP ID='TC_Eye33ft props',
      BEAD_DIAMETER=9.99998E-4,
      BEAD_DENSITY=8908.000003,
      BEAD_SPECIFIC_HEAT=0.439999/
&PROP ID='TC_Celling31ft props',
      BEAD_DIAMETER=9.99998E-4,
```

```
      BEAD_DENSITY=8908.000003,
      BEAD_SPECIFIC_HEAT=0.439999/
&PROP ID='TC_Eye31ft props',
      BEAD_DIAMETER=9.99998E-4,
      BEAD_DENSITY=8908.000003,
      BEAD_SPECIFIC_HEAT=0.439999/
&PROP ID='TC_Celling29ft props',
      BEAD_DIAMETER=9.99998E-4,
      BEAD_DENSITY=8908.000003,
      BEAD_SPECIFIC_HEAT=0.439999/
&PROP ID='TC_Eye29ft props',
      BEAD_DIAMETER=9.99998E-4,
      BEAD_DENSITY=8908.000003,
      BEAD_SPECIFIC_HEAT=0.439999/
&PROP ID='TC_Celling27ft props',
      BEAD_DIAMETER=9.99998E-4,
      BEAD_DENSITY=8908.000003,
      BEAD_SPECIFIC_HEAT=0.439999/
&PROP ID='TC_Eye27ft props',
      BEAD_DIAMETER=9.99998E-4,
      BEAD_DENSITY=8908.000003,
      BEAD_SPECIFIC_HEAT=0.439999/
&PROP ID='TC_Celling25ft props',
      BEAD_DIAMETER=9.99998E-4,
      BEAD_DENSITY=8908.000003,
      BEAD_SPECIFIC_HEAT=0.439999/
&PROP ID='TC_Eye25ft props',
      BEAD_DIAMETER=9.99998E-4,
      BEAD_DENSITY=8908.000003,
      BEAD_SPECIFIC_HEAT=0.439999/
&PROP ID='TC_Celling23ft props',
      BEAD_DIAMETER=9.99998E-4,
      BEAD_DENSITY=8908.000003,
      BEAD_SPECIFIC_HEAT=0.439999/
&PROP ID='TC_Eye23ft props',
      BEAD_DIAMETER=9.99998E-4,
      BEAD_DENSITY=8908.000003,
      BEAD_SPECIFIC_HEAT=0.439999/
&PROP ID='TC_Celling21ft props',
      BEAD_DIAMETER=9.99998E-4,
      BEAD_DENSITY=8908.000003,
      BEAD_SPECIFIC_HEAT=0.439999/
&PROP ID='TC_Eye21ft props',
      BEAD_DIAMETER=9.99998E-4,
      BEAD_DENSITY=8908.000003,
      BEAD_SPECIFIC_HEAT=0.439999/
&PROP ID='TC_Celling19ft_CY34.5ft props',
      BEAD_DIAMETER=9.99998E-4,
      BEAD_DENSITY=8908.000003,
      BEAD_SPECIFIC_HEAT=0.439999/
&PROP ID='TC_Eye19ft_CY34.5ft props',
      BEAD_DIAMETER=9.99998E-4,
      BEAD_DENSITY=8908.000003,
      BEAD_SPECIFIC_HEAT=0.439999/


      .
      .
      .
&PROP ID='TC_Eye_Corridor14 props',
      BEAD_DIAMETER=9.99998E-4,
      BEAD_DENSITY=8908.000003,
      BEAD_SPECIFIC_HEAT=0.439999/
&DEVC ID='TC_Celling35ft', PROP_ID='TC_Celling35ft props', QUANTITY='THERMOCOUPLE', XYZ=10.668,10.5156,2.8956/
&DEVC ID='TC_Eye35ft', PROP_ID='TC_Eye35ft props', QUANTITY='THERMOCOUPLE', XYZ=10.668,10.5156,1.524/
&DEVC ID='CO_Celling34.5ft', QUANTITY='MASS FRACTION', SPEC_ID='CARBON MONOXIDE', XYZ=10.5156,10.5156,2.8956/
&DEVC ID='CO_Eye34.5ft', QUANTITY='MASS FRACTION', SPEC_ID='CARBON MONOXIDE', XYZ=10.5156,10.5156,1.524/
&DEVC ID='CO_Celling32.5ft', QUANTITY='MASS FRACTION', SPEC_ID='CARBON MONOXIDE', XYZ=9.906,10.5156,2.8956/
&DEVC ID='TC_Celling33ft', PROP_ID='TC_Celling33ft props', QUANTITY='THERMOCOUPLE', XYZ=10.0584,10.5156,2.8956/
&DEVC ID='CO_Eye32.5ft', QUANTITY='MASS FRACTION', SPEC_ID='CARBON MONOXIDE', XYZ=9.906,10.5156,1.524/
&DEVC ID='TC_Eye33ft', PROP_ID='TC_Eye33ft props', QUANTITY='THERMOCOUPLE', XYZ=10.0584,10.5156,1.524/
&DEVC ID='CO_Celling30.5ft', QUANTITY='MASS FRACTION', SPEC_ID='CARBON MONOXIDE', XYZ=9.2964,10.5156,2.8956/
&DEVC ID='TC_Celling31ft', PROP_ID='TC_Celling31ft props', QUANTITY='THERMOCOUPLE', XYZ=9.4488,10.5156,2.8956/
&DEVC ID='CO_Eye30.5ft', QUANTITY='MASS FRACTION', SPEC_ID='CARBON MONOXIDE', XYZ=9.2964,10.5156,1.524/
&DEVC ID='TC_Eye31ft', PROP_ID='TC_Eye31ft props', QUANTITY='THERMOCOUPLE', XYZ=9.4488,10.5156,1.524/
&DEVC ID='CO_Celling28.5ft', QUANTITY='MASS FRACTION', SPEC_ID='CARBON MONOXIDE', XYZ=8.6868,10.5156,2.8956/
```

```
&DEVC ID='TC_Celling29ft', PROP_ID='TC_Celling29ft props', QUANTITY='THERMOCOUPLE', XYZ=8.8392,10.5156,2.8956/
&DEVC ID='CO_Eye28.5ft', QUANTITY='MASS FRACTION', SPEC_ID='CARBON MONOXIDE', XYZ=8.6868,10.5156,1.524/
&DEVC ID='TC_Eye29ft', PROP_ID='TC_Eye29ft props', QUANTITY='THERMOCOUPLE', XYZ=8.8392,10.5156,1.524/
&DEVC ID='CO_Celling26.5ft', QUANTITY='MASS FRACTION', SPEC_ID='CARBON MONOXIDE', XYZ=8.0772,10.5156,2.8956/
&DEVC ID='TC_Celling27ft', PROP_ID='TC_Celling27ft props', QUANTITY='THERMOCOUPLE', XYZ=8.2296,10.5156,2.8956/
&DEVC ID='CO_Eye26.5ft', QUANTITY='MASS FRACTION', SPEC_ID='CARBON MONOXIDE', XYZ=8.0772,10.5156,1.524/
&DEVC ID='TC_Eye27ft', PROP_ID='TC_Eye27ft props', QUANTITY='THERMOCOUPLE', XYZ=8.2296,10.5156,1.524/
&DEVC ID='CO_Celling24.5ft', QUANTITY='MASS FRACTION', SPEC_ID='CARBON MONOXIDE', XYZ=7.4676,10.5156,2.8956/
&DEVC ID='TC_Celling25ft', PROP_ID='TC_Celling25ft props', QUANTITY='THERMOCOUPLE', XYZ=7.62,10.5156,2.8956/
&DEVC ID='CO_Eye24.5ft', QUANTITY='MASS FRACTION', SPEC_ID='CARBON MONOXIDE', XYZ=7.4676,10.5156,1.524/
&DEVC ID='TC_Eye25ft', PROP_ID='TC_Eye25ft props', QUANTITY='THERMOCOUPLE', XYZ=7.62,10.5156,1.524/
&DEVC ID='CO_Celling22.5ft', QUANTITY='MASS FRACTION', SPEC_ID='CARBON MONOXIDE', XYZ=6.858,10.5156,2.8956/
&DEVC ID='TC_Celling23ft', PROP_ID='TC_Celling23ft props', QUANTITY='THERMOCOUPLE', XYZ=7.0104,10.5156,2.8956/
&DEVC ID='CO_Eye22.5ft', QUANTITY='MASS FRACTION', SPEC_ID='CARBON MONOXIDE', XYZ=6.858,10.5156,1.524/
&DEVC ID='TC_Eye23ft', PROP_ID='TC_Eye23ft props', QUANTITY='THERMOCOUPLE', XYZ=7.0104,10.5156,1.524/
&DEVC ID='CO_Celling20.5ft', QUANTITY='MASS FRACTION', SPEC_ID='CARBON MONOXIDE', XYZ=6.2484,10.5156,2.8956/
&DEVC ID='TC_Celling21ft', PROP_ID='TC_Celling21ft props', QUANTITY='THERMOCOUPLE', XYZ=6.4008,10.5156,2.8956/
&DEVC ID='CO_Eye20.5ft', QUANTITY='MASS FRACTION', SPEC_ID='CARBON MONOXIDE', XYZ=6.2484,10.5156,1.524/
&DEVC ID='TC_Eye21ft', PROP_ID='TC_Eye21ft props', QUANTITY='THERMOCOUPLE', XYZ=6.4008,10.5156,1.524/
&DEVC ID='CO_Celling_18.5ft_CY34.5ft', QUANTITY='MASS FRACTION', SPEC_ID='CARBON MONOXIDE', XYZ=5.6388,10.5156,2.8956/
&DEVC ID='TC_Celling19ft_CY34.5ft', PROP_ID='TC_Celling19ft_CY34.5ft props', QUANTITY='THERMOCOUPLE', XYZ=5.7912,10.5156,2.8956/
&DEVC ID='CO_Eye18.5ft__CY34.5ft', QUANTITY='MASS FRACTION', SPEC_ID='CARBON MONOXIDE', XYZ=5.6388,10.5156,1.524/
&DEVC ID='TC_Eye19ft_CY34.5ft', PROP_ID='TC_Eye19ft_CY34.5ft props', QUANTITY='THERMOCOUPLE', XYZ=5.7912,10.5156,1.524/

.
.
.

&DEVC ID='TC_Eye_Corridor14', PROP_ID='TC_Eye_Corridor14 props', QUANTITY='THERMOCOUPLE', XYZ=4.8768,21.9456,1.524/
&MATL ID='CONCRETE',
      FYI='NBSIR 88-3752 - ATF NIST Multi-Floor Validation',
      SPECIFIC_HEAT=1.040001,
      CONDUCTIVITY=1.800001,
      DENSITY=2279.999998,
      ABSORPTION_COEFFICIENT=5.0E4/
&MATL ID='Fabric',
      SPECIFIC_HEAT=1.000001,
      CONDUCTIVITY=0.1,
      DENSITY=1539.999995,
      ABSORPTION_COEFFICIENT=5.0E4/

&SURF ID='Wall',
      RGB=255,247,247,
      BACKING='VOID',
      MATL_ID(1,1)='CONCRETE',
      MATL_MASS_FRACTION(1,1)=1.0,
      THICKNESS(1)=3.9624E-3/
&SURF ID='Cloth Stack',
      RGB=40,180,99,
      HRRPUA=1528.000005,
      RAMP_Q='Cloth Stack_RAMP_Q',
      IGNITION_TEMPERATURE=253.0,
      BURN_AWAY=.TRUE.,
      BACKING='VOID',
      MATL_ID(1,1)='Fabric',
      MATL_MASS_FRACTION(1,1)=1.0,
      THICKNESS(1)=0.025/
&RAMP ID='Cloth Stack_RAMP_Q', T=0.0, F=0.0/
&RAMP ID='Cloth Stack_RAMP_Q', T=1.0, F=0.03018/
&RAMP ID='Cloth Stack_RAMP_Q', T=10.0, F=0.0325/
&RAMP ID='Cloth Stack_RAMP_Q', T=20.0, F=0.0375/
&RAMP ID='Cloth Stack_RAMP_Q', T=30.0, F=0.041014/
&RAMP ID='Cloth Stack_RAMP_Q', T=40.0, F=0.056491/
&RAMP ID='Cloth Stack_RAMP_Q', T=50.0, F=0.11685/
&RAMP ID='Cloth Stack_RAMP_Q', T=60.0, F=0.175662/
&RAMP ID='Cloth Stack_RAMP_Q', T=70.0, F=0.200425/
&RAMP ID='Cloth Stack_RAMP_Q', T=80.0, F=0.203521/
&RAMP ID='Cloth Stack_RAMP_Q', T=90.0, F=0.195782/
&RAMP ID='Cloth Stack_RAMP_Q', T=100.0, F=0.21745/
&RAMP ID='Cloth Stack_RAMP_Q', T=110.0, F=0.290191/

.
.
.

&RAMP ID='Cloth Stack_RAMP_Q', T=1800.0, F=0.0/
&SURF ID='Cloth Rack',
      RGB=130,255,124,
```

```
       HRRPUA=1528.0,
       RAMP_Q='Cloth Rack_RAMP_Q',
       IGNITION_TEMPERATURE=253.0,
       BURN_AWAY=.TRUE.,
       BACKING='VOID',
       MATL_ID(1,1)='Fabric',
       MATL_MASS_FRACTION(1,1)=1.0,
       THICKNESS(1)=0.025/
&RAMP ID='Cloth Rack_RAMP_Q', T=0.0, F=0.0/
&RAMP ID='Cloth Rack_RAMP_Q', T=1.0, F=0.03018/
&RAMP ID='Cloth Rack_RAMP_Q', T=10.0, F=0.0325/
&RAMP ID='Cloth Rack_RAMP_Q', T=20.0, F=0.0375/
&RAMP ID='Cloth Rack_RAMP_Q', T=30.0, F=0.041014/
&RAMP ID='Cloth Rack_RAMP_Q', T=40.0, F=0.056491/
&RAMP ID='Cloth Rack_RAMP_Q', T=50.0, F=0.11685/
&RAMP ID='Cloth Rack_RAMP_Q', T=60.0, F=0.175662/
&RAMP ID='Cloth Rack_RAMP_Q', T=70.0, F=0.200425/
&RAMP ID='Cloth Rack_RAMP_Q', T=80.0, F=0.203521/
&RAMP ID='Cloth Rack_RAMP_Q', T=90.0, F=0.195782/
&RAMP ID='Cloth Rack_RAMP_Q', T=100.0, F=0.21745/
&RAMP ID='Cloth Rack_RAMP_Q', T=110.0, F=0.290191/


.
.

.
&RAMP ID='Cloth Rack_RAMP_Q', T=1800.0, F=0.0/
&SURF ID='Cloth Displayed',
       RGB=93,173,226,
       HRRPUA=1528.0,
       RAMP_Q='Cloth Displayed_RAMP_Q',
       IGNITION_TEMPERATURE=253.0,
       BURN_AWAY=.TRUE.,
       BACKING='VOID',
       MATL_ID(1,1)='Fabric',
       MATL_MASS_FRACTION(1,1)=1.0,
       THICKNESS(1)=0.025/
&RAMP ID='Cloth Displayed_RAMP_Q', T=0.0, F=0.0/
&RAMP ID='Cloth Displayed_RAMP_Q', T=1.0, F=0.03018/
&RAMP ID='Cloth Displayed_RAMP_Q', T=10.0, F=0.0325/
&RAMP ID='Cloth Displayed_RAMP_Q', T=20.0, F=0.0375/
&RAMP ID='Cloth Displayed_RAMP_Q', T=30.0, F=0.041014/
&RAMP ID='Cloth Displayed_RAMP_Q', T=40.0, F=0.056491/
&RAMP ID='Cloth Displayed_RAMP_Q', T=50.0, F=0.11685/
&RAMP ID='Cloth Displayed_RAMP_Q', T=60.0, F=0.175662/
&RAMP ID='Cloth Displayed_RAMP_Q', T=70.0, F=0.200425/
&RAMP ID='Cloth Displayed_RAMP_Q', T=80.0, F=0.203521/
&RAMP ID='Cloth Displayed_RAMP_Q', T=90.0, F=0.195782/
&RAMP ID='Cloth Displayed_RAMP_Q', T=100.0, F=0.21745/
&RAMP ID='Cloth Displayed_RAMP_Q', T=110.0, F=0.290191/


.
.

.
&RAMP ID='Cloth Displayed_RAMP_Q', T=1800.0, F=0.0/
&SURF ID='Ignitor',
       COLOR='RED',
       TMP_FRONT=1000.0/
&SURF ID='Air curatin',
       RGB=122,226,209,
       VEL=-10.0/


&OBST ID='Obstruction', XB=-2.775558E-17,0.1524,3.048,22.2504,0.0,3.048, SURF_ID='Wall'/
&OBST ID='Obstruction', XB=11.43,11.5824,3.048,22.2504,0.0,3.048, SURF_ID='Wall'/
&OBST ID='Obstruction', XB=0.1524,3.9624,22.098,22.2504,0.0,3.048, SURF_ID='Wall'/
&OBST ID='Obstruction', XB=0.1524,3.9624,18.8976,19.05,0.0,3.048, SURF_ID='Wall'/
&OBST ID='Obstruction', XB=0.1524,3.9624,15.6972,15.8496,0.0,3.048, SURF_ID='Wall'/
&OBST ID='Obstruction', XB=0.1524,3.9624,12.4968,12.6492,0.0,3.048, SURF_ID='Wall'/
&OBST ID='Obstruction', XB=0.1524,3.9624,9.2964,9.4488,0.0,3.048, SURF_ID='Wall'/
&OBST ID='Obstruction', XB=0.1524,3.9624,3.048,3.2004,0.0,3.048, SURF_ID='Wall'/
&OBST ID='Obstruction', XB=7.4676,7.62,3.048,22.2504,0.0,3.048, SURF_ID='Wall'/
&OBST ID='Obstruction', XB=7.62,11.43,22.098,22.2504,0.0,3.048, SURF_ID='Wall'/
&OBST ID='Obstruction', XB=3.9624,4.1148,3.048,22.2504,0.0,3.048, SURF_ID='Wall'/
&OBST ID='Obstruction', XB=7.62,11.43,3.048,3.2004,0.0,3.048, SURF_ID='Wall'/
&OBST ID='Obstruction', XB=7.62,11.43,20.2692,20.4216,0.0,3.048, SURF_ID='Wall'/
&OBST ID='Obstruction', XB=7.62,11.43,18.7452,18.8976,0.0,3.048, SURF_ID='Wall'/
```

```
&OBST ID='Obstruction', XB=7.62,11.43,15.6972,15.8496,0.0,3.048, SURF_ID='Wall'/
&OBST ID='Obstruction', XB=7.62,11.43,12.4968,12.6492,0.0,3.048, SURF_ID='Wall'/
&OBST ID='Obstruction', XB=7.62,11.43,9.2964,9.4488,0.0,3.048, SURF_ID='Wall'/
&OBST ID='Obstruction', XB=7.62,11.5824,6.2484,6.4008,0.0,3.048, SURF_ID='Wall'/
&OBST ID='Stair part up', XB=2.8956,3.2766,9.4488,10.9728,3.048,3.2385, SURF_ID='Wall'/
&OBST ID='Stair part up', XB=2.5908,2.9718,9.4488,10.9728,2.8575,3.048, SURF_ID='Wall'/
&OBST ID='Stair part up', XB=2.286,2.667,9.4488,10.9728,2.667,2.8575, SURF_ID='Wall'/
&OBST ID='Stair part up', XB=1.9812,2.3622,9.4488,10.9728,2.4765,2.667, SURF_ID='Wall'/
&OBST ID='Stair part up', XB=1.6764,2.0574,9.4488,10.9728,2.286,2.4765, SURF_ID='Wall'/
&OBST ID='Stair part up', XB=1.3716,1.7526,9.4488,10.9728,2.0955,2.286, SURF_ID='Wall'/
&OBST ID='Stair part up', XB=1.0668,1.4478,9.4488,10.9728,1.905,2.0955, SURF_ID='Wall'/
&OBST ID='Stair part up', XB=0.762,1.143,9.4488,10.9728,1.7145,1.905, SURF_ID='Wall'/
&OBST ID='Stair part', XB=0.762,1.143,10.9728,12.4968,1.524,1.7145, SURF_ID='Wall'/
&OBST ID='Stair part', XB=1.0668,1.4478,10.9728,12.4968,1.3335,1.524, SURF_ID='Wall'/
&OBST ID='Stair part', XB=1.3716,1.7526,10.9728,12.4968,1.143,1.3335, SURF_ID='Wall'/
&OBST ID='Stair part', XB=1.6764,2.0574,10.9728,12.4968,0.9525,1.143, SURF_ID='Wall'/
&OBST ID='Stair part', XB=1.9812,2.3622,10.9728,12.4968,0.762,0.9525, SURF_ID='Wall'/
&OBST ID='Stair part', XB=2.286,2.667,10.9728,12.4968,0.5715,0.762, SURF_ID='Wall'/
&OBST ID='Stair part', XB=2.5908,2.9718,10.9728,12.4968,0.381,0.5715, SURF_ID='Wall'/
&OBST ID='Stair part', XB=2.8956,3.2766,10.9728,12.4968,0.1905,0.381, SURF_ID='Wall'/
&OBST ID='Stair part', XB=3.2004,3.5814,10.9728,12.4968,0.0,0.1905, SURF_ID='Wall'/
&OBST ID='Stair Slab', XB=0.1524,0.762,9.4488,12.4968,1.3716,1.7145, SURF_ID='Wall'/
&OBST ID='Prime Wall Stack Cloth Shop1', XB=7.62,11.43,12.0396,12.4968,0.0,3.048, BULK_DENSITY=387.576493, SURF_ID='Cloth Stack'/
&OBST ID='Side Wall Rack Shop1', XB=7.62,11.43,9.4488,10.0584,0.4572,3.048, BULK_DENSITY=77.515299, SURF_ID='Cloth Rack'/
&OBST ID='Back Wall Rack Shop1', XB=10.8204,11.43,10.0584,12.0396,0.4572,3.048, BULK_DENSITY=77.515299, SURF_ID='Cloth Rack'/
&OBST ID='Mid Stack Shop1', XB=7.62,10.0584,10.9728,11.5824,0.0,1.2192, BULK_DENSITY=387.576493, SURF_ID='Cloth Stack'/
&OBST ID='Shop Front Cloth Display Shop1', XB=7.3152,7.4676,10.9728,12.6492,0.0,3.048, BULK_DENSITY=19.378801, SURF_ID='Cloth Displayed'/
&OBST ID='Door Cloth Display Shop1', XB=6.5532,7.4676,10.0584,10.2108,0.0,2.1336, BULK_DENSITY=19.3788, SURF_ID='Cloth Displayed'/
&OBST ID='Front Rack 1 Shop1', XB=6.3246,7.0866,11.8872,12.3444,0.0,1.2192, BULK_DENSITY=77.5153, SURF_ID='Cloth Rack'/
&OBST ID='Front Rack 2 Shop1', XB=6.096,7.3152,9.2964,9.906,0.0,1.2192, BULK_DENSITY=77.5153, SURF_ID='Cloth Rack'/
&OBST ID='Celling Cloth Display Shop1', XB=7.62,10.8204,11.8872,12.0396,2.1336,3.048, BULK_DENSITY=19.3788, SURF_ID='Cloth Displayed'/
&OBST ID='Side Wall Stack Shop1', XB=7.62,11.43,9.4488,10.0584,0.0,0.4572, BULK_DENSITY=387.576493, SURF_ID='Cloth Stack'/
&OBST ID='Back Wall Stack Shop1', XB=10.8204,11.43,10.0584,12.0396,0.0,0.4572, BULK_DENSITY=387.576493, SURF_ID='Cloth Stack'/
&OBST ID='Ignitor', XB=10.668,10.7442,11.8872,11.9634,0.0762,0.1524, SURF_ID='Ignitor'/
&OBST ID='Air curtain 1', XB=7.3914,7.6962,10.0584,10.9728,2.1336,2.286, COLOR='BEIGE', SURF_ID='INERT'/
&OBST ID='Air curtain 2', XB=7.3914,7.6962,13.2588,14.1732,2.1336,2.286, COLOR='BEIGE', SURF_ID='INERT'/
&OBST ID='Air curtain 3', XB=7.3914,7.6962,7.0104,7.9248,2.1336,2.286, COLOR='BEIGE', SURF_ID='INERT'/
&OBST ID='Front Rack 2 Shop2', XB=6.096,7.3152,12.4968,13.1064,0.0,1.2192, BULK_DENSITY=77.5153, SURF_ID='Cloth Rack'/
&OBST ID='Front Rack 1 Shop2', XB=6.096,7.3152,15.0876,15.5448,0.0,1.2192, BULK_DENSITY=77.5153, SURF_ID='Cloth Rack'/
&OBST ID='Shop Front Cloth Display Shop2', XB=7.3152,7.4676,14.1732,15.8496,0.0,3.048, BULK_DENSITY=19.3788, SURF_ID='Cloth Displayed'/
&OBST ID='Door Cloth Display Shop2', XB=6.5532,7.4676,13.2588,13.4112,0.0,2.1336, BULK_DENSITY=19.3788, SURF_ID='Cloth Displayed'/
&OBST ID='Front upper Rack 1 Shop2', XB=6.7056,7.3152,15.0876,15.8496,1.8288,3.048, BULK_DENSITY=77.5153, SURF_ID='Cloth Rack'/
&OBST ID='Prime Wall Stack Cloth Shop2', XB=7.62,11.43,15.24,15.6972,0.0,3.048, BULK_DENSITY=387.576493, SURF_ID='Cloth Stack'/
&OBST ID='Side Wall Stack Shop2', XB=7.62,11.43,12.6492,13.1064,0.0,3.048, BULK_DENSITY=387.576493, SURF_ID='Cloth Stack'/
&OBST ID='Back Wall Stack Shop2', XB=10.9728,11.43,13.1064,15.24,0.0,3.048, BULK_DENSITY=387.576493, SURF_ID='Cloth Stack'/
&OBST ID='Mid Stack Shop2', XB=7.62,9.2964,14.1732,14.7828,0.0,1.2192, BULK_DENSITY=387.576493, SURF_ID='Cloth Stack'/
&OBST ID='Mid Stack 2 shop2', XB=9.906,10.5156,13.1064,14.7828,0.0,1.2192, BULK_DENSITY=387.576493, SURF_ID='Cloth Stack'/
&OBST ID='Celling Cloth Display Shop2', XB=7.62,10.9728,13.1064,13.2588,1.2192,3.048, BULK_DENSITY=19.378801, SURF_ID='Cloth Displayed'/
&OBST ID='Back Wall Display Shop2', XB=10.8204,10.9728,13.2588,15.24,1.2192,3.048, BULK_DENSITY=19.378801, SURF_ID='Cloth Displayed'/
&OBST ID='Side Wall Stack Shop3', XB=7.62,11.43,6.4008,7.0104,0.0,3.048, BULK_DENSITY=387.576493, SURF_ID='Cloth Stack'/
&OBST ID='Back Wall Stack Shop3', XB=10.2108,11.43,7.0104,9.2964,0.0,1.8288, BULK_DENSITY=387.576493, SURF_ID='Cloth Stack'/
&OBST ID='Prime Wall Stack Cloth Shop3', XB=7.62,10.2108,8.5344,9.2964,0.0,1.8288, BULK_DENSITY=387.576493, SURF_ID='Cloth Stack'/
&OBST ID='Prime Wall Stack 2 Cloth Shop3', XB=7.62,10.2108,7.9248,8.5344,0.0,1.2192, BULK_DENSITY=387.576493, SURF_ID='Cloth Stack'/
&OBST ID='Front Rack 3 Shop3', XB=6.4008,7.4676,6.2484,7.0104,0.0,1.8288, BULK_DENSITY=387.576493, SURF_ID='Cloth Stack'/
&OBST ID='Front Rack 2 Shop3', XB=6.4008,7.4676,7.9248,8.6868,0.0,1.2192, BULK_DENSITY=387.576493, SURF_ID='Cloth Stack'/
&OBST ID='Front Rack 1 Shop3', XB=6.4008,7.4676,8.6868,9.144,0.0,2.4384, BULK_DENSITY=387.576493, SURF_ID='Cloth Stack'/
&OBST ID='BackStackShop2', XB=10.8204,11.43,20.4216,22.098,0.0,3.048, BULK_DENSITY=387.576493, SURF_ID='Cloth Stack'/
&OBST ID='FrontStackShop2', XB=7.7724,8.382,20.4216,22.098,0.0,1.2192, BULK_DENSITY=387.576493, SURF_ID='Cloth Stack'/
&OBST ID='Front upper Rack 1 Shop2', XB=6.7056,7.3152,20.4216,21.0312,0.0,3.048, BULK_DENSITY=77.515299, SURF_ID='Cloth Rack'/
&OBST ID='Front upper Rack 2 Shop2', XB=6.7056,7.3152,21.6408,22.2504,0.0,3.048, BULK_DENSITY=77.515299, SURF_ID='Cloth Rack'/
&OBST ID='Side Wall Rack Shop2', XB=7.62,10.8204,21.6408,22.098,1.2192,3.048, BULK_DENSITY=77.515299, SURF_ID='Cloth Rack'/
&OBST ID='Side Wall Stack Shop2', XB=8.382,10.8204,20.4216,20.8788,0.0,3.048, BULK_DENSITY=387.576493, SURF_ID='Cloth Stack'/
&OBST ID='Celling Cloth Display Shop2', XB=8.382,10.8204,20.8788,21.0312,1.2192,3.048, BULK_DENSITY=19.378801, SURF_ID='Cloth Displayed'/
&OBST ID='Side Wall Stack SideShop3', XB=8.382,10.9728,18.8976,19.2024,0.0,3.048, BULK_DENSITY=387.576493, SURF_ID='Cloth Stack'/
&OBST ID='BackStackSideShop3', XB=10.9728,11.43,18.8976,20.2692,0.0,3.048, BULK_DENSITY=387.576493, SURF_ID='Cloth Stack'/
&OBST ID='Side Wall Stack SideShop3', XB=8.382,10.9728,19.9644,20.2692,0.0,3.048, BULK_DENSITY=387.576493, SURF_ID='Cloth Stack'/
&OBST ID='FrontStackSideShop3', XB=7.7724,8.382,18.8976,20.2692,0.0,1.2192, BULK_DENSITY=387.576493, SURF_ID='Cloth Stack'/
&OBST ID='Shop Front Cloth Display SideShop3', XB=7.1628,7.3152,18.7452,20.2692,1.8288,3.048, BULK_DENSITY=19.378801, SURF_ID='Cloth Displayed'/

&HOLE ID='Door1a', XB=3.81,4.2672,4.572,7.62,0.0,2.1336/
&HOLE ID='Door2b', XB=7.3152,7.7724,10.0584,10.9728,0.0,2.1336/
&HOLE ID='Door2c', XB=7.3152,7.7724,13.2588,14.1732,0.0,2.1336/
&HOLE ID='Door2d', XB=7.3152,7.7724,16.3068,17.2212,0.0,2.1336/
&HOLE ID='Door1b', XB=3.81,4.2672,14.1732,15.0876,0.0,2.1336/
&HOLE ID='Door1c', XB=3.81,4.2672,17.3736,18.288,0.0,2.1336/
```

```
&HOLE ID='Door1d', XB=3.81,4.2672,20.574,21.4884,0.0,2.1336/
&HOLE ID='Door2a', XB=7.3152,7.7724,7.0104,7.9248,0.0,2.1336/
&HOLE ID='Door2aa', XB=7.3152,7.7724,3.9624,4.8768,0.0,2.1336/
&HOLE ID='Door1front', XB=0.9144,3.048,2.8956,3.3528,0.0,2.1336/
&HOLE ID='Door2front', XB=8.5344,9.4488,2.8956,3.3528,0.0,2.1336/
&HOLE ID='Stair front', XB=3.81,4.2672,9.4488,12.4968,0.0,3.048/
&HOLE ID='Small Shop1', XB=7.3152,7.7724,20.4216,22.098,0.0,3.048/
&HOLE ID='Small Shop2', XB=7.3152,7.7724,18.8976,20.2692,0.0,3.048/

&VENT ID='Back Corridor', SURF_ID='OPEN', XB=4.1148,7.4676,22.2504,22.2504,0.0,3.048/
&VENT ID='Front Corridor', SURF_ID='OPEN', XB=0.0,11.5824,0.0,0.0,0.0,3.048/
&VENT ID='Left Corridor', SURF_ID='OPEN', XB=0.0,0.0,0.0,3.048,0.0,3.048/
&VENT ID='Right Corridor', SURF_ID='OPEN', XB=11.5824,11.5824,0.0,3.048,0.0,3.048/
&VENT ID='Air Curtain 1', SURF_ID='Air curatin', XB=7.5438,7.62,10.0584,10.9728,2.1336,2.1336/
&VENT ID='Stairs', SURF_ID='OPEN', XB=0.1524,4.1148,9.4488,12.4968,3.048,3.048/

&SLCF QUANTITY='VELOCITY', VECTOR=.TRUE., PBX=7.52856/
&SLCF QUANTITY='VELOCITY', VECTOR=.TRUE., PBY=10.5156/
&SLCF QUANTITY='TEMPERATURE', PBY=10.5156/
&SLCF QUANTITY='TEMPERATURE', PBX=5.7912/
&SLCF QUANTITY='VELOCITY', VECTOR=.TRUE., PBX=5.7912/
&SLCF QUANTITY='MASS FRACTION', SPEC_ID='CARBON MONOXIDE', VECTOR=.TRUE., PBX=5.7912/
&SLCF QUANTITY='MASS FRACTION', SPEC_ID='CARBON MONOXIDE', VECTOR=.TRUE., PBX=10.5156/

&DEVC ID='Convective Heat Flux_SURFACE INTEGRAL', QUANTITY='CONVECTIVE HEAT FLUX', STATISTICS='SURFACE INTEGRAL', XB=7.4676,7.4676,10.0584,10.9728,0.0,2.1336/
&DEVC ID='Radiative Heat Flux_SURFACE INTEGRAL', QUANTITY='RADIATIVE HEAT FLUX', STATISTICS='SURFACE INTEGRAL', XB=7.4676,7.4676,10.0584,10.9728,0.0,2.1336/

&TAIL /
```

Appendix C

List of Publications

C.1 Conference Papers

1. Shoshe, M. A. M. S. and Rahman, M. A. (2019), 'Effectiveness of Air Curtains as Thermal and Smoke Barrier Against High Gradients of Flow Parameters', *Proceedings of the 5th World Congress on Mechanical, Chemical, and Material Engineering (MCM'19),* Lisbon, Portugal, August 15-17, 2019, Paper No. HTFF 199, DOI: 10.11159/htff19.199.

2. Shoshe, M. A. M. S. and Rahman, M. A. (2019), 'Spread and Propagation of Generic Shopping Mall Fire of Bangladesh Under Different Scenarios', *Proceedings on International Conference on Disaster Risk Management,* Dhaka, Bangladesh, January 12-14, p. 641-648.